How Oomycete and Fungal Effectors Enter Host Cells and Promote Infection

Shiv Dutt Kale

Dissertation submitted to the Faculty of the
Virginia Polytechnic Institute and State University
in partial fulfillment of the requirements for the degree of

Doctor of Philosophy
in
Genetics, Bioinformatics, and Computational Biology

Brett M. Tyler, Chair
David R. Bevan
Daniel G. Capelluto
Christopher B. Lawrence
John M. McDowell

April 5th 2011

Keywords: Oomycete, Fungi, Effectors, RxLR, Phosphatidylinositol-3-phosphate

Abstract

The genus *Phytophthora* contains a large number of species that are known plant pathogens of a variety of important crops. *Phytophthora sojae*, a hemibiotroph, causes approximately 1-2 billion dollars (US) of lost soybean world-wide each year. *P. infestans*, the causative agent of the Irish potato famine, is responsible for over 5 billion dollars (US) worth of lost potato each year. These destructive plant pathogens facilitate pathogenesis through the use of small secreted proteins known as effector proteins. A large subset of effector proteins is able to translocate into host cells and target plant defense pathways. *P. sojae* Avr1b is able to suppress cell death triggered by BAX and hydrogen peroxide. The W-domain of Avr1b is responsible for this functionality, and is recognized by the Rps1b gene product to induce effector triggered immunity.

These oomycete effector proteins translocate into host cells via a highly conserved N-terminal motif known as RXLR-dEER without the use of any pathogen encoded machinery. In fungi an RXLR-like motif exists, [R,K,H] X [L,F,Y,M,~I] X, that is able to facilitate translocation without pathogen encoded machinery. Both functional RXLR and RXLR-like motifs are able to bind phosphatidylinositol-3-phosphate (PtdIns-3-P) to mediate entry into host cells. The use of novel inhibitory mechanisms has shown effector entry can be blocked either by sequestering PtdIns-3-P on the outer leaflet of plant and animal cells or by competitive inhibition of the binding pocket of the RXLR or RXLR-like motifs.

Acknowledgements

My journey to understand oomycete effectors, and in a broader sense eukaryotic protein translocation could not have been possible without the friendship, guidance, comradery, and support of many individuals. I must first thank my parents, Rajesh and Sarita Kale, for raising me to have an inquisitive mind. My strong work ethic and dedication can be attributed to them. Their philosophy on life being a continuum of knowledge acquisition really has shaped me to be a scientist. Thanks Mom and Dad!

I want to thank my wife Emily Kale who has been by my side to celebrate all of my successes and failures. Her support and encouragement throughout my PhD and also life is truly a blessing, and I consider myself fortunate to have someone like her as my better half. Emily I don't think I would have made it without you, always encouraging me and supporting me. You are the best cheering section a guy could ever ask for.

Scientifically, I have been very fortunate to have been surrounded by brilliant, hard-working, down to earth individuals. I sincerely thank my advisor Dr. Brett M. Tyler for being encouraging, supportive, and just about perfect. I have never met a person quite like Brett, and I consider myself incredibly lucky to have joined his lab to pursue my PhD. I would like to thank Dr. Chris "Obi-Wan Kenobi" Lawrence. Chris you have been a fantastic person to chat with about scientific and non-scientific matters and I am really grateful for all the lively discussion. I would also like to thank Dr. John McDowell for perspective changing discussions during the early years of my PhD. I am most grateful to John for his Disease Physiology and Development class where I gained tremendous knowledge, and also witnessed an excellent teacher in action. I would also like to thank Dr. Capelluto and Dr. Bevan for being very flexible committee members and for their guidance throughout my PhD.

Working in Tyler lab over the last 5 years has been fun. Challenging at times, but a lot of fun. I have to attribute the great atmosphere of the lab to Felipe Arredondo and Regina Hanlon. Felipe you somehow knew when I needed a coffee break and I am pretty sure I owe you $10 in soda not $20. Thank you for being a great friend, a good landlord for that one-year and an awesome lab manager. You have always been there for me in a lot of ways and I just want to say Thank You! Regina you always were someone to chat with about all of life's fun adventures. Thank you again for all your help after Madeline was born and for all of the books! We have shared a lot of laughs, and I am so lucky to have a friend like you because you plain and simply rock.

I would like to thank Dr. Lecong Zhou for teaching me as a young scientist to be meticulous. It was inspiring to see someone coordinate the processing of over 3000 RNA samples with such care. I have been forever inspired by your hardwork and diligenous throughout that long project. Thank you Lecong, I learned a lot!

I would like to thank Dr. Daolong Dou and Biao Gu for lively discussion and for being great people to work with in the lab. Daolong, your infinite positivity and enthusiasm for science are contagious. I fondly remember our late night discussion of how we should attack the mystery of the RXLR-dEER motif. Biao I enjoyed discussing science with you and we have some good memories drinking a lot of beer. I am glad our collaborative projects have had much success. You were a wonderful person to have in the lab for that year, and I wish you could have stayed. I look forward to seeing you in China someday!

I would like to thank Dennie Munson for being hilarious and for also being the best coordinator a program could ask for. Dennie you really spend a ton of time on us GBCB kids. Thank you for everything you do for the program and the students. Words cannot express how appreciative we are of you.

I would like to thank Nick Galloway and Marcus Chibucos for their friendship and for Tyler Lab Weight Lifting Team. I really miss going to the gym with you guys after work and hope life gives you immense success.

I would like to thank Trudy Torto-Alalibo, Amanda Rumore, Brydan Durham, Kwang-Hyung Kim, Vincenzo Antignani, Danielle Choi, Teresa Stuso Jewel, Sucheta Tripathy, Ryan Anderson, DevDutta Deb, Todd Brengal, Emily Feldman, Sara Marsico, Lachelle Waller, Maureen Lawrence-Kuether and the GBCB program for being great co-workers/collaborators/people.

Table of Contents

List of Tables

List of Figures

Chapter 5

Personal Attributions

Chapter 2

For the work presented in this chapter I invented the double barrel gene gun, performed all of the experiments, and wrote the first draft of the text. I would like thank Shultz-Creehan for fabricating a double barrel gene gun attachment based on my original design specifications.

Chapter 3

For the work presented in this chapter I designed and implemented the double barrel gene gun for analysis of suppression and induction of cell death. I performed 90% of the bombardment assays. I performed the statistical analysis of the bombardment data. I took part in cloning and screening for a large number of plasmids. I made contributions to the first draft of the manuscript.

Chapter 4

For the work presented in this chapter I designed and implemented the double barrel gene gun to assay cell re-entry activity. I performed 95% of the bombardment assays. I performed the statistical analysis of the bombardment data. I took part in cloning and screening for a large number of plasmids. I assisted with microscopy involving bombardment of onion epidermal cells and soybean root uptake assay. I expressed and purified the GFP fusion proteins. I made contributions to the first draft of the manuscript.

Chapter 5

For the work presented in this chapter I designed and implemented all of the protein expression constructs and approximately 50% of the bombardment constructs. I performed approximately half of the bombardment experiments. The remainder were done by Biao Gu. I expressed all of the proteins for this project with assistance from a variety of individuals. I performed the soybean root and suspension culture uptake assays with assistance from a variety of individuals. The leaf infiltration assays were performed by myself and Emily Feldman. Amanda Rumore prepared airway epithelial cells and I performed the uptake assays. I performed the lipid filter binding assay and the liposome binding assay with the assistance of several individuals. I wrote the first draft of the manuscript, and performed a significant amount of the editing.

Chapter 1: An overview of pathogenesis

Oomycete Pathogens

The genus *Phytophthora* contains over 100 identified species that are notorious for significant destruction to fruits and vegetables (**1**). Notable species include *Phytophthora sojae, P. infestans,* and *P. ramorum*. The genus *Phytophthora* is part of the order known as Peronosporales. The order Peronosporales also contains a variety of plant pathogens. These include but are not limited to: *Plasmopara viticola* (grape downy mildew) (**2**), *Hyaloperonospora arabidopsidis* (Arabidopsis downy mildew) (**3**), and *Bremia lactucae* (lettuce downy mildew) (**4**). The order Peronosporales is part of the Oomycota, which contain 10 different orders. The Oomycota contain a variety of organisms that are pathogens of human and animals (*Pythium insidiosum*) (**5**), insects (*Lagenidium giganteum*) (**6**), fish (*Saprolegnia parasitica)* (**7**), and plants (*Pythium ultimum*, *Albugo candida*) (**8,9**). The Oomycota belong to the stramenopiles, a broad group of organisms containing more than 100,000 diverse species, such as algae, kelp, and diatoms. Although pathogenic stramenopiles, such as the oomycetes, are evolutionarily distinct from fungi they share many similarities to pathogenic fungi in their mechanism of infection (**10**).

Field Damage

P. sojae is responsible for 1-2 billion dollars (US) worth of lost soybean (*Glycine max*) worldwide each year (**11**), and is second to soybean cyst nematode in lost product. There have been several instances of yield losses greater than 50% in individual fields infected with *P. sojae* (**12**). Fields with poor drainage support and high

clay content have suffered more severely (**12**). The disease manifests itself through root rot, stem rot, seed decay, and pre- and post-emergence damping-off (**12**). Of the 14 identified Resistance (*Rps*) genes, 6 are commercially deployed (*Rps*1a, *Rps*1b, *Rps*1c, *Rps*1k, *Rps*3a, and *Rps*6) individually or coupled with a form of partial resistance (**12**).

P. sojae is also prevalent in China and South Korea. The organism has only been recently identified in these countries, in 1993 and 1998 respectively. There is still a large degree of speculation as to the origin of *P. sojae*. Soybean cultivars analyzed from South Korea and China have a greater number of *Rps* genes and a greater diversity of partial resistance towards *P. sojae* (**12**) implying that the pathogen may have been present prior to the identification in the early 1990's.

Reproduction

P. sojae reproduces both sexually and asexually, and is able to produce three types of asexual spores: sporangia, zoospores, and chlamydospores (**11**). Sporangia have the ability to either produce zoospores or hyphae. Due to their thick walls, chlamydospores are produced for long-term survival and are generally found in dead plant material (**11**). Chlamydospores provide dormancy in low fitness environments. Zoospores are motile spores with two flagella that do not possess a cell wall (**11**). These spores produce adhesive cysts in relatively short periods of time. Zoospores play an important role in pathogenesis, as they are the primary means of pathogen movement (**11**).

Sexual reproduction in *P. sojae* requires only one mating type, while other *Phytophthora* species such as *P. infestans* are heterothallic and require two mating

types (**11**). Meiosis occurs in the oogonium (female organ) and antheridum (male organ) (**11**). The oogonium and antheridum fuse and a haploid nucleus is delivered to the oogonium (**11**). This mating process results in the production of an oospore, which then produces aseptate hyphae (**11**). *P. sojae* is able to infect soybean at any stage of its life cycle.

Early Infection

Infection of soybean by *P. sojae* occurs rapidly and predominantly in root tissue. Zoospores have been shown to migrate towards roots through a chemo-taxis mechanism of isoflavone recognition (**13**). Upon interacting with root tissue the zoospores turn into cysts that adhere to the plant tissue. At this point the cysts germinate into hyphae, which begins the penetration. At approximately 30 minutes after cyst germination the germ tube has penetrated between adjacent root epidermal cells (**11**). By 4 hours the hyphae has penetrated to the fourth layer of the root cortex and haustoria are abundant along the hyphae (**11**). At approximately 10 hours the endodermis is reached and haustoria are found budding throughout the hyphae (**11**). By 15 hours cells are being invaded directly and vascular tissue is thoroughly settled (**11**).

In an incompatible interaction, where the pathogen is unable to successfully infect the host, *P. sojae* zoospores still adhere to the plant tissue and penetration still occurs by the germ tube; however, at approximately 4 hours hyphae are unable to produce haustoria and many surrounding cells have induced program cell death (**11**). Interestingly, at 10 hours in an incompatible interaction the hyphae has still reached the endodermis, though there are few haustoria present and a large number of cells are

undergoing programmed cell death (**11**). At 15 hours hyphae penetration is halted at the endodermis and most cells in the cortex have now undergone a programmed cell death mechanism known as a hypersensitive response (**11**).

Pathogen-Host Gene for Gene Interactions

The concept that a single gene product in a host species could achieve immunity by "recognizing" a single gene product from a pathogen revolutionized the understanding of resistance for pathogen-host interactions. The concept was initially proposed based on the studies of the rust fungus *Melampsora lini* on flax, *Linum usitatissimum* (**14**). A population of flax with a single resistance gene were inoculated with a F_2 population of *M. lini* carrying a single avirulence gene, resulting in "monofactorial ratios" for inheritance of pathogenicity (**14**). A population of flax with multiple resistance (2 or 3) genes were inoculated with a F_2 population of avirulent *M. lini* resulted in "bi and tri-factorial ratios" for inheritance of pathogenicity (**14**). This concept was validated in several different pathogen-host model systems. As the concept of gene-for-gene interaction unfolded, many validated systems showed either a direct or indirect interaction between a resistance gene product and an avirulence gene product.

Pathogen Associated Molecular Patterns

Plants respond to infection through the activation of various defense response pathways. Initial recognition of the pathogen is believed to occur through perception of a foreign molecule through an extracellular receptor, such as a pattern recognition

receptor (PRR), that then triggers a series of events that primes the defense pathway and induces cell death. Flagellin, a key component of the bacterial flagellum, has the ability to activate the innate immune response in both plants and animals (**15,16**). Flagellin perception occurs by FLS2, a pattern recognition receptor (PRR) consisting of an extracellular receptor domain, a transmembrane domain, and an intercellular kinase domain (**17,18**). The interaction of flagellin and FLS2 results in (but is not limited to) the phosphorylation of AtMEKK1, a mitogen activated protein kinase kinase kinase (MAPKKK) (**19**). AtMEKK1 then phosphorylates AtMKK4/AtMKK5, a MAP kinase kinase (**19**). AtMKK4 then phosphorylates AtMPK3/AtMPK6, a MAP kinase (**19**). Phosphorylation of AtMPK3/AtMPK6 leads to the activation of WRKY22/29 and FRK1 (**19**). WRKY29 is believed to bind W-box DNA elements that then activate genes associated with an immune response leading to disease resistance (**19**). The disease resistance includes, but is not limited to the production of reactive oxygen species and callose deposition, production of salicylic acid, and growth inhibition of seedlings (**19**). These manifestations of defense through recognition of pathogen associated molecular patterns (PAMPS) allow the host to achieve immunity against the pathogen (PAMP triggered immunity). Similarly, the PAMP Ef-Tu leads to defense related phenomena through its interaction with ERF and overlapping, if not identical, MAPK pathways are known to be involved (**20,21,22**).

Several other PAMPs have been identified and their signal transduction pathways are being elucidated. Chitin (a homopolymer of unbranched β-1-4–linked N-acetyl-glucosamine) is a major component of the fungal cell membrane (**23,24,25**). Chitin functions as a PAMP in a large number of plants and animals (**23,24,25**). In rice

and Arabidopsis, mutants of PRR proteins that recognize chitin result in a greater host susceptibility phenotype (**26,27,28**). These PRR contain LysM domains directly responsible for binding to chitin, which then leads to a defense response (**29,30**). The pattern recognition receptor Xa21 recognizes sulfated Ax21 from *Magnaporthe oryzae* and leads to PTI (**31**). Xa21 is shown to be repressed, through autophsophorylation, by XB24 until an interaction with Ax21 occurs (**32**). Upon interaction, Xa21 is believed to initiate a pathway that leads to a defense response (**31**). *P. infestans* INF1 is able to induce a hypersensitive response in tomato and induces ethylene and jasmonic acid signaling pathways (**33**). These pathways are associated with defense signaling towards necrotrophs. Elicitins also induce a hypersensitive response in a variety of Solanaceae and Brassicaceae species in a non-race or cultivar specific manner (**33**). INF1 and elicitins are considered PAMPs, but currently there is no direct evidence for their role in inducing PAMP triggered immunity. Jones and Dangl argued that PRR activation leading to PAMP triggered immunity (PTI) provides a broad-spectrum defense response that is an initial priming/activation mechanism for the host defense (**34**). In many cases where PTI is not robust enough or is silenced by pathogen effectors, other forms of resistance such as effector-triggered immunity (ETI) have arisen to provide a much stronger defense response that is pathogen specific (**34**).

Bacterial Avirulence genes

Bacteria are able to deliver effector proteins through the use of a type-three secretion system. Several of these proteins are considered avirulence proteins due to their direct or indirect interaction with a resistance protein that results in immunity for the

plant (effector triggered immunity- ETI). Characterized *Avr* genes occur mostly in the genera *Pseudomonas* and *Xanthomonas*. The first bacterial avirulence gene characterized was the *Pseudomonas syringae* pv. *glycinea* AvrA (**35**). AvrA induced effector-triggered immunity on soybeans containing the Resistance gene *Rpg2* (**35**). AvrRxv from *Xanthomonas campestris* pv. *vesicatoria* was the first heterologous Avr gene identified (**36**). When expressed in *X. campestris* pv. *phaseoli* AvrRxv induces cultivar-specific resistance (**36**). Similar findings were seen with the effectors AvrRpt2 AvrD, AvrE and AvrPto from *P. syringae* pv. *tomato* when expressed in *P. syringae* pv. *glycinea* and inoculated on specific cultivars of soybean (**37,38,39,40**). Though these effectors play important functions in pathogenesis from the perspective of virulence and ETI, none of these effectors have been proposed as the lone determinants of host range.

Extensive work has been performed on AvrPto and AvrPtoB from *P. syringae* pv. *tomato* (*Pst*). AvrPto induces ETI in the presence of Pto, a serine/threonine kinase, and Prf, a NBS-LRR resistance protein (**41,42**). The mechanism of recognition occurs through Prf, which is believed to be guarding Pto. Interestingly, when AvrPto is not present in *Pst*, ETI is still triggered due to the presence of other effectors that may share a similar target with AvrPto (**43**). AvrPtoB contains a C-terminal E3 ubiquitin ligase, which was only identified through crystal structure (**44**). AvrPtoB lacking this E3 ubiquitin ligase induces ETI, while *Pst* with full length proteins are virulent. Full length AvrPtoB is able to ubiquitinate Fen, which leads to Fen degradation by a proteosome (**44**). This degradation prevents the signal for cell death generated by the interaction of the N-terminus of AvrPtoB and its interactor. Thus along with other virulence functions

AvrPtoB is able to suppress its own ETI.

Oomycete Avirulence genes

Several oomycete effectors are recognized by intracellular resistance proteins and lead to resistance of the host to the pathogen. Five virulence genes from *P. sojae* have been identified for the *P. sojae*-soybean pathogen-system (*Avr*1a, *Avr*1b, *Avr*3a, *Avr*3c, *Avr*4/6) (**45-48**). Currently five avirulence genes have been identified from *P. infestans* for the *P. infestans*-potato pathogen-system (*Avr*3a, *Avr*4, *Avr*2, *Avr*Blb1, and *Avr*Blb2) (**49-52**). *Hyaloperonospora arabidopsidis Atr*13 and *Atr*1 are two avirulence genes that mediate ETI on *Arabidopsis* containing *RPP*13 and *RPP*1 respectively (**53,54**). The exact mechanism of the interaction between these avirulence proteins and their respective R proteins is currently unknown. The oomycete avirulence genes share a common N-terminal motif known as RXLR (arginine-any amino acid-leucine, arginine) (**54,55, 56, 57**). The RXLR motif is followed by a series of amino acids known as the dEER motif for all known oomycete avirulence proteins with the exception of Atr13. The dEER motif is of variable length and location. Though the N-terminus of these avirulence proteins is conserved, the C-terminus varies in length and sequence. Interestingly, there is an example of one oomycete avirulence gene, *Atr5Emoy2* from *H. arabidopsidis* that does not contain an N-terminus canonical RXLR sequence (**58**). The protein does however contain two RXLR-like motifs and a RGD motif. Further analysis on their function will provide unique insight into the evolution of effectors.

The genomes of three *Phytophthora* species (*P. sojae, P. ramorum, P. infestans*) (**56,59**) and three other oomycetes (*Pythium ultimum*, *Hyaloperonospora arabidopsidis*,

Saprolegnia parasitica) (**3,8, unpublished**) have been sequenced using a variety of sequencing technologies. *P. sojae*, *P. ramorum*, and *P. infestans* each contain a large super family of candidate effector proteins that have been identified based on strong SignalP score and presence of an RXLR motif based on a Hidden Markov model (**56,57,59**). The members of these super families bare strong similarity to the known *Avr* genes and are thus referred to as avirulence homologs (*Avh*) (**57**). These *avh* genes have incidences of truncation, deletion, silencing, and variation in amino acid sequence, all instances of strong positive selection. Despite the variation, *Jiang et al* were able to show that a large subset of oomycete effectors contain conserved C-terminal domains known as W, Y, and L-domains (**57**). The W domain of Avr1b is responsible for the interaction with Rps1b and the ability of Avr1b to suppress BAX-triggered cell death (**60**). The W domain of Avr1k is also responsible for interaction with Rps1k (Kale et. al., unpublished).

Fungal Avirulence genes

Several instances of effector triggered immunity have been identified and validated between fungi and plants**.** *AvrL567*, *AvrM*, *P123*, and *P4* from *Melampsora lini* induce a hypersensitive response that results in ETI in specific cultivars of flax expressing respective resistance proteins (**61,62**). *AvrLm1*, *AvrLm4/7*, and *AvrLm6* from *Leptosphaeria maculans* also induce ETI in a cultivar specific manner on canola (*Brassica napus*) expressing *Lm1*, *Lm4*, *Lm7*, and *Lm6* respectively (**63,64,65**). Several avirulence genes have been identified in the rice blast fungus *Magnaporthe oryzae*. *AvrPi-ta*, *PWL1*, *PWL2*, and *ACE1* were identified by map-based cloning (**66,67,68,69**).

AvrPi-ta, PWL1, and PWL2 are recognized either directly or indirectly by their respective resistance proteins in rice (*Oryza sativa***)**. Interestingly, the secondary metabolite produced by ACE1 activates a cultivar specific response in rice (**69**). *Avr-Pia*, *Avr-Pii*, and *Avr-Pik/km/kp* were identified through a genome comparison of isolate Ina168 (known to contain 9 Avr genes) and isolate 70-15 (**70**). These three avirulence genes correspond to the phenotypes for five known avirulence proteins (**70**). *Avr1*, *Avr2*, and *Avr3* from *Fusarium oxysporum f. sp. lycopersici* were initially identified through a proteomics approach of tomato xylem sap (**71,72,73**). These effectors make up three of the 11 secreted in xylem (six) proteins. Avr1, Avr2, and Avr3 induce effector triggered immunity on cultivars of tomato through an interaction *of* I-1, I-2 and I-3 respectively (**71,72,73**). *Avr2, Avr4, Avr4E*, and *Avr9* from *Cladosporium fulvum* (syn. *Passalora fulva*), a biotrophic fungi responsible for tomato leaf mold, are race-specific avirulence genes (**74-77**). Though many avirulence genes have been identified in a diverse array of fungal-plant interactions, the precise mechanism of the interaction differs between many of the *Avr-R* gene interactions and is still unknown for several *Avr-R* gene interactions.

Avirulence proteins' contributions to virulence

Avr genes are assumed to play a contribution to virulence due to the development of resistance genes towards these *Avr* genes, and the fact that these *Avr* genes have not been lost due to selection pressure. Over-expression of Avr1b in *P. sojae* transformants causes increased virulence on soybean cultivars lacking *Rps*1b (**46**). Avr1b is able to suppress BAX mediated cell death *in-planta* and in yeast (**60**).

*Avr*3a is apparently required for full virulence of *P. infestans* (**78**). Avr3a has the ability to suppress the cell death induced by INF1 and is able to stabilize the U-box protein CMPG1 (**79**). *Atr13* expression *in-planta* shows its ability to suppress the production of reactive oxygen species and callose deposition, two responses associated with PAMP triggered immunity (**80**). *Atr1*, when delivered through *P. syringae* (*Pst*) DC3000, contributed positively to the virulence of *Pst* (**80**). *Avr2* from *F. oxysporum* contributes to the full virulence of the pathogen on susceptible tomato (**72**). *F. oxysporum* lacking *Avr3* suffers from a severe reduction in virulence (**73**). *Avr1* from *F. oxysporum* is able to suppress ETI triggered by I-2-Avr2 and I-3-Avr3 (**71**). AvrPto and AvrPtoB are able to suppress several forms of PTI, and are known to have several other intracellular targets that may contribute to virulence (**81,82,83**). Based on these findings avirulence genes play important roles in the overall fitness of the pathogen during infection and have the ability to suppress different types of cell death including PTI and ETI.

Effector contributions to virulence

Oomycetes and certain fungi contain large reservoirs of putative effectors (100-500+). This is in contrast to certain bacteria such as *Pst*, which contain anywhere from 30-50 effector proteins. Many of these effectors target suppression of PTI. AvrPphB cleaves the PAMP kinase BIK1 (**84**). HopF2 ADP-ribosylates MAP kinase kinase (MAPKK) (**85**). HopAI1 dephosphorylates MAP kinase (MAPK) (**86**). These MAP kinase pathways are associated predominately with PTI. Other effectors function to suppress ETI. HopF2 ADP-ribosylates RIN4 and thereby prevents ETI through prevention of cleavage of RIN4 by AvrRpt2 (**87**). *P. infestans* SNE1 is able to suppress program cell

death associated with a variety of *Avr-R* gene pairs (**88**). Other effectors have novel functions during pathogenesis. HopM1 induces the degradation of MIN7 thereby interferes with vesicle trafficking (**89**). HopU1 ADP-ribosylates RNA-binding proteins such as GRP7 (**90**). This function is believed to inhibit RNA pathways. HopI1 targets the chloroplasts to suppress SA production by activation Hsp70 (**91,92**). HopZ1 physically interacts with the isoflavone biosynthesis enzyme, 2-hydroxyisoflavanone dehydratase (**93,94**). microRNAs also play important role in the Arabidopsis defense response and effectors are inferred to play a role in their regulation though no direct evidence currently exists (**95**). By further studying effectors we can better understand the interplay between pathogen and host, leading to the discovery of novel components of the plant immune system.

Apoplastic Effectors

Though many effectors have the ability to translocate into host cells or their translocation is inferred by intracellular interactions, a growing number of effectors have been identified to localize and function in the apoplast. *Cladosporium fulvum* (syn. *Passalora fulva*) contains 6 extracellular effector protein (Ecp1, Ecp2, Ecp4, Ecp5, Ecp6, and Ecp7), all of which have been cloned (**96,97,98**). *C. fulvum* Avr2 interacts with Rcr3, a apoplastic Cys protease, and the interaction leads to Cf-2 mediated resistance (**99**). *C. fulvum* Avr4 and Avr4E are extracellular race-specific elicitors on tomato carrying the Cf-4 and *Hcr9-4E* resistance proteins (**100,101**). *C. fulvum* Avr9 is a 68 amino acid extracellular peptide that is processed by plant peptidases to 28 amino-acid and then triggers a race-specific resistance on Cf-9 tomatoes (**102**). Ecp6 contains

a LysM domain and is able to bind chitin oligosaccharides, a known elicitor of cell immune response (**23**). Sequestering of chitin by *C. fulvum* prevents the initiation of the defense response (**23**). Though work on extracellular effectors has been done extensively in *C. fulvum,* these effectors are also believed to be and are present in other fungi and oomycetes (**103**). EPIC1 and EPIC2 from *P. infestans* are two cystatin-like proteins that target the papain-like cysteine protease C14 from tomato and potato (**104**) as well as PIP1 and RCR3 (**103**), targets of *Cladisporium fulvum* apoplastic effectors. Silencing of C14 results in increased virulence of *P. infestans* of tomato indicating the important roles of apoplastic effectors in pathogenesis.

Bacterial Protein Translocation

The type three secretion system (T3SS) is founded in over 25 gram negative bacteria that are pathogens or symbionts of a wide array of organisms (**105**). The purpose of the T3SS is to deliver effector proteins from docked bacteria across the host plasma membrane and into the host cell cytoplasm. The core eight proteins of the flagellum share similarities with T3SS (**106-108**). Further similarities between the two components are seen through the visualization of the needle complex of *Salmonella enterica* serovar *typhimurium* by electron microscopy (**109**). These findings postulate that the T3SS evolved from the flagellum. Several phylogenetic studies disagree with this postulate due to evolution of T3SS occurring in seven different families (**110**). These studies argue that the T3SS is as old as the flagellum machinery and that both systems shared a common ancestor.

Plasmodium Effector Translocation

Plasmodium falciparum causes malaria, a disease associated with high morbidity in endemic areas. The parasite has an intimate life cycle with both mosquitoes and human. *P. falciparum* parasitizes erythrocytes leaving them rigid, malformed, and adhesive (**111**). This biophysical change associated with infected red blood cells severely impairs circulation and blood physiology (**111**). *P. falciparum* is able to enter erythrocytes forming a host-cell-derived parasitophorous vacuolar membrane (**112,113**). Over 300 putative effectors contain a plasmodium export element (PEXEL) RxLx(E/D/Q) motif. This motif is believed to mediate translocation into the erythrocyte. Analysis of several effectors has shown that requirement of the PEXEL motif in translocation (**114**). Interestingly, these PEXEL effectors contain a N-terminal signal peptide, though the signal peptide is not a requirement for trafficking for KAHRP (**115**). PEXEL effectors are cleaved by plasmepsin V (PMV) (**116,117**) and then acetylated (**118**). PMV is believed to function in a complex with other proteins, which have exclusive access to the cleaved and acetylated PEXEL protein. Sorting moves PEXEL cargoes to specific vesicles that localize to distinct locations on the parasitophorous vacuolar membrane containing the PTEX complex (**119**). PEXEL protein is then transported through a *Plasmodium*-specific pore complex known as PTEX (**119**). The PTEX complex is known to contain a heat shock protein 101 (Hsp101) whose homolog is commonly associated with protein translocons, a novel protein PTEX150, and an exported protein 2 (EXP2), which is believed to be the channel protein that bridges the cytosol of the erythrocyte and the parasitophorous vacuole. The translocation of PEXEL cargo is driven by ATP (**119**). The actual translocation is believed to involve unfolding of

the cargo protein (**119**) similar to what is believed to occur with bacterial effectors that transfer through the T3SS. This mechanism of protein delivery is unique to *Plasmodium* as no other apocomplexians possess these PEXEL protein, homologs to plasmepsin V, or the PTEX translocon (**114,119**).

Oomycete Effector Translocation

Oomycetes and fungi deploy a large number of effector proteins to facilitate infection. The oomycete effectors *Avr1b* from *P. sojae* and *Avr3a* from *P. infestans* have been used as models for effector translocation into host cells. *Whisson et al* showed the substitution of the RXLR and/or the dEER motif of Avr3a with alanines resulted in an inferred loss of translocation due to virulence on potato with Rps3a background (**120**). The N-terminus RXLR-dEER region of Avr3a was shown to translocate beta-glucuronidase (GUS) into host cells when secreted by the pathogen into the haustoria (**121**). *Dou et al* were able to show the translocation of Avr1b is mediated by the RXLR and the dEER motifs during pathogenesis of *P. sojae* on soybean (**121**). Interestingly, the N-terminus RXLR-dEER region of *Avr1b* could be substituted by the RXLR-dEER region of *Avr4/6* and *Ha341* (**121**). These findings imply the modularity of the RXLR-dEER motif. Through the use of a novel particle bombardment assay it was shown that Avr1b could re-enter soybean leaf cells and onion epidermal without any pathogen encoded machinery (**121**). These results were further supported through the uptake of exogenous Avr1b N-terminus fusion protein to GFP (**121**). Identical findings were found for Avr1k and Avh5 (**122**). Incubation of Avr1b, Avh5, and Avr1k GFP fusion proteins resulted in rapid internalization in airway epithelial cells indicating a conserved receptor

between plants and humans (**122**). Recently a putative RXLR effector from *Saprolegnia parasitica* SpHtp1 was identified to translocate into host fish cells without any pathogen encoded machinery (**7**). Oomycete RXLR effector proteins have the ability to translocate into host cells via the RXLR motif and do so without any pathogen encoded machinery. Detailed mutagenesis of *Avr1b*'s RXLR motif through the use of particle bombardment showed the motif retains functional activity in the presence of a variety of mutations. From a functional view RXLR can also encompass [R,K,H] X [L,F,Y,M,~I] X (**122**).

Fungal Effector Translocation

Fungal effectors, mainly avirulence proteins, are inferred to enter host cells. A major hindrance associated with identifying protein translocation domains is due to a lack of highly conserved N-terminal motifs amongst or between taxa of fungi. Currently there is no evidence for a highly conserved motif in the N-terminus of intracellular avirulence proteins from various fungi. A lack of a consensus motif makes bioinformatic identification of putative effectors challenging. Several model fungal avirulence genes are currently under investigation to identify their protein translocation domains. *Kale et al* and *Rafiqi et al* were able to independently identify the same protein translocation domain from AvrL567 and show its translocation independent of the pathogen (**122,123**). Interestingly, AvrL567 contains an RXLR-like motif RFYR. Mutation of this motif results in a loss of protein translocation. *Rafiqi et al* were also able to show another effector from *M. lini* AvrM containing a N-terminus protein translocation domain was sufficient to mediate protein translocation of GFP and the C-terminus of AvrM. Curiously, AvrM contains three RXLR-like motifs in its protein translocation domain

(**123**). Mutation of these RXLR motifs results in a loss of protein translocation. Several other known intracellular avirulence proteins contain a variety of RXLR-like motifs (see Chapter 5). These effectors translocate into cells via these RXLR-like motifs (**122**). Though identification of translocation motifs has been challenging the use of the flexible RXLR-like motif has identified a reservoir of putative effectors in *Leptosphaeria maculans* (**124**).

Phospholipid Mediated Cell Entry

The cell entry domain of oomycete and several fungal effectors contain RXLR and RXLR-like motifs respectively. These motifs mediate entry without the requirement of pathogen-encoded machinery. Remarkably, a beta-type phosphatidylinositol-4-phosphate kinase containing 11 tandem RXLR-dEER motifs is able to bind phosphatidylinositol-4-phosphate (**125**). The RXLR motif of Avr1b, Avr1k, and Avh5 is shown to bind phospholipids, specifically phosphatidylinositol-3-phosphate (PtdIns-3-P) (**122**). Mutation of the RXLR motif results in a loss of cell entry and a loss of phospholipid binding (**122**). Fungal RXLR-like motifs, such as the one found in AvrL567, were also able to bind phospholipids to mediate cell entry (**122**). Effector entry can be blocked by competitive inhibition through the use of 1,3-inositol diphosphate and by sequestration of PtdIns-3-P (**122**). (see Chapter 5).

Novel Protein Translocation Domains

Though the existence of the RXLR and RXLR-like effectors is present throughout oomycetes and fungi, several other putative protein translocation domains have been

identified in several oomycetes. Interestingly these motifs are present in a wide number of putative effectors and have small reservoirs in several oomycete pathogens. One such motif is the LXLFLAK motif identified in crinkler and necrosis (CRN) effectors (**126**). CRN effectors, when expressed inside the cell, produce a crinkling and necrosis phenotype and thus the N-terminus LXLFLAK motif is inferred to mediate protein translocation (**126**). To test the ability of the LXLFLAK motif for protein translocation the N-terminus of LXLFLAK domain was fused to the C-terminus of Avr3a (**127**). Transgenic *P. capsici* expressing LXLFLAK -C-term Avr3a induced a strong HR response on *N. benthamiana* expressing the R3a resistance protein (**127**). Mutation of the LXLFLAK motif to alanines resulted in a loss of translocation indicating that the KFLAK motif is able to translocate the C-terminus of Avr3a into host cells (**127**). Further work is required to identify if this translocation can occur without the pathogen and to identify the receptor that mediates translocation.

The sequence of the necrotrophic plant pathogen *Pythium ultimum* lead to the discovery of a novel YxSL[R/K] motif identified in approximately 91 putative effector proteins (**8**). Interestingly this necrotroph contains very few, if any RXLR or CRN effectors. A subset of barley powdery mildew, wheat stem rust, and wheat leaf rust fungi were found to have an N-terminus motif [Y/F/W]xC, (107,178, and 57 respectively) (**128**). These effectors have not been validated for effector translocation, though are presumed to play a role in effector translocation. Validation of these putative translocation motifs will help gain insight to novel methods of protein translocation.

Summary and Forward

Apoplastic and cytoplasmic effectors contribute to pathogenesis through silencing of PAMP signaling cascades or by suppression of defense responses such as effector-triggered immunity. Effectors are also able to target non-traditional sites that can contribute to virulence, such as vesicle movement or RNA pathways. Plants have evolved mechanisms to recognize effectors and trigger more robust defense responses. The arms race between pathogen-host highlights an intricate series of events that lead to either virulence or immunity. Chapter 3 describes how the effector Avr1b from *P. sojae* is able to suppress induction of cell death in a variety of systems. Suppression of cell death relies on W and Y domains found in C-terminus of Avr1b. These domains are found in many putative effector proteins. The work done with Avr1b supports the hypothesis that these modular domains contribute to virulence through suppression of different inducers of cell death. This hypothesis fits well due to *P. sojae*'s biotrophic life style during approximately the first 15 hours of infection.

Pathogens utilize a wide variety of mechanism to facilitate pathogenesis. One fundamental question that arises in every pathogen-host system is how are these effector proteins trafficked from pathogen to host? In the case of several bacteria, a T3SS is utilized to directly penetrate the host cell membrane and effectors are injected into the host cytosol. The entry mechanism of fungal and oomycete has remained a mystery. Chapter 4 shows that highly conserved RXLR-dEER motif of Avr1b is a translocation domain able to translocate Avr1b and GFP into soybean and onion epidermal cells without any pathogen-encoded machinery. Chapter 5 shows that the RXLR motif is still functional with a wide variety of amino acid substitutions. This finding enabled the identification of RXLR-like motifs in several fungal effectors leading to the

discovery that these RXLR-like motifs mediate translocation of fungal effectors without any pathogen-encoded machinery. Both fungal and oomycete translocation domains are able to enter a wide variety of cell types indicating that the host cell receptor is highly conserved and has an ancient origin. The receptor was identified as being phosphatidylinositol-3-phosphate (PtdIns-3-P). By binding PtdIns-3-P effectors enter host cells by endocytosis. The study of RXLR mediated entry has lead to several fundamental discoveries and has provided a proof of concept that is currently leading to the development of novel biotechnology applications.

References:

1. Erwin DC, Ribiero OK (1996) Phytophthora Diseases Worldwide. APS Press, St. Paul, Minnesota.
2. Kiefer B, et al (2002) The host guides morphogenesis and stomatal targeting in the grapevine pathogen *Plasmopara viticola*. *Planta*: 215, 387-393.
3. Baxter L, et al (2010) Signatures of adaptation to obligate biotrophy in the *Hyaloperonospora arabidopsidis* genome. *Science*: 330, 1549-1551.
4. Bonnier FJM, Reinink K, Groenwold R (1992) New sources of major gene resistance in *Lactuca* to *Bremia lactucae. Euphytica*: 61, 203–211.
5. Krajaejun T, et al (2010) The 74-Kilodalton immunodominant antigen of the pathogenic omycete *Pythium insidiosum* is a putative exo-1, 3-ß-glucanase. *Clinical Vaccine Immunology*: 17, 1203-1210.
6. Brey PT, Remaudiere G (1985) Recognition and isolation of *Lagenidium giganteum* couch. *Bull Soc Vector Ecol*: 10, 90-97.
7. van West P, et al (2010) The putative RxLR effector protein SpHtp1 from the fish pathogenic oomycete Saprolegnia parasitica is translocated into fish cells. *FEMS Microbiol Lett*: 310, 127-137.
8. Levesque CA, et al (2010) Genome sequence of the necrotrophic plant pathogen *Pythium ultimum* reveals original pathogenicity mechanisms and effector repertoire. *Genome Biol*: 11(7)R73 Epub.
9. Pound GS, Williams PH (1963) Biological races of *Albugo candida*. *Phytopathology:* 53, 1146-1149.
10. Meng S, et al (2009) Common processes in pathogenesis by fungal and oomycete plant pathogens, described with Gene Ontology terms. *BMC Microbio*: doi 10.1186/1471-2180-9-S1-S7.
11. Tyler BM (2007) *Phytophthora sojae*: root rot pathogen of soybean and model oomycete. *Molec Plant Path*: 8, 1-8.

12. Dorrance AE, et al (2007) Phytophthora root and stem rot of soybean. *The Plant Health Instructor*. DOI: 10.1094/PHI-I-2007-0830-07
13. Morris PF, Ward EWB (1992) Chemoattraction of zoospores of the soybean pathogen, *P. sojae*, by isoflavones. *Phys Mol Plant Pathol*: 40,17–22.
14. Flor HH (1971) Current status of the gene-for-gene concept. *Ann Rev Phytopath*: 7, 275-296.
15. Felix G, et al (1999) Plants recognize bacteria through the most conserved domain of flagellin. *Plant J:* 18, 265–276.
16. Eaves-Pyler T, et al (2001) Flagellin, a novel mediator of Salmonella-induced epithelial activation and systemic inflammation: I kappa B alpha degradation, induction of nitric oxide synthase, induction of proinflammatory mediators, and cardiovascular dysfunction. *J immunol*: 166, 1248-1260.
17. Chinchilla D, et al (2006) The *Arabidopsis* receptor kinase FLS2 binds flg22 and determines the specificity of flagellin perception. *The Plant Cell*: 18, 465-476.
18. Gomez-Gomez L, Boller T (2000) FLS2: An LRR receptor–like kinase Involved in the perception of the bacterial elicitor flagellin in *Arabidopsis. Mol Cell: 5, 1003-1011.*
19. Asai T, et al (2002) MAP kinase signaling cascade in *Arabidopsis* innate immunity. *Nature* 415, 977-983.
20. Zipfel C, et al (2006) Perception of the bacterial PAMP EF-Tu by the receptor EFR restricts agrobacterium-mediated transformation. *Cell*: 125, 749-760.
21. Kunze G, et al (2004) The N-Terminus of bacterial elongation factor Tu elicits innate immunity in *Arabidopsis* plants. *The Plant Cell*: 16:3496-3507.
22. Nekrasov V, et al (2009) Control of the pattern-recognition receptor EFR by an ER protein complex in plant immunity. *The EMBO J*: 28, 3428-3438.
23. de Jonge R, et al (2010) Conserved fungal LysM effector Ecp6 prevents chitin-triggered immunity in plants. *Science*: 328, 953-955.
24. Boller T (1995) Chemoperception of microbial signaling plant cells. *Annu Rev Plant Physiol Plant Mol Biol*: 46, 189-214.
25. Lee CG, et al (2008) Chitin regulation of immune responses: An old molecule with new roles. *Curr Opin Immunol*: 20, 684-689.
26. Felix G (1993) Specific perception of subnanomolar concentrations of chitin fragments by tomato cells: Induction of extracellular alkalinization, changes in protein phosphorylation, and establishment of a refractory state. *Plant J*: 4, 307-316.
27. Kakuet H, et al (2006) Plant cells recognize chitin fragments for defense signaling through a plasma membrane receptor. *Proc Natl Acad Sci USA*: 103, 11086-11091.
28. Miyaet A, et al (2007) CERK1, a LysM receptor kinase, is essential for chitin elicitor signaling in *Arabidopsis*. *Proc Natl Acad Sci USA:* 104, 19613-19618.
29. Wanet J, et al (2008) A LysM receptor-like kinase plays a critical role in chitin signaling and fungal resistance in *Arabidopsis*. *The Plant Cell*: 20, 471-481.
30. Lizasa E, et al (2010) Direct binding of a plant LysM receptor-like kinase, LysM RLK1/CERK1, to chitin in-vitro. *J Biol Chem*: 285, 2996-3004.
31. Song WY, et al (1995) A receptor kinase-like protein encoded by the rice disease resistance gene, Xa21. *Science*: 270, 1804–1806.

32. Chen X (2010) An ATPase promotes autophosphorylation of the pattern recognition receptor XA21 and inhibits XA21-mediated immunity. *Proc Nat Acad Sci*: 107, 8029-8034.
33. Kawamura Y, et al (2009) INF1 elicitin activates jasmonic acid- and ethylene-mediated signalling pathways and induces resistance to bacterial wilt disease in tomato. *J Phytopath*: 157, 287-297.
34. Jones JDG, Dangl JL (2006) The plant immune system. *Nature:* 444, 323-329.
35. Staskawicz B, Dahlbeck D, Keen NT (1984) Cloned avirulence gene of *Pseudomonas syringae* pv. glycinea determines race-specific incompatiblity on *Glycines max* (L.) Merr. *Proc Natl Acad Sci USA:* 81, 6024–6028.
36. Whalen MC, Stall RE, Staskawicz BJ (1988) Characterization of a gene from a tomato pathogen determining hypersensitive resistance in non-host species and genetic analysis of this resistance in bean. *Proc Natl Acad Sci USA:* 85, 6743–6747.
37. Keen NT, et al (1990) Bacteria expressing avirulence gene D produce a specific elicitor of the soybean hypersensitive reaction. *Mol Plant Micro Interact:* 3, 112–121.
38. Kobayashi DY, Tamaki SJ, Keen NT (1989) Cloned avirulence genes from the tomato pathogen *Pseudomonas syringae* pv. tomato confer cultivar specificity on soybean. *Proc Natl Acad Sci USA:* 86,157–161.
39. Lorang JM, Shen H, Kobayashi D, Cooksey D, Keen NT (1994) *avrA* and *avrE* in *Pseudomonas syringae* pv. tomato PT23 play a role in virulence on tomato plants. *Mol Plant Micro Interact:* 7, 508–515.
40. Ronald PC, Salmeron JM, Carland FM, Staskawicz BJ. (1992) The cloned avirulence gene *avrPto* induces disease resistance in tomato cultivars containing the *Pto* resistance gene. *J Bacteriol:* 174,1604–1611.
41. Pedley,KF, Martin, GB (2003) Molecular basis of Pto-mediated resistance to bacterial speck disease in tomato. *Annu Rev Phytopathol*: 41, 215–243.
42. Rathjen JP, et al (1999) Constitutively active Pto induces a Prf-dependent hypersensitive response in the absence of avrPto. *EMBO J*: 18, 3232–3240.
43. Tang X, et al (1996) Initiation of plant disease resistance by physical interaction of AvrPto and Pto kinase. *Science*: 20, 2060-2063.
44. Rosebrock TR, et al (2007) A bacterial E3 ubiquitin ligase targets a host protein kinase to disrupt plant immunity. *Nature:* 448, 370-374.
45. Qutob D, et al (2009) Copy number variation and transcriptional polymorphisms of *Phytophthora sojae* RXLR effector genes Avr1a and Avr3a. *PLoS One*: 4(4):e5066
46. Shan W, et al (2004) The Avr1b locus of Phytophthora sojae encodes an elicitor and a regulator required for avirulence on soybean plants carrying resistance gene Rps1b. *Mol Plant Micro Interact:* 17, 394-403.
47. Dong S, et al (2009) The *Phytophthora sojae* avirulence locus Avr3c encodes a multi-copy RXLR effector with sequence polymorphisms among pathogen strains*. PLoS One.* 2009;4(5):e5556.
48. Dou D, et al (2010) Different domains of *Phytophthora sojae* effector Avr4/6 are recognized by soybean resistance genes Rps4 and Rps6. Mol Plant Micro Interact 23, 425-435.

49. Armstrong MR, et al (2005) An ancestral oomycete locus contains late blight avirulence gene Avr3a, encoding a protein that is recognized in the host cytoplasm. *Proc Nat Acad Sci USA:* 102, 7766-7771.
50. Van Poppel PM, et al (2008). The *Phytophthora infestans* avirulence gene Avr4 encodes an RXLR-dEER effector. *Mol Plant Microbe Interact*: 21, 1460-1470.
51. Vleeshouwers VG, et al (2008) Effector genomics accelerates discovery and functional profiling of potato disease resistance and phytophthora infestans avirulence genes. *PLoS ONE*: 3, e2875.
52. Oh SK, et al (2009) In planta expression screens of *Phytophthora infestans* RXLR effectors reveal diverse phenotypes, including activation of the Solanum bulbocastanum disease resistance protein Rpi-blb2. *Plant Cell*: 21, 2928-2947.
53. Allen RL, et al (2004) Host-parasite coevolutionary conflict between *Arabidopsis* and downy mildew. *Science*: 306, 1957-1960.
54. Rehmany AP, et al (2005) Differential recognition of highly divergent downy mildew avirulence gene alleles by RPP1 resistance genes from two *Arabidopsis* lines. *The Plant Cell:* 17, 1839-1850.
55. Birch, PR et al (2006) Trafficking arms: Oomycete effectors enter host plant cells. *Trends Microbiol:* 14, 8–11.
56. Tyler BM, et al (2006) Phytophthora genome sequences uncover evolutionary origins and mechanisms of pathogenesis. *Science*: 313, 1261–1266.
57. Jiang RHY, et al (2008) RXLR effector reservoir in two *Phytophthora* species is dominated by a single rapidly evolving super-family with more than 700 members. *Proc Natl Acad Sci USA*: 105, 4874–4879.
58. Bailey K (2011) Molecular cloning of ATR5Emoy2 from *Hyaloperonospora arabidopsidis*, an avirulence determinant that triggers RPP5-mediated defense in *Arabidopsis*. *Mol Plant Micro Interact: doi: 10.1094/MPMI-12-10-0278*
59. Haas BJ, et al (2009) Genome sequence and analysis of the Irish potato famine pathogen *Phytophthora infestans. Nature:* 461, 393-398.
60. Dou D, et al (2008) Conserved C-terminal motifs required for avirulence and suppression of cell death by *Phytophthora sojae* effector Avr1b. *The Plant Cell*: 20,1118-1133.
61. Dodds PN, et al (2004) The *Melampsora lini AvrL567* avirulence genes are expressed in haustoria and their products are recognized inside plant cells. *Plant Cell:* 16, 755-768.
62. Catanzariti AM, et al (2005) Haustorially expressed secreted proteins from flax rust are highly enriched for avirulence elicitors. *Plant Cell*: 18, 243-256.
63. Gout L, et al (2006) Lost in the middle of nowhere: the *AvrLm1* avirulence gene of the Dothideomycete *Leptosphaeria maculans. Molec Microbiol:* 60, 67–80.
64. Fudal I, et al (2007) Heterochromatinlike regions as ecological niches for avirulence genes in the *Leptosphaeria maculans* genome: map-based cloning of *AvrLm6. Molec Plant Micro Interac:* 20, 459–470.
65. Parlange F, et al (2009) *Leptosphaeria maculans* avirulence gene *AvrLm4-7* confers a dual recognition specificity by the *Rlm4* and *Rlm7* resistance genes of oilseed rape, and circumvents *Rlm4*–mediated recognition through a single amino acid change. *Molec Microbiol:* 71, 851–863.

66. Jia Y, et al (2000) Direct interaction of resistance gene and avirulence gene products confers rice blast resistance. *The EMBO Journal*: 19, 4004 – 4014
67. Valent B, et al (1986) Genetic studies of fertility and pathogenicity in *Magnaporthe grisea*. *Iowa State J Res*: 60, 569-594.
68. Sweigard JA, et al (1995) Identification, cloning, and characterization of *PWL2,* a gene for host species specificity in the rice blast fungus. *Plant Cell*: 7, 1221-1233.
69. Fudal I, et al (2007) Expression of *Magnaporthe grisea* avirulence gene *ACE1* Is connected to the initiation of appressorium-mediated penetration. *Euk Cell*: 6, 546-554.
70. Yoshida K, et al (2009) Association genetics reveals three novel avirulence genes from the rice blast fungal pathogen *Magnaporthe oryzae. Plant Cell:* 21, 1573-1591.
71. Houterman PM, et al (2008) Suppression of plant resistance gene-based immunity by a fungal effector. PLoS Pathog 4(5): e1000061.
72. Houterman PM, et al (2009). The effector protein Avr2 of the xylem-colonizing fungus *Fusarium oxysporum* activates the tomato resistance protein I-2 intracellularly. *Plant Journal:* 58, 970-8.
73. Rep M, et al (2004) A small, cysteine-rich protein secreted by *Fusarium oxysporum* during colonization of xylem vessels is required for I-3-mediated resistance in tomato. *Molec Microbiol:* 53, 1373–1383.
74. van Kan JAL, et al (1991) Cloning and characterization of cDNA of avirulence gene *Avr9* of the fungal pathogen *Cladosporium fulvum*, causal agent of tomato leaf mold. *Mol Plant Micro Interact*: 4, 52–59.
75. Joosten MHAJ, et al (1994) Host resistance to a fungal tomato pathogen lost by a single base-pair change in an avirulence gene. *Nature*: 367, 384–386.
76. Luderer R, et al (2002) *Cladosporium fulvum* overcomes *Cf-2*-mediated resistance by producing truncated AVR2 elicitor proteins. *Mol Microbiol*: 45, 875–884.
77. Westerink N, et al (2004) *Cladosporium fulvum* circumvents the second functional resistance gene homologue at the *Cf-4* locus (*Hcr9-4E*) by secretion of a stable avr4E isoform. *Mol Microbiol*: 54, 533–545.
78. Bos JIB, et al (2010) *Phytophthora infestans* effector AVR3a is essential for virulence and manipulates plant immunity by stabilizing host E3 ligase CMPG1. *Proc Nat Acad Sci USA*: 107, 9909-9914.
79. BOS JIB, et al (2006) The C-terminal half of Phytophthora infestans RXLR effector AVR3a is sufficient to trigger R3a-mediated hypersensitivity and suppress INF1-induced cell death in *Nicotiana benthamiana. The Plan J:* 48, 165-176.
80. Sohn KH, et al (2007) The downy mildew effector proteins ATR1 and ATR13 promote disease susceptibility in *Arabidopsis thaliana. The Plant Cell:* 19, 4077-4090.
81. Xiang T, et al (2008) *Pseudomonas syringae* effector AvrPto blocks innate immunity by targeting receptor kinases. *Curr Biol:* 18, 74–80.
82. Göhre V, (2008) Plant pattern-recognition receptor FLS2 is directed for degradation by the bacterial ubiquitin ligase AvrPtoB, *Curr Biol:* 18, 1824–1832.
83. Gimenez-Ibanez S, et al (2009) AvrPtoB targets the LysM receptor kinase

CERK1 to promote bacterial virulence on plants, *Curr Biol:* 19, 423–429.
84. Zhang J, et al (2010) Receptor-like cytoplasmic kinases integrate signaling from multiple plant immune receptors and are targeted by a *Pseudomonas syringae* effector. *Cell Host Microbe:* 7, 290–301.
85. Wang Y, et al (2010) A *Pseudomonas syringae* ADP-ribosyltransferase inhibits Arabidopsis mitogen-activated protein kinase kinases, *Plant Cell:* 22, 2033–2044.
86. Zhang J, et al (2007) A *Pseudomonas syringae* effector inactivates MAPKs to suppress PAMP-induced immunity in plants, *Cell Host Microbe:* 1, 175–185.
87. Wilton M, et al (2010) The type III effector HopF2Pto targets Arabidopsis RIN4 protein to promote *Pseudomonas syringae* virulence, *Proc Natl Acad Sci USA:* 107, 2349–2354.
88. Kelley BS, et al (2010) A secreted effector protein (SNE1) from *Phytophthora infestans* is a broadly acting suppressor of programmed cell death. *Plant J*: 62, 357-366.
89. Nomura K, et al (2006) A bacterial virulence protein suppresses host innate immunity to cause plant disease. *Science:* 313, 220–223.
90. Fu ZQ, et al (2007) A type III effector ADP-ribosylates RNA-binding proteins and quells plant immunity. *Nature:* 447, 284–288.
91. Jelenska J, et al (2007) A domain virulence effector of *Pseudomonas syringae* remodels host chloroplasts and suppresses defenses, *Curr Biol:* 17, 499–508.
92. Jelenska J, et al (2010) *Pseudomonas syringae* hijacks plant stress chaperone machinery for virulence. *Proc Natl Acad Sci USA:* 107, 13177–13182.
93. Lewis JD, et al (2008) The HopZ family of *Pseudomonas syringae* type III effectors require myristoylation for virulence and avirulence functions in *Arabidopsis thaliana*. *J Bacteriol:* 190, 2880–2891.
94. Zhou H, et al (2009) Allelic variants of the *Pseudomonas syringae* type III effector HopZ1 are differentially recognized by plant resistance systems, *Mol Plant Microbe Interact:* 22, 176–189.
95. Navarro L, et al (2008) Suppression of the microRNA pathway by bacterial effector proteins. *Science*: 321, 964-967.
96. Bolton MD, et al (2008) The novel *Cladosporium fulvum* lysine motif effector Ecp6 is a virulence factor with orthologs in other fungal species. *Mol Microbiol*: 69, 119–136.
97. van den Ackerveken GFJM, et al (1993) Characterization of two putative pathogenicity genes of the fungal tomato pathogen *Cladosporium fulvum*. *Mol Plant Micro Interact*: 6, 210–215.
98. Laugé R, et al (2000) Specific HR-associated recognition of secreted proteins from *Cladosporium fulvum* occurs in both host and non-host plants. *Plant J*: 6, 735-745.
99. Peter van Esse H, et al (2008) The *Cladosporium fulvum* virulence protein Avr2 inhibits host proteases required for basal defense. *The Plant Cell*: 20, 1948-1963.
100. Westerink N, et al (2004) *Cladosporium fulvum* circumvents the second functional resistance gene homologue at the *Cf-4* locus (*Hcr9-4E*) by secretion of a stable avr4E isoform. *Mol Microbiol:* 54, 533-545.
101. Joosten MHAJ, et al (1994) Host resistance to a fungal tomato pathogen lost by a single base-pair change in an avirulence gene. *Nature*: 367, 384-386.

102. Van den Ackerveken GFJM, et al (1992) Molecular analysis of the avirulence gene *avr9* of the fungal tomato pathogen *Cladosporium fulvum* fully supports the gene-for-gene hypothesis. *Plant J*: 2, 359-366
103. Song J, et al (2009) Apoplastic effectors secreted by two unrelated eukaryotic plant pathogens target the tomato defense protease Rcr3. *Proc Nat Acad Sci USA:* 106**,** 1654-1659.
104. Kaschani F, et al (2010) An effector-targeted protease contributes to defense against *Phytophthora infestans* and is under diversifying selection in natural hosts. *Plant Physiol*: 154, 1794-1804.
105. Cornelis GR (2006) The type III secretion injectisome. *Nature Reviews Microbiology:* 4, 811-825.
106. van Gijsegem F, et al (1995) The hrp gene locus of *Pseudomonas solanacearum*, which controls the production of a type III secretion system, encodes eight proteins related to components of the bacterial flagellar biogenesis complex. *Mol. Microbiol:* 15,1095–1114.
107. Fields KA, et al (1994) A low-Ca2+ response (LCR) secretion (ysc) locus lies within the lcrB region of the LCR plasmid in *Yersinia pestis*. *J. Bacteriol:* 176, 569–579.
108. Woestyn S, et al (1994) YscN, the putative energizer of the *Yersinia* Yop secretion machinery. *J. Bacteriol:* 176, 1561–1569.
109. Kubori T et al (1998) Supramolecular structure of the *Salmonella typhimurium* type III protein secretion system. *Science:* 280, 602–605.
110. Gophna U, et al (2003) Bacterial type III secretion systems are ancient and evolved by multiple horizontal-transfer events. *Gene:* 312, 151–163.
111. Miller LH, et al (1994) Malaria pathogenesis. *Science: 264*, 1878-1883.
112. Maier AG, et al (2009) Malaria parasite proteins that remodel the host erythrocyte. *Nature Rev Microbiol*: 7, 341–354.
113. Marti M, et al (2004) Targeting malaria virulence and remodeling proteins to the host erythrocyte. *Science*: 306, 1930–1933.
114. Hiller NL, et al (2004) A host-targeting signal in virulence proteins reveals a secretome in malarial infection. *Science*: 306, 1934–1937.
115. Boddey JA, et al (2009) Role of the Plasmodium export element in trafficking parasite proteins to the infected erythrocyte. *Traffic*: 10, 285–299.
116. Boddey JA, et al (2010) An aspartyl protease directs malaria effector proteins to the host cell. *Nature:* 463, 627-631.
117. Russo I, et al (2010) Plasmepsin V licenses Plasmodium proteins for export into the host erythrocyte. *Nature*: 463, 632-636.
118. Chang HH, et al (2008) N-terminal processing of proteins exported by malaria parasites. *Mol Biochem Parasitol*: 160, 107-115.
119. de Koning-Ward TF, et al (2009) A novel protein export machine in malaria parasites. *Nature*: 459, 945-949.
120. Whisson SC, et al (2007) A translocation signal for delivery of oomycete effector proteins into host plant cells. *Nature:* 450, 115-118.
121. Dou D, et al (2008) RXLR-Mediated Entry of *Phytophthora sojae* Effector *Avr1b* into Soybean Cells Does Not Require Pathogen-Encoded Machinery. *The Plant Cell* 20:1930-1947.

122. Kale SD, et al (2010) External lipid PI3P mediates entry of eukaryotic pathogen efectors into plant and animal host cells. *Cell:* 142, 284-295.
123. Rafiqi M, et al (2010) Internalization of flax rust avirulence proteins into flax and tobacco cels can occur in the absence of the pathogen. *The Plant Cell*: 22, 2017-2032.
124. Rouxel T, et al (2011) Effector diversification within compartments of the *Leptosphaeria maculans* genome affected by Repeat-Induced Point mutations. *Nat Comm*: doi:10.1038/ncomms1189.
125. Lou Y, et al (2006) The highly charged region of plant beta-type phosphatidylinositol 4-kinase is involved in membrane targeting and phospholipid binding. *Plant Molec Biol*: 60, 729-746.
126. Torto TA, et al (2003) EST Mining and Functional Expression Assays Identify Extracellular Effector Proteins From the Plant Pathogen *Phytophthora. Genome Res: 13, 1675-1685.*
127. Schornack S, et al (2010) Ancient class of translocated oomycete effectors targets the host nucleus. *Proc Nat Acad Sci: doi: 1008491107v1-201008491.*
128. Godrey D, et al (2010) Powdery mildew fungal effector candidates share N-terminal Y/F/WxC-motif. *BMC Genomics*: 11:317.

Chapter 2: Assaying effector function *in planta* using double-barreled particle bombardment

Shiv D. Kale and Brett M. Tyler

The following is a book chapter from:

Springer Plant Immunity: Methods and Protocols Vol. 712, 2011. McDowell, John M. (Ed.). Currently in press.

page 153-172, *Assaying effector function in planta using double-barreled particle bombardment,*

Shiv D. Kale and Brett M. Tyler, Figures 1-4, Table 1.

i. Summary/Abstract

The biolistic transient gene expression assay is a beneficial tool for studying gene function *in vivo*. However, biolistic transient assay systems have inherent pitfalls that often cause experimental inaccuracies such as poor transformation efficiency, which can be confused with biological phenomena. The double-barreled gene gun device is a cheap and highly effective attachment that enables statistically significant data to be obtained with one-tenth the number of experimental replicates compared to conventional biolistic assays. The principle behind the attachment is to perform two simultaneous bombardments with control and test DNA preparations onto the same leaf. The control bombardment measures the efficiency of the transformation while the ratio of the test bombardment to the control bombardment measures the activity of the gene of interest. With care, the ratio between the pair of bombardments can be highly reproducible from bombardment to bombardment. The double-barreled attachment has been used to study plant resistance *(R)* gene-mediated responses to effectors, induction and suppression of cell death by a wide variety of pathogen and host molecules, and the role of oömycete effector RXLR motifs in cell re-entry.

ii. Key Words

Transient expression; biolistic; double-barreled gene-gun; effectors; *R* gene; avirulence; soybean; tobacco; BAX; PAMP triggered immunity; effector triggered immunity; suppression of PCD.

1. Introduction

Biolistic transformation has been used extensively to create stable and transiently genetically modified plant, animal, fungal and bacterial cells **(1)**. This process has been used in a variety of applications, such as the creation of genetically modified crops **(2)**, the delivery of DNA vaccines into animals **(3)**, and the transformation of mitochondria and chloroplasts **(4,5)**. Biolistic transformation has also been used to study the transient expression of individual gene products *in vivo* **(6, 7)**. Biolistic transient gene expression has been particularly useful for the characterization of plant pathogen effector proteins **(6, 7, 8)**. This application uses cells that are biolistically transformed with a reporter gene and the gene(s) of interest using a particle delivery system such as a gene gun. The most commonly used reporter gene encodes beta-glucuronidase (GUS); when expressed in a living cell, GUS produces a blue precipitate (indigo blue) in the region of the transformed cells in the presence of X-Gluc and a oxidizing agent such as potassium ferri(III) cyanide that speeds up the reaction **(9)**. In the presence of genes that encode inducers of cell death, fewer viable cells expressing GUS are produced and so fewer blue tissue patches (spots) are observed in comparison to a control (a process called ablation). Taking this approach one step further, when a GUS reporter together with an inducer of cell death are used as the control, the ability to suppress the cell death of a protein encoded by a third added gene can be measured. In summary, biolistic delivery can be used for transient assays of effector avirulence activity (induction of *R* gene-dependent plant cell death) and virulence activity (suppression of *R* gene-dependent plant cell death). Additionally, biolistic delivery has also been used

to study the structure and function of host-targeting sequences in oömycete effector proteins **(7, 8).**

When using conventional bombardment assays, large sets of replicates are required to produce precise and accurate results due to the high variability between individual assays, especially in three-gene assays. This variability is attributable to fluctuations in transformation efficiency caused by inconsistent particle acceleration, as well as the natural variations in tissue physiology among samples (e.g. individual leaves). In the most commonly used form of the gene gun, a large helium burst produced by a rupture disk that breaks at an approximate pressure is used to induce particle acceleration **(10)**. The strength of this burst appears to be quite variable between bombardments. The double-barreled attachment was designed to circumvent the variability associated with the gene gun.

The concept behind the double-barreled attachment (Figure 1c) is to allow for the simultaneous bombardment of two different preparations of particle-bound DNA, thereby controlling for variations in transformation efficiency from bombardment to bombardment (Figure 1b). The first preparation is most commonly a control consisting of a reporter gene (GUS) that measures the number of transformed cells. The second preparation consists of the reporter gene and a gene of interest that is expected to alter the number of viable transformed cells, for example an avirulence gene that encodes an inducer of cell death. The simultaneous bombardment of the two preparations avoids the variability associated with particle acceleration, since both particle preparations are bombarded at the same time. The ratio between the variable bombardment and the control is highly reproducible from assay to assay. Therefore, a treatment bombardment

that produces more or fewer blue spots than a control bombardment is more likely to result from a biological phenomenon than from variation in transformation efficiency. The greatly increased consistency allows statistically significant results to be obtained in less than one-tenth the number of assays performed using conventional biolistic transformation. Therefore, it becomes feasible to measure much smaller variations in cell killing, such as variations resulting from mutations in a death-inducing or death-suppressing gene.

The double-barreled gene gun attachment we have developed fits into the existing Bio-Rad PDS-1000/He (Figure 1a) (*see* **Note 1**). The attachment replaces the internal spacer rings nested inside of the support manifold. The single-wide opening that particles travel through in the PDS-1000/He is replaced by two barrels that channel the control and variable preparations of particles into targeted regions of the sample (usually a leaf) (*see* **Note 2**). To date, the double-barreled gene gun attachment has been used for a variety of published studies on plant *R* gene-mediated responses to effectors, induction and suppression of cell death by a variety of pathogen and host molecules, and functional studies of the RXLR-dEER motif from oömycete effectors **(7, 8)**. However, this attachment can in principle be used to minimize variability in any gene function assay that utilizes biolistic delivery.

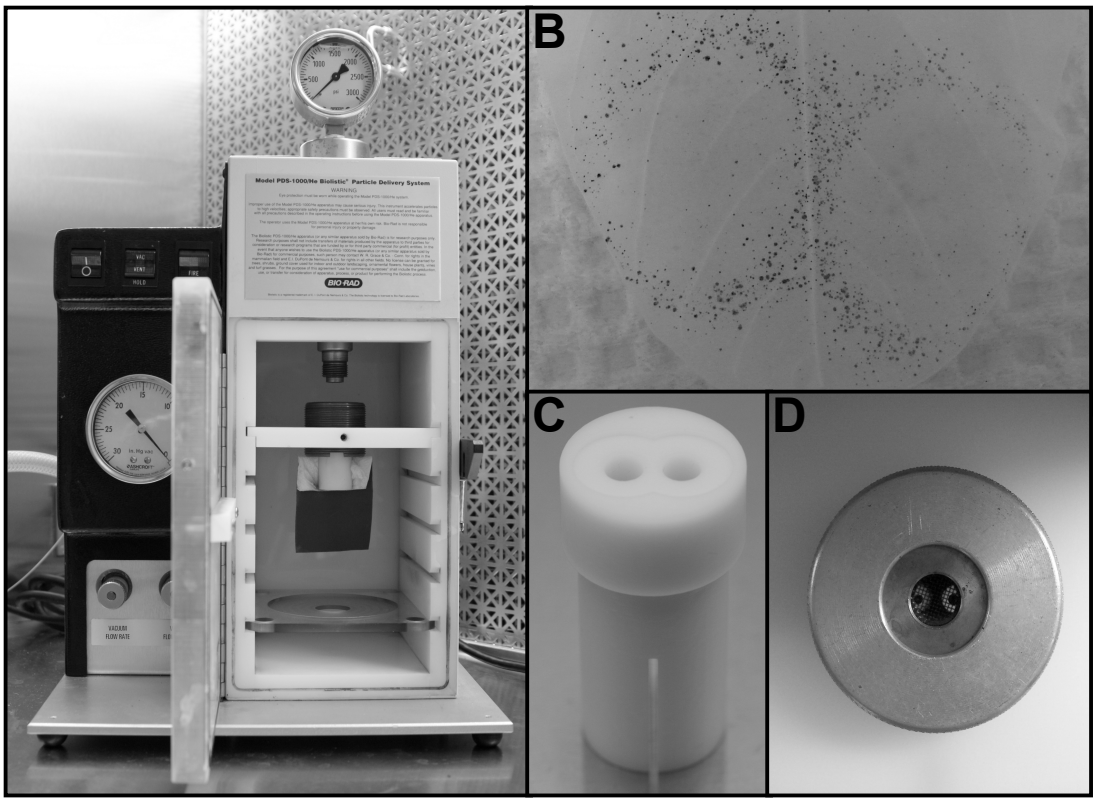

Figure 1 Double-Barreled Gene Gun Attachment
A) Double-barreled gene gun attachment setup inside of PDS-1000/He. B) Leaf after co-bombardment with two control preparations, incubation, staining, and destaining. C) Double-barreled gene gun attachment (Not shown is the dividing screen to separate overlap between bombardments). D) Alignment of macrocarrier with preparations in the PDS-1000/He with double-barreled gene gun attachment.

2. Materials

2.1 Hardware and Disposables

1. PDS-1000/He (Bio-Rad Inc., Hercules, CA).
2. Double-barreled attachment (Figure 1c).
3. Dissecting microscope with minimum 10X magnification.
4. Hand held counter.

5. Soil (Miracle Grow Potting Mix).
6. Trays (Griffin Greenhouse).
7. Pots (Griffen Greenhouse).
8. Soybean seeds.
9. Qiagen maxi prep kit (Qiagen Inc., Valencia, CA).
10. M-10 tungsten microcarriers (Bio-Rad Inc., Hercules, CA).
11. Macrocarrier (Inbio Gold Inc., Victoria, Australia).
12. Macrocarrier holder (Bio-Rad Inc., Hercules, CA).
13. Rupture disks 650 PSI (Soybean and Tobacco) (Inbio Gold Inc., Victoria, Australia).
14. Stopping screens (Inbio Gold Inc., Victoria, Australia).
15. Petri-dishes.
16. Whatman filter paper 70 mm (Fisher Scientific, Pittsburgh, PA).
17. Nescofilm (parafilm).
18. 100% methanol.

2.2 Solutions

1. Spermidine: 25 µL aliquots (Sigma-Aldrich Inc., St. Louis, MO) in 0.6 mL eppendorf tubes. Make 30 aliquots and store at 4°C in a container with drierite (W.A. Hammond Drierite Co. LTD, Xenia, OH).

2. 2.5 M sodium chloride (NaCl)*: Dissolve 7.305 g of NaCl in 30 mL of sterile deionized water (dH_20) and increase the final volume to 50 mL.

3. LB Plates: 5 g tryptone, 5 g sodium chloride, 2.5 g yeast extract, 7.5 g agar, raise the volume to 500 mL with water. Autoclave the media for 40 minutes on a liquid cycle. Cool

the media until it can be held then pour approximately 25 mL into sterile Petri dishes in a sterile hood. Allow plates to solidify and store at 4°C until use.

4. 0.2 M potassium phosphate monobasic* (KH_2PO_4): Dissolve 12 g anhydrous KH_2PO_4 (Sigma-Aldrich, St. Louis, MO) in 400 mL of sterile dH_20. Raise the volume to 500 mL. Filter Sterilize*.

5. 0.2 M potassium phosphate dibasic (K_2HPO_4)*: Dissolve 14.2 g anhydrous K_2HPO_4 (Sigma-Aldrich, St. Louis, MO) in 400 mL of sterile dH_20. Raise the volume to 500 mL.

6. 0.1 M potassium ferricyanide(III)** ($K_3[Fe(CN)_6]$): Dissolve 1.65 g ($K_3[Fe(CN)_6]$ (Sigma-Aldrich, St. Louis, MO) in 50 mL sterile dH_20. Highly light sensitive.

7. 0.1 M potassium hexacyanoferrate(II) trihydrate** ($K_4[Fe(CN)_6]3H_20$): Dissolve 2.11 g of $K_4[Fe(CN)_6]3H_20$ (Sigma-Aldrich, St. Louis, MO) in 50 mL sterile dH_20. Highly light sensitive.

8. 0.5 M sodium ethylenediaminetetraacetic acid (Na_2EDTA)*: Dissolve 18.612 g of Na_2EDTA (Fischer Scientific, Pittsburgh, PA) in 50 mL of sterile dH_20. Raise the volume to 100mL.

9. Staining Solution (500 mL): Prepare 200 mL of 0.2 M potassium phosphate buffer pH 7.0* in a sterile bottle with 124 mL 0.2 M K_2HPO_4* and 76 mL 0.2M KH_2PO_4*. Add 177 mL sterile dH_20 to the 200 mL stain solution. Add 2 mL of 0.1 M $K_3[Fe(CN)_6]$** and 2 mL of 0.1 M $K_4[Fe(CN)_6]3H_20$** to the 377 mL stain solution. Wrap the stain solution bottle in aluminum foil as it is light sensitive. Add 8 mL 0.5 M Na_2EDTA to the 381 mL stain solution. Mix the solution thoroughly. Dissolve 400 mg of X-Gluc (5-bromo-4-chloro-3-indolyl-beta-D-glucuronic acid; Gold BioTechnology, St. Louis, MO) in 8 mL of DMSO, mix, and immediately add to the 389 mL stain solution. Mix the stain solution well. X-

Gluc is highly light sensitive. Add 100 mL of 100% Methanol to the 397 mL stain solution and mix. Add 3 mL of 10% Triton X-100 (Sigma-Aldrich, St. Louis, MO) to the 497 mL stain solution and mix thoroughly. Store the solution at 4°C. It is stable for up to 1 year when stored in the dark.

*filter sterilized (0.22 μm)

**Contact with acids liberates very toxic cyanide gas. Read Material Safety Data Sheet (MSDS) before handling chemical.

3. Methods

3.1 Experimental Design

This section describes assays for induction of cell death and suppression of cell death. The assay for induction of cell death consists of 16 co-bombardments per experimental replicate. A co-bombardment is comprised of two simultaneous bombardments using the double-barreled gene gun attachment. If the inducer of cell death being used is independent of plant genotype (for example DNA encoding the mouse BAX that induced cell death equally well on all tested soybean lines), then 16 co-bombardments (16 pairs) are recommended to achieve a high level of statistical reliability (*see* **Note 3**). If the leaf is of sufficient size, then two co-bombardments may be fired onto the same leaf, with the BAX containing preparation being fired through one barrel and the control preparation being fired through the other barrel. The leaf is then rotated so that the preparations are bombarded on the alternate side of the leaf for the second bombardment (Figure 2a). This is done for the first 4 co-bombardments. For the next four co-bombardments, the BAX preparation and control preparation should be

fired through the other barrel (Figure 2a). The preparations are reversed so that not all control preparations are fired on only one side of the leaf throughout the experiments. By switching the preparations the control and variable bombardments are delivered to all sides the target area an even number of times throughout the experiment. These 8 co-bombardments should then be repeated to give a total of 16 co-bombardments. These 16 co-bombardments are equivalent to one experimental replicate. Ablation due to the plant cell death response can then be calculated as 1 - (treatment spot number) / (control spot number).

If the inducer of cell death being used is dependent on plant genotype, for example the *Phytophthora sojae Avr1b* protein that is dependent of the presence of the soybean *R* gene *Rps1b* to trigger cell death, then leaves from plants lacking the *Rps1b* gene may be used as an additional control. Following the *Rps1b* example, 8 co-bombardments would be performed on the leaves expressing *Rps1b*, and 8 co-bombardments would be performed on leaves lacking *Rps1b*, arranged as follows: 4 co-bombardments on *Rps1b* leaves followed by 4 co-bombardments on *Rps* leaves with treatment (*Avr1b*) and control fired through the two barrels. The treatment and control barrels are then switched and the 8 co-bombardments are repeated (Figure 2b). Ablation due to the plant cell death response can then be calculated as 1- [(treatment spot number in presence of gene) / (control spot number in presence of gene)] / [(treatment spot number in absence of gene) / (control spot number in absence of gene)].

For assays to test whether an effector can suppress cell death (e.g. triggered by BAX), we recommend carrying out both a direct and an indirect assay (*see* **Note 3**). In

the direct assay, one barrel contains a suppressor preparation (GUS + cell death trigger + suppressor) and the other barrel contains the cell death preparation (GUS + cell death trigger + empty vector control). In the indirect assay, two assay results are compared to determine the relative ablation: a suppressor preparation (GUS + cell death trigger + suppressor) versus a control preparation (GUS + control) are compared to the cell death preparation (GUS + cell death trigger + control) versus the control preparation (GUS + control). 16 co-bombardments are required for the two parts of the indirect assay, while 8 co-bombardments are required for the direct measurement (Figure 2c). Preparations are fired through alternate barrels every 8 co-bombardments in the indirect assay and every four bombardments in the direct assay. Leaves are rotated as described for the in the inducer of cell death assay between the 2 co-bombardments for each leaf.

The procedure described below is optimized for assays to test the function of effectors from *P. sojae* on leaves of soybean (*Glycine max*).

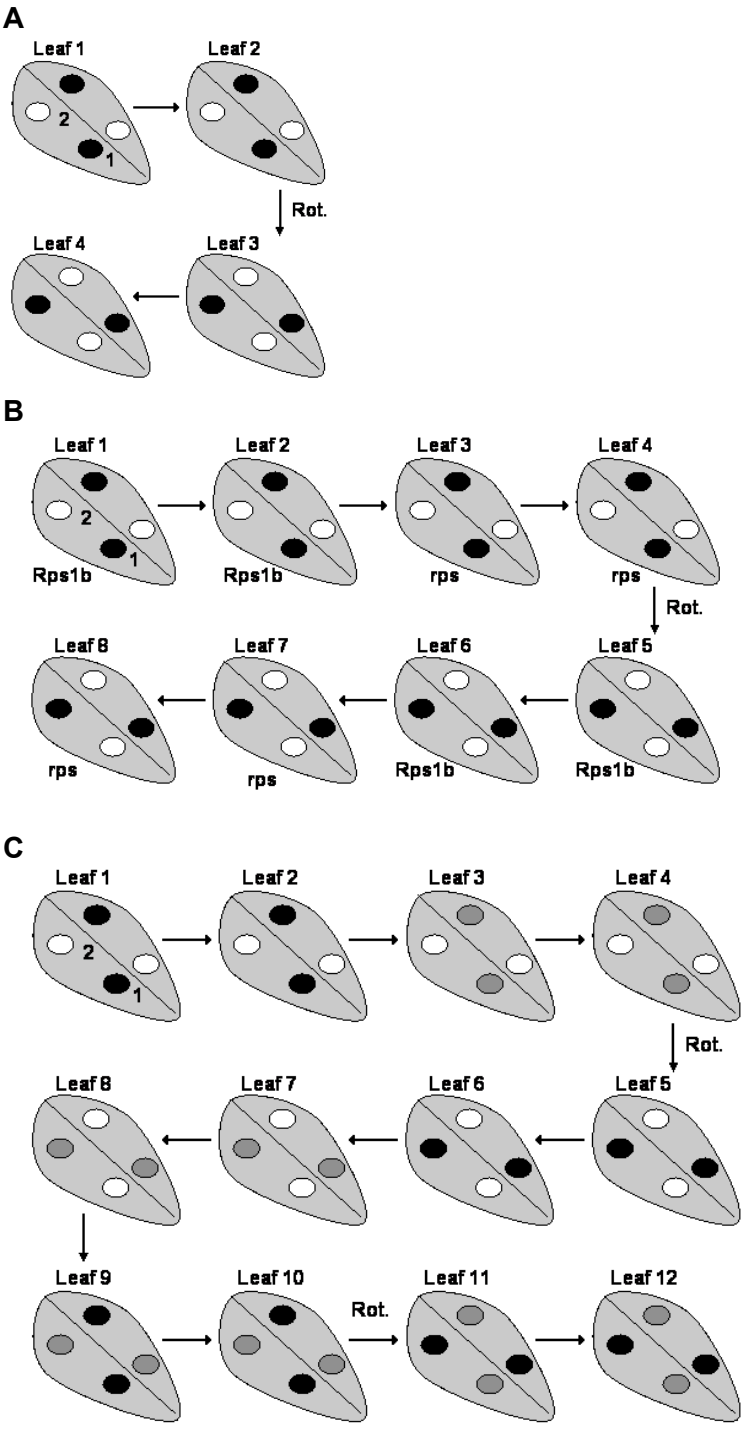

Figure 2 Order of Co-Bombardments for Various Type of Experiments

A) Inducer of cell death independent of plant genotype. B) Induction of cell death based on plant genotype, using the *Avr1b-Rps1b* interaction as an example. C) Suppression of cell death. White circles are bombardments of the control preparation; black circles are bombardment of preparations containing an inducer of cell death. Gray circles are bombardments of preparations containing the inducer of cell death and the suppressor of cell death. 1 signifies that first co-bombardment. 2 signifies the second co-bombardment. The two co-bombardments on a leaf are switched by rotating the leaf. Rot. signifies rotating/ switching the preparations so that they are fired through the other barrel.

3.2 Plasmid Design

1. Plasmids are designed for transient expression under the control of the cauliflower mosaic virus 35s promoter and terminator. pUC19 serves as the vector backbone so that the bombardment plasmid will be small in size and therefore easier to prepare.
2. Genes can be cloned into the bombardment vector using these template primer designs. Forward primer 5'AGATCCCGGGGGAGCAATGAGAT**ATG**…. 3'. The reverse primer consists of 5'….**TGA**GGTACCcatgc 3' **(7)**. Underlined sequences represent restriction sites used for cloning. Bold sequences represent actual gene sequence.
3. The PCR product and bombardment vector should be digested with XmaI and KpnI and then ligated **(7)**.

3.4 Soybean Growth

1. Approximately two weeks before the assay is to be performed, plant 10 pots of soybeans in the greenhouse, with 5 plants per pot. Set the day length for 14 hours at 28°C and the night length for 10 hours at 25°C. Water as required.
2. Select the first (monofoliate) true leaves for bombardment 14 to 18 days after planting. If the monofoliate leaves are too old or too young the transformation efficiency will drop drastically. Leaves must be in very good health for bombardment.

3.5 DNA Purification

1. Prepare two 4-Liter flasks with 500 mL of LB and autoclave for 60 minutes.
2. Add sterile ampicillin to reach a final concentration of 100 µg/mL.
3. Inoculate flasks from a freshly streaked plate of *E.coli* containing the plasmid and gene of interest.
4. Grow culture in a shaker at 240 RPM at 37°C for approximately 14 hours.

5. Harvest cells at 6,000 g for 15 minutes.
6. Perform purification using Qiagen Maxi Prep kits. 500 mL of culture pelleted culture should receive 10 mL of P1, 10 mL of P2, 10 mL P3, and should follow the maxi prep protocol. Columns can be used twice. Columns must be washed twice with QBT between each purification if they are being reused (*see* **Note 4**).
7. Dried DNA should be resuspended in water and set to a final concentration between 3-5 μg/μL. Concentration can be determined using a spectrophotometer; we use a nanodrop-1000. Measurement should be taken of a 1 to 20 dilution since high concentrations fall outside the linear conversion range.
8. DNA should be portioned into aliquots of roughly 25 μL and stored at -20°C.

3.6 Setup and Calibration of PDS-1000/He

1. Replace spacer rings and stop-screen support inside of the fixed nest with the double-barreled attachment.
2. Attach the rupture disk retaining cap. Attach the macrocarrier holder and the macrocarrier cover lid to the macrocarrier launch assembly. Set the spacing between the rupture retaining cap and the macrocarrier launch assembly using the ¼ inch gap adjustment tool so that the adjustment tool just fits between the two.
3. Place the target shelf on the lowest setting in the PDS-1000/He.
4. The chamber vacuum must be able to reach 23 PSI.
5. Set the pressure on the He-tank gauge to exceed no more than 200PSI of the rupture disk pressure. Rupture disk = 650 PSI, tank pressure = 825-850 PSI.
6. Adjust the helium metering valve so that upon firing the rupture disk takes 15 seconds to fire.

3.7 Double-Barreled Attachment

1. Remove internal spacer rings and stop-screen support ring nested inside the fixed nest with retaining spring (*see* **Note 5**).
2. Place the double-barreled attachment into the fixed nest with retaining spring.
3. Lock the double-barreled attachment and nest with retaining spring into the adjustable brass nest. Place the adjustable brass shelf on the top shelf inside the PDS-1000/He.

3.8 Tungsten

1. Add 90 mg of tungsten to 1 mL 95% EtOH in a 1.5 mL eppendorff tube and vortex for 1 minute, followed by centrifugation at 13,000 g for 10 minutes. Remove all of the ethanol by gently pipetting. Repeat once (*see* **Note 6**).
2. Add 1 mL of sterile dH_20 to the dried tungsten and vortex for 1 minute followed by centrifugation at 13,000 g for 15 minutes. Remove all of the dH_20 by gently pipetting Repeat once (*see* **Note 7**).
3. Add 1 mL of sterile 50% glycerol to the dried tungsten and store at -20°C. Can be stored indefinitely. Making 20-50 tubes of tungsten is recommended.

3.9 Bombardment Mixture

1. Thoroughly vortex stored tungsten (2 minutes) and transfer 100 µL into two 0.6 mL eppendorf tubes (Control and Test). Minimizing surface area in smaller tubes helps reduce degradation and keeps mixture homogenous (*see* **Note 8**).
2. Centrifuge tubes for 1 minute at 13,000 g and remove 50 µL of supernatant.
3. 25 µL of volume is reserved for DNA. This step is discussed in depth below in the sections titled “DNA mixture for induction of cell death” and “DNA mixture for

suppression of cell death." Once DNA is added, vortex thoroughly for 1 minute and keep tubes on ice from here until the end of the actual bombardments (*see* **Note 9**).

4. Add 65µL of 2.5M NaCl, vortex thoroughly for 1 minute, and place back on ice.
5. Add 4µL of aliquot spermidine to 246 µL sterile dH_20 to make 0.1M spermidine and vortex thoroughly.
6. Add 25 µL 0.1 M spermidine to the bombardment mixture. Vortex thoroughly for 2 minutes and put on ice for a minimum of 30 minutes. Discard 0.1 M spermidine after 1 day if not used again.
7. Particle mixture can be stored at -20°C for up to 8 hours.
8. Centrifuge mixture for 1 minute at 13,000 g and remove 135 µL of the supernatant. Be very careful to not disturb the tungsten-DNA pellet.
9. Thoroughly vortex mixture for 2-3 minutes and store on ice. The mixture will begin to clump after 3 hours. Bombardments must be carried out immediately and will usually take 2.5 hours for a novice user and 1.5 hours for an experienced user.

3.10 DNA mixture for Induction of Cell Death

Two preparations are created, each with a final volume of 25 µL. Each preparation provides 16 bombardments. The first is a control preparation consisting of 50 µg of DNA encoding GUS, and 50 µg of DNA encoding an inducer of cell death. The second is an induction of cell death preparation consisting of 50 µg of DNA encoding GUS and 50 µg of DNA encoding an inducer of cell death. If the inducer of cell death is very strong, the amount of inducer of cell death and control pUC19 should be lowered so that an equal amount and ratio of plasmids are present in each preparation.

Example

Control preparation: 8 µL GUS (50 µg) + 10 µL pUC19 (30 µg) + 7 µL water = 25 µL total.

Test preparation 8 µL GUS (50 µg) + 9 µL pUCBomb-*Avr1b* (30 µg) + 8 µL water = 25 µL total.

3.11 DNA mixture for Suppression of Cell Death

Three preparations are created, each with a total volume of 25 µL. Each preparation provides 16 bombardments. The first is an induction of cell death preparation consisting of 50 µg of DNA encoding GUS, 25 µg of DNA encoding an inducer of cell death (BAX) and 50 µg of control DNA (pUC19). The second is a cell death suppressor preparation consisting of 50 µg DNA encoding GUS, 25 µg DNA encoding an inducer of cell death (BAX), and 50 µg of DNA encoding a suppressor of cell death (*Avr1b*). The control preparation consists of 50 µg of DNA encoding GUS, and 75 µg of control DNA (pUC19).

Example

Control preparation: 8 µL GUS (50 µg) + 15 µL pUC19 (75 µg) + 2 µL water = 25 µL total.

Cell death preparation 8 µL GUS (50 µg) + 7 µL BAX (25 µg) + 10 µL pUC19 (50 µg) = 25 µL total.

Suppression preparation: 8 µL GUS (50 µg) + 7 µL BAX (25 µg) + 7 µL pUC*Avr1b* (50 µg) + 2 µL water = 25 µL total.

3.12 Bombardment

1. Place 650 PSI rupture disk inside the rupture disk retaining cap and tighten fully.

2. Load 1 µL of each preparation (control and gene of interest) onto a macrocarrier placed inside a macrocarrier holder. Vortex preparations thoroughly for (15-30 seconds) and pipette 1 µL onto the macrocarrier. The preparations are put immediately back on ice.
3. The macrocarrier holder is placed on top of the fixed nest with the retaining spring and the 1 µL preparations are aligned with each barrel so that they are directly in the center of each barrel opening.
4. Add the macrocarrier lid cover and tighten completely. Visually make sure that the 1 µL preparations are still aligned completely. If a shift has occurred re-align the preparations (Figure 1D).
5. Place the microcarrier launch assembly into the PDS-1000/He.
6. Remove a leaf from the plant and place it flat on a media Petri-dish. Cover the petiole portion of the leaf. The distal portion of the leaf should be shot first then the petiole portion immediately after.
7. Place the Petri-dish onto the target shelf and align the sample with the barrels. The major vein of the leaf should be directly under the spacer of the double-barreled attachment and there should be adequate exposed tissue (*see* **Note 10**).
8. Close the door to the vacuum chamber and begin vacuum. Wait until vacuum reaches 23 PSI and then set the Vac/Vent/Hold switch to Hold.
9. Hold the fire button until rupture disk ruptures and then quickly release.
10. Set the Vac/Vent/Hold switch to Vent and wait until chamber depressurizes.

11. Change the rupture disk and dispose of the macrocarrier and stopping screen. Clean the barrels with a paper towel soaked in 70% ethanol. Dry double-barreled attachment using compressed air.
12. Repeat above bombardment protocol on the petiole portion of the leaf. With each of the two preparations bombarding the other side of the leaf. Do this by rotating the leaf to produce the opposite alignment of samples.
13. Once the leaf has been co-bombarded twice, place the leaf in a Petri-dish containing Whatman filter paper soaked in water so that the stem is in contact with the filter paper. There should be 0.5-1 mL of free water in the Petri-dish. Wrap in parafilm.
14. A bombardment experiment usually entails 16 or 24 bombardments (as described in experimental design). All bombardments for an experiment must be carried out successively as soon as possible (*see* **Note 11**).

3.13 Incubation, Staining, Destaining, and Counting

1. Store Petri dishes at 25°C (*see* **Note 12**) for approximately 72 hours.
2. Completely drain water from each Petri-dish.
3. Add 1 mL of stain solution to each leaf and blot using a kim-wipe until the leaf is completely covered in stain solution. Add more stain if required to cover the entire leaf.
4. Re-wrap Petri dishes in nescofilm and incubate at 25°C for 24 hours.
5. Soak leaves in methanol and shake at 85 RPM on an orbital shaker until they fully destain. Methanol should be replaced if leaves are not fully destained. Petri dishes must be wrapped in parafilm during the detaining.

6. Perform counting using a dissecting scope and a hand held counter. If the co-bombardment fails due to misalignment then the bombardment is not counted. An example would be having a bombardment from one barrel miss the leaf or a portion of the leaf. If the target region is not completely occupied by leaf tissue then the co-bombardment is considered a failure (Table 1).
7. Input results of the counting into a spreadsheet (Table 1). Every two rows in the spreadsheet correspond to a leaf. The area of the co-bombardment falls under either distal or petiole. The spreadsheet rows are ordered in the same order the leaves were bombarded.

A	B	C	D	E	F	G
Leaf	Plasmid for Petiole Area	GUS+ Petiole Area	R for Petiole	Plasmid for Distal Area	GUS+ Distal Area	R for Distal
1	BAX(25µg)+Gus	25	-0.852	Control+Gus	182	-1.660
	Control+Gus	184		BAX(25µg)+Gus	3	
2	BAX(25µg)+Gus	18	-1.105	Control+Gus	399	-0.312
	Control+Gus	241		BAX(25µg)+Gus	194	
3	Control+Gus	262	-1.517	BAX(25µg)+Gus	16	-1.003
	BAX(25µg)+Gus	7		Control+Gus	170	
4	Control+Gus	304	-0.861	BAX(25µg)+Gus		
	BAX(25µg)+Gus	41		Control+Gus		
5	BAX(25µg)+Avh331(50µg)+Gus	156	-0.166	Control+Gus	96	-0.187
	Control+Gus	229		BAX(25µg)+Avh331(50µg)+Gus	62	
6	BAX(25µg)+Avh331(50µg)+Gus	138	-0.177	Control+Gus	194	-0.135
	Control+Gus	208		BAX(25µg)+Avh331(50µg)+Gus	142	
7	Control+Gus	194	-0.193	BAX(25µg)+Avh331(50µg)+Gus	111	-0.163
	BAX(25µg)+Avh331(50µg)+Gus	124		Control+Gus	162	
8	Control+Gus	272	-0.243	BAX(25µg)+Avh331(50µg)+Gus	37	-0.547
	BAX(25µg)+Avh331(50µg)+Gus	155		Control+Gus	133	
9	BAX(25µg)+Avh331(50µg)+Gus	12	0.637	BAX(25µg)+Gus	3	0.916
	BAX(25µg)+Gus	2		BAX(25µg)+Avh331(50µg)+Gus	32	
10	BAX(25µg)+Avh331(50µg)+Gus	146	0.576	BAX(25µg)+Gus	14	0.815
	BAX(25µg)+Gus	38		BAX(25µg)+Avh331(50µg)+Gus	97	
11	BAX(25µg)+Gus	21	0.788	BAX(25µg)+Avh331(50µg)+Gus	72	1.085
	BAX(25µg)+Avh331(50µg)+Gus	134		BAX(25µg)+Gus	5	
12	BAX(25µg)+Gus	69	-0.067	BAX(25µg)+Avh331(50µg)+Gus		
	BAX(25µg)Avh331(50µg)+Gus	59		BAX(25µg)+Gus		

Table 1 Data Analysis Table for Suppression of BAX by *Avh331*
A) Table is sorted by order of co-bombarded leaf. B) DNA for co-bombardment shot in the petiole portion of the leaf. C) Number of GUS+ spots for each co-bombardment in the petiole portion. D) Calculated *R* value for co-bombardments shot on the petiole portion of the leaf. E) DNA for co-bombardment shot in the distal portion of the leaf. F) Number of GUS+ spots for each co-bombardment in the distal portion. G) Calculated *R* value for co-bombardments shot on the distal portion of the leaf. Blacked out cells indicate failed co-bombardments.

3.14 Statistical Analysis

Statistical analysis is performed by using two different statistical tests designed for nonparametric data sets **(11)**. The Wilcoxon signed ranks test is employed for measuring the statistical significance for a direct assay of an inducer or suppressor of cell death. The direct assay directly compares cell killing by two preparations

bombarded side-by-side in the gene gun. Indirect measurements of suppression of cell death or *Avr-R* gene interaction can be assessed for significance using the Wilcoxon rank sum test. The indirect assay directly compares cell killing by two preparations bombarded in two separate experiments that include a common control preparation as reference (Table 1).

In both cases, the log ratio of the number of blue cells is calculated for each pair of bombardments log $[(1+b_1) / (1+b_2)]$, where b_1 and b_2 are the number of blue cells produced by each member of the paired sample. Each blue cell number is incremented by 1 to avoid zeros and to slightly decrease the influence of very small denominators; this adjustment makes the statistical tests slightly more conservative.

The Wilcoxon rank sum test is a non-parametric test used to determine the statistical difference between two small samples that need not have a normal distribution **(11)**. Figure 4a illustrates the procedure of the test using Excel. The two sample groups (BAX (column 4a-1) and *Avh331*+BAX (4a-2) are considered together (4a-3) and ranked from 1 (smallest value) to 16 (largest value) (4a-4). Ties are resolved by averaging the ranks of the tied samples. The sum of the ranks for the two sample groups (4a-5, 4a-6, 4a-7, 4a-8) is calculated separately. In this example, the sum for BAX is 27 and for BAX + *Avh331* is 91. These values are used in the following equations to calculate W_a and W_b: $W_a = (n_1*n_2)+((n_2*(n_2+1))/2) - R_1$ and $W_b = n_1*n_2 - W_a$, where n_1 is equal to the number of values in the larger sample, n_2 is equal to the number of values in the smaller sample, and R_1 is equal to the sum of the ranks from the smaller sample (e.g., $W_a = (8*7)+[7*(7+1)] / 2 -27 =55$. $W_b = (7*8)- 55 = 1$). The larger W value becomes the Wilcoxon's two-sample statistic to determine the statistical

significance for sample size n_1 and n_2 using a statistical table **(12, table CC)**. In this case the P value corresponds to <0.001 and the null hypothesis that there is no difference between the two sample groups is rejected.

a Wilcoxon Rank Sum Test							
4a-1	**4a-2**	**4a-3**	**4a-4**	**4a-5**	**4a-6**	**4a-7**	**4a-8**
BAX	**Avh331+BAX**	**Sort**	**Rank**	**BAX Sort**	**Rank**	**Avh331+BAX Sort**	**Rank**
-0.852	-0.166	-1.66	1	-1.66	1	-0.547	7
-1.105	-0.177	-1.517	2	-1.517	2	-0.243	9
-1.517	-0.193	-1.105	3	-1.105	3	-0.193	10
-0.861	-0.243	-1.003	4	-1.003	4	-0.187	11
-1.66	-0.187	-0.861	5	-0.861	5	-0.177	12
-0.312	-0.135	-0.852	6	-0.852	6	-0.166	13
-1.003	-0.163	-0.547	7	-0.312	8	-0.163	14
-1.04429	-0.547	-0.312	8	**N=7**	**29**	-0.135	15
9.030552	**-0.22638**	-0.243	9			**N=8**	**91**
	59.37792	-0.193	10				
		-0.187	11				
		-0.177	12	**Wilcoxon**	**55**	**Wilcoxon(2)**	**0**
		-0.166	13				
		-0.163	14	**Alpha 0.001**	**54**		
		-0.135	15				

b Wilcoxon signed ranks test				
4b-1	**4b-2**		**4b-3**	
Ratio	**Rank**			
-0.067	-1		**N**	**7**
0.637	+2		**Sum of Negative**	**1**
0.737	+3		**Sum of Positive**	**27**
0.788	+4		**T(s)**	**1**
0.815	+5		**T(s) = 1**	**Alpha 0.0156**
0.916	+6		**Log Ratio Avh331+BAX/BAX**	**0.794**
1.085	+7		**Ratio Avh331+BAX/BAX**	**6.216**

Figure 4 Statistical Analysis of *Avh331* suppression of BAX Triggered Cell Death. A) Wilcoxon Rank Sum Test. Non-parametric test used to measure difference between two small samples. 5a-1) Co-bombardment *R* values for induction of cell death by BAX in comparison to a control. 5a-2) Co-bombardments *R* values for suppression of BAX triggered cell death by *Avh331* in comparison to a control. 5a-3) *R* values for 5a-1 and 4a-2 combined and sorted smallest to largest. 5a-4) Rank assigned to sorted values. 5a-5, 6) Sorted *R* values for BAX bombardment and respective rank. 5a-7, 8) Sorted *R* values for BAX+*Avh331* bombardment and respective rank. B) Wilcoxon Signed Rank

Test. Statistical test for significance in small nonparametric samples. 5b-1) Sorted co-bombardment *R* values of suppression of BAX triggered cell death by *Avh331* in comparison to BAX triggered cell death. 5b-2) Signed ranks for co-bombardments. 5b-3) Calculations for statistical analysis.

The Wilcoxon signed ranks test is designed to test for significance in small nonparametric samples **(11)**. It is usually used to compare the differences between paired samples and determines if the magnitudes of the differences greater than zero are significantly different than the magnitudes of the differences less than zero. In this case, the log ratio is considered to be the relevant difference [i.e. $\log(1+b_1) - \log(1+b_2)$]. Figure 4 shows the procedure of the test using Excel. All of the ratios from the 8 co-bombardments (8 pairs) are listed in a column. These ratios are the log[(inducer of cell death +1) / (control +1)] from each co-bombardment. These ratios are then ordered from smallest to largest regardless of their sign (positive or negative) and then ranked from 1 (smallest) to 8 (largest, for example if you have 16 co-bombardments the rank for the largest number is now 16). Ties are resolved by averaging the ranks of the tied samples. If a ratio is negative the rank gets assigned to a negative value. Figure 4b shows that there are no negative log-ratios and therefore the sum of the negative ranks is 0, while the sum of the positive ratio ranks is 28. The sums of the positive and negative ranks are added, such that the contribution of the negative ranks decreases the sum. In this case the negative sum was 0 and the positive value was 28. The smaller sum is assigned to T. The number of samples is assigned to n. In this example we had 8 values so n=8. The values are then looked up in a Wilcoxon signed ranks table **(12, table DD)**. At n=8 with a T=0, the alpha value is 0.0156. In this example, we

can thus reject the null hypothesis that there is no difference between the bombardments from either barrel with a significance value (p value) of 0.0156.

The cut off for significance is usually considered to be a p value of less than 0.05. Note that a p value of 0.05 means there is a 5% chance that a result will be called significant when there really is no difference between the samples. Thus if 20 experiments are carried out with identical DNA preparations, one experiment may be expected to give a p value less than 0.05, just by chance. Therefore a lower p value (e.g. 0.01) is recommended when large numbers of experiments are carried out. For a rigorous treatment of this multiple testing issue, and procedures for accounting for it, see **(13, 14)**. In our hands, the recommended numbers of replicates produce p values less than 0.001, thus multiple testing is rarely an issue.

4. Notes

Note 1

The first embodiment of the double barreled gene gun attachment consisted of two metal pipes that were fused to a custom made metal ring that fit inside the PDS-1000/He. The current double barreled gene gun attachment is produced using a mold tool (Figure 1C). Plans for large scale commercial manufacturing are in progress. Please contact Dr. Brett Tyler (bmtyler@vt.edu) about acquiring the technology.

Note 2

The leaf width perpendicular to the mid vein at the center of the leaf should measure a minimum 4.5 cm and should range between 4.5-6 cm. The length of the leaf should be

measured using the mid vein. The length should be a minimum of 6.5 cm and should range between 6.5-8.5 cm.

Note 3

The amount of DNA encoding an inducer of cell death should be varied to determine the ideal amount that produces an adequate level of cell death (50-90% reduction in blue spots; an example is shown in Figure 3). Likewise the amount of suppressor of cell death should also be determined. We find using double the amount of suppressor works well for the suppression of mouse BAX by Avr1b and Avh331.

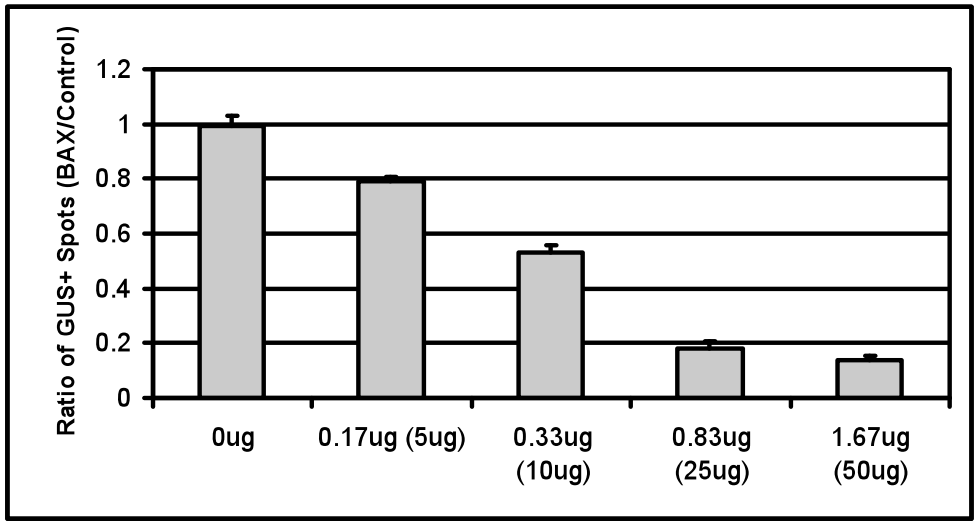

Figure 3 Ablation of GUS Activity Due to Cell Death Caused by Varying Concentrations of BAX
Soybean leaves were bombarded using a double-barreled gene gun attachment that delivered varying concentrations of mouse BAX DNA and GUS DNA preparation to one side of the leaf and a control preparation of empty vector and GUS DNA to the other side. The ratio of blue spots in comparison to the BAX preparation and the control preparation was calculated for varying concentrations of mouse BAX. # µg signifies the amount of BAX DNA bombarded from a barrel during a co-bombardment. (# µg) indicate overall amount of BAX DNA used to make the preparation.

Note 4

The terms used to describe the various components of the PDS-1000/He are the exact names used in the user's manual. Pictures of components are included in the manual to avoid confusion. This manual is available online through Bio-rad.

Note 5

Occasionally a column will clog due to high viscosity of the solution after centrifugation. We do not recommend running these samples through the column since the purification time will increase significantly and the quality of the purification will diminish greatly. If the pellet achieved from harvesting is larger than normal adjust the amount of P1, P2, and P3. Do not decrease the amount of the buffer solutions, only increase them.

Note 6

The tungsten pellet requires extra centrifugation to pellet on occasion. Repeat the centrifugation step to further pellet the tungsten. The pellet is not as densely packed as it is in other aqueous solutions. Take care in slowly removing the ethanol from the top of the solution. If a small amount of residual ethanol is present after the second wash proceed to the water washes as this will help remove any small amounts of ethanol

Note 7

The tungsten pellet requires extra centrifugation time to pellet on occasion. Repeat the centrifugation step to further pellet the tungsten. The pellet should be dried after water removal. In all cases a little tungsten is removed during pipetting.

Note 8

The homogeneity of the tungsten solution plays a significant role in the transformation efficiency of the preparations. Less tungsten in one of the two tubes will cause the results from the bombardment to be skewed. From a 1 mL preparation of tungsten we

only recommend using the first 800 µL and disregarding the rest. Sometimes the tungsten will pellet at the bottom of the eppendorf tube. This pellet must be fully resuspended before transferring tungsten to the new tube. Flip the tube upside down and flick the tube; if the tungsten comes away from the bottom conical area the tungsten is appropriately resuspended. Vortex again for 15-20 seconds and then pipette quickly.

Note 9

Mixing DNA is one of the most important steps involved in this process. DNA at high concentrations is very viscous and error due to pipetting is common. DNA should be pipetted up and down several times slowly. Using DNA at very high concentrations will increase variability. The best advice is to maximize volume for the DNA (e.g., 12.5 µL of GUS at 4 µg/µl and 12.5 µL pUC19 at 4 µg/µl is preferable to 5 µL GUS at 10 µg/µl , 5µL pUC19 at 10 µg/µl , and 15 µL of water.

Note 10

The alignment of the leaf under the bombardment is critical to the success of the assay. Wide leaves that are symmetrical in shape and size across the major vein should be used for bombardment. Bombardments are comparable only across the mid vein, not together on the same side. Transformation efficiency varies between the distal portion of the leaf and the petiole. The minimal media plate used to hold the leaves can dehydrate the bombarded area of the leaf after a short period of time since this is wounded tissue. Minimizing the amount of time the leaf spends on the minimal media after bombardment is important.

Note 11

The double-barreled gene gun should first be mastered by bombarding a control sample through both barrels. Initially the user should use one preparation for both barrels. The ratio between the barrels should be approximately 1, but a 10% deviation is considered acceptable. Once successful with this bombardment requirement the user should prepare two separate control preparations and repeat the assay. This will ensure that the user can prepare the solutions for bombardment accurately.

Note 12

Resistance through effector triggered immunity can be temperature dependent **(15)**. We found that 25°C is an appropriate temperature to trigger cell death through the recognition of Avr1b by Rps1b and for cell death induction by mouse BAX. A temperature that is physiologically relevant for infection should be used for incubation.

References

1. Klein, T. et al. (1992). Transformation of microbes, plants, and animals by particle bombardment. *Nature Biotechnology*, **10**, 286-291.
2. Liang, G.H. and Skinner, D.Z. (2004). Genetically modified crops: their development, uses, and risks. Haworth Press. Binghamton, New York.
3. Barry, M.A. and Johnston, S.A. (1997). Biological features of genetic immunization. *Vaccine*, **15**, 788-791.
4. Daniel, H. et al. (1990). Transient foreign gene expression in chloroplasts of cultured tobacco cells after biolistic delivery of chloroplast vectors. *Proc. Nat. Acad. Sci.* USA, **87**, 88-92.
5. Remacle C. et al. (2005). High-efficiency biolistic transformation of Chlamydomonas mitochondria can be used to insert mutations in complex I genes. *Proc. Nat. Acad. Sci. USA*, **103**, 4771-4776.
6. Qutob, D., Kamoun, S., and Gijzen, M. (2002). Expression of a Phytophthora sojae necrosis-inducing protein occurs during transition from biotrophy to necrotrophy. *Plant Journal*, **32**, 361–373.
7. Dou, D., Kale, S.D. et al. (2008). Conserved C-Terminal Motifs Required for Avirulence and Suppression of Cell Death by Phytophthora sojae Effector Avr1b.*The Plant Cell*, **20**, 1118-1133.
8. Dou, D., Kale, S.D. et al. (2008). RXLR-Mediated Entry of Phytophthora sojae Effector Avr1b into Soybean Cells Does Not Require Pathogen-Encoded Machinery. *The Plant Cell*, **20**, 1930-1947.

9. Jefferson, R.A. (1987) Assaying chimeric genes in plants: the GUS gene fusion system. Plant Mol. Biol. Rep. **5**, 387-405.
10. Sanford, J.C., et al. (1991). An improved, helium-driven biolistic device. *Technique*, **3**, 3-16.
11. Sokal, R.R. and Rohlf F.J. Biometry. W.H. Freeman and Company San Francisco.
12. Sokal, R.R. and Rohlf F.J. Statistical Tables. W.H. Freeman and Company San Francisco.
13. Benjamini, Y. and Hochberg, Y. (1995). Controlling the false discovery rate - a practical and powerful approach to multiple testing. *J R Stat Soc Ser B*, **57**, 289-300.
14. Benjamini, Y. and Yekutieli, D. (2001). The control of the false discovery rate in multiple testing under dependency. *Ann Stat*, **29**, 1165-1188.
15. Gijzen, M. et al. (1996) Temperature induced susceptibility to *Phytophthora sojae* in soybean isolines carrying different *Rps* genes. *Physiol and Molec Plant Pathol*, **48**, 209-215.

The Plant Cell, Vol. 20: 1118–1133, April 2008, www.plantcell.org © 2008 American Society of Plant Biologists

Conserved C-Terminal Motifs Required for Avirulence and Suppression of Cell Death by *Phytophthora sojae effector* Avr1b [W]

Daolong Dou,[a,1] Shiv D. Kale,[a,1] Xinle Wang,[b] Yubo Chen,[b] Qunqing Wang,[b] Xia Wang,[a] Rays H.Y. Jiang,[a,c,2] Felipe D. Arredondo,[a] Ryan G. Anderson,[d] Poulami B. Thakur,[d] John M. McDowell,[d] Yuanchao Wang,[b] and Brett M. Tyler[a,d,3]

[a] Virginia Bioinformatics Institute, Virginia Polytechnic Institute and State University, Blacksburg, Virginia 24061
[b] Department of Plant Pathology, Nanjing Agricultural University, Nanjing 210095, China
[c] Laboratory of Phytopathology, Wageningen University, NL-6709 PD Wageningen, The Netherlands
[d] Department of Plant Pathology, Physiology, and Weed Science, Virginia Polytechnic Institute and State University, Blacksburg, Virginia 24061

The sequenced genomes of oomycete plant pathogens contain large superfamilies of effector proteins containing the protein translocation motif RXLR-dEER. However, the contributions of these effectors to pathogenicity remain poorly understood. Here, we show that the *Phytophthora sojae* effector protein Avr1b can contribute positively to virulence and can suppress programmed cell death (PCD) triggered by the mouse BAX protein in yeast, soybean (*Glycine max*), and *Nicotiana benthamiana* cells. We identify three conserved motifs (K, W, and Y) in the C terminus of the Avr1b protein and show that mutations in the conserved residues of the W and Y motifs reduce or abolish the ability of Avr1b to suppress PCD and also abolish the avirulence interaction of Avr1b with the *Rps*1b resistance gene in soybean. W and Y motifs are present in at least half of the identified oomycete RXLR-dEER effector candidates, and we show that three of these candidates also suppress PCD in soybean. Together, these results indicate that the W and Y motifs are critical for the interaction of Avr1b with host plant target proteins and support the hypothesis that these motifs are critical for the functions of the very large number of predicted oomycete effectors that contain them.

INTRODUCTION

Oomycete plant pathogens, including >80 species of *Phytophthora*, are destructive to a vast variety of plants important to agriculture and forestry and to natural ecosystems. The economic damage to crops in the United States by *Phytophthora* species is estimated in the billions of dollars, and worldwide it is many times that (Erwin and Ribiero, 1996). Some species of *Phytophthora*, such as *P. cinnamomi* and *P. parasitica*, each attack hundreds of different plant host species. Others, like the soybean (*Glycine max*) pathogen *P. sojae* and the potato (*Solanum tuberosum*) and tomato (*Solanum lycopersicum*) pathogen *P. infestans*, have narrow host ranges. In addition to *Phytophthora*, the oomycete class Peronosporomycetidae includes many other destructive plant pathogens, such as the downy mildews and >100 species of *Pythium* (Agrios, 2005). The downy mildew pathogen of *Arabidopsis thaliana*, *Hyaloperonospora parasitica*, has been used extensively as a model for understanding plant responses to oomycete infection (Slusarenko and Schlaich, 2003). Despite morphological and physiological resemblances to fungi, oomycetes belong to the kingdom Stramenopila, which includes diatoms and golden brown algae (Sogin and Silberman, 1998).

P. sojae and *P. infestans* are hemibiotrophic, which means they have an initial phase of biotrophic growth followed by a transition to necrotrophy. During the early stages of infection, biotrophic and hemibiotrophic oomycetes form specialized feeding structures called haustoria. Haustoria are formed when hyphae penetrate the host plant cell wall but remain separated from the host cytoplasm by the plant plasma cell membrane (Erwin and Ribiero, 1996; Hahn and Mendgen, 2001; Tyler, 2007). Haustoria are thought to play a key role in exploitation of the plant by actively importing carbon, water, and inorganic nutrients. Haustoria are also likely structures through which pathogens might deliver effector molecules into the plant cell to modulate plant defense circuitry and enable parasitic colonization (Hahn and Mendgen, 2001).

The role of effector proteins in pathogenesis has been characterized most extensively in bacteria (Alfano and Collmer, 2004; Chang et al., 2004; Mudgett, 2005; Chisholm et al., 2006). During animal infection, pathogen effector proteins can alter specific host cell functions, such as phagocytosis, proinflammatory responses, apoptosis, and intracellular trafficking (Mota and

[1] These authors contributed equally to this work.
[2] Current address: Broad Institute, Massachusetts Institute of Technology, 7 Cambridge Center, Cambridge, MA 02142.
[3] Address correspondence to bmtyler@vt.edu.
The author responsible for distribution of materials integral to the findings presented in this article in accordance with the policy described in the Instructions for Authors (www.plantcell.org) is: Brett M. Tyler (bmtyler@vt.edu).
[W] Online version contains Web-only data.
www.plantcell.org/cgi/doi/10.1105/tpc.107.057067

Cornelis, 2005). In plant pathogenesis, many bacterial effectors suppress defense responses, triggered by either microbe-associated molecular patterns (MAMPs) or by other effectors due to recognition by resistance (R) proteins (Kjemtrup et al., 2000; Alfano and Collmer, 2004; Chang et al., 2004; Mudgett, 2005; Chisholm et al., 2006; Jones and Dangl, 2006). Many bacterial effectors are Cys proteases that presumably target positive regulators of defense (Hotson and Mudgett, 2004). On a similar theme, AvrPtoB from *Pseudomonas syringae* suppresses programmed cell death (PCD) triggered by diverse elicitors, including the mouse BAX protein via a C-terminal E3 ubiquitin ligase domain (Abramovitch et al., 2003, 2006). As an alternative mechanism, several bacterial effectors are transcription factors and can stimulate the expression of host genes that promote disease susceptibility (Arbibe et al., 2007; Kay et al., 2007). Several fungal plant pathogens secrete effector proteins that contribute to virulence (reviewed in Chisholm et al., 2006), including the toxins NIP1 from *Rhynchosporium secalis* and PtrA from *Pyrenophora tritici-repentis* and the chitin binding protein Avr4 from *Cladosporium fulvum*. Several additional secreted proteins are presumed to be effectors since they interact with plant resistance proteins, but their contribution to pathogen virulence has not yet been directly demonstrated. These include the metalloproteases Avr-Pita and Avr-YAMO from *Magnaporthe grisea* and the proteinase inhibitors Avr2 from *C. fulvum* and AvrP123 from *Melampsora lini* (reviewed in Chisholm et al., 2006). Some of these fungal effectors can cross into the plant cell cytoplasm, or are inferred to do so, but the mechanisms of entry are unknown. Many potential effector proteins have been identified in oomycetes through structural and functional genomics studies, including toxins, proteases, and proteinase inhibitors (reviewed in Kamoun, 2007), but the contributions of these proteins to virulence are currently only inferred.

Many plant disease resistance genes that confer resistance against oomycete pathogens encode nucleotide binding site, leucine-rich repeat (NBS-LRR) proteins. These include the *Arabidopsis RPP*1, *RPP*2, *RPP*4, *RPP*5, *RPP*7, *RPP*8, and *RPP*13 genes against *H. parasitica* (Slusarenko and Schlaich, 2003), the lettuce (*Lactuca sativa*) *Dm*3, *Dm*14, and *Dm*16 resistance genes against *Bremia lactucae* (Wroblewski et al., 2007), the potato *R*1 (Ballvora et al., 2002), *Rb*/*RpiBlb*1 (Song et al., 2003; van der Vossen et al., 2003), *RpiBlb*2 (van der Vossen et al., 2005), and *R*3a (Huang et al., 2005) genes against *P. infestans*, and the soybean *Rps*1k (Gao et al., 2005), *Rps*4, and *Rps*6 (Sandhu et al., 2004) genes against *P. sojae*. Five oomycete avirulence genes that interact with these *R* genes in a gene-for-gene manner have been cloned, namely, *P. sojae Avr1b*-1 (Shan et al., 2004), *P. infestans Avr3a* (Armstrong et al., 2005), *H. parasitica ATR13* (Allen et al., 2004) and *ATR1* (Rehmany et al., 2005), and *P. sojae Avr4/6* (D. Dou, S.D. Kale, F.D. Arredondo, and B.M. Tyler, unpublished data). All five of these genes encode small secreted hydrophilic proteins that are recognized by their cognate resistance gene products in the cytoplasm of the plant host (Allen et al., 2004; Armstrong et al., 2005; Rehmany et al., 2005). These effector proteins share an N-terminal motif, RXLR-dEER (Rehmany et al., 2005; Birch et al., 2006; Tyler et al., 2006), that is required to carry these proteins across the host plasma cell membrane into the cytoplasm (Whisson et al., 2007). The RXLR-dEER motif resembles the host targeting signal of *Plasmodium* effectors that carries those effectors across the parasitiphorous vacuolar membrane in erythrocytes (Hiller et al., 2004; Marti et al., 2004) and is functionally exchangeable with the *Plasmodium* host targeting signal (Bhattacharjee et al., 2006).

Bioinformatic analysis of the genome sequences of *P. sojae* and *P. ramorum* has identified an extraordinarily large superfamily of predicted proteins with sequence similarity to the *P. sojae Avr1b*-1 and *P. infestans Avr3a* genes (Tyler et al., 2006; Win et al., 2007; Jiang et al., 2008). These genes all encode small secreted proteins that contain an N-terminal RXLR-dEER motif, which leads us to the hypothesis that the proteins can enter host cells and so may be considered as candidate effector proteins (Tyler et al., 2006; Win et al., 2007; Jiang et al., 2008). The members of the superfamily also share sequence similarity in the C-terminal regions, indicating they have a common evolutionary origin (Jiang et al., 2008). In more than half of the members of the superfamily, bioinformatic analysis has identified three conserved motifs, termed W, Y, and L motifs. Many of these effector candidates contain multiple copies of the three motifs, in which case, the three motifs are repeated in tandem as a single W-Y-L module (Jiang et al., 2008).

Since RXLR-dEER–containing proteins can enter plant cells, they are presumed to act to promote the virulence of these pathogens. However, this has not yet been directly demonstrated, and the mechanisms by which they might do this are poorly understood. The oomycete avirulence genes cloned to date are not essential for pathogenicity since virulent races of the respective pathogens exist in which the avirulence genes are either not expressed or have accumulated many mutations. Bos et al. (2006) demonstrated that transient expression of *Avr3a* in *Nicotiana benthamiana* could suppress PCD triggered by the INF1 elicitin protein, which is a MAMP (Nurnberger et al., 2004); this suggests that Avr3a may contribute to the pathogenicity of *P. infestans* by suppressing MAMP-triggered immunity. The C terminus of the protein was required for this activity. However, Avr3a has not been demonstrated directly to be required for or to contribute to the virulence of *P. infestans*.

We show here that overexpression of the *P. sojae* effector gene *Avr1b*-1 measurably increases the virulence of *P. sojae* transformants. We further show that expression of the *Avr1b*-1 gene can suppress PCD triggered by the mouse BAX protein in yeast, soybean, and *N. benthamiana*, identifying a mechanism by which Avr1b may contribute to virulence. We show that the C-terminal W and Y motifs of Avr1b are required for suppression of PCD and for interaction with the Rps1b resistance gene product. Finally, we show that three bioinformatically identified oomycete effector candidates that contain W and Y motifs can also suppress BAX-induced PCD, suggesting that suppression of PCD is a major function of the >214 *P. sojae* effector candidates that contain these motifs.

RESULTS

Avr1b Contributes Positively to Virulence

Loss of *Avr1b*-1 expression does not compromise the virulence of *P. sojae* (Shan et al., 2004), presumably because the genome

encodes a very large number of effectors of similar function. Therefore, to test whether the Avr1b gene product contributes positively to virulence, we produced *P. sojae* transformants that overexpress *Avr1b*-1. We obtained two *P. sojae* transformants (T17 and T20) that contain multiple copies of the *Avr1b*-1 gene and produce high levels of *Avr1b*-1 mRNA (Figures 1A and 1B). Both transformants killed soybean seedlings slightly more quickly than the recipient strain P7076 in a hypocotyl inoculation assay (Figure 1C). To measure the difference quantitatively, we used an assay routinely used to measure quantitative resistance in soybean cultivars (Vega-Sánchez et al., 2005). In this assay, in which the rate of lesion progression up the roots of soybean seedlings is measured, both transformants produced lesions that progressed statistically significantly faster than the recipient ($P < 0.05$; Figure 1D).

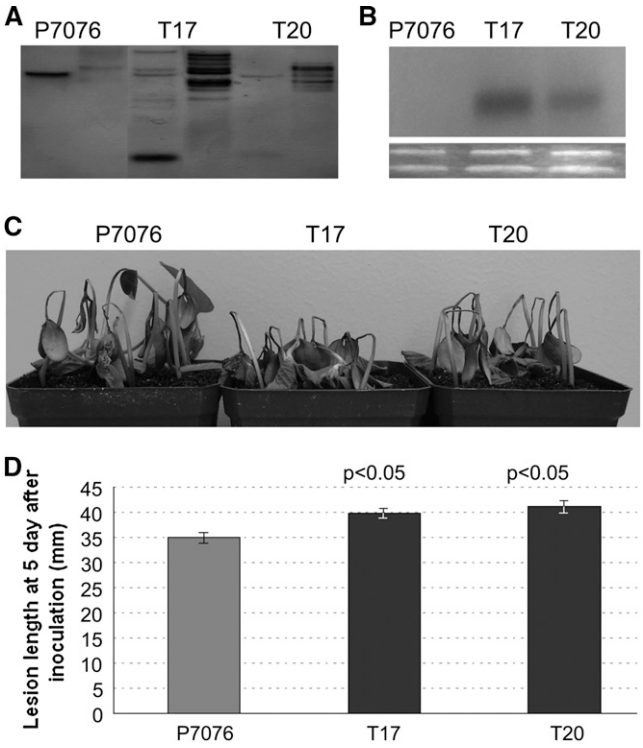

Figure 1. Overexpression of *Avr1b*-1 Confers Increased Virulence on Soybean.

(A) DNA gel blots hybridized with the *Avr1b*-1 probe, demonstrating multiple copies of *Avr1b*-1 transgenes. P7076 is the transformation recipient, and T17 and T20 are two transformants. DNA from each strain was digested with *Kpn*I (lanes 1, 3, and 5) or *Xho*I (lanes 2, 4, and 6). A band around 400 bp is released when transgenic DNA is cut with *Kpn*I.

(B) RNA gel blots of RNA extracted from in vitro grown mycelium and hybridized with an *Avr1b*-1 probe. The bottom panel shows ethidium bromide staining of RNA prior to transfer.

(C) Seven-day-old seedlings of soybean cultivar Williams were inoculated on the hypocotyls and photographed 4 d later.

(D) Root lesion lengths 5 d after inoculation. Lesions on the roots of 30 seedlings inoculated with wild-type or transgenic *P. sojae* were measured in each of five independent experiments. Combined data for all 150 plants are shown. Error bars show SE. P values were determined with a *t* test.

Avr1b Can Suppress PCD Induced by Mouse BAX Protein in Soybean and *Nicotiana*

To explore the mechanisms by which Avr1b contributes to virulence, we tested whether, like many bacterial effectors, Avr1b could suppress PCD induced by the proapoptotic protein BAX. We used a particle bombardment assay that introduces DNA encoding β-glucuronidase (GUS) into soybean leaf cells. When DNA encoding an elicitor of PCD is cotransformed with the *GUS* gene, PCD results in the elimination of most cells expressing *GUS* (Mindrinos et al., 1994; Qutob et al., 2002) (Figures 2A and 2B). When a third gene is introduced on the same particles, the ability of the protein encoded by the gene to suppress PCD can be measured by the restoration of cells expressing *GUS* (Figure 2A). To facilitate the comparison of test and control bombardments, we invented a novel, double-barreled attachment for the Bio-Rad Gene Gun (see Supplemental Figure 1 online) that enables us to shoot two different DNA samples side by side into a leaf in the same shot, which greatly improves the reproducibility of the results (see Supplemental Figure 2 online).

To trigger PCD in soybean cells, we used a mouse *Bax* cDNA that triggers PCD when expressed in *Nicotiana* (Lacomme and Cruz, 1999) and *Arabidopsis* (Baek et al., 2004). Figure 2B and Table 1 show that expression of *Bax* reduced the number of GUS-positive blue patches by 88% (experiment a compared with experiment c in Table 1), confirming that mouse BAX protein can trigger PCD in soybean cells. When *Avr1b*-1 was coexpressed with the *Bax* cDNA, the number of surviving GUS-positive blue patches was tripled, indicating that Avr1b could partially suppress BAX-induced PCD. This result was obtained both when the cobombardment of *Bax* and *Avr1b*-1 was compared directly to cobombardment of *Bax* and empty vector using the double-barreled bombardment (direct assay; Figure 2C, Table 1) and when each mixture was separately compared with a reference consisting of *GUS* plus empty vector (indirect assay) (Table 1). *Avr1b*-1 expression did not increase the number of blue spots when BAX was omitted from the experiment (Figure 2D, Table 1).

To independently confirm that Avr1b could suppress BAX-induced PCD in plant cells, we used *Agrobacterium tumefaciens* cells to deliver a potato virus X (PVX) vector carrying *Avr1b*-1 and the *Bax* cDNA into *N. benthamiana* leaves. *A. tumefaciens*–mediated transient expression was used previously to demonstrate suppression of BAX-induced PCD by bacterial effectors (Jamir et al., 2004) and suppression of elicitin-induced PCD by *P. infestans Avr3a* (Bos et al., 2006). When *N. benthamiana* leaves were infiltrated with *A. tumefaciens* cells containing a *Bax* cDNA driven by the cauliflower mosaic virus (CaMV) 35S promoter, obvious cell death symptoms were observed (Figures 3A and 3C), confirming that BAX could trigger PCD in *N. benthamiana* cells (Lacomme and Cruz, 1999). However, when the leaves were infiltrated with *A. tumefaciens* cells containing an *Avr1b*-1 gene, 1 d (Figure 3C) or 2 d (Figure 3B) prior to infiltration with the *Bax* cDNA-containing cells, no cell death symptoms were observed except in regions of the leaf that failed to receive *Avr1b*-1 gene–containing cells. *Avr1b*-1 gene expression also protected *N. benthamiana* tissue from cell death triggered by *Bax* cDNA

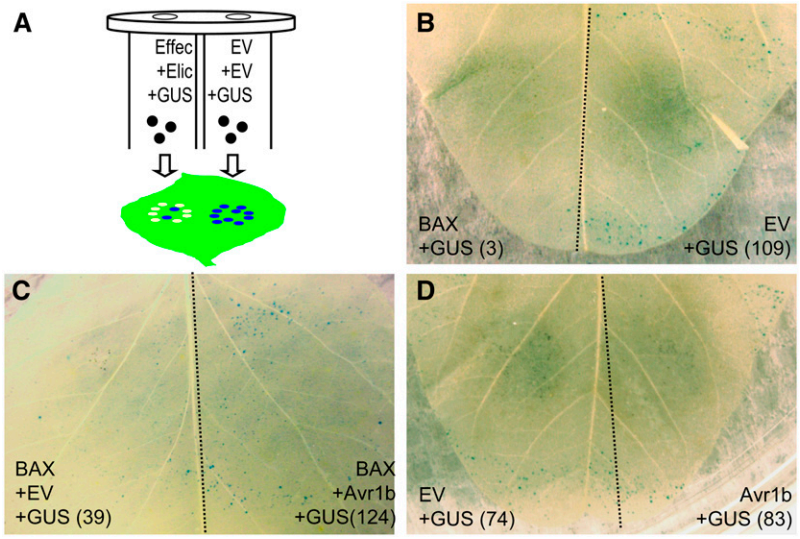

Figure 2. Measuring Suppression of BAX-Mediated PCD by Avr1b Using Double-Barreled Particle Bombardment of Soybean Leaves.

(A) Experimental design using the double-barreled particle bombardment assay. The diagram illustrates the indirect assay in which the number of GUS-positive blue spots produced by a mixture of an effector (e.g., Avr1b) and elicitor (e.g., BAX) is measured as a ratio to an empty vector (EV) control. PCD triggered by BAX protein reduces the appearance of blue spots because the GUS-producing cells are killed. Avr1b partially restores the appearance of blue spots by suppressing PCD.

(B) to **(D)** Leaves bombarded with the pairs of DNA mixtures indicated. Dotted line indicates the position of a divider used to prevent overlap of the two bombardment areas. Numbers of blue spots counted are indicated in parentheses. Blue spots cannot be counted in the central area of a shot due to tissue damage. Conclusions are based on statistical analysis of results from 14 to 16 leaves similar to those illustrated (Table 1).

(B) Ablation of blue spots by BAX-triggered PCD.

(C) Suppression of BAX-triggered PCD by Avr1b.

(D) A control experiment verifying that Avr1b does not significantly increase the number of blue spots in the absence of BAX.

expression when *A. tumefaciens* strains containing the two genes were infiltrated simultaneously (Figure 3A). Prior infiltration of *N. benthamiana* leaves with buffer or with *A. tumefaciens* cells containing a green fluorescent protein (*GFP*) gene did not protect the leaves from BAX-induced PCD (Figure 3C). Furthermore, as expected, infiltrations of *A. tumefaciens* cells containing *Avr1b*-1 alone failed to elicit visible cell death (Figures 3A and 3C). These results support the conclusion from the soybean particle bombardment assay that *Avr1b*-1 gene expression can suppress BAX-induced PCD in plant cells.

Suppression of PCD in Yeast Indicates That Avr1b Has a Highly Conserved Target

To address whether Avr1b targets a host protein specific to plants or a highly conserved protein in the pathway leading to PCD, we tested whether, like some bacterial effectors (Abramovitch et al., 2003), Avr1b can suppress PCD in the yeast *Saccharomyces cerevisiae*. We introduced the *Avr1b*-1 gene into yeast strain W303 under the control of the *GAL*1 promoter and then tested the resistance of several transformants to PCD induced by hydrogen

Table 1. Suppression of BAX-Mediated PCD by Avr1b, Measured by Double-Barreled Particle Bombardment

Experiment	Barrel 1[a]	Barrel 2[a]	Direct Ratio[b]	Indirect Ratio[c]	P Value[d]
a	EV + GUS	EV + GUS	0.99 ± 0.03		
b	Avr1b + GUS	EV + GUS	1.03 ± 0.15	b/a = 1.04	>0.100
c	BAX + GUS	EV + GUS	0.12 ± 0.02		
d	Avr1b + BAX + GUS	EV + EV + GUS	0.34 ± 0.04	d/c = 2.84	<0.001
e	Avr1b + BAX + GUS	EV + BAX + GUS	3.36 ± 0.7		<0.004

[a] Barrels 1 and 2 are physically identical. Half of all the replicates were conducted using the configuration of DNA samples indicated, and half were conducted with the samples reversed between barrels 1 and 2. In all cases, the mass of DNA in each barrel was identical. EV, empty vector.

[b] Ratios between the numbers of spots produced by each barrel. Geometric averages and SE were calculated from log ratios obtained from 14 to 16 pairs of shots.

[c] Comparison of the two averaged ratios from the experiments indicated by the lowercase letters.

[d] P values for the indirect comparisons were calculated from the log ratios using the Wilcoxon rank sum test. P value for the direct comparison (experiment e) was calculated from the log ratios using the Wilcoxon signed ranks test. A significant P value indicates significant suppression of PCD.

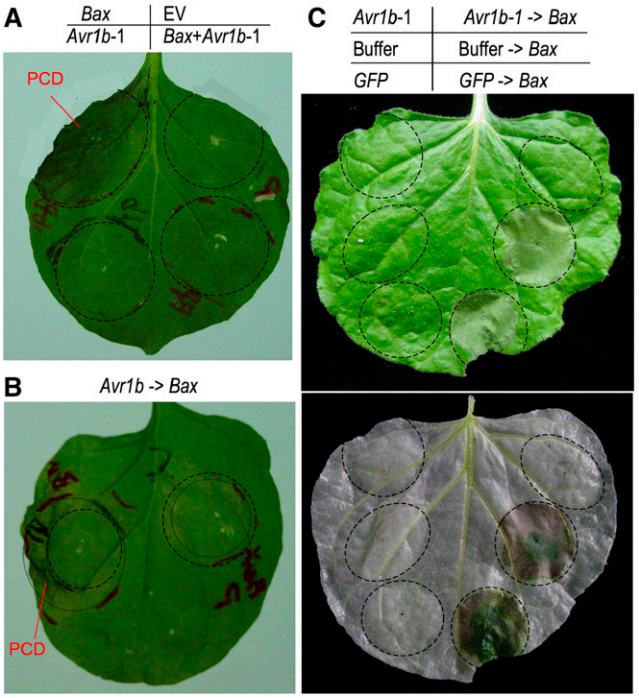

Figure 3. Avr1b Suppresses BAX-Induced Cell Death in *N. benthamiana*.

N. benthamiana leaves were infiltrated with *A. tumefaciens* cells containing a PVX vector carrying a mouse *Bax* cDNA, the *P. sojae Avr1b*-1 gene, a *GFP* gene or an empty vector (EV) within the regions indicated by the dashed lines. Photos were taken 5 or 6 days after the last infiltration. In **(A)**, the *Bax*- and *Avr1b*-1–containing cells were infiltrated at the same time. In **(B)**, *Avr1b*-1–containing cells were infiltrated into the areas marked by the dashed lines, followed 2 d later by infiltration with cells carrying the *Bax* cDNA into the region marked with the dotted line. In **(C)**, buffer or cells carrying the *Avr1b*-1 or *GFP* genes were infiltrated into the leaf, followed after 24 h either by no further challenge (left side) or by infiltration with cells carrying the *Bax* cDNA. The bottom panel shows the same leaf as the top panel after decolorization with ethanol.

peroxide. We observed that Avr1b protected yeast from the PCD induced by 15 mM H_2O_2 compared with control transformants (Figure 4A). We also observed that *Avr1b*-1 expression could weakly suppress PCD induced by BAX (Figure 4B), although the activity is not as strong as the cell death suppressor Bcl2 (see Supplemental Figure 3 online). In yeast, production of reactive oxygen species was shown to play a key role in BAX-induced apoptosis (Madeo et al., 1999). Therefore, we conclude that the components of the PCD machinery of the plants and yeast targeted by Avr1b are substantially conserved.

Identification of Conserved C-Terminal Motifs in Avr1b and Close Paralogs

To identify the regions of Avr1b responsible for mediating the suppression of PCD, we performed an amino acid sequence alignment of Avr1b with *P. infestans* Avr3a (Armstrong et al., 2005) and with Avr1b paralogs that we identified in the genome sequences of *P. sojae*, *P. infestans*, and *P. capsici* (see Supplemental Table 1 online). The genome sequences of *P. ramorum* and *H. parasitica* do not encode any effector-like proteins with strong similarity to Avr1b. As shown in Figure 5A, the sequence alignment identifies three regions of sequence conservation in the C terminus of these proteins, in addition to the secretory leader and RXLR-dEER domain in the N terminus. Two of the conserved regions correspond to W and Y motifs found in more than half of the RXLR-dEER–containing effectors in the *P. sojae* and *P. ramorum* genomes (Jiang et al., 2008). In addition to the W and Y motifs, the alignment reveals a conserved Lys-rich motif that we have called the K motif. Adding an allele of Avr1b to the sequence alignment together with the product of *Avh*1, a highly similar paralog of *Avr1b*-1 found in some strains of *P. sojae* (Shan et al., 2004), reveals that the K, W, and Y regions are also the locations of highly polymorphic residues. These residues are under strong positive selection (Shan et al., 2004; Jiang et al., 2008).

To resolve why the most conserved regions corresponding to the K, W, and Y motifs are also the most polymorphic, we mapped the polymorphic and conserved residues onto the predicted secondary structure of Avr1b protein. The predicted

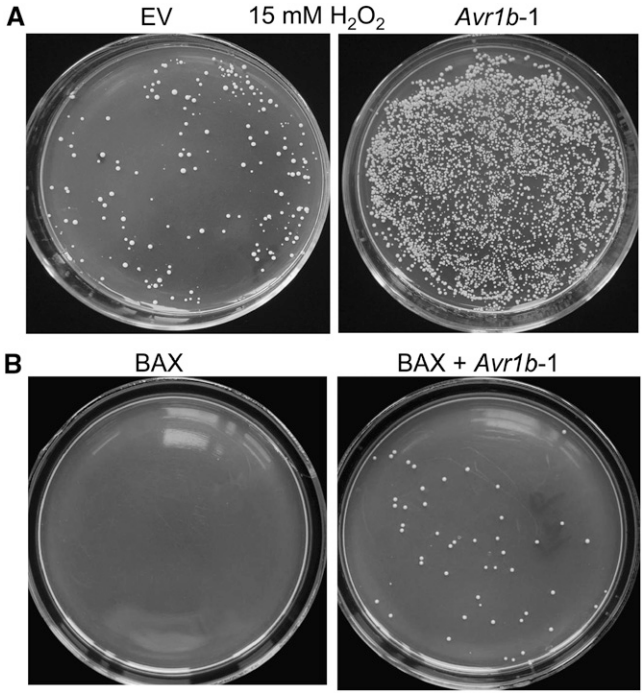

Figure 4. Avr1b Suppresses H_2O_2- and BAX-Induced Cell Death in Yeast.

(A) Yeast cells of strain W303 containing an empty vector (EV) or *Avr1b*-1 under control of the galactose-inducible *GAL*1 promoter were grown in galactose-containing medium, harvested, treated with 15 mM H_2O_2 for 6.5 h, and then diluted and plated as detailed in Methods.
(B) Yeast cells of strain W303 containing the Bax cDNA under control of the galactose-inducible *GAL1* promoter either alone (BAX) or together with *Avr1b*-1 under control of the *GAL1* promoter (BAX + Avr1b) were grown on glucose-containing medium and then harvested, diluted, and plated on galactose-containing medium as detailed in Methods.

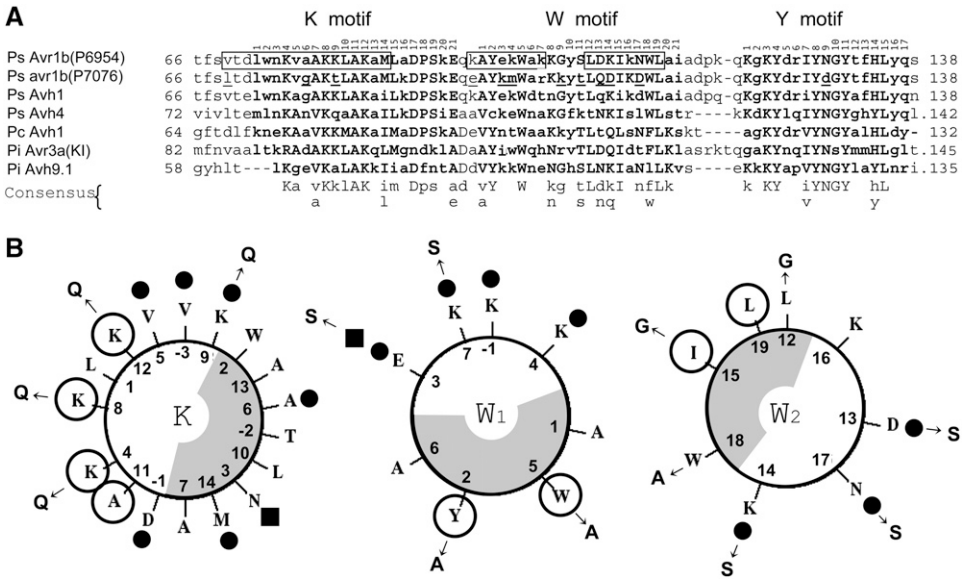

Figure 5. Conserved Motifs in the Avr1b C Terminus Correspond to Predicted Polymorphic Amphipathic α-Helices.

(A) Sequence alignment of C-terminal regions of Avr1b family proteins reveals three conserved C-terminal motifs, K, W, and Y, shown in bold. In the alignment, uppercase letters indicate the most highly conserved residues in the sequences and the consensus. Dots at the end of sequences indicate residues omitted from the figure. Boxed regions indicate predicted α-helices. Ps Avr1b(P6954) sequence is from avirulent strain P6954 (AAM20937); Ps avr1b(P7076) sequence is from virulent strain P7076 (AF449624) (Shan et al., 2004). Underlined sequences are polymorphic among *Avr1b*-1 alleles (Shan et al., 2004). Ps Avh1 (AF449626) and Avh4 indicate Avr1b paralogs in *P. sojae* strain P6497 (Shan et al., 2004; Tyler et al., 2006; Jiang et al., 2008). Pc Avh1 from *P. capsici* is representative of seven nearly identical paralogs (see Supplemental Table 1 online) in the genomic sequence (www.jgi.doe.gov). *P. infestans* Avh9.1 (gene model PITG_05911.1) is representative of seven nearly identical paralogs (see Supplemental Table 1 online) in the genomic sequence (www.broad.mit.edu). *P. infestans* Avr3a (Armstrong et al. 2005) represents five nearly identical paralogs; the KI allele from an avirulent strain (Armstrong et al., 2005) is shown.
(B) Helical wheel projections of the predicted α-helices that overlap the Avr1b K and W motifs. The shaded and unshaded regions indicate hydrophobic and hydrophilic faces of the helices, respectively. Black circles indicate residues polymorphic in *Avr1b*-1 alleles and in *Avh*1. Black squares indicate positions corresponding to polymorphic residues in *P. infestans* Avr3a. Open circles indicate the most conserved residues. Arrows indicate substitutions in the mutants Avr1bK1 (Q substitutions), Avr1bW1 (A and G substitutions), and Avr1bW2 (S substitutions). Numbering refers to positions within each motif as designated in **(A)**.

secondary structure of the C terminus of Avr1b contains three α-helices separated by turns (Shan et al., 2004). One helix corresponds to the K motif and two to the W motif (Figure 5A). Figure 5B shows a helical wheel projection of the residues in the K and W regions. All three helices are predicted to be amphipathic with hydrophobic residues clustered primarily on one side of the helix (shaded in Figure 5B) and hydrophilic residues primarily on the other. The pattern is particularly strong in the two helices associated with the W motif. Figure 5B also shows that in the two helices associated with the W motif, the polymorphic residues are exclusively located on the hydrophilic sides of the two helices, while the most conserved residues are located on the hydrophobic sides. In the K motif helix, the most conserved residues are hydrophilic, and so the hydrophilic side of the helix is well conserved. However, the polymorphic residues form two clusters located ~180° from one another.

Conserved Residues in the W Motif Are Required for Suppression of PCD

To test the roles of the conserved and polymorphic residues of the three conserved C-terminal motifs in the function of Avr1b, we introduced substitution mutations into the residues and tested the ability of genes encoding the mutant Avr1b proteins to suppress BAX-induced PCD using the soybean leaf bombardment assay. Initially five multipoint mutations were introduced into the K, W, and Y motifs. The Avr1bK1 mutation replaced each of the four Lys residues with Gln, which is uncharged but has a similar size to Lys and is hydrophilic (Figures 5B and 6). This mutation did not significantly affect the suppression of PCD by *Avr1b*-1 ($P > 0.1$; Figure 6, Table 2; see Supplemental Table 2 online). The Avr1bW1 mutation replaced the six most highly conserved hydrophobic residues in the W motif with Ala or Gly residues (Figures 5B and 6); this mutant lost all ability to suppress PCD (Figure 6, Table 2; see Supplemental Table 2 online). The Avr1bW2 mutation replaced five of the six polymorphic hydrophilic residues of the W motif with Ser residues (Figures 5B and 6); this mutation did not affect the suppression of PCD (Figure 6, Table 2; see Supplemental Table 2 online). The Avr1bW3 mutation changed four consecutive residues in the second W motif helix to Gly; this also abolished suppression of PCD (Figure 6, Table 2; see Supplemental Table 2 online). The Y1 mutation replaced eight conserved residues in the Y motif; this mutation partially reduced the suppression of PCD (Figure 6, Table 2; see Supplemental Table 2 online). We also tested whether the allele of *Avr1b*-1 found in strain P7076

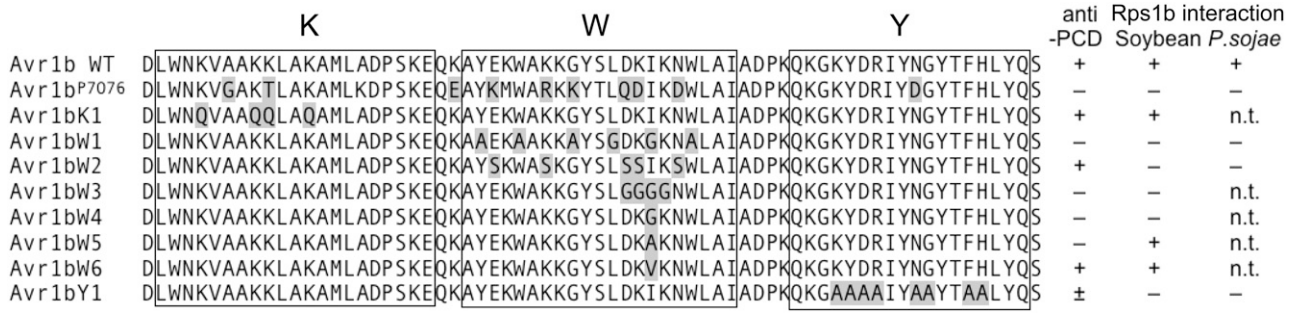

Figure 6. Mutational Analysis of Avr1b C-Terminal K, W, and Y Motifs.

Sequences of the mutants and summary of phenotypes. Mutations are shaded. Avr1b^{P7076} is an allele from virulent strain P7076. Anti-PCD indicates the ability to suppress PCD in the particle bombardment assays. Avirulence was determined using the particle bombardment assay (soybean) and/or in *P. sojae* transformants (*P. sojae*). +, active; −, inactive; ±, partially active; n.t., not tested. Detailed assay data are given in Table 2 and in Supplemental Tables 2 to 4 online.

could suppress PCD; P7076 is virulent against soybean cultivars containing *Rps*1b, and the encoded protein contains substitutions at most of the polymorphic sites in the K, W, and Y motifs. This allele was inactive in suppressing PCD (Figure 6, Table 2; see Supplemental Table 2 online).

A further set of mutations was targeted to a highly conserved Ile residue (position 15 in the W motif; position 109 in the protein) that had been changed to Gly in the Avr1bW1 and Avr1bW3 mutants. I109 was changed to Gly (W4), Ala (W5), and Val (W6). I109G and I109A abolished suppression of PCD, but the more conservative I109V did not (Figure 6, Table 2; see Supplemental Table 2 online).

Conserved and Polymorphic Residues in the W and Y Motifs Are Required for the Functional Interaction of *Avr1b*-1 with *Rps*1b

To determine whether the same residues required for suppression of PCD were also required for the interaction that makes an *Avr1b*-1–expressing *P. sojae* strain avirulent on an

Table 2. Effects of Avr1b Mutations on PCD Suppression and Interaction with Rps1b

	PCD Suppression[b]				Rps1b Interaction				
					Particle Bombardment[c]		*P. sojae* Transformants[d]		
	Direct		Indirect		Rps1b to rps		No. of Transformants	Phenotype	
Mutant[a]	Ratio to Control	P Value	Ratio to Control	P Value	Ratio	P Value		Rps1b	rps
Avr1b^{+}	3.36	<0.001	2.84	<0.001	0.22	<0.001	2	A	V
Avr1b^{P7076}	0.74	>0.5	0.74	>0.1	1.01	>0.1	2	V	V
Avr1bK1	2.41[e]	<0.001	4.87[e]	<0.001	0.12	<0.001	nt		
Avr1bW1	0.99	>0.4	0.68	>0.1	1.02	>0.1	4	V	V
Avr1bW2	3.48	<0.001	3.81	<0.001	0.93	<0.001	4	V	V
Avr1bW3	0.85	>0.5	0.67	>0.1	1.01	>0.1	nt		
Avr1bW4	1.03	>0.2	0.82	>0.1	1.05	>0.1	nt		
Avr1bW5	0.93	>0.5	1.06	>0.1	0.17	<0.001	nt		
Avr1bW6	3.12	<0.001	3.46	<0.001	0.18	<0.001	nt		
Avr1bY1	1.80[f]	<0.01	1.55[g]	<0.05	1.00	>0.1	2	V	V

[a] Sequences of Avr1b mutant proteins given in Figure 6.

[b] PCD suppression was measured using both the direct and indirect assays as described in the Methods and in the legend of Table 1. Significant deviation above 1.0 indicates activity in PCD suppression.

[c] A significant reduction in GUS expression on *Rps*1b leaves compared with *rps* leaves indicates a positive interaction with Rps1b.

[d] Two to four independent transformants carrying each tested mutant *Avr1b*-1 gene were inoculated onto soybean Rps1b or rps seedlings to determine virulence (V) or avirulence (A). To test the P7076 allele, strain P7076 itself was transformed with a GUS gene. More detailed data are presented in Supplemental Table 4 online. nt, not tested.

[e] Not significantly different than wild-type Avr1b ($P > 0.100$).

[f] Significantly different than wild-type Avr1b ($P < 0.025$).

[g] Significantly different than wild-type Avr1b ($P < 0.001$).

*Rps*1b-expressing soybean plant, we introduced *Avr1b*-1 genes carrying the W1, W2, and Y1 mutations into *P. sojae* by transformation. All three mutations abolished the ability of *Avr1b*-1 to make the transformants avirulent upon infection of *Rps*1b-containing cultivars (Figure 6, Table 2; see Supplemental Table 4 online). To confirm these results and to test additional mutations, we used the soybean leaf bombardment assay. In this version of the assay, ablation of the GUS-positive tissue patches is caused by the hypersensitive response (HR) of the soybean tissue to the Avr1b gene product when the resistance gene *Rps*1b is expressed. Wild-type *Avr1b*-1 DNA caused a 78% reduction in the number of GUS-positive spots on *Rps*1b-containing leaves relative to an empty vector control (Table 2, line 1, indirect assay) but caused no reduction on leaves lacking *Rps*1b (rps) (Table 1, line 2, experiment b; Figure 2D; see Supplemental Table 3 online). Of the multipoint mutations, W1, W2, W3, and Y1 all abolished triggering of the HR in the presence of *Rps*1b, but K1 had no effect (Figure 6, Table 2; see Supplemental Table 3 online). Of the five mutations, only W2 abolished the interaction with Rps1b but did not abolish suppression of PCD. The P7076 allele of *Avr1b*-1 (*Avr1b*-1^{P7076}) did not trigger a reaction in *Rps*1b-expressing tissue, as expected since P7076 is virulent on *Rps*1b-containing cultivars. Of the three point mutations at Ile-109, I109G abolished the Rps1b interaction, but I109A and I109V did not (Figure 6, Table 2; see Supplemental Table 3 online). Thus, I109A abolished suppression of BAX-triggered PCD but did not abolish the Rps1b reaction.

Three Bioinformatically Identified Effectors Containing W and Y Motifs Suppress PCD

The experiments described in the previous section demonstrated that residues in the W motif are required for Avr1b to suppress PCD. To determine if other putative RXLR-dEER effectors that contain W motifs also can suppress PCD, we selected two such effectors from the genome sequence of *P. sojae* and one from the genome sequence of *H. parasitica*. One of the *P. sojae* genes, Ps *Avh*331, was selected because it is located 5 kb from *Avr1b*-1. The other two genes, Ps *Avh*163 and Hp *RxL*96, were selected because they display significant sequence similarity with each other. As illustrated in Figure 7A and Supplemental Figure 4 online, all three of these putative effectors contain multiple W and Y motifs, together with an additional conserved motif not found in Avr1b, called an L motif (Jiang et al., 2008). Many predicted oomycete effectors contain multiple modules consisting of adjacent W, Y, and L motifs (W-Y-L modules), though some motifs may be degenerate or missing in some modules (Jiang et al., 2008). All three of these putative effectors could suppress BAX-mediated PCD in the soybean leaf bombardment assay (Figure 7; see Supplemental Table 2 online). Ps Avh331 suppressed PCD even more strongly than Avr1b. Ps Avh331 also could suppress BAX-induced PCD in the *Agrobacterium* infiltration assay in *N. benthamiana* leaves (Figure 7C); the other two genes were not tested in *N. benthamiana*. As an example of an oomycete effector that lacks W, Y, and L motifs, we tested the ability of *P. sojae* avirulence gene Avr4/6 to suppress BAX-induced PCD. Avr4/6 was identified as an RXLR-containing protein encoded in the genetic interval defined

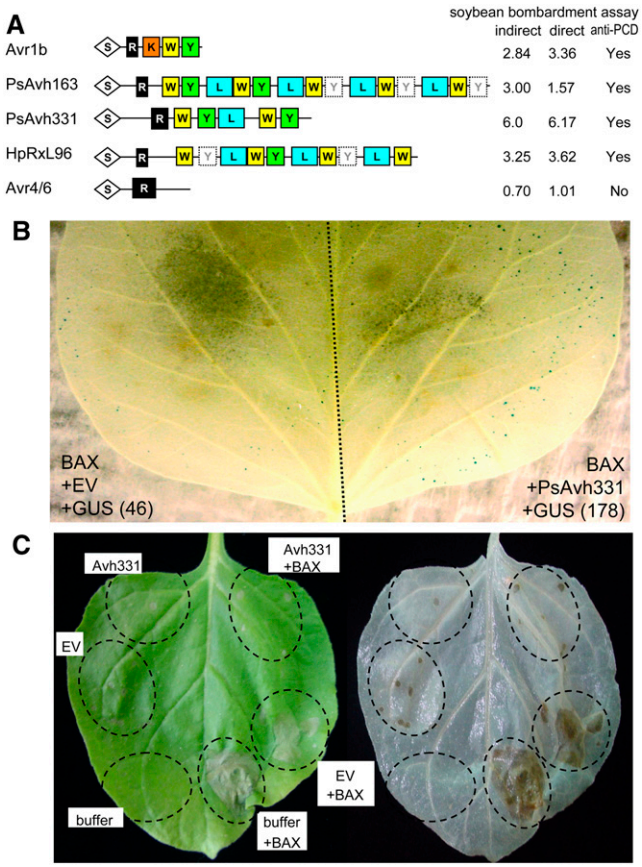

Figure 7. Suppression of BAX-Mediated PCD by Diverse Predicted Effectors Containing W and Y Motifs.

(A) Structure of the predicted effector proteins and their suppression of BAX-mediated cell death in soybean bombardment assays. The positions of each motif are approximately to scale. S, secretory leader; R, RXLR-dEER motif; K, K motif; W, W motif; L, L motif (Jiang et al., 2008). Dotted outlines and gray lettering indicate weak matches to the respective motifs. Each effector was tested for suppression of PCD using both the direct and indirect bombardment assays as described in the Methods and the legend to Figure 2. All effectors with significant suppression activity had P values <0.01 in both assays. Detailed assay data are given in Supplemental Table 2 online.

(B) A leaf bombarded with the pair of DNA mixtures indicated (empty vector [EV]). Dotted line indicates the position of a divider used to prevent overlap of the two bombardment areas. Numbers of blue spots counted are indicated in parentheses. Blue spots cannot be counted in the central area of a shot due to tissue damage. Conclusions are based on statistical analysis of results from 14 to 16 leaves similar to the one illustrated (see Supplemental Table 2 online).

(C) Suppression of BAX-triggered cell death by PsAvh331 confirmed in *N. benthamiana* leaves using *Agrobacterium* infiltration. Buffer or *Agrobacterium* cells carrying PsAvh331 in a PVX vector or an empty vector were infiltrated into the indicated leaf panels. After 2 d, *Agrobacterium* cells carrying BAX in a PVX vector were infiltrated into the same panels as indicated. After 5 d, the leaves were photographed, decolorized in ethanol to visualize the necrotic tissue more clearly, and then photographed again. Two photographs of a representative leaf (before and after decolorization) are shown.

by Whisson et al. (2004). Avr4/6 triggers HR in both *Rps*4 and *Rps*6 soybean plants in the bombardment assay, and silencing of the gene in *P. sojae* eliminates avirulence on both *Rps*4 and *Rps*6 cultivars (D. Dou, S.D. Kale, F.D. Arredondo, and B.M. Tyler, unpublished data). As indicated in Figure 7A, Avr4/6 caused no suppression of BAX-mediated PCD at all.

DISCUSSION

In the first part of this study, we used *P. sojae* overexpression transformants to obtain evidence that avirulence protein Avr1b is an effector that contributes positively to the virulence of the pathogen. In the second part of the study, we demonstrated that Avr1b can suppress PCD triggered in soybean and *N. benthamiana* plants by expression of a mouse *Bax* cDNA, suggesting that one of the mechanisms by which Avr1b contributes to virulence is by suppressing the host plant's HR. We further showed that *Avr1b*-1 gene expression could suppress PCD in yeast, suggesting that the PCD signaling protein(s) targeted by the effector is highly conserved. In the final part of this study, we showed that a conserved C-terminal motif (W motif) found in many predicted oomycete effectors was required for the ability to suppress PCD and that a second motif (Y motif) also may play a role. The hypothesis suggested by these results, namely, that many of the other predicted effectors that contain W motifs may also act to suppress PCD, was reinforced by our confirmation that three predicted effectors containing W and Y motifs (W-Y motif effectors) could suppress PCD, whereas a functional avirulence protein (Avr4/6) that lacked the motif could not. We further demonstrated that many of the residues of Avr1b required for suppression of PCD were also involved in eliciting an Rps1b-mediated HR, though two mutations could be identified that separated the two activities.

This study also introduces two technical improvements that are of general value to researchers studying *P. sojae* and plant–microbe interactions in general. First, we have introduced three major improvements to the efficiency and reliability of *P. sojae* transformation (Judelson et al., 1991), namely, use of a new protoplast transformation procedure (McLeod et al., 2008), use of G418 selection, and the use of the strong constitutive promoter of the *P. sojae* rpL41 ribosomal protein gene. Our second major innovation has been the invention of a double-barreled modification of the Bio-Rad Gene Gun, which enables all quantitative particle bombardment experiments to be internally controlled. This innovation greatly increases the reproducibility and, hence, sensitivity of these experiments.

Avr1b Is an Effector Protein That Can Suppress PCD

Our results show that although Avr1b is not essential to virulence, presumably because the *P. sojae* genome contains a very large number of similar effectors (Tyler et al., 2006; Jiang et al., 2008), its contribution to virulence can be seen when magnified by strong overexpression. Suppression of PCD constitutes an important potential mechanism by which Avr1b may contribute to virulence. A key cytological difference between a compatible and an incompatible interaction between *P. sojae* and soybean is the appearance of many dying plant cells during ingress of *P. sojae* hyphae during the early hours of an incompatible interaction and a paucity of cells containing pathogen haustoria. Haustoria are a major site of nutrition for the pathogen, and suppression of PCD by haustorial cells would be of major benefit to the pathogen.

Plant defenses to infection by biotrophic and hemibiotrophic pathogens are induced by a multilayered set of pathways that respond to common pathogen molecules (MAMPs; also called pathogen-associated molecular patterns) (Nurnberger et al., 2004) and also to specific pathogen effector molecules (Jones and Dangl, 2006). Both MAMP- or PAMP-triggered immunity (MTI or PTI) and effector-triggered immunity (ETI) can be suppressed by bacterial effector proteins (reviewed in Chisholm et al., 2006). There is considerable evidence for extensive overlap and crosstalk between the signaling pathways for MTI and ETI (He et al., 2007), and a number of effectors can interfere with both types of responses (Chisholm et al., 2006). Other bacterial effectors, such as AvrBs3 (Kay et al., 2007) and *Shigella flexneri* OspF (Arbibe et al., 2007), modify host transcription by acting as transcription factors.

Both MTI and ETI responses can include a form of PCD termed the HR. The HR is very effective against obligate biotrophic pathogens, such as downy mildews and viruses. PCD is similarly effective against obligate biotrophic pathogens of animals. Consequently, several animal viruses produce proteins that suppress PCD (Clem, 2007). HR can also be effective against hemibiotrophic pathogens if it is triggered very quickly before the pathogens have switched to necrotrophic growth. Thus, numerous bacterial effectors have been identified that suppress PCD (e.g., Jamir et al., 2004; Nomura et al., 2006). However, if HR is delayed, hemibiotrophic pathogens, especially filamentous ones such as fungi and oomycetes, can grow out of the region affected by HR, resulting in a lethal spreading HR that favors necrotrophic proliferation of the pathogen. *P. sojae* is a hemibiotroph. It typically switches from biotrophic to necrotrophic growth 16 to 24 h following invasion of host tissue (Enkerli et al., 1997). Therefore, the ability of *P. sojae* to suppress or delay the HR of soybean tissue is likely a major component of its pathogenic strategy.

The sequence similarity of the *P. infestans* Avr3a protein to Avr1b, including the presence of W and Y motifs (Figure 5A), suggests that the two effectors have a similar function. Bos et al. (2006) showed that Avr3a could suppress the PCD triggered in *Nicotiana* by the *P. infestans* MAMP INF1. Thus, oomycete W-Y motif effectors may share the ability to suppress PCD associated with MAMP perception. The spectrum of responses that W-Y motif effector proteins can suppress needs to be more fully explored. For example, do such effectors have some specificity as suggested by the fact that Avr3a could not suppress PCD triggered by the MAMP NEP1 (Bos et al., 2006)? Do oomycete pathogens have large numbers of diverse W-Y motif effectors, some with multiple W and Y (and L) motifs, to suppress PCD responses to a wide diversity of MAMPs? Can these effectors suppress PCD triggered by interactions between *R* gene products and effectors that are avirulence proteins?

The Avr1b Target Is Conserved and Lies at or Downstream of the Point at Which BAX Acts

All four W-Y motif effectors that we tested suppressed BAX-induced PCD in soybean, and the two that were tested in

N. benthamiana, Avr1b and Ps Avh331, also suppressed BAX-induced PCD in that plant species. Mouse BAX protein triggers PCD in animal cells by inserting into the mitochondrial outer membrane, destabilizing the mitochondria and releasing cytochrome c and reactive oxygen species. The reactive oxygen species further destabilize the mitochondrial outer membrane, creating a positive feedback loop as more reactive oxygen species are released. Cytochrome c is recognized by ApaF1, leading to the activation of the caspase cascade; ApaF1 is an NBS-LRR protein that has similarity to plant NBS-LRR resistance proteins. In plants, the oxidative burst plays a key role in initiating the HR in response to pathogen infection. Current evidence suggests that H_2O_2 and NO produced by the oxidative burst act together to activate caspases via a mitogen-activated protein kinase pathway. Since Avr1b can suppress PCD in both yeast and plants, it presumably targets a molecule(s) that is common to the PCD signal transduction pathways in both kingdoms.

Avr1b and other W-Y motif effectors could potentially suppress PCD by directly interfering with a host component necessary for PCD or by altering host gene expression or cell physiology to create an antiapoptotic cellular environment. Numerous pathogen proteins have been identified as suppressors of BAX-induced PCD in yeast or plants (reviewed in Hoeberichts and Woltering, 2002; Madeo et al., 2004; see also Abramovitch et al., 2006; Janjusevic et al., 2006). Avr1b and other W-Y motif effectors lack any recognizable sequence similarity to enzymes, such as peroxidases, proteases, or E3 ligases, that could conceivably interfere with PCD signaling. The effectors also lack hydrophobic domains common to anti-apoptotic proteins in the Bcl-2 family or anti-apoptotic proteins, such as *Arabidopsis* At BI-l (for Bax inhibitor-1) (Watanabe and Lam, 2006), the BON family (Yang et al., 2006), and the BON-associated protein family (Yang et al., 2007). Furthermore, the W-Y motif effectors do not resemble any bacterial effector proteins, and most lack canonical nuclear localization signals. However, it is intriguing that many W-Y motif effectors, including the three tested here, have multiple copies of the W-Y-L module and in this regard resemble the IAP proteins that contain multiple zinc finger domains involved in caspase binding (Fesik and Shi, 2001). W-Y-L modules are very diverse in sequence (Jiang et al., 2008). While this diversity may result from coevolutionary conflict with plant resistance gene products (Rehmany et al., 2005; Jiang et al., 2008), it is also possible that the modules have evolved to attack a diversity of targets in the plant defense and/or PCD pathways. Further biochemical and structural studies of Avr1b and other W-Y motif effectors and their interaction with proteins in yeast and plants will be required to uncover their molecular mechanisms of action. These studies may in turn shed additional light on the processes of PCD signaling in these organisms.

C-Terminal Motifs Conserved across the RXLR-dEER Superfamily Are Required for Suppression of PCD

The W, Y, and L motifs are the most prominent C-terminal motifs conserved across the RXLR-dEER superfamily. Of the 397 family members, 214 have at least a W motif, and many have multiple copies of the module consisting of the W, Y, and L motifs (Jiang et al., 2008), though in many modules, one or both of the Y and L motifs cannot readily be recognized (Figure 7A). The predicted secondary structure for the region of Avr1b containing the W and Y motifs is three α-helices separated by turns, two shorter ones spanning the W motif, and one longer one spanning the K motif. The three predicted helices are all amphipathic, suggesting that they form a helical bundle with the hydrophobic faces of the helices turned inwards. Mutagenesis of six conserved hydrophobic residues of the W motif (W1 mutation) abolished the ability of Avr1b to suppress PCD, but mutagenesis of five variable hydrophilic residues (W2 mutation) did not. This suggests that the overall structure of the region carrying the W and Y motifs may be important for suppression of PCD but that none of the exterior residues altered in W2 are required. Mutagenesis of the Y motif significantly reduced the suppression of PCD by Avr1b ($P < 0.001$) but did not abolish it. Thus, the Y motif may not be directly involved in the suppression of PCD, but the Y1 mutation may have partially disrupted the structure of the region containing the W and Y motifs.

Replacement of I109 with Ala (mutation W5; I109A) abolished the ability of Avr1b to suppress PCD. However, the mutation is not predicted to disrupt the structure of the helix, as Ala is a helix-promoting residue, and the mutation did not disrupt the interaction of Avr1b with Rps1b. Thus, Ile-109 may define a site that is important in the suppression of PCD. All three bioinformatically predicted W motif–containing effectors that we tested could suppress BAX-mediated PCD, one of them (Ps Avh331) exceptionally well. The position in the W motif corresponding to Ile-109 is either Val, Leu, or Ile in 85% of the predicted W motifs, and replacement of Ile-109 with Val (W6 mutation) did not disrupt the ability of Avr1b to suppress PCD. At the position corresponding to Ile-109 in the second predicted helix of the W motif in Avr1b, Avr3a also has an Ile residue. Since 174 of the 350 predicted effectors encoded in the *P. sojae* genome contain W motifs and many contain multiple W-Y-L modules, it appears that as much as half of the oomycete effector repertoire may be dedicated to the suppression of host PCD. Very many bacterial effectors can also suppress PCD (e.g., Jamir et al., 2004; Nomura et al., 2006), leading to the hypothesis that suppression of PCD is central to pathogenicity in both bacterial and oomycete plant pathogens.

Avr4/6 lacks any recognizable W, Y, or L motifs, and it was unable to suppress PCD, consistent with its lack of a W motif. Assuming that Avr4/6 contributes to virulence, this observation suggests that Avr4/6 may have a different mechanism than Avr1b for doing so. This may also be true of the 175 other predicted *P. sojae* RXLR-dEER effectors that lack any W, Y, or L motifs. Many of these effectors have relatively well-conserved paralogs in *P. ramorum*, indicating that they are not pseudogenes (Jiang et al., 2008). Further investigation is needed to determine what those functions might be.

The *R* Gene Rps1b Targets the C-Terminal Functional Domain of Avr1b

Mutations in the W motif not only abolish the ability of Avr1b to suppress PCD but also abolish its ability to trigger an Rps1b-mediated HR. The Y1 mutation also abolished triggering of the Rps1b-mediated response. Thus, the *Rps*1b resistance gene in soybean has evolved to respond to the region of Avr1b that is

involved in its ability to suppress PCD. Presumably, *Rps*1b was selected during evolution because it targeted a region of Avr1b that was essential for virulence. The allele of Avr1b found in P7076 has many mutations in the W and Y motifs, and the encoded protein can no longer trigger an Rps1b-mediated response nor suppress PCD. Five of the residues polymorphic in P7076 were targeted in the W2 mutation, and W2 also abolishes the triggering of an Rps1b-mediated response by Avr1b. However, W2 does not interfere with suppression of PCD, suggesting that some of the four other residues in the W motif that are altered in P7076 may play a role in this function of Avr1b. All of the nine DNA sequence changes within the region of the *Avr1b*-1 gene encoding the W motif cause amino acid substitutions, indicating that this part of the protein is under extremely strong positive selection (Shan et al., 2004; Jiang et al., 2008), presumably due to pressure from *Rps*1b and/or other similar resistance genes.

In contrast with Avr1b, *P. infestans* Avr3a has only one polymorphic site in the W motif, and that mutation does not strongly affect the ability of Avr3a to interact with the R3a gene product. The Lys at position 80 in Avr3a near the K motif was more important to the interaction. Furthermore, mutations spanning large regions of the Avr3a protein restored the interaction with R3a (J. Bos and S. Kamoun, unpublished data). It has been proposed that there are two mechanisms by which plant resistance gene products detect the presence of pathogen effectors. One mechanism is direct interaction and the other is indirect interaction. Direct interaction has been documented in the case of the Pi-ta resistance protein of rice (*Oryza sativa*) and the AvrPi-ta avirulence protein of the fungus *Magnaporthe grisea* (Jia et al., 2000), and in the case of the flax resistance protein L and the avirulence protein AvrL567 of the rust fungus *M. lini* (Dodds et al., 2006). Indirect interaction has been hypothesized in the case of many bacterial effectors that appear to be detected by the cognate *R* gene product indirectly through changes in a plant protein targeted by the effector; this situation has been termed the guard hypothesis (Van der Biezen and Jones, 1998; Jones and Dangl, 2006). The W2 mutation abolishes the triggering of the Rps1b-mediated response but does not interfere with suppression of PCD. This suggests that the interaction with Rps1b is not mediated by the PCD-signaling protein that is presumably targeted by Avr1b. It remains to be determined whether Avr1b interacts directly with Rps1b or whether there is another plant protein targeted by Avr1b and guarded by Rps1b. In the case of Avr3a, the same two polymorphisms that abolish the suppression of PCD also abolish the interaction with R3a (Bos et al., 2006), consistent with indirect guard recognition of Avr3a by R3a.

METHODS

Plasmids and Strain Construction

The oligonucleotides used for the following plasmid constructions are documented in Supplemental Table 5 online. *Phytophthora sojae* transformation plasmids pHamAvr1b (full sequence of *Avr1b*-1, AAR05402, driven by Ham34 promoter; Judelson et al., 1991), pHamGUS (modified *Staphylococcus* GUS gene [Cambia *GUSPlus*; www.cambia.org]) driven by Ham34 promoter), and pUN (NptII gene driven by *P. sojae* rpL41 promoter) were constructed as follows. For pHamAvr1b, the NptII gene of pHAMT35N (Judelson et al., 1991) was replaced with *P. sojae Avr1b*-1 using PrimerC and PrimerD. For pHamGUS, the NptII gene of pHAMT35N was replaced with the CAMBIA *GUSPlus* gene using primers GusR and GusF. For pUN, the Ham34 promoter of pHAMT35N was replaced by the *P. sojae* rpL41 promoter (EF681129) using primers UF and UR.

Soybean (*Glycine max*) transient expression plasmids pUCAvr1b (leaderless *Avr1b*-1 driven by the CaMV 35S promoter) and pUCGUS (GUSPlus gene driven by the CaMV 35S promoter) were constructed as follows. For pUCGUS, a cassette containing the CaMV 35S promoter, CAMBIA *GUSPlus* gene, and nos terminator was amplified from pCambia1305.2 using primers GusF_EcoRI and GUSR_HindIII, cleaved with *Eco*RI and *Hin*dIII, and ligated into pUC19. For pUCAvr1b, the hygromycin resistance of pCambia1305.2 was replaced by Avr1b-1 lacking its secretory leader (replaced by ATG codon) using primers Avr1bF and Avr1bR, creating pCambia-mAvr1b. Then, the Avr1b expression cassette, including the double 35S promoter was amplified from pCambia-mAvr1b using primers Avr1b_EcoRI, Avr1b_HindIII, and Avr1b_genegun_KpnI and subcloned into pUC19. These primers also created *Xma*I and *Kpn*I sites for later manipulation of the *Avr1b*-1 gene.

To construct *Avr1b*-1 C-terminal mutants for soybean transient expression, we used a two-step amplification procedure to create an *Avr1b*-1 amplicon containing the desired mutation and then replaced *Avr1b*-1 in pUCAvr1b with the mutant gene. For example, to construct Avr1b K1, we amplified the C terminus of *Avr1b*-1 from pUCAvr1b using oligonucleotide Avr1bK1F in combination with Avr1bR and the N terminus using Avr1bK1R and Avr1bF. Then, the full sequence of Avr1bK1 was obtained by combining the N-terminal and C-terminal amplicons and amplifying them with primers Avr1bF and Avr1bR. We used the same two-step PCR strategy to construct Avr1bW1, Avr1bW2, Avr1bW3, Avr1bW4, Avr1bW5, Avr1bW6, and Avr1bY1 with the following oligonucleotide pairs: Avr1bW1F and Avr1bW1R, Avr1bW2F and Avr1bW2R, Avr1bW3F and Avr1bW3R, Avr1bW4F and Avr1bW4R, Avr1bW5F and Avr1bW5R, Avr1bW6F and Avr1bW6R, and Avr1bYF and Avr1bYR. We cleaved the above eight amplicons with *Nco*I and *Kpn*I and inserted them into *Nco*I- and *Kpn*I-digested pUCAvr1b to obtain pUCAvr1bK1, pUCAvr1bW1, pUCAvr1bW2, pUCAvr1bW3, pUCAvr1bW4, pUCAvr1bW5, pUCAvr1bW6, and pUCAvr1bY1, respectively. We amplified the *Avr1b*-1 allele from *P. sojae* strain P7076 using oligonucleotides Avr1bF and AP7076R. The amplicons obtained were inserted into *Xma*I- and *Kpn*I-digested pUCAvr1b to obtain pUCAvr1bP7076. Plasmids pUCAvr46, pUCBax, pUCHpRxL96, pUCAvh163, and pUCAvh331 were obtained by insertion into *Xma*I- and *Kpn*I-digested pUCAvr1b with the amplicons obtained with oligonucleotides Avr4F and Avr4R, BaxF and BaxR, Hp96F and Hp96R, Avh163F and Avh163R, and Avh331F and Avh331R, respectively.

The identification of the Avr4/6 gene (ABS50087) will be described in detail elsewhere. Briefly, Avr4/6 was identified as the only RXLR-containing gene in the region identified by Whisson et al. (2004). Particle bombardment confirmed an avirulence interaction with both the soybean *Rps*4 and *Rps*6 genes, and silencing of the gene in *P. sojae* showed that it was responsible for the avirulence phenotype of the pathogen on cultivars containing either *Rps*4 or *Rps*6 (D. Dou, S.D. Kale, F.D. Arredondo, and B.M. Tyler, unpublished data).

To make the constructs for *P. sojae* transformation, three amplicons (Avr1bW1, Avr1bW2, and Avr1bY1) were digested with *Nco*I and *Kpn*I and inserted into pHamAvr1b digested with the same enzymes to obtain pHamAvr1bW1, pHamAvr1bW2, and pHamAvr1bY1, respectively. All the plasmids were further confirmed by sequencing at the Virginia Bioinformatics Institute core facility.

To make constructs for the yeast cell death assay, *Avr1b*-1 was amplified from pHamAvr1b with the oligonucleotides AvrYeastF and AvrYeastR. The amplicon was inserted into *Eco*RI- and *Sal*I-digested

pGilda (Clontech). For the PVX assay, *Avr1b-1*, *Avh331*, and Bax were amplified using combinations of oligonucleotides Avr1bPVXF and Avr1bPVXR, Avh331PVXF and Avh331PVXR, or BaxPVXF and BaxPVXR, respectively. Then, the amplicons were cloned using appropriate restriction enzymes into the PVX vector pGR106 (Lu et al., 2003). The constructs were further confirmed by sequence by Invitrogen Biotechnology.

P. sojae Strains, Manipulation, and Inoculation Assay

P. sojae isolates P6954 (Race 1), P6497 (Race 2), P7064 (Race 6), and P7076 (Race 19) (Forster et al., 1994) were routinely grown and maintained on V8 agar (Erwin and Ribiero, 1996). For transformation experiments, pea broth medium was made by autoclaving 120 g of frozen peas in 1 liter of distilled water for 15 min, filtering through four layers of cheesecloth, and then autoclaving again after bringing the volume up to 1 liter.

The following protocol was modified from that kindly provided by A. McLeod and W. Fry (McLeod et al., 2008). Three-day-old *P. sojae* mycelial mats, cultured in pea broth medium, were rinsed and washed in 0.8 M mannitol, then placed in enzyme solution (0.4 M mannitol, 20 mM KCl, 20 mM MES, pH 5.7, 10 mM $CaCl_2$, 10 mg/mL β-1.3 glucanase [InterSpec 0439-1], and 5 mg/mL cellulysin [Calbiochem 219466]) and incubated for 40 min at 22°C with 100 rpm shaking. The protoplasts were harvested by centrifugation at 1500 rpm for 3 min and resuspended in W5 solution (5 mM KCl, 125 mM $CaCl_2$, 154 mM NaCl, and 31 mg/mL glucose) at a concentration of 2×10^6 protoplasts/mL or higher. After 30 min, the protoplasts were centrifuged at 1500 rpm for 4 min and resuspended in an equal volume of MMg solution (0.4 M mannitol, 15 mM $MgCl_2$, and 4 mM MES, pH 5.7) to allow protoplasts to swell. To each of 1 mL MMg solution, 25 μg transforming DNA was added and incubated for 10 min on ice. For cotransformation experiments, 10 μg of DNA containing the selectable marker and 30 μg of DNA containing the gene of interest were used. Then, three aliquots of 580 μL each of freshly made polyethylene glycol solution (40% [v/v] polyethylene glycol 4000, 0.3 M mannitol, and 0.15 M $CaCl_2$) were slowly pipetted into the protoplast suspension and gently mixed. After 20 min incubation on ice, 10 mL pea broth containing 0.5 M mannitol were added, and the protoplasts were incubated overnight to regenerate. The regenerated protoplasts were suspended in liquid pea agar (40°C) containing 0.5 M mannitol and 50 μg/mL G418 (AG Scientific) and plated. The visible colonies could be observed after 2 to 3 d incubation at 22°C. All transformants were propagated on V8 agar with 50 μg/mL G418 at 22°C.

This procedure is very reliable. Approximately 30 to 100 putative transformants were obtained from each experiment, of which 80% would continue growing through the third round of antibiotic selection. Of these, 20 to 45% were generally confirmed to contain and express the transgene. When cotransformation was used, 4 to 13% of the transformants contained the nonselected plasmid.

Putative *P. sojae* transformants containing wild-type and mutant *Avr1b*-1 transgenes were screened in three steps. First, DNA from each line was amplified with oligonucleotides HamF (see Supplemental Table 5 online) and HamR, which are primers for the Ham34 promoter and terminator, respectively. Next, RT-PCR was performed on RNA extracted from each line using oligonucleotides Avr1bReF and Avr1bReR to confirm *Avr1b*-1 expression. Finally, the mRNA levels derived from the *Avr1b*-1 transgenes were accurately measured by quantitative real-time PCR performed by the Virginia Bioinformatics Institute core facility. To perform DNA gel blot hybridization analysis of *P. sojae* transformants, we purified genomic DNA from mycelium as described by Judelson et al. (1991) and digested 10 μg total genomic DNA with *Kpn*I or *Xho*I purchased from New England Biolabs. The digested DNA was size fractionated on a 0.7% agarose gel followed by transfer to Hybond N^+ nylon membrane (Amersham). For RNA gel blot analysis, total RNA from the transformants and wild-type *P. sojae* were isolated using the RNeasy plant mini kit (Qiagen) according to the manufacturer's recommendations. We electrophoresed 5 to 10 μg total RNA samples in a 1% agarose gel in MOPS running buffer at 45 mV for 50 min. The gel was then stained with an RNA staining buffer for 15 min. The gel was transferred overnight with 20× SSC buffer. DNA probes of *Avr1b*-1 were synthesized using a PCR digoxigenin probe synthesis kit according to the manufacturer's manual (Roche Diagnostics). The membrane was hybridized, and chemiluminescent detection was performed following the kit instructions.

The avirulence phenotypes of selected transformants were evaluated by hypocotyl inoculation (Tyler et al., 1995) using soybean (*Glycine max*) cultivars HARO(1-7) (rps), Haro13 (Harosoy background, *Rps*1b), Williams (rps), and L77-1863 (Williams background, *Rps*1b). The differences between the numbers of surviving plants from *rps* and *Rps*1b cultivars were compared using Fisher's exact test. Only the transformants producing significant differences between rps and *Rps*1b cultivars were judged as avirulent. Each avirulence determination was repeated at least three times. Quantitative virulence of *P. sojae* transformants was measured using a lesion length assay described by Vega-Sánchez et al. (2005) for measuring soybean partial resistance levels against *P. sojae*. There were three replications of 10 plants each within each experiment, and each experiment was repeated five times.

Particle Bombardment Assays for Avirulence and Virulence Phenotypes

Soybean plants were grown in the growth chamber; the day was 12 h at 28°C and the night was 12 h at 25°C. The first (monofoliate) true leaves were selected for bombardment 9 to 14 d after planting.

Plasmid DNA was isolated using Qiagen brand Maxi preparation kits and concentrated to 5 to 6 μg/μL in sterile deionized water. M-10 tungsten particles (Bio-Rad) were washed twice with 95% ethanol and twice with sterile deionized water, then resuspended in 50% sterile glycerol to a concentration of 90 mg/mL. For bombardment, 9 mg of tungsten particles were combined with 50 μg of GUS plasmid DNA (pCambia1305.2) and 50 μg of either test DNA (e.g., pCaAvr1b) or empty vector [pCa-GUS(−) or pUC19] as the control in a total of 100 μL of 25% glycerol on ice in a 0.5 mL centrifuge tube. Sixty-five microliters of 2.5 M $CaCl_2$ was added followed by 25 μL of freshly prepared 0.1 M spermidine. The preparation was vortexed for 2 min and then placed on ice for 20 min. The particle preparation was then concentrated to 30 μL by brief centrifugation.

Bombardment was performed using the Bio-Rad He/1000 particle delivery system with a double-barreled extension attached (see Supplemental Figure 1 online) to enable leaves to be bombarded with two DNA preparations simultaneously. A patent application has been submitted for this device. One microliter of each DNA particle preparation was loaded onto the macrocarrier so that the mixtures were directly over their respective barrels (see Supplemental Figure 1D online). The distance from the stopping screen to the target shelf was 12 cm. The distance between the rupture disk and macrocarrier was set to 3/8 inch. and the highest position was used for the macrocarrier in the macrocarrier assembly; 650 p.s.i. rupture disks were used. The chamber vacuum was 26 p.s.i. The pressure build time was set to 12 to 14 s. The two barrels of the extension were cleaned with 70% ethanol and then dried with compressed air between shots.

The target leaves were bombarded twice: first the petiole-proximal half of the leaf and then the petiole-distal half, resulting in a total of four bombardment sites. A cover was used to prevent overlapping bombardments.

After bombardment, the leaves were incubated for 5 d in darkness at 28°C. The leaves were then stained for 16 h at 28°C using 0.8 mg/mL X-gluc (5-bromo-4-chloro-3-indolyl-β-D-glucuronic acid, cyclohexylammonium salt), 80 mM Na phosphate, pH 7.0, 0.4 mM $K_3Fe(CN)_6$, 0.4 mM

$K_4Fe(CN)_6$, 8 mM Na_2EDTA, 0.8 mg/mL 20% methanol, and 0.06% (v/v) Triton X-100 and then de-stained in 100% methanol. Blue spots were counted using a dissecting microscope at ×5 to ×20 magnification.

To quantitate the avirulence activity of *Avr1b*-1 constructs, DNA carrying the constructs (1.7 μg per shot) was cobombarded into soybean leaves along with DNA carrying a GUS reporter gene (1.7 μg per shot). Avirulence activity was measured as the reduction in the number of blue staining GUS-positive spots in leaves carrying Rps1b compared with leaves lacking Rps1b. The double-barreled device was used to deliver a parallel control shot in every case that contained GUS DNA plus empty vector DNA. For each pair of shots, the logarithm of the ratio of the blue spots with Avr1b to that with the empty vector control was calculated. Each assay consisted of eight pairs of shots and was conducted at least twice. The log ratios from all the *Rps*1b leaves were then compared with those from the non-*Rps*1b leaves using the Wilcoxon rank sum test.

To quantitate suppression of BAX-mediated cell death, two assays were used: an indirect assay and a direct assay. For the indirect assay, *Avr1b*-1 DNA (1.7 μg/shot) was mixed with Bax DNA (pUCBax; 0.83 μg/shot) and GUS DNA (1.7 μg/shot) and bombarded into soybean leaves lacking Rps1b. The control shot in the second barrel was empty vector (pUC19; 2.53 μg/shot) plus GUS DNA (1.7 μg/shot). The log ratios for these shots were then compared with the log ratios obtained when *Avr1b*-1 DNA was replaced by empty vector DNA; 14 to 16 pairs of shots were performed for each comparison, and the results were evaluated using the Wilcoxon rank sum test. The indirect assay had the advantage that the level of PCD triggered by BAX could be monitored in every shot. For the direct assay, Avr1b + BAX + GUS was compared directly with empty vector + BAX + GUS in the second barrel. The log ratios obtained were then tested for significance using the Wilcoxon signed ranks test. Again 14 to 16 pairs of shots were performed. The direct assay had the advantage that the activity of *Avr1b*-1 could be compared with a control (or another *Avr1b*-1 construct) directly on the same leaves. Other effectors or mutants were tested by replacing the *Avr1b*-1 DNA with the relevant DNA.

Agrobacterium tumefaciens Infiltration Assays

A. tumefaciens strain GV3101 (Hellens et al., 2000) was used. For infiltration, recombinant strains were cultured in Luria-Bertani media supplemented with 50 μg/mL kanamycin and then harvested, washed three times in 10 mM $MgCl_2$, and resuspended in 10 mM $MgCl_2$ to an OD_{600} of 0.3. Infiltration experiments were performed on 4- to 6-week-old *Nicotiana benthamiana* plants. Plants were grown and maintained throughout the experiments in a greenhouse with an ambient temperature of 25° and high light intensity. *A. tumefaciens* cell suspensions carrying the *Avr1b*-1 gene (pGR106*Avr1b*-1) or PsAvh331 (pGR106*Avh331*) were infiltrated into *N. benthamiana* leaves (Bos et al., 2006) by pressure infiltration; a small nick was placed in each leaf with a razor blade and then 100 μL of cell suspension was infiltrated through the nick using a syringe without a needle. *A. tumefaciens* cells carrying the *Bax* gene (pGR106: *Bax*) were infiltrated into the same site 24 or 48 h later. As controls, *A. tumefaciens* strains carrying *Bax* or *Avr1b*-1 were replaced with *A. tumefaciens* strains carrying empty vectors. Symptom development was monitored from 3 to 8 d after infiltration, and pictures were taken after 5 d. The experiments were repeated at least three times. Although it is likely that PVX replication occurred in the transformed plant cells, resulting in amplified expression of the genes in the PVX vector, no attempt was made to quantitate PVX replication.

Yeast Cell Death Assays

The *Saccharomyces cerevisiae* strain W303 (MATa; ura3-52; trp1Δ2; leu2-3,112; his3-11; ade2-1; can1-100) was used, and the culture and transformation of the cells were performed essentially as described by Kampranis et al. (2000). To test if *Avr1b*-1 could suppress PCD triggered by H_2O_2, *Avr1b*-1 was introduced into W303 cells on the plasmid pGilda under the control of the galactose-inducible *GAL*1 promoter. Cells from W303 and the transformants were pelleted, washed, and resuspended in SD medium [0.17% YNB-AA/AS; 0.5%$(NH_4)_2SO_4$] containing 2% galactose and 1% raffinose as carbon sources (SD/gal/raff/±his) to induce expression of the Avr1b protein from the *GAL*1 promoter. After 12 h of induction, cells were diluted to $OD_{600} = 0.05$ and treated with 15 mM H_2O_2 added to the medium, and cultures were incubated at 30°C with vigorous shaking for 6 h. After treatment, viability was determined by plate counting. Treated and untreated cells were sampled and spread onto YPD medium (1% yeast extract, 2% peptone, 2% dextrose) with 2% agar and then incubated at 30°C for 48 h. The number of colony-forming units from treated cells were compared with the colony-forming units of untreated cells, and photos were taken. All the experiments were repeated least three times.

To test if *Avr1b*-1 expression could suppress PCD triggered in yeast cells by BAX, the plasmid pGildaBax that carries a mouse *Bax* cDNA under the control of the *GAL*1 promoter (Kampranis et al., 2000) was introduced into W303 cells. *Avr1b*-1 was introduced on the plasmid pYES2, also under the control of the *GAL*1 promoter. Cells containing pGildaBax, with or without pYES2*Avr1b*-1, were grown in SD-glucose medium. After 24 h, the cells were harvested and resuspended in water to an OD_{600} of 1.0. One hundred microliters of the cell suspension were then plated on SD-galactose and cultured at 30°C for 3 d, and the colonies were photographed and counted.

Sequence Search, Alignment, and Structure Prediction

The sequenced oomycete genomes were accessed at the following sites: *P. sojae*, *P. ramorum*, and *Hyaloperonospora parasitica* at vmd.vbi.vt.edu, *P. infestans* at www.broad.mit.edu, and *P. capsici* at shake.jgi-psf.org/Phyca1 (Department of Energy Joint Genome Institute). Avr1b paralogs were identified by tBLASTN search (Altschul et al., 1997) with a cutoff of $E = 10^{-7}$. Paralogs were selected with an amino acid similarity of at least 45%. Two such Avr1b paralogs were found in *P. sojae*, seven in *P. capsici*, and eight in *P. infestans*. The two *P. sojae* paralogs were *Avh*1 (Shan et al., 2004) and *Avh*4 (Jiang et al., 2008). The seven paralogs in *P. capsici* were nearly identical, and one was selected for the sequence alignment shown in Figure 4. The paralogs in *P. infestans* fell into two classes with near identity within each class; one from each class, including Avr3a, were selected for the sequence alignment. RXLR-dEER family members PsAvh331 and PsAvh163 were described by Jiang et al. (2008), and HpRxL96 was identified from the *H. parasitica* sequence by the procedures described by Jiang et al. (2008) together with Smith Waterman alignment to identify candidate effectors conserved between *P. sojae* and *H. parasitica*. PsAvh163 and HpRxL96 show 26% identity and 43% similarity over their aligned sequences. Multiple alignments were created using the program ClustalW (Thompson et al., 1994) with minor manual adjustment to optimize the alignment as necessary. Secondary structure prediction was performed using 3D-pssm (Imperial College of Science, Technology and Medicine, London, UK) and by using PredictProtein (www.PredictProtein.org).

Accession Numbers

Sequence data from this article can be found in the GenBank/EMBL data libraries under the following accession numbers: Ps *Avh*4 (EU282486), Ps *Avh*331 (EU282487), Ps *Avh*163 (EU282485), Hp *RXL*96 (EU282490), Pc *Avh*1 (EU282489), Pi05911 (EU282488), Ps *RpL*41 (EF681129), and Ps Avr4/6 (ABS50087).

Supplemental Data

The following materials are available in the online version of this article.

Supplemental Figure 1. The Double-Barreled Particle Bombardment Device.

Supplemental Figure 2. Correlation between Replicate Bombardments Produced by Double-Barreled Bombardment.

Supplemental Figure 3. Comparison of Ability of Avr1b and Bcl2 to Suppress BAX-Mediated Cell Death in Yeast.

Supplemental Figure 4. Sequences and Motif Structures of Avr and Avh Proteins.

Supplemental Table 1. Details of Avr1b Family Proteins.

Supplemental Table 2. Complete Data for Soybean Bombardment Assays of Suppression of BAX-Mediated PCD by Avr1b-1 Mutants and Other W-Y-Motif Effectors.

Supplemental Table 3. Assay Data for Bombardment Tests of Avr1b Avirulence Function.

Supplemental Table 4. Assay Data for Avirulence Tests of *P. sojae* Stable Transformants.

Supplemental Table 5. Summary of Oligonucleotides Used.

ACKNOWLEDGMENTS

We thank Adele McLeod and William Fry (Cornell University) for providing their *P. sojae* transformation protocol prior to publication, Terry Anderson (Agriculture Canada) and Saghai Maroof (Virginia Tech) for soybean seed, and Carol Volker for manuscript preparation. This work was supported by grants to B.M.T. from the National Research Initiative of the USDA Cooperative State Research, Education, and Extension Service (Grants 2001-35319-14251, 2002-35600-12747, 2004-35600-15055, and 2007-35319-18100) and from the U.S. National Science Foundation (Grants MCB-0242131 and EF-0412213), by funds from the Virginia Bioinformatics Institute, and by a 111 International Cooperation grant (B07030) to Nanjing Agricultural University from the Chinese government. R.H.Y.J. was supported in part by fellowship NGI 050-72-404 from the Netherlands Genomics Initiative.

Received November 20, 2007; revised February 26, 2008; accepted March 17, 2008; published April 4, 2008.

REFERENCES

Abramovitch, R.B., Janjusevic, R., Stebbins, C.E., and Martin, G.B. (2006). Type III effector AvrPtoB requires intrinsic E3 ubiquitin ligase activity to suppress plant cell death and immunity. Proc. Natl. Acad. Sci. USA **103:** 2851–2856.

Abramovitch, R.B., Kim, Y.-J., Chen, S., Dickman, M.B., and Martin, G.B. (2003). *Pseudomonas* type III effector AvrPtoB induces plant disease susceptibility by inhibition of host programmed cell death. EMBO J. **22:** 60–69.

Agrios, G.N. (2005). Plant Pathology, 5th ed. (New York: Academic Press).

Alfano, J.R., and Collmer, A. (2004). Type III secretion system effector proteins: Double agents in bacterial disease and plant defense. Annu. Rev. Phytopathol. **42:** 385–414.

Allen, R.L., Bittner-Eddy, P.D., Grenvitte-Briggs, L.J., Meitz, J.C., Rehmany, A.P., Rose, L.E., and Beynon, J.L. (2004). Host-parasite coevolutionary conflict between *Arabidopsis* and downy mildew. Science **306:** 1957–1960.

Altschul, S.F., Madden, T.L., Schaffer, A.A., Zhang, J.H., Zhang, Z., Miller, W., and Lipman, D.J. (1997). Gapped BLAST and PSI-BLAST: A new generation of protein database search programs. Nucleic Acids Res. **25:** 3389–3402.

Arbibe, L., Kim, D.W., Batsche, E., Pedron, T., Mateescu, B., Muchardt, C., Parsot, C., and Sansonetti, P.J. (2007). An injected bacterial effector targets chromatin access for transcription factor NF-kappaB to alter transcription of host genes involved in immune responses. Nat. Immunol. **8:** 47–56.

Armstrong, M.R., et al. (2005). An ancestral oomycete locus contains late blight avirulence gene Avr3a, encoding a protein that is recognized in the host cytoplasm. Proc. Natl. Acad. Sci. USA **102:** 7766–7771.

Baek, D., et al. (2004). Bax-induced cell death of *Arabidopsis* is meditated through reactive oxygen-dependent and -independent processes. Plant Mol. Biol. **56:** 15–27.

Ballvora, A., Ercolano, M.R., Weiss, J., Meksem, K., Bormann, C.A., Oberhagemann, P., Salamini, F., and Gebhardt, C. (2002). The R1 gene for potato resistance to late blight (*Phytophthora infestans*) belongs to the leucine zipper/NBS/LRR class of plant resistance genes. Plant J. **30:** 361–371.

Bhattacharjee, S., Hiller, N.L., Liolios, K., Win, J., Kanneganti, T.D., Young, C., Kamoun, S., and Haldar, K. (2006). The malarial host-targeting signal is conserved in the Irish potato famine pathogen. PLoS Pathog. **2:** 453–465.

Birch, P.R., Rehmany, A.P., Pritchard, L., Kamoun, S., and Beynon, J.L. (2006). Trafficking arms: Oomycete effectors enter host plant cells. Trends Microbiol. **14:** 8–11.

Bos, J.I.B., Kanneganti, T.-D., Young, C., Cakir, C., Huitema, E., Win, J., Armstrong, M., Birch, P.R.J., and Kamoun, S. (2006). The C-terminal half of *Phytophthora infestans* RXLR effector AVR3a is sufficient to trigger R3a-mediated hypersensitivity and suppress INF1-induced cell death in *Nicotiana benthamiana.* Plant J. **48:** 165–176.

Chang, J.H., Goel, A.K., Grant, S.R., and Dangl, J.L. (2004). Wake of the flood: Ascribing functions to the wave of type III effector proteins of phytopathogenic bacteria. Curr. Opin. Microbiol. **7:** 11–18.

Chisholm, S.T., Coaker, G., Day, B., and Staskawicz, B.J. (2006). Host-microbe interactions: Shaping the evolution of the plant immune response. Cell **124:** 803–814.

Clem, R.J. (2007). Baculoviruses and apoptosis: A diversity of genes and responses. Curr. Drug Targets **8:** 1069–1074.

Dodds, P.N., Lawrence, G.J., Catanzariti, A.M., Teh, T., Wang, C.I., Ayliffe, M.A., Kobe, B., and Ellis, J.G. (2006). Direct protein interaction underlies gene-for-gene specificity and coevolution of the flax resistance genes and flax rust avirulence genes. Proc. Natl. Acad. Sci. USA **103:** 8888–8893.

Enkerli, K., Hahn, M.G., and Mims, C.W. (1997). Ultrastructure of compatible and incompatible interactions of soybean roots infected with the plant pathogenic oomycete *Phytophthora sojae.* Can. J. Bot. **75:** 1494–1508.

Erwin, D.C., and Ribiero, O.K. (1996). *Phytophthora* Diseases Worldwide. (St. Paul, MN: APS Press).

Fesik, S.W., and Shi, Y. (2001). Structural biology. Controlling the caspases. Science **294:** 1477–1478.

Forster, H., Tyler, B.M., and Coffey, M.D. (1994). *Phytophthora-sojae* races have arisen by clonal evolution and by rare outcrosses. Mol. Plant Microbe Interact. **7:** 780–791.

Gao, H., Narayanan, N.N., Ellison, L., and Bhattacharyya, M.K. (2005). Two classes of highly similar coiled coil-nucleotide binding-leucine rich repeat genes isolated from the *Rps*1-k locus encode *Phytophthora* resistance in soybean. Mol. Plant Microbe Interact. **18:** 1035–1045.

Hahn, M., and Mendgen, K. (2001). Signal and nutrient exchange at biotrophic plant-fungus interfaces. Curr. Opin. Plant Biol. **4:** 322–327.

He, P., Shan, L., and Sheen, J. (2007). Elicitation and suppression of microbe-associated molecular pattern-triggered immunity in plant-microbe interactions. Cell. Microbiol. **9:** 1385–1396.

Hellens, R., Mullineaux, P., and Klee, H. (2000). Technical focus: A guide to *Agrobacterium* binary Ti vectors. Trends Plant Sci. **5:** 446–451.

Hiller, N.L., Bhattacharjee, S., van Ooij, C., Liolios, K., Harrison, T., Lopez-Estrano, C., and Haldar, K. (2004). A host-targeting signal in virulence proteins reveals a secretome in malarial infection. Science **306:** 1934–1937.

Hoeberichts, F.A., and Woltering, E.J. (2002). Multiple mediators of plant programmed cell death: interplay of conserved cell death mechanisms and plant-specific regulators. Bioessays **25:** 47–57.

Hotson, A., and Mudgett, M.B. (2004). Cysteine proteases in phytopathogenic bacteria: Identification of plant targets and activation of innate immunity. Curr. Opin. Plant Biol. **7:** 384–390.

Huang, S., van der Vossen, E.A., Kuang, H., Vleeshouwers, V.G., Zhang, N., Borm, T.J., van Eck, H.J., Baker, B., Jacobsen, E., and Visser, R.G. (2005). Comparative genomics enabled the isolation of the *R*3a late blight resistance gene in potato. Plant J. **42:** 251–261.

Jamir, Y., Guo, M., Oh, H.S., Petnicki-Ocwieja, T., Chen, S.R., Tang, X.Y., Dickman, M.B., Collmer, A., and Alfano, J.R. (2004). Identification of *Pseudomonas syringae* type III effectors that can suppress programmed cell death in plants and yeast. Plant J. **37:** 554–565.

Janjusevic, R., Abramovitch, R.B., Martin, G.B., and Stebbins, C.E. (2006). A bacterial inhibitor of host programmed cell death defenses is an E3 ubiquitin ligase. Science **311:** 222–226.

Jia, Y., McAdams, S.A., Bryan, G.T., Hershey, H.P., and Valent, B. (2000). Direct interaction of resistance gene and avirulence gene products confers rice blast resistance. EMBO J. **19:** 4004–4014.

Jiang, R.H.Y., Tripathy, S., Govers, F., and Tyler, B.M. (2008). RXLR effector reservoir in two *Phytophthora* species is dominated by a single rapidly evolving super-family with more than 700 members. Proc. Natl. Acad. Sci. USA **105:** 4874–4879.

Jones, J.D., and Dangl, J.L. (2006). The plant immune system. Nature **444:** 323–329.

Judelson, H.S., Tyler, B.M., and Michelmore, R.W. (1991). Transformation of the oomycete pathogen, *Phytophthora infestans.* Mol. Plant Microbe Interact. **4:** 602–607.

Kamoun, S. (2007). Groovy times: Filamentous pathogen effectors revealed. Curr. Opin. Plant Biol. **10:** 358–365.

Kampranis, S.C., Damianova, R., Atallah, M., Toby, G., Kondi, G., Tsichlis, P.N., and Makris, A.M. (2000). A novel plant glutathione S-transferase/peroxidase suppresses Bax lethality in yeast. J. Biol. Chem. **275:** 29207–29216.

Kay, S., Hahn, S., Marois, E., Hause, G., and Bonas, U. (2007). A bacterial effector acts as a plant transcription factor and induces a cell size regulator. Science **318:** 648 –651.

Kjemtrup, S., Nimchuk, Z., and Dangl, J.L. (2000). Effector proteins of phytopathogenic bacteria: Bifunctional signals in virulence and host recognition. Curr. Opin. Microbiol. **3:** 73–78.

Lacomme, C., and Cruz, S.S. (1999). Bax-induced cell death in tobacco is similar to the hypersensitive response. Proc. Natl. Acad. Sci. USA **96:** 7956–7961.

Lu, R., Malcuit, I., Moffett, P., Ruiz, M.T., Peart, J., Wu, A.J., Rathjen, J.P., Bendahmane, A., Day, L., and Baulcombe, D.C. (2003). High throughput virus-induced gene silencing implicates heat shock protein 90 in plant disease resistance. EMBO J. **22:** 5690–5699.

McLeod, A., Fry, B.A., Zuluaga-Duque, A.P., Meyers, K.L., and Fry, W.E. (2008). Towards improvements of oomycete transformation protocols. J. Eukaryot. Microbiol. **55:** 103–109.

Madeo, F., Frohlich, E., Ligr, M., Grey, M., Sigrist, S.J., Wolf, D.H., and Frohlich, K.U. (1999). Oxygen stress: A regulator of apoptosis in yeast. J. Cell Biol. **145:** 757–767.

Madeo, F., Herker, E., Wissing, S., Jungwirth, H., Eisenberg, T., and Froehlich, K.-U. (2004). Apoptosis in yeast. Curr. Opin. Microbiol. **7:** 655–660.

Marti, M., Good, R.T., Rug, M., Knuepfer, E., and Cowman, A.F. (2004). Targeting malaria virulence and remodeling proteins to the host erythrocyte. Science **306:** 1930–1933.

Mindrinos, M., Katagiri, F., Yu, G.L., and Ausubel, F.M. (1994). The *A. thaliana* disease resistance gene RPS2 encodes a protein containing a nucleotide-binding site and leucine-rich repeats. Cell **78:** 1089–1099.

Mota, L.J., and Cornelis, G.R. (2005). The bacterial injection kit: Type III secretion systems. Ann. Med. **37:** 234–249.

Mudgett, M.B. (2005). New insights to the function of phytopathogenic bacterial type iii effectors in plants. Annu. Rev. Plant Biol. **56:** 509–531.

Nomura, K., Debroy, S., Lee, Y.H., Pumplin, N., Jones, J., and He, S.Y. (2006). A bacterial virulence protein suppresses host innate immunity to cause plant disease. Science **313:** 220–223.

Nurnberger, T., Brunner, F., Kemmerling, B., and Piater, L. (2004). Innate immunity in plants and animals: Striking similarities and obvious differences. Immunol. Rev. **198:** 249–266.

Qutob, D., Kamoun, S., and Gijzen, M. (2002). Expression of a *Phytophthora sojae* necrosis-inducing protein occurs during transition from biotrophy to necrotrophy. Plant J. **32:** 361–373.

Rehmany, A.P., Gordon, A., Rose, L.E., Allen, R.L., Armstrong, M.R., Whisson, S.C., Kamoun, S., Tyler, B.M., Birch, P.R., and Beynon, J.L. (2005). Differential recognition of highly divergent downy mildew avirulence gene alleles by RPP1 resistance genes from two *Arabidopsis* lines. Plant Cell **17:** 1839–1850.

Sandhu, D., Gao, H., Cianzio, S., and Bhattacharyya, M.K. (2004). Deletion of a disease resistance nucleotide-binding-site leucine-rich-repeat-like sequence is associated with the loss of the *Phytophthora* resistance gene *Rps*4 in soybean. Genetics **168:** 2157–2167.

Shan, W.X., Cao, M., Dan, L.U., and Tyler, B.M. (2004). The *Avr1b* locus of *Phytophthora sojae* encodes an elicitor and a regulator required for avirulence on soybean plants carrying resistance gene *Rps*1b. Mol. Plant Microbe Interact. **17:** 394–403.

Slusarenko, A.J., and Schlaich, N.L. (2003). Pathogen profile. Downy mildew of *Arabidopsis thaliana* caused by *Hyaloperonospora parasitica* (formerly *Peronospora parasitica*). Mol. Plant Pathol. **4:** 159–170.

Sogin, M.L., and Silberman, J.D. (1998). Evolution of the protists and protistan parasites from the perspective of molecular systematics. Int. J. Parasitol. **28:** 11–20.

Song, J., Bradeen, J.M., Naess, S.K., Raasch, J.A., Wielgus, S.M., Haberlach, G.T., Liu, J., Kuang, H., Austin-Phillips, S., Buell, C.R., Helgeson, J.P., and Jiang, J. (2003). Gene *Rb* cloned from *Solanum bulbocastanum* confers broad spectrum resistance to potato late blight. Proc. Natl. Acad. Sci. USA **100:** 9128–9133.

Thompson, J.D., Higgins, D.G., and Gibson, T.J. (1994). CLUSTAL W: Improving the sensitivity of progressive multiple sequence alignment through sequence weighting, position-specific gap penalties and weight matrix choice. Nucleic Acids Res. **22:** 4673–4680.

Tyler, B.M. (2007). *Phytophthora sojae*: Root rot pathogen of soybean and model oomycete. Mol. Plant Pathol. **8:** 1–8.

Tyler, B.M., Forster, H., and Coffey, M.D. (1995). Inheritance of avirulence factors and restriction-fragment-length-polymorphism markers in outcrosses of the oomycete *Phytophthora sojae.* Mol. Plant Microbe Interact. **8:** 515–523.

Tyler, B.M., et al. (2006). *Phytophthora* genome sequences uncover evolutionary origins and mechanisms of pathogenesis. Science **313:** 1261–1266.

Van der Biezen, E.A., and Jones, J.D. (1998). Plant disease-resistance proteins and the gene-for-gene concept. Trends Biochem. Sci. **23:** 454–456.

van der Vossen, E., Sikkema, A., Hekkert, B.L., Gros, J., Stevens, P., Muskens, M., Wouters, D., Pereira, A., Stiekema, W., and Allefs, S. (2003). An ancient R gene from the wild potato species *Solanum bulbocastanum* confers broad-spectrum resistance to *Phytophthora infestans* in cultivated potato and tomato. Plant J. **36:** 867–882.

van der Vossen, E.A.G., Gros, J., Sikkema, A., Muskens, M., Wouters, D., Wolters, P., Pereira, A., and Allefs, S. (2005). The *Rpi-blb2* gene from *Solanum bulbocastanum* is an *Mi*-1 gene homolog conferring broad-spectrum late blight resistance in potato. Plant J. **44:** 208–222.

Vega-Sánchez, M.E., Redinbaugh, M.G., Costanzo, S., and Dorrance, A.E. (2005). Spatial and temporal expression analysis of defense-related genes in soybean cultivars with different levels of partial resistance to *Phytophthora sojae.* Physiol. Mol. Plant Pathol. **66:** 175–182.

Watanabe, N., and Lam, E. (2006). *Arabidopsis* Bax inhibitor-1 functions as an attenuator of biotic and abiotic types of cell death. Plant J. **45:** 884–894.

Whisson, S.C., Basnayake, S., Maclean, D.J., Irwin, J.A., and Drenth, A. (2004). *Phytophthora sojae* avirulence genes *Avr4* and *Avr6* are located in a 24kb, recombination-rich region of genomic DNA. Fungal Genet. Biol. **41:** 62–74.

Whisson, S.C., et al. (2007). A translocation signal for delivery of oomycete effector proteins into host plant cells. Nature **450:** 115–118.

Win, J., Morgan, W., Bos, J., Krasileva, K.V., Cano, L.M., Chaparro-Garcia, A., Ammar, R., Staskawicz, B.J., and Kamoun, S. (2007). Adaptive evolution has targeted the C-Terminal domain of the RXLR effectors of plant pathogenic oomycetes. Plant Cell **19:** 2349–2369.

Wroblewski, T., Piskurewicz, U., Tomczak, A., Ochoa, O., and Michelmore, R.W. (2007). Silencing of the major family of NBS-LRR-encoding genes in lettuce results in the loss of multiple resistance specificities. Plant J. **51:** 803–818.

Yang, H., Yang, S., Li, Y., and Hua, J. (2007). The *Arabidopsis BAP*1 and *BAP2* genes are general inhibitors of programmed cell death. Plant Physiol. **145:** 135–146.

Yang, S.H., Yang, H.J., Grisafi, P., Sanchatjate, S., Fink, G.R., Sun, Q., and Hua, J. (2006). The *BON*/*CPN* gene family represses cell death and promotes cell growth in *Arabidopsis.* Plant J. **45:** 166–179.

Conserved C-Terminal Motifs Required for Avirulence and Suppression of Cell Death by *Phytophthora sojae effector* Avr1b

Daolong Dou, Shiv D. Kale, Xinle Wang, Yubo Chen, Qunqing Wang, Xia Wang, Rays H.Y. Jiang, Felipe D. Arredondo, Ryan G. Anderson, Poulami B. Thakur, John M. McDowell, Yuanchao Wang and Brett M. Tyler

Plant Cell 2008;20;1118-1133; originally published online April 4, 2008;
DOI 10.1105/tpc.107.057067

Supplemental Data. Dou et al. (2008) Conserved C-terminal motifs required for avirulence and suppression of cell death by *Phytophthora sojae* effector Avr1b.

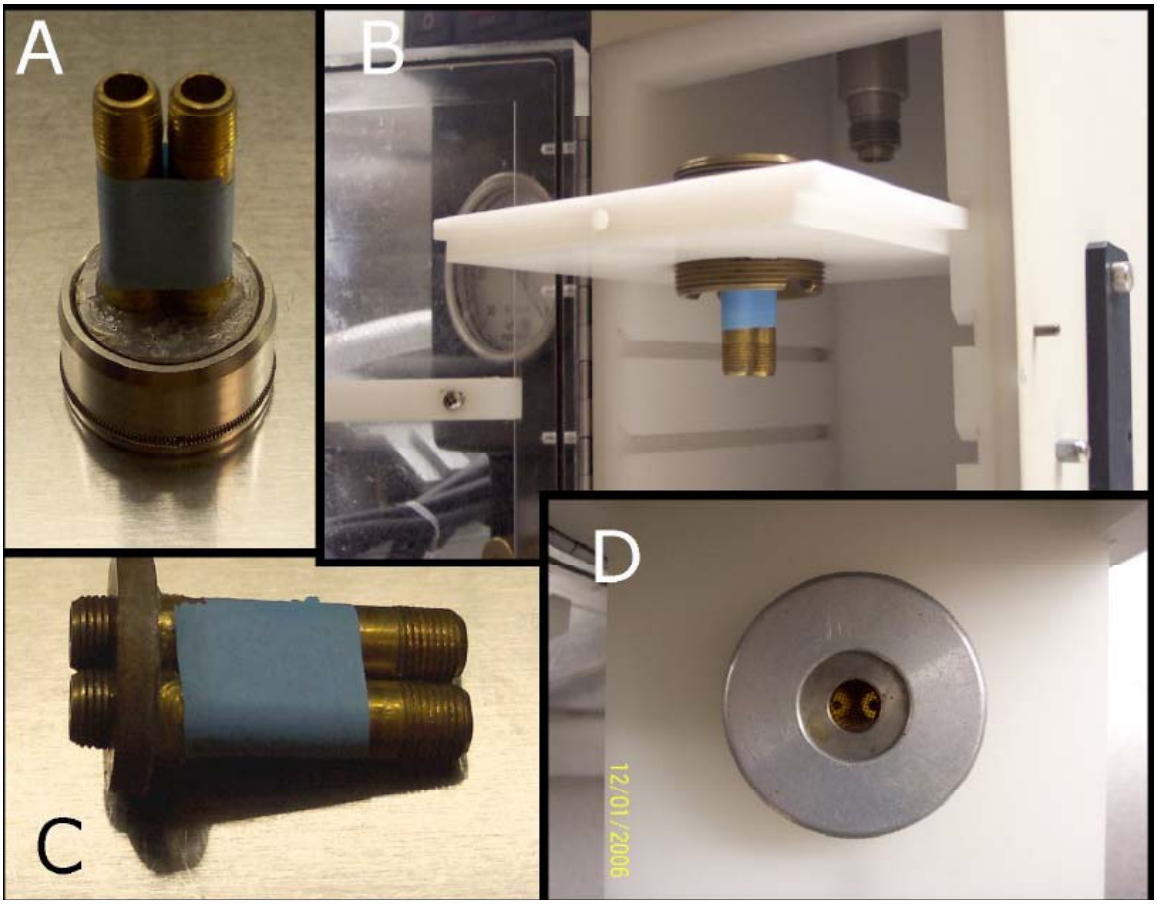

Supplemental Figure S1. The double-barreled particle bombardment device.

(A) – **(D)** show four views of the device. **(B)** shows the device inserted into the Gene Gun.

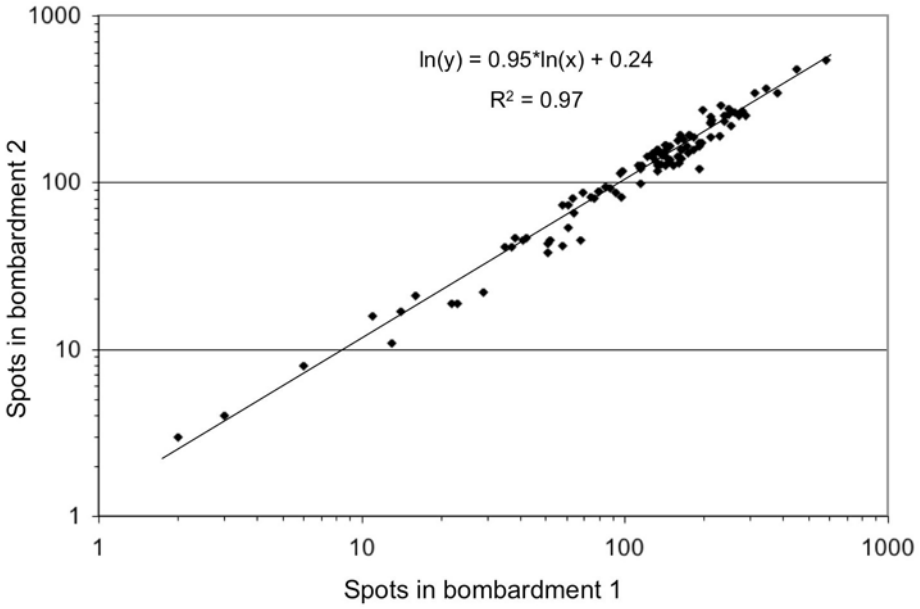

Supplemental Figure S2. Correlation between replicate bombardments produced by double-barreled bombardment. Results are plotted from 104 pairs of shots from 18 experiments in which there was no significant difference between the constructs in the two replicates.

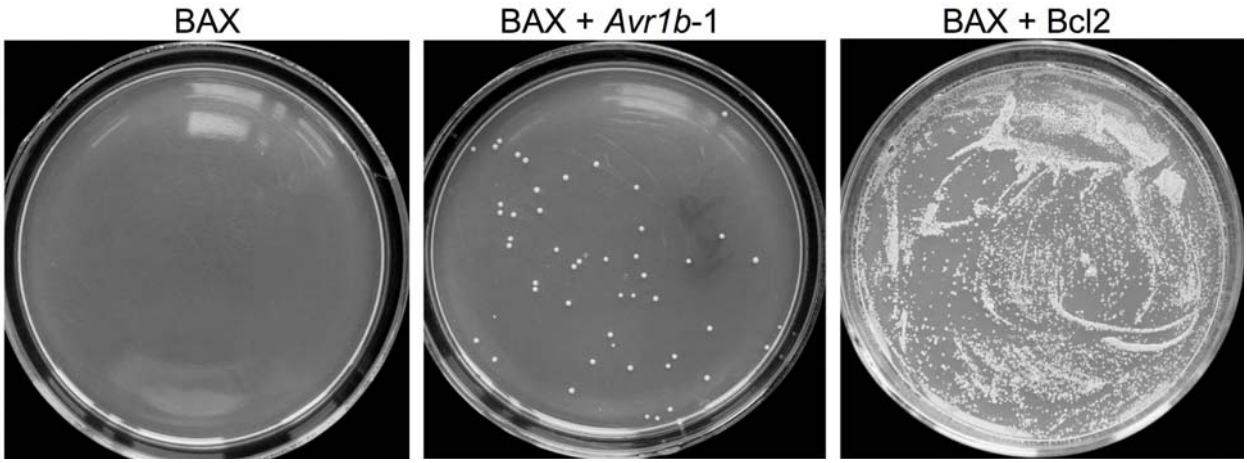

Supplemental Figure 3. Comparison of ability of Avr1b and Bcl2 to suppress BAX-mediated cell death in yeast. Yeast cells of strain W303 containing the Bax cDNA under control of the galactose inducible *GAL1* promoter either alone (BAX) or together with *Avr1b*-1 or Bcl2 under control of the *GAL1* promoter (BAX + Avr1b) were grown on glucose-containing medium, then harvested, diluted and plated on galactose-containing medium as detailed in the Methods section.

Supplemental Figure 4. Sequences and motif structures of Avr and Avh proteins

Supplemental Table 1. Details of Avr1b family proteins.

Gene Name[a]	Species[b]	Accession Number	Location in genome sequence[c]	Protein Length	Leader Length[d]	RXLR position[e]	dEER position	Similarity (%)[f]
Ps*Avr1b*-1	Ps	AAM20937	Sc37: 171847-172263	138	21	52-55	58-65	138/138 (100%)
PsAvr1b^{P7064}	Ps	AAM20936	P7064 (A)	138	21	52-55	58-65	137/138 (99%)
PsAvr1b^{P7076}	Ps	AF449624	P7076 (V)	138	21	52-55	58-65	131/138 (94%)
PsAvr1b^{P7081}	Ps	AF449623	P7081 (V)	138	21	52-55	58-65	131/138 (94%)
PsAvr1b^{P7074}	Ps	AF449625	P7074 (V)	138	21	52-55	58-65	131/138 (94%)
PsAvh1	Ps	AAM20941	Sc60: 179783-180199	138	21	52-55	58-65	129/138 (93%)
PsAvh4	Ps	EU282486	Sc108: 128933-129385	151	21	55-58	62-71	89/154 (57%)
PcAvh1	Pc	EU282489	Sc6: 931495-931893	132	21	46-49	53-63	86/141 (60%)
PcAvh2	Pc		Sc6: 1028084-1028452	122	21	45-48	52-58	80/136 (58%)
PcAvh3[g]	Pc		Sc6:943301-943698	132	21	46-49	55-60	87/144 (60%)
PcAvh4	Pc		Sc6:981362-981739	125	21	48-51	55-62	82/139 (59%)
PcAvh5[g]	Pc		Sc10: 1176255-1176640	128	21	48-51;56-59;64-67	None	72/139 (52%)
PcAvh6	Pc		Sc6:914793-915194	111	21	46-49	53-64	67/144 (46%)
PcAvh7[g]	Pc		Sc6: 894097-894486	129	21	45-48	52-62	81/145 (56%)
PITG_13593 [g]	Pi		Sc29: 1252049-1252471	141	24	42-45	49-54	75/136 (55%)
PITG_05918.1	Pi		Sc9: 1600969-1601373	135	21	54-57	58-66	73/137 (53%)
PiAvh9.1	Pi	EU282488	Sc9: 1500623-1501027	135	21	54-57	58-66	77/138 (55%)
PITG_05912.1	Pi		Sc9: 1502803-1503207	135	21	54-57	58-66	77/138 (55%)
PEX147-3	Pi	CAI72350	Pi T30-4	147	21	44-47	50-59	71/150 (47%)
PITG_14374.1	Pi		Sc34: 578150-578590	147	21	44-47	50-59	71/150 (47%)
PEX147-2	Pi	CAI72329	Pi T30-4	148	21	44-47	50-59	70/151 (46%)
PITG_14368.1	Pi		Sc34: 532802-533245	148	21	44-47	50-59	70/151 (46%)
PITG_22089.1	Pi		Sc1810: 1165-1569	135	21	54-57	58-66	74/138 (53%)
PITG_14371.1	Pi		Sc34: 566355-566795	147	21	44-47	50-59	69/150 (46%)
Pi Avr3a^{KI}	Pi	AAN31507	Sc29: 1252049-1252471	147	21	44-47	50-59	69/150 (46%)
Pi avr3a^{EM}	Pi	CAI72345	Pi T30-4 (V)	147	21	44-47	50-59	68/150 (45%)

[a] Superscripts indicate alleles. Gene names starting with PITG indicate gene models from the *P. infestans* genome sequence. Underlined genes were used for the alignment in Figure 3A

[b] Ps, *P. sojae*; Pc, *P. capsici* and Pi, *P. infestans*.

[c] Locations indicate scaffold (Sc) and coordinates for versions 1.1, 1.0 and 1.0 of the *P. sojae*, *P. capsici* and *P. infestans* genomes sequences respectively. Where genes come from strains that have not been sequenced, the strain name is given. Where an avirulence gene has been obtained from a non-sequenced strains, the avirulence phenotype of the strain is also given (A= avirulent; V = virulent).

[d] Leader indicates secretory leader predicted by the algorithm SignalP available at http://www.cbs.dtu.dk/services.

[e] PcAvh5 has three possible RXLR motifs. Avr1b has two RXLR strings but the coordinates are given only for the functional motif determined experimentally by Dou et al (2008). PITG_13593 contains the RXLR-like motif KRIR

[f] percentage similarity to Avr1b from sequenced strain P6497 determined by Smith-Waterman.

[g] PcAvh3 and PcAvh5 include frameshifts in codons 20 and 80, respectively and PcAvh7 includes two frameshifts in codons 11 and 27; these may be true mutations or may be sequencing errors. PITG_13593 contains RXLR similar motif KRIR.

Supplemental Table 2. Complete data for soybean bombardment assays of suppression of BAX mediated PCD by Avr1b-1 mutants and other W-Y-motif effectors

Gene	Indirect assay				Direct assay		Anti-PCD Activity[d]
	(BAX+EV) /EV[a]	(Gene+BAX) /EV[a]	Ratio [b]	p value [b]	(BAX+Gene)/ (BAX+EV)[a]	p value [c]	
Avr1b WT	0.12±0.02	0.34±0.04	2.84	p<0.001	3.36±0.66	p<0.001	Yes
Avr1b^{P7076}	0.07±0.01	0.08±0.02	1.07	p>0.1	0.74±0.09	p>0.1	No
Avr1bK1	0.07±0.01	0.36±0.04	4.87	p<0.001	2.41±0.13	p<0.001	Yes
Avr1bW1	0.11±0.02	0.08±0.02	0.68	p>0.1	0.99±0.27	p>0.1	No
Avr1bW2	0.08±0.02	0.30±0.02	3.81	p<0.001	3.48±0.81	p<0.001	Yes
Avr1bW3	0.10±0.02	0.08±0.02	0.82	p>0.1	1.03±0.10	p>0.1	No
Avr1bW4	0.11±0.02	0.08±0.02	0.72	p>0.1	0.87±0.07	p>0.1	No
Avr1bW5	0.11±0.02	0.12±0.01	1.06	p>0.1	0.93±0.09	p>0.1	No
Avr1bW6	0.12±0.01	0.40±0.16	3.46	p<0.001	3.12±0.55	p<0.001	Yes
Avr1bY1	0.11±0.02	0.17±0.02	1.55	p<0.05	1.80±0.49	p<0.01	Medium
PsAvh163	0.10±0.02	0.30±0.13	3.00	p<0.001	1.57±0.26	p<0.001	Yes
PsAvh331	0.10±0.01	0.60±0.03	6.93	p<0.001	6.17±0.66	p<0.001	Yes
HpRXL96	0.12±0.03	0.39±0.06	3.25	p<0.001	3.62±0.74	p<0.001	Yes
Avr4/6	0.10±0.01	0.07±0.02	0.70	p>0.1	1.01±0.33	p>0.1	No

[a] average ratio and standard error from 14-16 pairs of shots

[b] Ratio from indirect assay is calculated as (BAX+gene/EV ratio)/(BAX/EV ratio). p value was calculated for the comparison using the Wilcoxon rank sum test.

[c] p value for direct assay calculated using the Wilcoxon signed rank test

[d] The Anti-PCD Activity of each gene is determined by whether the ratios for both direct and indirect assays are statistically significantly greater than 1.0

Supplemental Table 3. Assay data for bombardment assay Avr1b avirulence function

Gene[a]	GUS spot ratio [b]		Ratio of Rps1b/rps[c]	p value[c]	Avirulence[d]
	rps	Rps1b			
Avr1b WT	1.26±0.07	0.28±0.03	0.22	<0.001	Yes
Avr1b^{P7076}	0.99±0.03	1.00±0.03	1.01	>0.1	No
Avr1bK1	1.02±0.05	0.16±0.04	0.16	<0.001	Yes
Avr1bW1	1.02±0.06	1.04±0.06	1.02	>0.1	No
Avr1bW2	1.00±0.04	0.96±0.07	0.96	>0.1	No
Avr1bW3	1.03±0.04	1.05±0.03	1.02	>0.1	No
Avr1bW4	1.03±0.04	1.05±0.04	1.01	>0.1	No
Avr1bW5	0.99±0.04	0.20±0.03	0.20	<0.001	Yes
Avr1bW6	0.98±0.03	0.18±0.01	0.18	<0.001	Yes
Avr1bY1	1.04±0.05	1.04±0.06	1.00	>0.1	No

a Gene indicates Avr1b allele and mutants shown in Figure 4A of the main text.

b Ratio of blue spots in the presence of the assayed *Avr1b*-1 gene, compared to the empty vector (EV) when bombarded onto leaves from *rps* plants (Williams) or *Rps*1b plants (L77-1863). Averages and standard errors are from 16 pairs of shots.

c Ratio is calculated as (Rps1b ratio)/(rps ratio). p values were calculated using the Wilcoxon rank sum test.

d Avirulence based on an Rps1b/rps ratio statistically significantly less than 1.0.

Supplemental Table 4. Assay data for avirulence tests of *P. sojae* stable transformants.

Gene[a]	*P. sojae* Recipient[b]	Number[c]	Transgene DNA PCR[d]	Transgene RT-PCR[d]	Inoculation results[e]			
					rps		Rps1b	
Avr1b WT	P7076	2	+	+	1/12	V	12/14	A
Avr1bW1	P7076	4	+	+	1/9	V	5/18	V
Avr1bW2	P7076	4	+	+	3/15	V	3/31	V
Avr1bY1	P7076	2	+	+	2/15	V	1/30	V
GUS	P7076	2	-	-	1/8	V	2/16	V
None	P7064	n.a.	-	-	0/10	V	15/17	A

[a] All genes were driven by the strong constitutive promoter HAM34. GUS represents the gene coding for ß-glucuronidase.

[b] *P. sojae* strains P7076 and P7064 are virulent and avirulent respectively on Rps1b cultivars.

[c] number of independent positive *P. sojae* transformants. n.a. = not applicable.

[d] The presence of the transgenes in the transformants were verified by genomic DNA PCR. Expression of the transgenes was confirmed by both qualitative RT-PCR and quantitative real time PCR. RNA was extracted from mycelium grown in V8 broth. No *Avr1b*-1 transgene RNA were found in the Gus transformants nor in untransformed P7064.

[e] Surviving seedlings number in total inoculated seedlings by hypocotyl inoculations as methods on the cultivar Williams (rps) or the near-isogenic lines L77-1863 (Rps1b) and Haro (1-7) (rps) or the near-isogenic lines Haro13 (Rps1b), only one time inoculation results, in three duplications, are shown. V indicates virulence and A for avirulence.

Supplemental Table 5. Summary of oligonucleotides used

No.	Name	Sequences (from 5' to 3')	Usage
1	HamF	TTCTCCTTTTCACTCTCACG	Primers in Ham34 promoter and terminator, for screening *P. sojae* transformants
2	HamR	AGACACAAAATCTGCAACTTC	
3	Avr1bReF	ACCTTCAGCGTGACTGACCT	Internal primers of *Avr1b*-1, used for RT-PCR and real time PCR assay for *Avr1b*-1 mRNA
4	Avr1bReR	GCGATTGCCAACCAGTTCT	
5	ActinF	CGACATCCGTAAGGACCTGT	Internal primers of *P. sojae* Actin gene, for RT-PCR and real time PCR mRNA assays
6	ActinR	TTCGAGATCCACATCTGCTG	
7	PrimerC	ggggtaccgacaaca**ATG**CGTCTATCTTTTGTGCT	For insertion of *Avr1b*-1 genes into *P. sojae* transformation vector
8	PrimerD	ggggtacc**TCA**GCTCTGATACCGGTGAA	
9	Avr1bF	atcgcactcgagctttcgcagatcccgggggcaatgagat**atg**ACTGAGTACTCCGACGAA	For insertion of *Avr1b*-1 genes into plant transient expression assay vector, pCambia1305.2
10	Avr1bR	gaaactcgagcttgtcgatcgacagatccggtcggcaggtacc**TCA**GCTCTGATACCGGTG	
11	Avr1bP7076R	taaggtacc**TCA**GCTCTGATACAGGTG	Use with Avr1bF to amplify *Avr1b*-1 allele from *P. sojae* strain P7076
12	BaxF	agatcccgggggcaatgagat**ATG**GACGGGTCCGGGGAG	Insertion of BAX gene into soybean transient expression assay vector
13	BaxR	ggcaggtacc**TCA**GCCCATCTTCTTCCAG	
14	Avh163F	agatcccgggggcaatgagat**atg**GTATCAGCACTCCAGCTCCCCG	Insertion of PsAvh163 gene into soybean transient expression vector
15	Avh163R	ggcaggtacc**CTA**AGAGCGCCGAGGGGTCACAT	
16	Hp96F	agatcccgggggcaatgagat**atg**GTGGTGGTAGCCACCTTCCAGGCT	Insertion of HpRXL96 into soybean transient expression assay vector
17	Hp96R	cggcaggtacc**TCA**CGATGACGATGAGGGCGGGTGCCA	
18	Avr4F	agatcccgggggcaatgagat**atg**ATCACAGATGAGTCTCAG	Insertion of *Avr4/6* gene into soybean transient expression assay vector
19	Avr4R	ggcaggtacc**TTA**CGTTAGGTGGTGTAG	
20	Avh331F	agatcccgggggcaatgagat**atg**CTCACTTGCGCCACCTCC	Insertion of PsAvh331 gene into soybean transient expression assay vector
21	Avh331R	Ggcaggtacc**TCA**GATAATCATGATGCT	
22	Avr1bK1F	CcAGGTGGCGGCCcAAcAGTTGGCCcAGGCGATG	Creation of Avr1bK1 mutation
23	Avr1bK1R	CTgTTgGGCCGCCACCTgGTTCCAC	
24	Avr1bW1F	AGAAGgcGTACgGCCTGGATAAGggCAAGAACTGGgcGGCAATCG	Creation of Avr1bW1 mutation
25	Avr1bW1R	CCAGGCcGTACgcCTTCTTTGCCgcCTTCTCGgcCGCTTTCT	
26	Avr1bW2F	gcAAGGGGTACAGCCTGagTAgcATCAAGAgCTGGTTG	Creation of Avr1bW2 mutation
27	Avr1bW2R	CAGGCTGTACCCCTTgcTTGCCCACTTgctGTACGCT	
28	Avr1bW3F	GTACAGCCTGGgTggAggTggGAACTGGTTGG	Creation of Avr1bW3 mutation
29	Avr1bW3R	CCAACCAGTTCCcAccTccAccCAGGCTGTAC	
30	Avr1bW4F	CTGGATAAGggtAAGAACTGGTTG	Creation of Avr1bW4 mutation
31	Avr1bW4R	CAACCAGTTCTTaccCTTATCCAG	
32	Avr1bW5F	CTGGATAAGgcCAAGAACTGGTTG	Creation of Avr1bW5 mutation
33	Avr1bW5R	CAACCAGTTCTTGgcCTTATCCAG	
34	Avr1bW6F	CTGGATAAGgTCAAGAACTGGTTG	Creation of Avr1bW6 mutation
35	Avr1bW6R	CAACCAGTTCTTGAcCTTATCCAG	
36	Avr1bY1F	cTgcCTACgcCGcgTACACCgcTgcCCGGTATC	Creation of Avr1bY1 mutation
37	Avr1bY1R	TGTAcgCGgcGTAGgcAgcTgCAgcCTTCCCCTTCT	
38	AvrYeastF	cgcgaattc**ATG**CGTCTATCTTTTGTGCT	Insertion of *Avr1b*-1 into yeast expression vector
39	AvrYeastR	tatgtcgac**TCA**GCTCTGATACAGGTGAA	

40	Avr1bPVXF	ggcatcgat**ATG**CGTCTATCTTTTGTGC	Insertion of *Avr1b*-1 into PVX vector
41	Avr1bPVXR	catgtcgac**TCA**GCTCTGATACAGGTG	
42	BaxPVXF	ggcatcgat**ATG**GACGGGTCCGGGGAG	Insertion of BAX into PVX vector
43	BaxPVXR	catgtcgac**TCA**GCCCATCTTCTTCCAG	
44	Avh331PVXF	gtacccgggT**ATG**ATGCAATGGAGCGCAATC	Insertion of *PsAvh331* into PVX vector
45	Avh331PVXR	ggcgtcgac**TCA**GATAATCATGATGCTGTTC	
46	GusF_EcoRI	TCCCGaaTTCAGTTTAGCTTCATG	Transfer of GUSPlus expression cassette from pCambia1305.2 to pUC19
47	GusR_HindIII	TAGTaagcTTCCCGATCTAGTAACAT	
48	GusF	CAcccgggAAGA**ATG**GTCCGTCCTGTAGAAACCC	Transfer of GUSPlus coding region from pCambia1305.2 to pHAMT35N
49	GusR	TAggtaccTCATTGTTTGCCTCCCTGCTGC	
50	Avr1b_EcoRI	GGAGgaaTTcGCTGGCTGGTGGCAGGAT	Transfer of Avr1b expression cassette from pCambia1305.2 into pUC19 vector with addition of *Xma* I and *Kpn* I sites flanking *Avr1b*-1 gene
51	Avr1b_HindIII	GTATTGGCTAGAGaAGCTTGCCA	
52	Avr1b_genegun_KpnI	AGAAACTCGAGCTTGTCGATCGACAGATCCGGTCGGCAggTACcTCAGCTCTGATAC	

Notes: Uppercase letters indicate bases that match the initial template. Lower case letters indicate mutations or 5' extensions that do not match the initial template. Restriction sites introduced into the amplicon are underlined and start or stop codons are both in bold.

The Plant Cell, Vol. 20: 1930–1947, July 2008, www.plantcell.org © 2008 American Society of Plant Biologists

RXLR-Mediated Entry of *Phytophthora sojae* Effector *Avr1b* into Soybean Cells Does Not Require Pathogen-Encoded Machinery [W]

Daolong Dou,[1] Shiv D. Kale,[1] Xia Wang, Rays H.Y. Jiang,[2] Nathan A. Bruce, Felipe D. Arredondo, Xuemin Zhang,[3] and Brett M. Tyler[4]

Virginia Bioinformatics Institute, Virginia Polytechnic Institute and State University, Blacksburg, Virginia 24061

Effector proteins secreted by oomycete and fungal pathogens have been inferred to enter host cells, where they interact with host resistance gene products. Using the effector protein Avr1b of *Phytophthora sojae*, an oomycete pathogen of soybean (*Glycine max*), we show that a pair of sequence motifs, RXLR and dEER, plus surrounding sequences, are both necessary and sufficient to deliver the protein into plant cells. Particle bombardment experiments demonstrate that these motifs function in the absence of the pathogen, indicating that no additional pathogen-encoded machinery is required for effector protein entry into host cells. Furthermore, fusion of the Avr1b RXLR-dEER domain to green fluorescent protein (GFP) allows GFP to enter soybean root cells autonomously. The conclusion that RXLR and dEER serve to transduce oomycete effectors into host cells indicates that the >370 RXLR-dEER–containing proteins encoded in the genome sequence of *P. sojae* are candidate effectors. We further show that the RXLR and dEER motifs can be replaced by the closely related erythrocyte targeting signals found in effector proteins of *Plasmodium*, the protozoan that causes malaria in humans. Mutational analysis of the RXLR motif shows that the required residues are very similar in the motifs of *Plasmodium* and *Phytophthora*. Thus, the machinery of the hosts (soybean and human) targeted by the effectors may be very ancient.

INTRODUCTION

Oomycetes are fungal-like organisms that are evolutionarily related to marine algae (Förster et al., 1990; Sogin and Silberman, 1998; Harper et al., 2005). Many oomycete species are destructive plant pathogens, including the potato late blight pathogen that caused the Irish potato famine, *Phytophthora infestans*, the Sudden Oak Death pathogen, *Phytophthora ramorum*, and the soybean root and stem rot pathogen *Phytophthora sojae* (Erwin and Ribiero, 1996). *P. sojae* alone causes $200 to $300 million in annual soybean (*Glycine max*) losses in the US and around $1 to $2 billion in losses per year worldwide (Wrather and Koenning, 2006).

Many bacterial pathogens of plants and animals deliver effector proteins into host cells using the type III secretion machinery, which consists of a pilus that transfers the proteins across the membranes of the bacteria and the host, directly into the host cytoplasm (reviewed in Staskawicz et al., 2001). Most of the disease resistance genes that protect against these pathogens encode intracellular proteins with a nucleotide binding site–leucine-rich repeat (NBS-LRR) domain (Dangl and Jones, 2001). There are some exceptions, such as *Pto*, which encodes a protein kinase (Martin et al., 1993), and *Bs*3, which encodes a flavin monooxygenase (Romer et al., 2007). Many disease resistance genes that protect against fungal and oomycete pathogens also encode NBS-LRR proteins with a predicted intracellular location. Fungal resistance genes include the L, M, N, and P families of flax against flax rust (Lawrence et al., 1995; Anderson et al., 1997; Dodds et al., 2001a, 2001b), the rice (*Oryza sativa*) genes *Pib* (Wang et al., 1999), *Pi-ta* (Bryan et al., 2000), and Pi9 (Qu et al., 2006) against *Magnaporthe grisea*, the *Mla* resistance gene of barley (*Hordeum vulgare*) against the powdery mildew pathogen *Blumeria graminis* f. sp *hordei* (Halterman et al., 2001), the wheat (*Triticum aestivum*) *Lr1* (Cloutier et al., 2007) and *Lr10* (Feuillet et al., 2003) genes against leaf rust, and four alleles of the wheat *Pm3* gene against powdery mildew (Yahiaoui et al., 2004; Srichumpa et al., 2005).

Oomycete resistance genes include the *Arabidopsis thaliana* *Rpp1*, *Rpp2*, *Rpp4*, *Rpp5*, *Rpp7*, *Rpp8*, and *Rpp13* genes against *Hyaloperonospora parasitica* (Slusarenko and Schlaich, 2003), the lettuce (*Lactuca sativa*) *Dm3*, *Dm14*, and *Dm16* resistance genes against *Bremia lactucae* (Shen et al., 2002; Wroblewski et al., 2007), the potato (*Solanum tuberosum*) *R1* (Ballvora et al., 2002), *Rb* (Song et al., 2003; van der Vossen et al., 2003), and *R3a* (Huang et al., 2005) genes against *P. infestans*, and the soybean *Rps*1k (Gao et al., 2005), *Rps*4, and *Rps*6 (Sandhu et al., 2004) genes against *P. sojae*.

The predicted intracellular location of the cognate resistance gene products implies that the fungal and oomycete avirulence factors that interact with these resistance gene products must be

[1] These authors contributed equally to this work.
[2] Current address: Laboratory of Phytopathology, Wageningen University, NL-6709 PD Wageningen, The Netherlands.
[3] Current address: Center for Biosystems Research, University of Maryland Biotechnology Institute, 9600 Gudelsky Dr., Rockville, MD 20850.
[4] Address correspondence to bmtyler@vt.edu.
The author responsible for distribution of materials integral to the findings presented in this article in accordance with the policy described in the Instructions for Authors (www.plantcell.org) is: Brett M. Tyler (bmtyler@vt.edu).
[W] Online version contains Web-only data.
www.plantcell.org/cgi/doi/10.1105/tpc.107.056093

able to enter the cytoplasm of plant cells (Tyler, 2002). Several fungal and oomycete avirulence genes have been cloned that interact genetically with host NBS-LRR resistance genes. Most of these encode secreted proteins, including the flax rust AvrL567, AvrM, AvrP4, and AvrP123 genes (Dodds et al., 2004; Catanzariti et al., 2006), the AvrPita gene of *M. grisea* (Orbach et al., 2000), the *Avr1b*-1 gene from *P. sojae* (Shan et al., 2004), the *Avr3a* gene from *P. infestans* (Armstrong et al., 2005), and the *ATR13* (Allen et al., 2004) and *ATR1* (Rehmany et al., 2005) genes from the *Arabidopsis* downy mildew pathogen *H. parasitica*. Furthermore, in many of these cases, expression of the pathogen avirulence gene inside the host cytoplasm resulted in recognition of the avirulence proteins by the plant receptors, confirming that the cytoplasm was the site of interaction between the resistance gene products and the avirulence proteins (Allen et al., 2004; Dodds et al., 2004; Armstrong et al., 2005; Rehmany et al., 2005; Catanzariti et al., 2006). The AVR_{k1} and AVR_{a10} genes of *B. graminis* f. sp *hordei* do not encode proteins with conventional secretory leader sequences; nevertheless, the proteins trigger resistance responses when expressed in the cytoplasm of barley cells (Ridout et al., 2006). Since each of these avirulence proteins appears to enter the host cells, they have been inferred to be effector proteins. Several fungal and oomycete effector proteins that are not associated with resistance gene interactions have also been shown or inferred to enter plant cells, including *Phytophthora* elicitin (Tyler, 2002) and crinkler (Torto et al., 2003) proteins, the RTP1p protein of the bean rust *Uromyces fabae* (Kemen et al., 2005), and the ToxA protein toxin of *Pyrenophora tritici-repentis* (Manning and Ciuffetti, 2005). In all cases, the mechanisms by which these proteins might enter the cell are unknown.

The *Avr1b*-1 gene of *P. sojae* was cloned by a map-based strategy (Shan et al., 2004). It encodes a small, secreted hydrophilic protein with a mature length of 117 amino acids. The protein has no disulfide bonds. The C terminus of the protein is highly polymorphic, especially in *P. sojae* isolates that can overcome resistance provided by *Rps*1b (Shan et al., 2004). Constitutive expression of *Avr*1b in *P. sojae* transformants renders the strains unable to infect soybean cultivars containing the resistance gene *Rps*1b, and mutations in the C terminus of the protein abolish this property of *Avr1b*-1 (Dou et al., 2008). High-level constitutive expression of *Avr*1b in *P. sojae* transformants makes the strains more virulent on soybean, indicating that *Avr1b*-1 contributes positively to virulence. Avr1b proteins can suppress programmed cell death triggered in soybean, *Nicotiana benthamiana*, and *Saccharomyces cerevisiae* cells by the pro-apoptotic protein BAX, suggesting that suppression of defense-related host cell death is a mechanism by which Avr1b contributes to virulence (Dou et al., 2008).

Comparison of the sequences of the four cloned oomycete avirulence genes with each other and with large diverse families of similar genes in the *P. sojae* and *P. ramorum* genome sequences (*Avh* genes) identified two conserved motifs, termed RXLR (Arg-X-Leu-Arg) and dEER (Asp-Glu-Glu-Arg; the Asp is less well conserved than the other three residues), near the N terminus of these secreted proteins (Rehmany et al., 2005; Birch et al., 2006; Tyler et al., 2006; Jiang et al., 2008) (Figure 1). The RXLR motif closely resembles a motif (Pexel or VTF; $RXLX^{E}/_{Q}$) that enables effector proteins of the malaria pathogen *Plasmodium* to cross the parasitiphorous vacuolar membrane into the cytoplasm of human erythrocytes (Hiller et al., 2004; Marti et al., 2004). Furthermore, one RXLR motif, that of Avr3a, was shown to function in targeting proteins from *Plasmodium* into the erythrocyte cytoplasm (Bhattacharjee et al., 2006). The structural and functional similarity between the RXLR and Pexel/VTF motifs encouraged the hypothesis that the RXLR motif was responsible for transit of the oomycete effector proteins into the cytoplasm of host cells (Rehmany et al., 2005; Birch et al., 2006; Tyler et al., 2006). Here, we experimentally verify this hypothesis by testing mutations in the RXLR and dEER motifs of the *P. sojae* Avr1b protein in both transgenic *P. sojae* and transgenic soybean tissue, supporting similar recent findings for the *P. infestans* Avr3a protein (Whisson et al., 2007). Furthermore, we demonstrate that RXLR-mediated transit does not require presence of the pathogen, indicating that transit depends only on the RXLR protein and host molecules.

RESULTS

RXLR2 and dEER Motifs of Avr1b Are Required for Its Avirulence Function in Transgenic *P. sojae* Lines

To test the function of the RXLR and dEER motifs of Avr1b, we created transgenic *P. sojae* strains that expressed either wild-type or mutant *Avr1b*-1 genes. Wild-type Avr1b contains two RXLR motifs, RXLR1 and RXLR2 (Figure 1A). We created mutations in either or both of the RXLR motifs, in addition to a mutation in the dEER motif (Figure 1A). The *Avr1b*-1 gene constructs were fused to a strong constitutive promoter, HAM34 (Judelson et al., 1991), and introduced into a strain, P7076, that expresses a variant Avr1b protein that does not confer avirulence against *Rps*1b-containing soybeans (Shan et al., 2004). Two independent transformants (T17 and T20) expressing wild-type *Avr1b*-1 (Figures 1B and 1C) lost the ability to infect soybean plants carrying *Rps*1b but were unaffected in their ability to infect plants lacking *Rps*1b (Figure 1E, Table 1). This demonstrated that they had acquired avirulence against *Rps*1b as a result of a functional Avr1b gene product. This result was confirmed using two different pairs of isolines of soybean (Buzzell et al., 1987) that differed only in the presence of *Rps*1b, namely, Williams (no *Rps* gene) with L77-1863 (*Rps*1b; Williams background) and HARO(1-7) 1 (No *Rps*; Harosoy background) with HARO13 (*Rps*1b; Harosoy background) (Figure 1E, Table 1).

By contrast, in five independent transformants expressing the $RXLR2^{AAAA}$ mutant, there was no gain of avirulence against *Rps*1b cultivars, despite the presence of abundant mRNA from the transgene (Figure 1E, Table 1). Thus, the RXLR2 motif is necessary for Avr1b activity when the protein is delivered by the pathogen. Since the RXLR1 motif was intact in the $RXLR2^{AAAA}$ mutant, the motif appeared to be nonfunctional. Consistent with this inference, the $RXLR1^{AAAA}$ mutation did not abolish avirulence in three independent transformants (Figure 1E, Table 1). As expected, avirulence was lost in the $RXLR1^{AAAA}$ $RXLR2^{AAAA}$ double mutants (Figure 1E, Table 1). A mutation in the dEER motif also abolished avirulence (in two independent transformants),

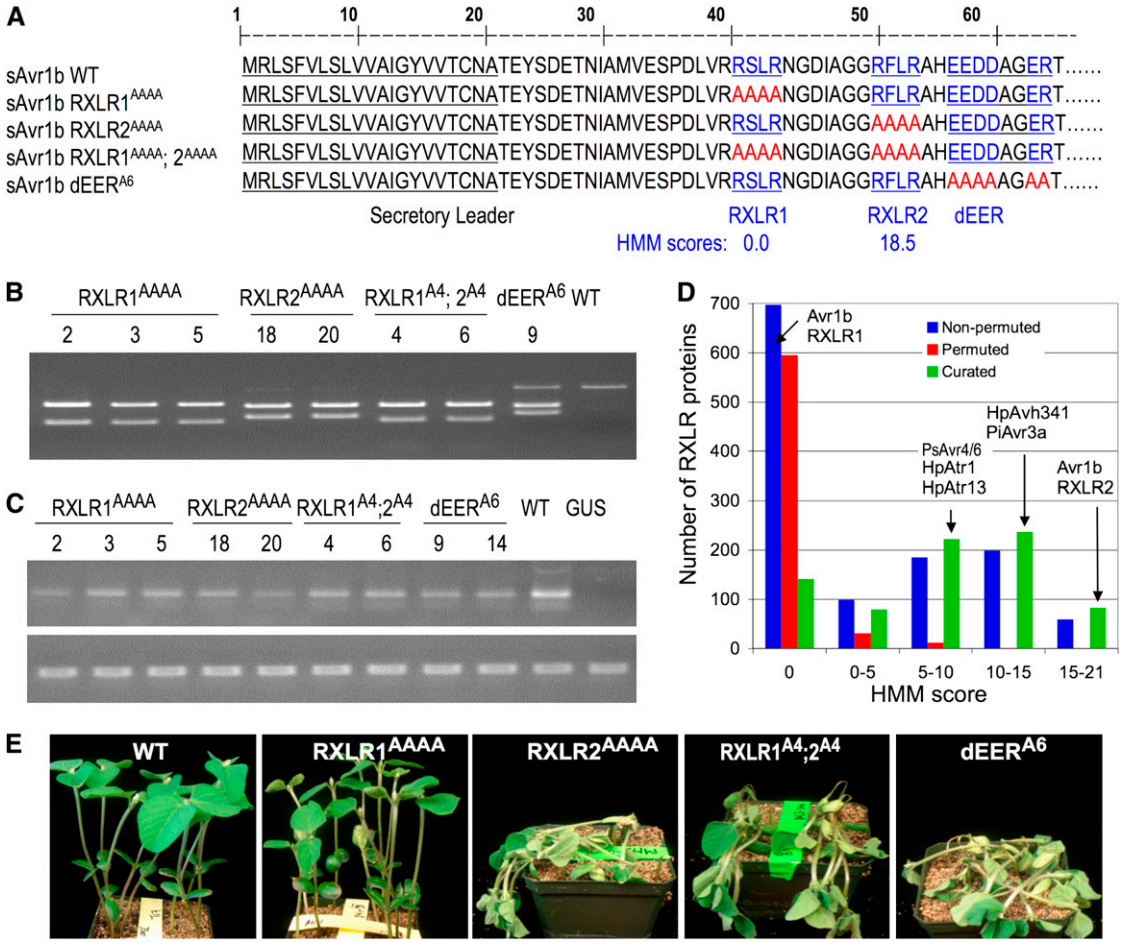

Figure 1. RXLR and dEER Motifs Are Required for Avr1b Function in *P. sojae* Transformants.

(A) Sequences of mutations in the RXLR1, RXLR2, and dEER motifs. Blue represents wild-type amino acids targeted for replacement by Ala residues (red).

(B) *Pst*I restriction analysis of PCR products amplified from *Avr1b*-1 transformants using primers specific for the HAM34 promoter and terminator regions. *Pst*I restriction profiles of Avr1b(RXLR1^{AAAA}), Avr1b(RXLR2^{AAAA}), Avr1b(RXLR1^{AAAA}, 2^{AAAA}), Avr1b(dEER^{A6}), and wild-type Avr1b are distinguished from each other because the mutations introduce a *Pst*I site. Avr1b(dEER^{A6})-9 was confirmed by sequencing the PCR product.

(C) Detection of Avr1b mRNA in *P. sojae* stable transformants by RT-PCR. Top panel shows amplification with primers internal to the Avr1b C terminus. Bottom panel shows amplification with *P. sojae* actin primers. *P. sojae* stable transformants were the same as for **(B)** except that an amplification reaction is also shown from RNA from a *P. sojae* transformant containing a GUS gene. No amplification was observed when reverse transcriptase was omitted from the reactions.

(D) Distributions of HMM scores of RXLR flanking regions for all RXLR-containing secreted proteins from *P. sojae* and *P. ramorum* (nonpermuted), for all secreted proteins retaining an RXLR string after sequence permutation (permuted), and for all high-quality RXLR-effector candidates identified by Jiang et al. (2008) (curated). The locations on the distribution of the HMM scores of the RXLR strings of known avirulence proteins and HpAvh341 are shown by the arrows.

(E) Phenotype of L77-1863 (*Rps*1b) seedlings inoculated on the hypocotyls with transformants carrying the indicated wild-type or mutant *Avr1b*-1 genes and photographed 4 d later.

indicating that this motif is also required for the function of the protein (Figure 1E, Table 1).

The difference in activity between RXLR1 and RXLR2 suggests that surrounding sequences are important to the activity of an RXLR motif. To define the differences in the surrounding sequences, we created a hidden Markov model (HMM) using the 10–amino acid residues to the left and right of the RXLR motifs of all of the *P. sojae* and *P. ramorum* Avh genes (Tyler et al., 2006; Jiang et al., 2008). Using this HMM, the sequences surrounding RXLR2 had a high score of 18.5, representing an excellent match to the consensus flanking sequence, very unlikely to have been found in a random sequence. By contrast, sequences surrounding RXLR1 had a low, nonsignificant score of 0.0. Using the same HMM, the sequences surrounding the RXLR motif of *P. infestans* Avr3a scored 10.9. Using a similar HMM derived from *H. parasitica* Avh genes, the sequences surrounding the RXLR motifs of

Table 1. Molecular Characterization and Avirulence Testing of *P. sojae* Stable Transformants

Strains	Transgene (PCR)[a]	Expression (RT-PCR)[b]	Transformant Validation[c]	Avirulence (Surviving Seedlings)[d]		P[e]
				Rps1b	*rps*	
P7076 (GUS)						
GUS	–	–		1/23	1/22	0.77
P7076 (s*Avr1b* WT)						
T17	+	+	*Pst*I	20/30	0/21	3.9 E-07
T20	+	+	Sequence	25/44	2/28	1.2 E-05
P7076 (s*Avr1b* RXLR1^{AAAA})						
RXLR1-2	+	+	*Pst*I	32/36	3/20	5.0 E-08
RXLR1-3	+	+	*Pst*I	31/54	3/21	6.4 E-04
RXLR1-5	+	+	*Pst*I	37/57	7/23	5.1 E-03
P7076 (s*Avr1b* RXLR2^{AAAA})						
RXLR2-18	+	+	*Pst*I	6/44	3/17	0.48
RXLR2-20	+	+	*Pst*I	4/46	3/19	0.33
P7076 (s*Avr1b* RXLR1^{AAAA}; RXLR2^{AAAA})						
RXLR1+2-4	+	+	*Pst*I	5/31	2/16	0.55
RXLR1+2-6	+	+	*Pst*I	4/43	1/21	0.47
P7076 (s*Avr1b* dEER^{A6})						
dEER-9	+	+	Sequence	4/59	2/23	0.79
dEER-14	+	+	*Pst*I	4/40	3/15	0.28
Ps *Avr4/6-Avr1bCt*						
4/6-1b-3	+	+	Size	15/24	3/11	0.057
4/6-1b-19	+	+	Size	14/26	3/16	0.025
Hp *341-Avr1bCt*						
341-1b-13	+	+	Size	16/19	0/11	6.6 E-06
341-1b-17	+	+	Size	23/24	0/7	3.0 E-06
mAvr1bCt						
mAvr1bCt-4	+	+	Size	3/20	3/16	0.77
mAvr1bCt-5	+	+	Size	2/21	1/15	0.63

[a] The presence of transgenes was verified by PCR as described in Methods. +, transgene present; – transgene not detected.

[b] Transgene expression was determined by qualitative RT-PCR and by quantitative RT-PCR as described in Methods. +, transgene transcripts present; –, transgene transcripts not detected.

[c] The presence of the relevant mutation in the transforming plasmid was verified by sequencing in every case. The presence of the correct mutation within the transgenes of each transformed strain was verified after PCR amplification of the *Avr1b*-1 transgene by *Pst*I digestion, by sequencing in the case of the mutants (e.g., Figure 1), or by size in the case of the Avh gene fusions and N-terminal deletion (e.g., Figure 4).

[d] The avirulence of each transgenic strain was tested by inoculation of seedlings containing *Rps*1b (L77-1863) or no *rps* gene (Williams) as described in Methods. The number of surviving seedlings/total inoculated seedlings is shown, summed from all replicates

[e] Fisher's exact test (one tailed) was used to compare the frequency of seedling survival between *rps* and *Rps*1b plants. A significant P value (0.05) indicates that the transformant's phenotype is avirulent.

the *H. parasitica* Atr1 and Atr13 proteins had scores of 9.8 and 6.3, respectively.

To establish the significance of these HMM scores, we used the *Phytophthora* HMM to score the RXLR motifs of 1240 RXLR-containing sequences identified from a pool of all putative secreted *P. sojae* and *P. ramorum* proteins by Jiang et al. (2008). As a control, we scored 639 RXLR-containing sequences found after permuting the sequences of all the putative secreted *P. sojae* and *P. ramorum* proteins (Jiang et al., 2008). As shown in Figure 1D, the RXLR strings of 698 (56%) of the 1240 real proteins had an HMM score of zero, while the RXLR strings of 595 (93%) of the permuted proteins had a zero score, and only 13 (1.8%) scored above 5.0. By contrast, of 765 proteins that Jiang et al. (2008) identified as high-quality candidate effectors, only 18% had an HMM score of zero, and 543 (72%) had a score >5.0. From this comparison, we conclude that HMM scores of zero, such as that of Avr1b RXLR1, are characteristic of RXLR strings found at random, while scores >5.0 are characteristic of non-random occurrences of RXLR strings and of the RXLR strings of functional avirulence proteins. HMM scores between 0 and 5 are equivocal. The curated Avh genes with a score of zero may represent pseudogenes as many of them were identified principally by C-terminal sequence similarity.

The Interaction between Avr1b and the *Rps*1b Gene Product Occurs within Host Cells and Does Not Require the RXLR and dEER Motifs

To confirm that the site of interaction of Avr1b with the *Rps*1b gene product is within plant cell, we used particle bombardment

to introduce DNA encoding Avr1b proteins lacking a secretory leader into soybean cells together with DNA encoding β-glucuronidase (GUS). This assay measures the functional interaction of the Avr1b protein with the intracellular product of the soybean *Rps*1b gene; when the two proteins interact, programmed cell death is triggered in the transformed cells ablating the development of tissue patches expressing GUS (Mindrinos et al., 1994; Qutob et al., 2002). Since the Avr1b protein lacks its normal secretory leader, the protein should be synthesized in the plant cytoplasm. To facilitate the comparison of test and control bombardments, we used a novel double-barreled attachment for the Bio-Rad Gene Gun (Dou et al., 2008) that enables us to shoot two different DNA samples side by side into a leaf in the same shot, which greatly improves the reproducibility of the results (Dou et al., 2008). Figure 2 shows that delivery of DNA encoding leaderless Avr1b protein into soybean cells significantly reduced the number of blue GUS-positive patches when the *Rps*1b gene was present but not when *Rps*1b was absent (Figure 2A). This is consistent with a cytoplasmic location for the Avr1b–Rps1b interaction. When RXLR2 or dEER motifs were replaced by four or six Ala residues, respectively [Figure 2A, mAvr1b(RXLR2^{AAAA}) and mAvr1b(dEER^{A6})], the interaction of the cytoplasmic, leaderless Avr1b with Rps1b was unaffected (Figures 2A and 2B), indicating that the RXLR2 and dEER motifs were not required for the interaction.

RXLR-Mediated Transit into Soybean Cells Does Not Require the Pathogen

To test whether RXLR function requires the presence of the pathogen, we used the bombardment assay to determine the effect of the RXLR2^{AAAA} mutation on secreted Avr1b protein. When soybean cells were bombarded with DNA encoding wild-type Avr1b, including its normal secretory leader, a reduction in GUS-positive blue spots was observed comparable to that observed for the nonsecreted protein [Figure 2A, sAvr1b(WT)]. However, when the RXLR2^{AAAA} or dEER^{A6} mutations were present in the bombarded DNA, there was no reduction in the number of blue spots [Figure 2A, sAvr1b(RXLR2^{AAAA}) and sAvr1b (dEER^{A6})]. Figure 2C shows a leaf bombarded simultaneously side by side with the sAvr1b(WT) and sAvr1b(RXLR2^{AAAA}) constructs, illustrating the reduction observed with the wild-type construct compared with the mutant. From these results, we infer first that the secretory leader is functional in soybean and targets Avr1b protein to the outside of the cell. Second, we infer that the RXLR2 (but not RXLR1) and dEER motifs are required for Avr1b protein to reenter the cell, which confirms the conclusion from the *P. sojae* transformation experiments. Importantly, the results also show that RXLR-dEER–mediated entry does not require the presence of the pathogen.

To support our inference that the secretory leader of Avr1b was correctly exporting the protein from the plant cells in the bombardment assay, we constructed a gene encoding *Aequorea coerulescens* green fluorescent protein (acGFP; abbreviated GFP in this article) fused either to the Avr1b leader or to full-length Avr1b. These fusions enabled us to track the proteins and check their stability. To aid in visualization, we used onion bulb epidermal cells for these experiments rather than soybean cells.

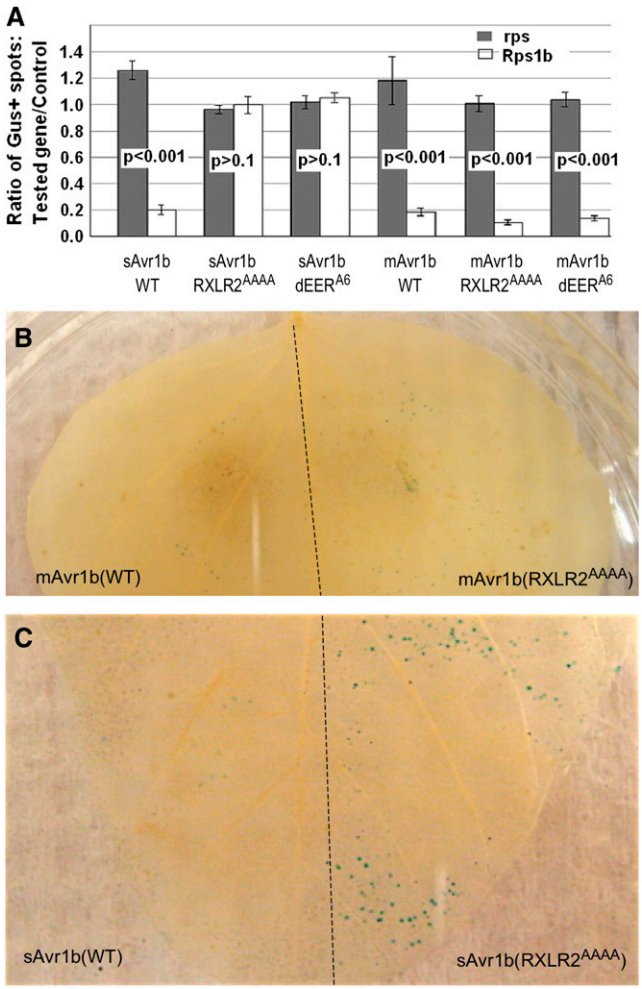

Figure 2. RXLR and dEER Functions Confirmed by Particle Bombardment Assay.

Soybean leaves were bombarded using a double-barreled device that delivered *Avr1b*-1 DNA-bearing particles to one side of the leaf and control (empty vector) DNA to the other; both sides received GUS DNA.
(A) Ratio of blue spots in the presence of *Avr1b*-1 compared with the control. sAvr1b indicates a gene encoding secretory Avr1b, and mAvr1b indicates one encoding mature Avr1b (lacking the secretory leader). WT indicates wild-type RXLR motif, RXLR2^{AAAA} indicates the four Ala replacement of the RXLR2 motif, and dEER^{A6} indicates the six Ala replacement of the dEER motif. Averages and SE are from 16 pairs of shots. P values comparing results from cultivars with *Rps*1b (L77-1863) or without (rps; Williams) were calculated using the Wilcoxon rank sum test.
(B) Direct comparison of bombardment with mature Avr1b.
(C) Direct comparison of bombardment with secretory Avr1b.
In both **(B)** and **(C)**, DNA encoding wild-type (left) and RXLR2^{AAAA} (right) versions of mAvrb or sAvr1b, respectively, were bombarded onto the same leaf of L77-1863 (*Rps*1b). The dashed lines indicate the positions of a divider that prevents particles from the two shots from overlapping. In both photographs, the brightness and contrast were adjusted uniformly to improve the visibility of the blue spots.

GFP was exported from the cells and accumulated in the apoplast when the secretory leader was attached to GFP (Figure 3A) but accumulated in the cytoplasm and nucleus when the leader was not attached (Figure 3B), as has been observed by others (e.g., Bonello et al., 2002; Yamane et al., 2005). When full-length Avr1b was fused to GFP, the proteins also accumulated in the apoplast if a mutation was present in either the RXLR2 motif (Figure 3C) or in the dEER motif (Figure 3D). This observation confirmed that the protein encoded by these mutants was stable and correctly targeted outside of the cells. When cells expressing Avr1b-GFP fusion proteins with RXLR mutations were plasmolyzed by treatment with 0.8 M mannitol for 15 min, the GFP was

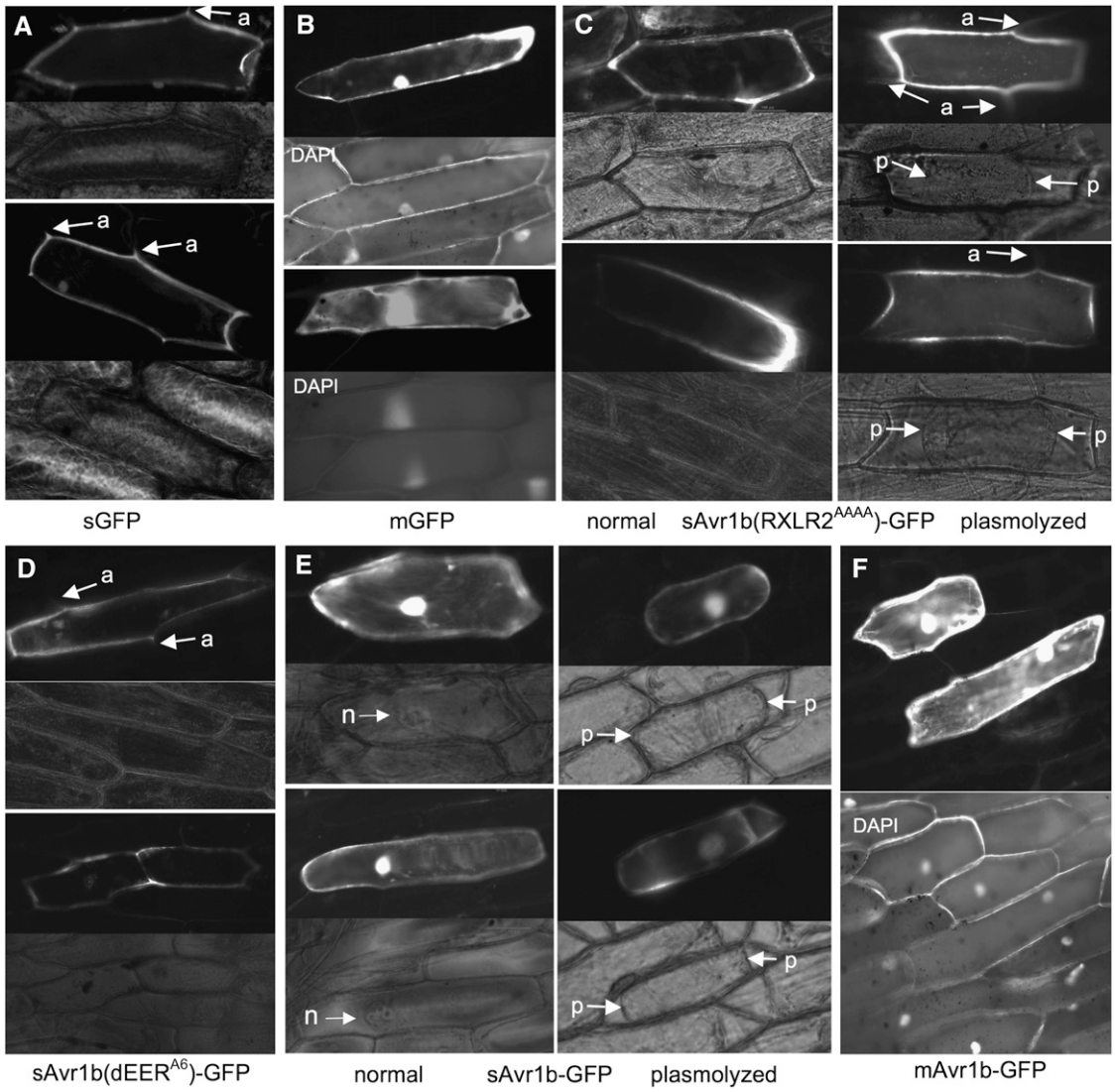

Figure 3. Secretion and Reentry of Avr1b-GFP Fusion Proteins Expressed in Onion Cells.

DNA encoding various fusions of Avr1b with *A. coerulescens* GFP was bombarded into onion epidermal cells using the Gene Gun without the double-barrel attachment. Cells were photographed under both UV and white light illumination 12 to 24 h after bombardment. a, sites where secreted GFP has begun to spread into the apoplast between pairs of neighboring cells; n, nuclei visualized under white light; p, plasma membrane in plasmolyzed cells; DAPI, cells stained with 4′,6-diamidino-2-phenylindole and photographed under UV illumination.

(A) Fusion of GFP to the secretory leader of Avr1b alone.

(B) GFP with no secretory leader (native GFP). DAPI-stained cells are shown instead of white light–illuminated cells.

(C) GFP fused to the Avr1b RXLR2^{AAAA} mutant, including its secretory leader. In the top right panel, a white trace of the plasma membrane from the panel below has been added. The right-side panels show photographs of plasmolyzed cells.

(D) GFP fused to Avr1b dEER^{A6} mutant, including its secretory leader.

(E) GFP fused to wild-type Avr1b, including its secretory leader. The right-side panels show photographs of plasmolyzed cells.

(F) GFP fused to mature Avr1b lacking its secretory leader. DAPI-stained cells are shown instead of white light–illuminated cells.

associated with the cell wall and not with the plasma cell membrane (Figure 3C, right panels; see Supplemental Figure 1 online). Furthermore, GFP protein could be seen diffusing into the apoplast between pairs of neighboring cells (arrows marked by "a" in Figures 3A, 3C, and 3D). Similar observations were made when cells expressing secreted GFP or Avr1b-GFP fusion proteins with a dEER mutation were plasmolyzed (see Supplemental Figure 1 online). If the RXLR2 and dEER motifs were intact, however, the sAvr1b-GFP protein fusion accumulated in the cytoplasm and nucleus of the cells (Figure 3E), similar to the mAvr1b-GFP fusion lacking the leader (Figure 3F). When cells expressing sAvr1b-GFP fusion proteins were plasmolyzed by treatment with 0.8 M mannitol for 15 min, the GFP could be observed to have either fully or partially returned to the inside of the cells (Figure 3E, right panels). These results supported our conclusion that the RXLR2 and dEER motifs act together to enable Avr1b protein to reenter the plant cells.

The Avr1b RXLR and dEER Motifs Are Sufficient to Target GFP to Soybean Cells

Shan et al. (2004) showed that culture filtrates of *Pichia pastoris* cells secreting Avr1b proteins could trigger the hypersensitive response in soybean leaves expressing the *Rps*1b resistance gene. Subsequently, it proved extremely difficult to consistently produce enough soluble Avr1b protein in *P. pastoris* or any other expression system to repeat this observation. As an alternative, we fused the RXLR-dEER region of Avr1b to GFP, synthesized the fusion protein in *Escherichia coli*, and partially purified it (Figure 4A). Root tips of soybean seedlings were incubated with the isolated fusion protein for 12 h, washed for 4 h in water, and then observed under light and UV microscopy to localize the GFP. As shown in Figure 4C, GFP accumulated inside many of the root cells, whereas buffer alone did not produce any fluorescence (Figure 4B). The optical sections produced by the confocal microscope (Figure 4C) revealed that the protein penetrated ~10 cell layers deep during the 12-h incubation. The characteristic accumulation of GFP in the nuclei of the treated cells (Figure 4G) is comparable to the pattern observed when GFP is expressed in planta (Figures 3B, 3E, and 3F) and verifies that the GFP is located inside the cells. The nuclear localization of the protein also indicates that the cells are alive. If mutations were present in the RXLR or dEER motifs of the fusion protein, GFP did not accumulate inside the soybean root cells (Figures 4E and 4F, respectively). When the RXLR-dEER region was replaced by the artificial protein transduction motif Arg_9 (Chang et al., 2005, 2007; see below), GFP once again entered the soybean root cells (Figure 4E) and accumulated in the nuclei (Figure 4H).

Avr1b RXLR and dEER Motifs Can Be Replaced by RXLR-dEER–Containing Protein Sequences Encoded by Bioinformatically Identified Avh Genes

To determine if the RXLR and dEER motifs of bioinformatically identified *Avh* genes could functionally replace the RXLR2 and dEER motifs of *Avr1b*-1, we fused full-length *Avh* genes from *P. sojae* and *H. parasitica* to an *Avr1b*-1 N-terminal deletion mutant lacking the RXLR and dEER motifs. The fusion genes were then introduced into *P. sojae*, and the transformants were tested for avirulence on *Rps*1b-containing soybean cultivars. Both *Avh* genes, *P. sojae Avh*171 (since identified as Avr4/6; Dou et al., 2008) and *H. parasitica Avh*341, could replace the requirement for the RXLR2 and dEER motifs as judged by the avirulence of the transformants on *Rps*1b-containing cultivars, whereas transformants containing only the C terminus of Avr1b fused to an initiator Met remained virulent (Figure 5, Table 1). This result indicates that the RXLR and dEER motifs form a distinct transferable functional domain of Avr1b and other Avh proteins. The HMM scores of the RXLR-dEER motifs of Ps Avr4/6 and Hp Avh341 are both well within the functional range (6.9 and 14.2, respectively) (Figure 1D).

The Avr1b Host Targeting Signal Can Be Functionally Replaced by Autonomous Protein Transduction Motifs

Protein transduction domains (PTDs) capable of autonomously carrying proteins across plasma cell membranes have been described and characterized in the HIV-1 Tat protein (Joliot, 2005). Arg-rich peptides such as Arg_9 can also perform this function (Futaki, 2002). To compare RXLR-dEER–mediated effector delivery with the function of PTDs, we replaced the RXLR2 motif of Avr1b with TAT PTD or with Arg_9 (Figure 6A). When we tested the resultant proteins using the particle bombardment assay, both PTDs could functionally replace the RXLR2 motif of Avr1b, restoring the avirulence reaction of Avr1b with Rps1b (Figure 6B). Furthermore, when we fused the version of secreted Avr1b that contained the Arg_9 sequence in place of the RXLR2 motif to GFP, the fusion protein accumulated in the cytoplasm and the nucleus of bombarded onion bulb cells rather than the apoplast, confirming that Arg_9 could functionally replace RXLR2 (Figure 6C). Similar results were obtained when we fused the version of secreted Avr1b that contained the TAT PTD in place of the RXLR2 motif to GFP (Figure 6D). Finally, when Arg_9 was fused to GFP, the isolated proteins could enter soybean root cells directly (Figures 4D and 4H), as also observed for onion root cells (Chang et al., 2005). TAT PTD-GFP fusion proteins also could enter onion root cells (Chang et al., 2005).

The Avr1b Host Targeting Signal Is Interchangeable with Host Targeting Signals from *Plasmodium* Effectors

To test if the erythrocyte targeting signals of *Plasmodium* effector proteins could functionally replace the RXLR-dEER region of Avr1b, we replaced the residues of Avr1b from the end of the secretory leader to the end of the dEER motif with the mature N termini of three different *Plasmodium* effector proteins that are targeted to the erythrocyte cytoplasm, namely, PfGBP-130, PfHRPII, and PfPFE1615c (Bhattacharjee et al., 2006). The entire 37– to 41–amino acid region of each *Plasmodium* effector required for transduction (Bhattacharjee et al., 2006) was used (Figure 6A). As shown in Figure 6B, all three *Plasmodium* host targeting domains could functionally replace the Avr1b N terminus in targeting Avr1b to the soybean cytoplasm, assuming that they do not simply interfere with secretion.

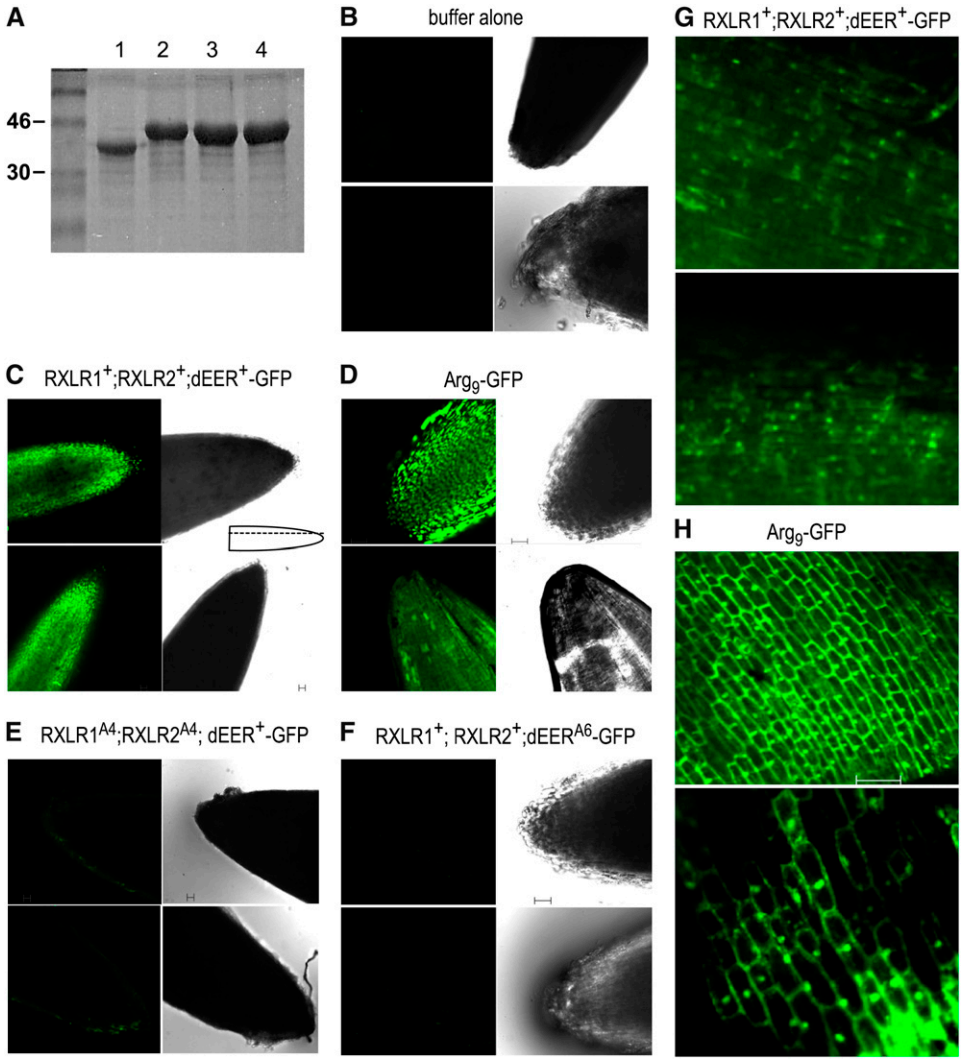

Figure 4. RXLR-dEER-GFP Fusion Proteins Isolated from *E. coli* Can Enter Soybean Cells in the Absence of the Pathogen.

GFP fusion proteins were expressed in *E. coli*, partially purified, and incubated with soybean root tips for 12 h. The root tips were then washed for 4 h and photographed under UV and white light illumination.

(A) Protein gel electrophoresis analysis of GFP fusion proteins partially purified from *E. coli* cells: lane 1, Arg_9-GFP; lane 2, GFP fused to the N-terminal 44 amino acids of mature wild-type Avr1b protein (RXLR1$^+$,RXLR2$^+$-dEER-GFP); lane 3, same as lane 2 with both RXLR1 and RXLR2 mutations (RXLR1^{AAAA},RXLR2^{AAAA}-dEER-GFP); lane 4, same as lane 2 except with dEER mutation (RXLR1$^+$,RXLR2$^+$-dEER^{AAAAAA}-GFP). The left lane contained molecular mass markers; the sizes of the markers are shown on the left (in kD). All expressed GFP proteins fluoresce normally under UV illumination.

(B) to **(F)** UV (left panels) and back-lit white light (right panels) illumination of roots after incubation with the indicated GFP protein fusion. The UV photographs represent longitudinal optical sections taken using the confocal microscope as illustrated by the dashed line in the inset of **(C)**. The GFP concentration, illumination, and exposure of the UV photographs was identical in all 10 panels shown.

(B) Buffer alone with no fusion protein.

(C) RXLR1$^+$,RXLR2$^+$-dEER-GFP.

(D) Arg_9-GFP.

(E) RXLR1^{AAAA},RXLR2^{AAAA}-dEER-GFP.

(F) RXLR1$^+$,RXLR2$^+$-dEER^{AAAAAA}-GFP.

(G) and **(H)** Higher-magnification photographs after the root tips were gently squashed following washing, showing nuclear accumulation of GFP.

(G) RXLR1$^+$,RXLR2$^+$-dEER-GFP.

(H) Arg_9-GFP.

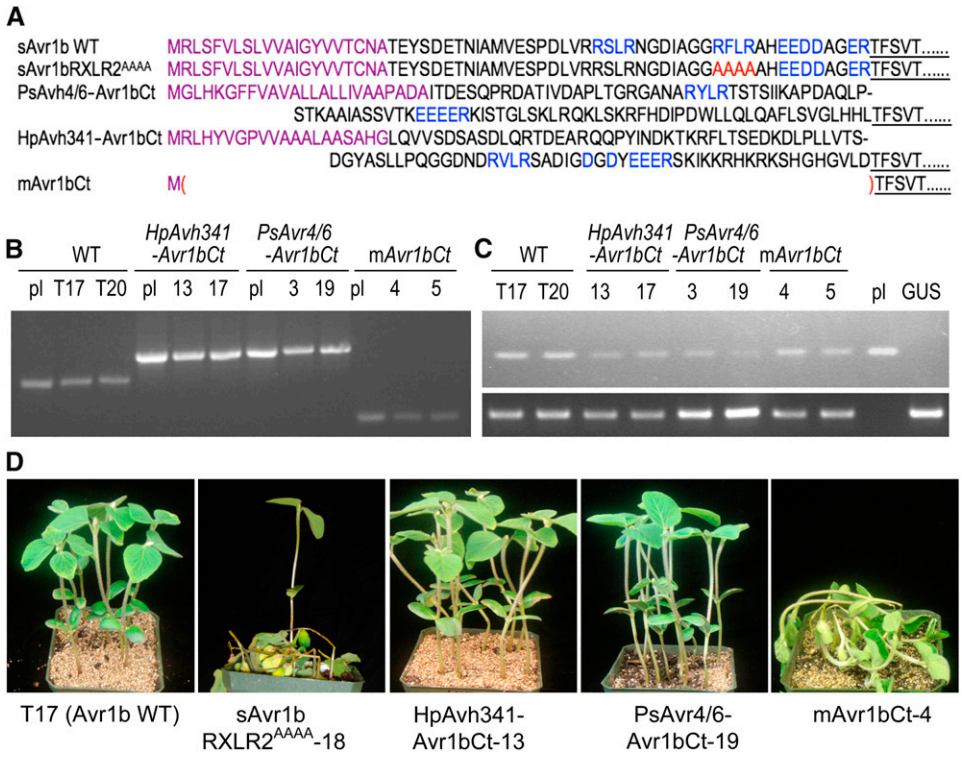

Figure 5. *P. sojae* Stable Transformants Show That Two Other Avh Proteins Can Replace the RXLR-dEER Region of Avr1b.

(A) Sequences of the N termini of wild-type and mutant Avr1b proteins and of fusions with two other Avh proteins. Purple, secretory leader; blue, RXLR motif; red, dEER motif. The C-terminal sequence of Avr1b is underlined.

(B) PCR analysis of DNA from *P. sojae* stable transformants. WT: pI, pHamAvr1b plasmid DNA; T17 and T20, two transformants with wild-type *Avr1b*-1 transgenes. *HpAvh341-Avr1bCt*: pI, pHamAvh341 plasmid DNA (encoding Hp Avh341-Avr1bCt); 13 and 17, two transformants containing pHamAvh341. PsAvr4/6-Avr1bCt: pI, pHamAvh171 plasmid DNA (encoding Ps Avr4/6-Avr1bCt); 3 and 19, two transformants containing pHamAvh171. *mAvr1bCt*: pI, pHamAvr1bCt plasmid DNA (encoding mAvr1bCt protein); 4 and 5, two transformants containing pHamAvr1bCt. The sizes of the PCR products for *Avr1b*-1, pHamAvh341, pHamAvh171, and pHamAvr1bCt are 577, 721, 748, and 385 bp, respectively.

(C) Detection of Avr1b mRNA in *P. sojae* stable transformants by RT-PCR. Top panel shows amplification with primers internal to the Avr1b C terminus. Bottom panel shows amplification with *P. sojae* actin primers. *P. sojae* stable transformants were the same as for **(B)** except that an amplification reaction is also shown from RNA from a *P. sojae* transformant containing GUS. PI, pHamAvr1b plasmid DNA as template. No amplification was observed when reverse transcriptase was omitted from the reactions.

(D) Phenotype of L77-1863 (*Rps*1b) seedlings inoculated on the hypocotyls with the indicated transformants carrying wild-type or mutant *Avr1b*-1 genes and photographed 4 d later. HpAvh341-Avr1b-17, PsAvr4/6-Avr1b-3, and mAvr1bCt-5 gave similar results to HpAvh341-Avr1b-13, PsAvr4/6-Avr1b-19, and mAvr1bCt-4 (Table 1).

Functional Characterization of the RXLR Motif

To begin to experimentally characterize the sequence requirements of the RXLR motif, we introduced a series of mutations into the motif in a version of the *Avr1b*-1 gene that retained the secretory leader and assayed the mutants using the bombardment assay (Table 2). Mutations that targeted the Arg at position 1 or the Leu at position 3 have the strongest effect on the ability of Avr1b to ablate GUS-positive tissue patches. Replacement of R1 with Lys reduced function significantly (33% ablation compared with 78%; $P < 0.001$), while Gln replacement completely abolished it. Replacement of L3 with Ala or even the relatively conservative Val also completely abolished function. Replacement of the Arg at position 4 with a Gln slightly but significantly reduced function (58% ablation compared with 72%; $P < 0.001$). Reversing the order within the first and second two pairs of positively charged and hydrophobic residues (RFLR → FRLR; RFLR → RFRL) completely abolished avirulence activity, indicating that positions of R1 and L3 were critical, not just their presence.

DISCUSSION

Since many resistance genes against oomycetes encode intracellular proteins and since several cognate oomycete avirulence genes encode secreted proteins, it has been inferred that there must be a mechanism for translocating the avirulence proteins into the plant cells (Tyler, 2002; Allen et al., 2004; Armstrong et al., 2005; Rehmany et al., 2005). Since the RXLR and dEER

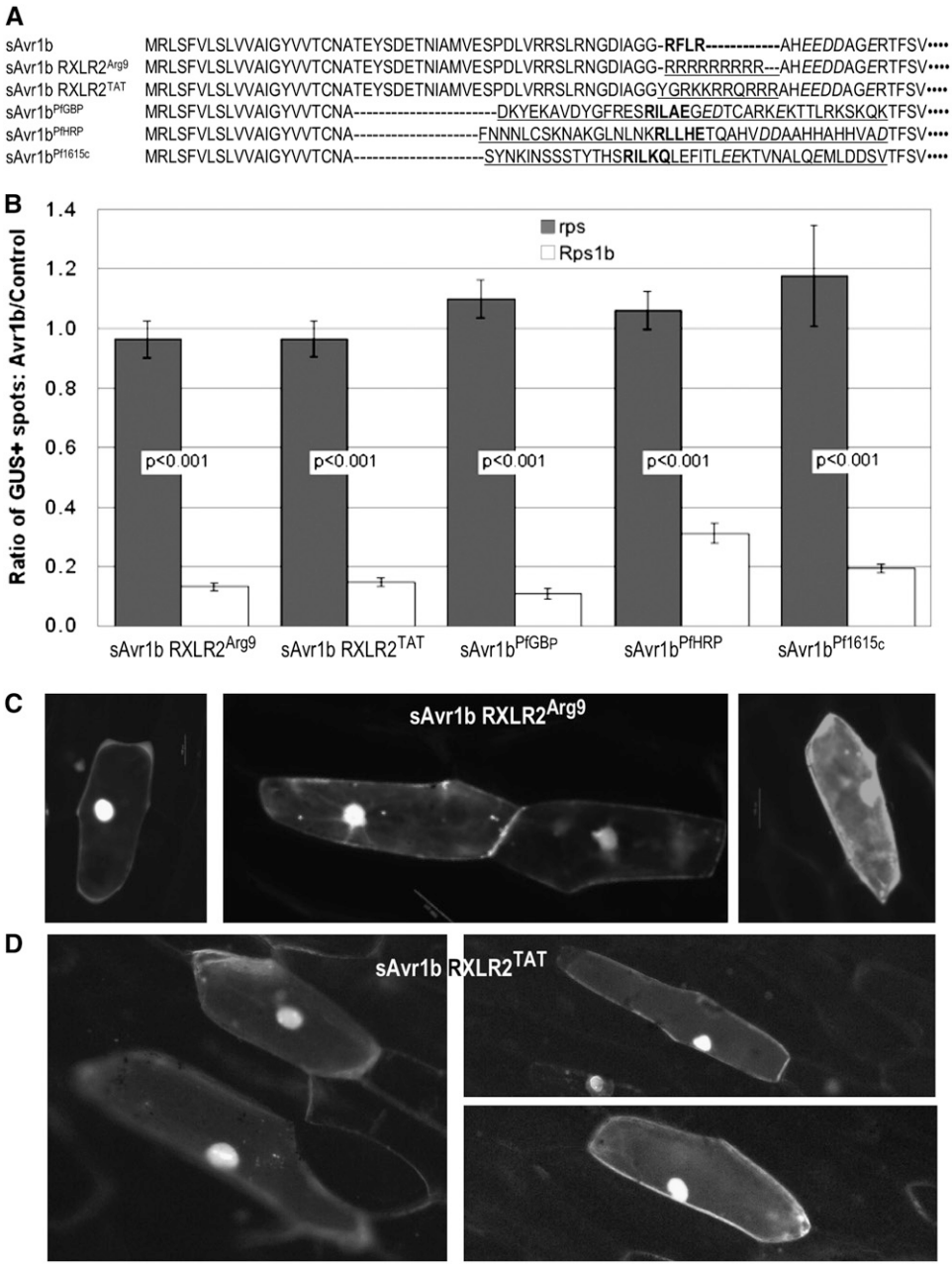

Figure 6. Functional Replacement of Avr1b Host Targeting Signal with Protein Transduction Motifs and *Plasmodium* Host Targeting Signals.

(A) Sequences of modified Avr1b proteins. PfGBP, PfHRP, and Pf1615c refer to the *Plasmodium* Pf GBP-130, Pf HRPII, and Pf PFE1615c proteins (Bhattacharjee et al., 2006). All nonnative Avr1b sequences are underlined, Avr1b RXLR2 and *Plasmodium* $RXLX^{E}/_{Q}$ motifs are in bold, and acidic residues in the dEER region are in italics. The Avr1b secretory leader was used in all constructs. Details of all constructs are given in Supplemental Table 2 online.

(B) Ratio of blue spots in the presence of *Avr1b*-1 compared with the control, assayed as described in Figure 2. Constructs are as in **(A)**. Averages and SE are from eight pairs of shots.

(C) Secretion and reentry of GFP protein fused to Avr1b protein containing Arg_9 in place of RXLR2, expressed in onion cells.

(D) Secretion and reentry of GFP protein fused to Avr1b protein containing the TAT protein transduction signal in place of RXLR2, expressed in onion cells.

In **(C)** and **(D)**, DNA encoding the fusion proteins was bombarded into onion epidermal cells using the Gene Gun without the double-barrel attachment. Cells were photographed 24 h after bombardment.

Table 2. Function of RXLR2 Mutants of Avr1b Assayed by Particle Bombardment

RXLR2 Sequence[a]	Ratio of GUS-Positive Spots[b]		Ablation[c]	P Value[d]	Activity
	rps	*Rps1b*			
RFLR	1.26 ± 0.07	0.28 ± 0.03	0.78	<0.001	Yes
AAAA	0.93 ± 0.04	0.96 ± 0.05	0	>0.100	No
KFLR	1.04 ± 0.04	0.70 ± 0.04	0.33[e]	<0.001	Partial
QFLR	0.95 ± 0.03	0.99 ± 0.03	0	>0.100	No
FRLR	1.00 ± 0.04	0.98 ± 0.05	0	>0.100	No
RFLQ	0.98 ± 0.07	0.41 ± 0.08	0.58[e]	<0.001	Partial
QFLQ	1.03 ± 0.05	1.05 ± 0.05	0	>0.100	No
RFAR	0.94 ± 0.03	0.91 ± 0.05	0	>0.100	No
RFVR	0.95 ± 0.05	1.03 ± 0.07	0	>0.100	No
RFRL	1.02 ± 0.04	0.96 ± 0.04	0	>0.100	No

[a] Amino acid sequence of RXLR2 in the wild type and mutants. RFLR is the wild type. Altered residues are underlined.
[b] Ratio of blue spots in the presence of various RXLR2 mutants of *Avr1b*-1 compared with the control empty vector when bombarded onto leaves from *rps* plants (Williams) or *Rps*1b plants (L77-1863). Averages and SE are from 16 pairs of shots.
[c] Ablation calculated as 1 − (Rps1b ratio)/(rps ratio) for ratios significantly different between *rps* and *Rps*1b.
[d] P values comparing results from *rps* and *Rps*1b cultivars were calculated using the Wilcoxon rank sum test.
[e] Ablations for KFLR and RFLQ were significantly different than the wild type (RFLR) with $P < 0.001$.

motifs were first identified during the *Phytophthora* genome sequence annotation (Rehmany et al., 2005; Govers and Gijzen, 2006), there has been extensive speculation that these motifs are involved in transporting avirulence proteins into host cells (Rehmany et al., 2005; Birch et al., 2006). We have demonstrated here experimentally that the RXLR and dEER motifs do indeed have this function.

As summarized in Figure 7, we first demonstrated that both the RXLR2 and dEER motifs of Avr1b are required for this protein to confer avirulence on *P. sojae* transformants. Next, using a particle bombardment assay, we confirmed that the RXLR2 and dEER motifs are not required to trigger an interaction with the *Rps*1b gene product when the Avr1b protein is synthesized in the soybean cytoplasm. Furthermore, we showed that when Avr1b protein is directed to be secreted out of the soybean cell, the RXLR2 and dEER motifs are once more required for the protein to trigger an interaction with Rps1b, which is consistent with the motifs being required for the Avr1b protein to reenter the soybean cell across the plasma cell membrane. The inferred targeting of Avr1b was supported using GFP fusions. Finally, we showed that fusion of the RXLR-dEER region to GFP enabled the isolated fusion protein to enter soybean root cells in the absence of the pathogen but only if the RXLR and dEER motifs were both intact.

Our findings that the RXLR and dEER motifs are required for Avr1b entry into plant cells are consistent with the finding that RXLR and dEER motifs are required for the *P. infestans* effector Avr3a to enter potato cells (Whisson et al., 2007). Furthermore, our results show that the RXLR and dEER motifs, together with the surrounding sequences, are sufficient for entry into plant cells. Whisson et al. (2007) found that Avr3a protein secreted into the apoplast by *Pectobacterium atrosepticum* could not trigger an interaction with the R3a gene product of potato and concluded that *P. infestans* must be present for Avr3a to enter the plant cell. Two related issues may explain the conflict with our findings. First, the amount of Avr3a secreted by *P. atrosepticum* may have been insufficient to overcome proteolysis in the apoplast, whereas a much larger amount of protein was present when we added isolated RXLR-dEER-GFP fusion protein directly to soybean roots. Second, both during formation of a *Phytophthora* haustorium, in which the host cell wall but not the plasma membrane are breached, and in our particle bombardment experiments, the secreted effector protein accumulates close to the host plasma cell membrane; this close localization may facilitate efficient transport into the cells.

We have begun to experimentally define the RXLR motif, which has previously been defined principally from sequence alignments of the hypothetical proteins encoded by the Avh genes. These findings are very important in guiding more reliable bioinformatics searches for RXLR effector candidates. We have shown that the Arg at position 1 and the Leu residue at position 3 are essential for function of the motif. A Lys at position 1 allows some function, but significantly less than Arg. However, there is not a strong requirement for the Arg at position 4. Therefore, by functional assays, the oomycete RXLR motif resembles the *Plasmodium* motif ($RxLx^{E}/_{Q}$) even more closely than previously noted. The positioning of Arg-1 and Leu-3 within RXLR also is critical because reversing the order of either of the first or the second pairs in the motif residues abolishes function.

Our results also show that the amino acid sequences flanking the RXLR2 and dEER motifs are required in addition to the motifs themselves for the transit of Avr1b into soybean cells (summarized in Figure 8A). Furthermore, our GFP fusion protein experiments showed that the region from residues 33 to 71 (19 amino acids to the left of RXLR2 and 6 amino acids to the right of dEER) were sufficient for protein translocation. A similar observation was made in the case of the *Plasmodium* host targeting motifs. In *Plasmodium*, seven residues upstream of the motifs and 16 residues downstream were required for the targeting function (Bhattacharjee et al., 2006) (Figure 8A). Our results do not indicate which specific flanking sequences are required. However, HMMs constructed from the 10–amino acid residues

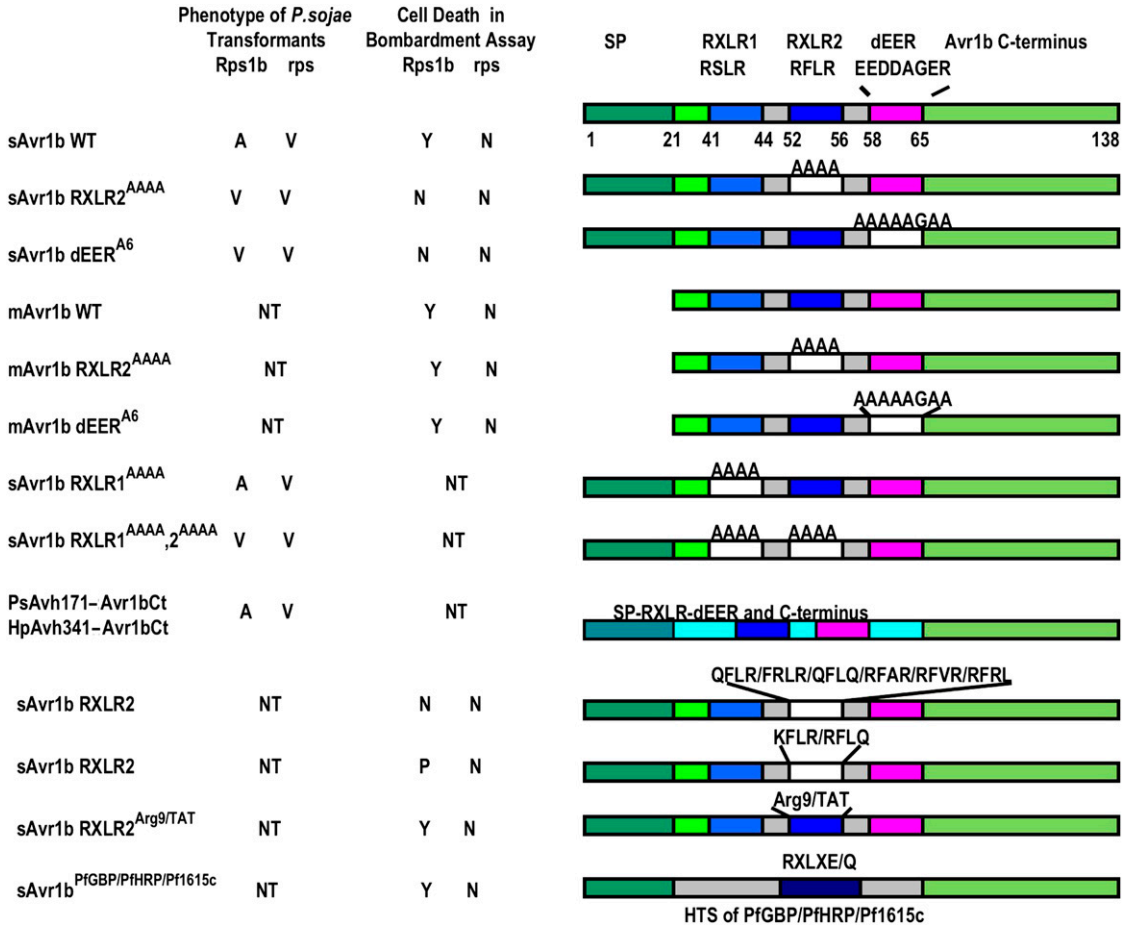

Figure 7. Summary of *Avr1b*-1 Mutations and Their Phenotypes in *P. sojae* Stable Transformants and Soybean Transient Expression Assays.

A, avirulent; V, virulent; NT, not tested; Y, significantly fewer blue (GUS-positive) tissue patches from GUS expression resulting from Avr1b-induced cell death; N, not significantly fewer blue tissue patches; P, partial reduction in blue tissue patches; SP, signal peptide.

flanking the upstream and downstream sides of all *P. sojae* and *P. ramorum* Avh RXLR motifs could clearly separate the RXLR motifs of functional avirulence proteins from RXLR motifs obtained by chance from real or permuted protein sequences (Figure 1D). These findings indicate that reliable bioinformatic searches for RXLR effector candidates should include the use of HMMs to evaluate the sequences flanking putative RXLR and dEER motifs (e.g., Jiang et al., 2008).

One of the most important conclusions from this study is that RXLR-dependent entry of Avr1b does not require the presence of the pathogen. Bacterial plant pathogens have evolved an elaborate mechanism, the type III secretion machinery, for delivering effector proteins into the cytoplasm of plant cells (Plano et al., 2001; Alfano and Collmer, 2004). Nematode plant pathogens deliver effectors into the host cytoplasm through their stylet (Davis and Mitchum, 2005). However, no mechanism has been identified by which filamentous eukaryotic pathogens, such as fungi and oomycetes, deliver effectors to the host cytoplasm. Many oomycete and fungal pathogens, especially those that are biotrophic or hemibiotrophic, form differentiated feeding structures inside host cells called haustoria (Hahn and Mendgen, 2001; Hardham, 2007). The hyphae displace, but do not penetrate, the plant plasma cell membrane, resulting in the formation of a specialized haustorial interface consisting of the plasma cell membranes of the two organisms, separated by a modified pathogen cell wall (Figure 8) (Hahn and Mendgen, 2001; Hardham, 2007). Haustoria are an obvious site for the release of effector proteins from the pathogen into the plant tissue, as the secreted effectors will be concentrated in close proximity with the plant plasma cell membrane.

PTDs capable of autonomously carrying proteins across plasma cell membranes have been described and characterized in several animal proteins (Joliot, 2005; Langel, 2006), most notably the HIV-1 Tat protein, the *Drosophila* transcription factor antennapedia, the neuropeptide dynorphin, and the defensin Bac7 (reviewed in Langel, 2006; Tomasinsig et al., 2006). Like the targeting sequences of these proteins, the oomycete RXLR motif and the *Plasmodium* Pexel/VTF motif ($RXLX^{E}/_{Q}$) are rich in basic and hydrophobic residues. Characterization of the mechanisms by which PTDs transport proteins suggests that an electrostatic

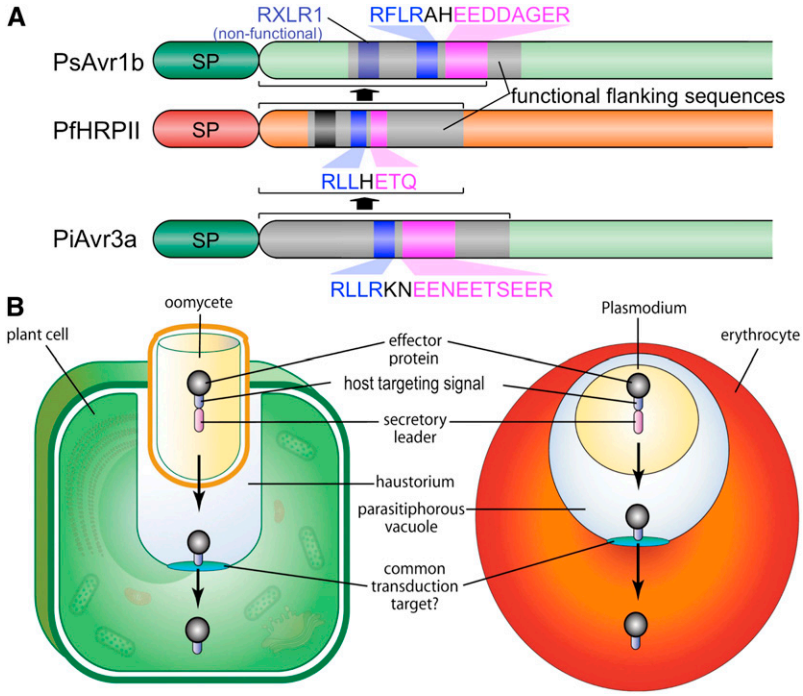

Figure 8. Common Host Targeting Mechanism in Oomycetes and *Plasmodium*.

(A) Features and functional exchange of host targeting signals in *P. sojae* Avr1b, *Plasmodium falciparum* HRPII, and *P. infestans* Avr3a. Common RXL(R) and dEER-like motifs are shown in blue and pink, respectively, and were defined experimentally (this article; Marti et al., 2004; Hiller et al., 2004; Whisson et al., 2007). Flanking regions inferred also to be required are shown in gray. In Ps Avr1b, the flanking regions are defined as the 19 residues upstream and 16 residues downstream of RXLR2 shown to be sufficient for translocation in the GFP fusion experiments. In Pf HRPII, the eight residues upstream and 13 residues downstream were defined experimentally (Bhattacharjee et al., 2006). In Pi Avr3a, the flanking regions are defined by the region tested in *Plasmodium* (Bhattacharjee et al., 2006). The region of Pi Avr3a tested in *Plasmodium* and the region of Pf HRPII tested in *P. sojae* (this article) are shown by the brackets.

(B) Anatomical contexts of oomycete and *Plasmodium* effector entry are similar. The haustorium is a specialized invagination of the plant cell formed by oomycete (and fungal) pathogens. The plant cell wall is pierced during formation of the haustorium, while the oomycete cell wall is retained but differentiates into the haustorial wall. Both the haustorial membrane and the parasitiphorous vacuolar membrane are derived from the host plasma cell membrane during pathogen invasion.

interaction between cationic PTDs and the anionic surface of the plasma membrane leads to transport via a specialized form of endocytosis called macropinocytosis (Snyder and Dowdy, 2004; Kaplan et al., 2005) that occurs in plant cells (Chang et al., 2007) and animal cells. Thus, macropinocytosis is one candidate mechanism by which RXLR-dEER proteins might enter cells. Concordant with this hypothesis, our results show that two of these PTDs can functionally replace RXLR in Avr1b.

The Avr1b protein requires not only the RXLR motif itself but also nonrandom surrounding sequences, including the dEER motif. These surrounding sequences are not enriched in positive and hydrophobic residues but instead are enriched in acidic and hydrophilic residues. Furthermore, our RXLR mutagenesis results show that the presence of basic and hydrophobic residues is not sufficient for RXLR function; instead, the order of the amino acid residues is very important, and very subtle mutations, such as RFLR → RFVR or QFLR, abolish function. Therefore, an alternative hypothesis is that oomycete effectors use a novel mechanism for translocation across the membrane, possibly involving host cell surface machinery (such as a receptor) that is more complex than just the phospholipid bilayer. As summarized in Figure 8A, the *Plasmodium* Pexel/VTF motif also requires surrounding sequences that are enriched in acidic and hydrophilic residues (Bhattacharjee et al., 2006); in fact, the motif is functionally interchangeable with the oomycete RXLR domain in both erythrocytes (Bhattacharjee et al., 2006) and in soybean tissue (this study). Thus, oomycetes and *Plasmodium* both may target host cell surface machinery that is common to plants and vertebrate animals (Figure 8B) but different than that targeted by animal PTDs. A recent study (Bhattacharjee et al., 2008) demonstrated that the *Plasmodium* PTD motif functions by sorting secreted proteins into host cell surface vesicles (Maurer's clefts) that are subsequently internalized, implying the involvement of a cell surface receptor. The targeted machinery, if common, must not only be very ancient but also must serve an irreplaceable function in the host organisms since it must have been preserved against strong negative selection pressure resulting from exploitation by the pathogens. The kingdoms containing oomycetes and *Plasmodium* have a common evolutionary origin within the chromalveolate group (Yoon et al., 2002; Tyler et al., 2006) and so

the RXLR and Pexel/VTF motifs might have a common evolutionary origin. Alternatively, the two pathogens may have acquired a common transduction mechanism through convergent evolution (Figure 8B). If convergent evolution is the explanation, then a much broader array of pathogens might also have acquired this transduction mechanism by convergent evolution, lending considerable importance to characterizing this transduction mechanism.

In fungal pathogens, as discussed in the Introduction, the PtrToxA toxin of *P. tritici-repentis* (Manning and Ciuffetti, 2005) and the RTP1p protein of *U. fabae* (Kemen et al., 2005) have been shown biochemically to enter into host cells, and the products of several avirulence genes have been inferred to do so, namely Avr-Pita (Orbach et al., 2000) of *Magnaporthe oryzae*, AvrL567 (Dodds et al., 2004), AvrM, AvrP4, and AvrP123 (Catanzariti et al., 2006) of *Melampsora lini*, and AVR_{k1} and AVR_{a10} of *B. graminis* f. sp *hordei* (Ridout et al., 2006). So far, no common motif or mechanism has been identified by which these fungal proteins enter plant cells. An RGD vitronectin-like motif has been implicated in PrtToxA transfer into cells (Manning and Ciuffetti, 2005), and the authors suggest that receptor-mediated endocytosis may be involved. Interestingly, an RGD motif overlaps the RXLR motifs of several oomycete effectors (Senchou et al., 2004), and receptors that bind the RGD motifs have been identified (Gouget et al., 2006). The four flax rust Avr gene products share a GxxR motif, but mutagenesis of the motif had no effect on the relevant R gene interactions (Catanzariti et al., 2006). AVR_{k1} and AVR_{a10} of *B. graminis* f. sp *hordei* share a motif ([R/K]VY[L/I]R) with some resemblance to the oomycete RXLR motif, but no functional data are available as to its role (Ridout et al., 2006). The ability to use Avr1b as a reporter protein for entry into plant cells may facilitate the experimental identification of the motifs required for entry of these fungal proteins into plant cells.

METHODS

Plasmids and oligonucleotides used in the study are described in Supplemental Tables 1 and 2 online, respectively.

Phytophthora sojae Isolates and Transformation

P. sojae isolate P7076 (Race 19) (Forster et al., 1994) was routinely grown and maintained on V8 agar (Erwin and Ribiero, 1996). The *P. sojae* transformation procedure was described by Dou et al. (2008) and was kindly provided by A. McLeod and W. Fry (Cornell University) prior to publication. (McLeod et al., 2008).

Characterization of *P. sojae* Transformants

P. sojae transformants were selected that grew well on V8 medium with 50 μg/mL G418 and were cultured in V8 liquid medium for 3 d. The mycelia were harvested, frozen in liquid nitrogen, and ground to a powder for DNA or RNA extraction.

Genomic DNA was isolated from mycelium as described by Judelson et al. (1991). DNA samples were quantified using a Nanodrop ND-1000 spectrophotometer (Thermo Scientific). The presence of *Avr1b*-1 transgenes was verified by PCR amplification from 100 ng genomic DNA using a program of 94°C for 2 min, 30 cycles of 94°C for 30 s, 56°C for 30 s, 72°C for 30 s, and 72°C for 5 min with primers of HamF and HamR (TS1). All the transformed *P. sojae* were double-checked by *Pst*I restriction and/or sequence.

RNA was extracted from each sample using RNeasy plant mini kit (Qiagen) with β-mercaptoethanol added buffer RLT, and genomic DNA was removed using RNase-Free DNase (Qiagen) according to the manufacturer's recommendations. RNA was quantified using a Nanodrop ND-1000 spectrophotometer. *Avr1b*-1 transgene transcription was verified by RT-PCR using the internal primers, Avr1bReF and Avr1bReR (TS1), and *P. sojae* actin was used as the reference.

Phenotypic Assays for Avirulence

Avr1b phenotypic expression was assayed using soybean (*Glycine max*) cultivars HARO(1-7) (rps), Haro13 (Harosoy background, Rps1b), Williams (rps), and L77-1863 (Williams background, Rps1b) (Buzzell et al., 1987). The seed was kindly provided by Terry Anderson (Agriculture Canada). Seedlings were grown in the greenhouse or in a growth chamber (Percival AR-36L) with a program of 24°C at daytime and 22°C at night with a 14-h daylength under fluorescent light (250 μmol photons s^{-1} m^{-2}).

The virulence of each transformant was evaluated using hypocotyl inoculation (Tyler et al., 1995). One to two days after the first primary leaf appeared, the hypocotyl of the soybean was wounded with a short incision and the incision was inoculated with a small piece of V8 agar cut from the edge of a 3-d-old colony. Thereafter, the plants were incubated in a growth chamber under the conditions described above. The numbers of dead and surviving plants were counted 4 d after inoculation and summed over two to five replicates. The differences between the numbers of surviving plants from *rps* and *Rps*1b cultivars were compared using Fisher's exact test (Sokal and Rohlf, 1995). Only the transformants producing a significant difference between rps and Rps1b cultivars were judged as avirulent.

Particle Bombardment Assays

Particle bombardment assays were performed using a double-barreled extension of the Bio-Rad He/1000 particle delivery system (Dou et al., 2008). Analyzing the bombardment data as a ratio between the test and control shots improves the reproducibility of the measurements greatly (Dou et al., 2008).

The avirulence activity of the *Avr1b*-1 constructs was measured as the reduction in the number of blue spots comparing the *Avr1b*-1 + GUS bombardment with the GUS + control bombardment. For each paired shot, the logarithm of the ratio of the spot numbers of *Avr1b*-1 to that of the control was calculated, and then the log ratios obtained from the *Rps*1b and non-*Rps*1b leaves were compared using the Wilcoxon rank sum test (Sokal and Rohlf, 1995).

Bombardment Assays of Onion Bulb Cells with GFP Constructs

Preparation of DNA-particle mixtures was as described above. Five-millimeter hemispherical layers of yellow and white onion bulbs were bombarded without the double barrel attachment under a 26-p.s.i. vacuum, using a rupture pressure of 1100 p.s.i. The onion layers were incubated between 24 and 48 h at 25°C, and then viewed with a Zeiss Axioskop2 Plus microscope using a 480-nm filter for GFP fluorescence. Images were captured using a Qimaging Retiga 1300 camera. To further confirm that the GFP had been secreted out of the onion cells, plasmolysis was performed for 15 min in 0.8 M mannitol and cells were observed in a Zeiss LSM510 laser scanning confocal microscope with an argon laser excitation wavelength of 488 nm.

RXLR-GFP Fusion Protein Expression and Purification

Residues 33 to 71 of Avr1b (VESPDLVRRSLRNGDIAGGRFLRAHEED-DAGERTFSVTD), including the RXLR1, RXLR2, and dEER motifs, were

fused to GFP (see Supplemental Table 2 online), replacing the Arg_9 encoding sequences in vector pR9GFP (called pR9 by Chang et al., 2005). pR9GFP, which also adds an N-terminal His_6 tag, was derived by Chang et al. (2005) from pTAT-HA provided by Steven Dowdy (Washington University, St. Louis, MO).

C43(DE3) *Escherichia coli* cells containing RXLR-GFP fusion constructs or pR9 were grown in 200 mL of Luria-Bertani medium containing 100 μg/mL ampicillin in a 1-liter baffled flask shaken at 240 rpm at 37°C until reaching an OD of 0.4, at which point the cells were induced by addition of 1 mL of 1 M isopropylthio-β-galactoside (final [5 mM]). After 4 h of further growth at the same conditions, the cells were harvested by centrifugation at 4°C and then stored at −20°C. Visual confirmation of GFP expression was noted by the green color of the bacterial cell pellet.

To extract the GFP fusion proteins, cells were thawed on ice for 20 min, and then 4 mL of lysis buffer (50 mM NaH_2P0_4, 300 mM NaCl, and 10 mM imidazole, pH 8.0) were added per 1 g of wet cell weight. Lysozyme (Sigma-Aldrich) was added to a final concentration of 1 mg/mL, and then the suspension was incubated for 20 min on ice. Sonication (Branson Sonifier 150D, with double stepped microtip, 3 mm) was done at 300 W at 15-s bursts four times with 15-s cooling periods between each burst. The lysate was centrifuged at 10,000*g* for 30 min at 4°C, and then the supernatant was transferred to a fresh tube and kept on ice until use. Five microliters of each sample was stored for SDS-PAGE analysis.

Protein purification using Ni-NTA affinity chromatography was performed using the QiaExpressionist protocol. Two milliliters of 50% Ni-NTA superflow slurry (Qiagen) was loaded on a column. The column was washed twice with 5 mL of wash buffer (50 mM NaH_2P0_4, 300 mM NaCl, and 20 mM imidazole, pH 8.0). The protein sample was loaded onto the column, and then the column was washed twice with 10 volumes (10 mL) of wash buffer. The protein was eluted with 4 mL of elution buffer (50 mM NaH_2P0_4, 300 mM NaCl, and 200 mM imidazole, pH 8.0) into 1-mL fractions. These fractions were pooled and concentrated to 300 μL using a centrifugal protein concentrator (Amicon Centriplus Centrifugal Filter Device MWCO-3kDa) at 13,500*g*. The sample was then mixed with an equal volume of 50 mM MES buffer, pH 5.8. The protein concentration was measured at 280 nm using a nanodrop spectrophotometer (ND-1000) and adjusted to 8 mg/mL. All purified GFP preparations fluoresced normally under UV illumination.

RXLR-GFP Fusion Protein Root Cell Transduction Assay

Root tips were cut into lengths of between 0.5 and 1 cm and then were washed with water. Each root tip was completely submerged in 20 μL of the protein solution (8 mg/mL in 25 mM MES, pH 5.8) in an Eppendorf tube. The samples were incubated overnight at 28°C (~12 h). The roots were then washed in 200 mL of water for 4 h while shaken at 100 rpm on a rotary shaker. The roots were then viewed using a Zeiss LSM510 laser scanning confocal microscope with an argon laser excitation wavelength of 488 nm. For nuclear staining, the roots were stained with DAPI (Sigma-Aldrich) and viewed with a 405-nm filter.

HMM Analysis

Using the program HMMER 2.3.2 (Eddy, 1998) (http://hmmer.janelia.org), an HMM was built from the full set of 765 high-quality candidate effectors identified from the *P. sojae* and *Phytophthora ramorum* genomes by Jiang et al. (2008), using the 10 amino acids on the left side of each RXLR motif together with the 10 amino acids on the right side each RXLR motif. The same procedure was used to build an HMM from a curated list of 191 high-quality candidate effectors from *Hyaloperonospora parasitica* developed at the *H. parasitica* genome annotation jamboree in August 2007 and available at pmgn.vbi.vt.edu. To estimate the significance of HMM scores, all proteins (1240) with a predicted N-terminal signal peptide and the string RXLR located between 30 and 60 amino acids after the signal peptide cleavage site were obtained by translating the genome sequences of *P. sojae* and *P. ramorum* in all reading frames (Jiang et al., 2008). The sequences of all the putative secreted proteins were permuted (other than the signal peptide), and RXLR-containing sequences were again identified; 639 of the permuted proteins had RXLR strings, indicating that ~639 of the 1240 detected RXLR motifs could be expected by chance (Jiang et al., 2008). The distributions of HMM scores from the set of 1240 real proteins, the 639 permuted proteins and the 765 curated proteins were then calculated. The frequency that a permuted protein received a score between 0 and 5.0 was 0.044. The frequency that a permuted protein received a score better than 5.0 was 0.018.

Accession Numbers

Sequence data from this article can be found in the GenBank/EMBL database under accession number EF681127 (Hp *Avh*341). Accession numbers for sequences already in GenBank are as follows: Ps *Avr1b*-1 (AAM20936), Ps *Avr4/6* (ABS50087), Pi *Avr3a* (CAI72345), Hp *Atr1* (AY842877), and Hp *Atr13* (AY785301).

Supplemental Data

The following materials are available in the online version of this article.

Supplemental Figure 1. Plasmolysis of Onion Cells Expressing Secreted GFP Fusion Proteins.

Supplemental Table 1. Oligonucleotides Used for PCR and Plasmid Construction.

Supplemental Table 2. Description of Plasmids Used.

Supplemental Table 3. Efficiency of PEG-Mediated *P. sojae* Protoplast Transformation.

ACKNOWLEDGMENTS

We thank Han-jung Lee (National Dong Hwa University, Taiwan) for providing us with plasmid pR9GFP and for helpful discussions, Adele McLeod (University of Stellenbosch, South Africa) and William Fry (Cornell University) for providing their *P. sojae* transformation protocol prior to publication, Terry Anderson (Agriculture Canada) and Saghai Maroof (Virginia Tech) for soybean seed, Yinghui Dan, Robert Presler, and Nickolaus Galloway (all of Virginia Tech) for assistance with particle bombardment assays, Ryan Anderson and John McDowell (both of Virginia Tech) for the Hp *Avh*341 gene, Emily Berisford and Carol Volker for manuscript preparation, and June Mullins (Virginia Tech) for illustrations. This work was supported by grants to B.M.T. from the National Research Initiative of the USDA Cooperative State Research, Education, and Extension Service (Grants 2001-35319-14251, 2002-35600-12747, 2004-35600-15055, and 2007-35319-18100) and from the U.S. National Science Foundation (Grants MCB-0242131 and EF-0412213) and by funds from the Virginia Bioinformatics Institute. R.H.Y.J. was supported in part by fellowship NGI 050-72-404 from the Netherlands Genomics Initiative.

Received October 11, 2007; revised June 6, 2008; accepted June 27, 2008; published July 11, 2008.

REFERENCES

Alfano, J.R., and Collmer, A. (2004). Type III secretion system effector proteins: Double agents in bacterial disease and plant defense. Annu. Rev. Phytopathol. **42:** 385–414.

Allen, R.L., Bittner-Eddy, P.D., Grenville-Briggs, L.J., Meitz, J.C., Rehmany, A.P., Rose, L.E., and Beynon, J.L. (2004). Host-parasite coevolutionary conflict between *Arabidopsis* and downy mildew. Science **306:** 1957–1960.

Anderson, P.A., Lawrence, G.J., Morrish, B.C., Ayliffe, M.A., Finnegan, E.J., and Ellis, J.G. (1997). Inactivation of the flax rust resistance gene M associated with loss of a repeated unit within the leucine-rich repeat coding region. Plant Cell **9:** 641–651.

Armstrong, M.R., et al. (2005). An ancestral oomycete locus contains late blight avirulence gene *Avr3a*, encoding a protein that is recognized in the host cytoplasm. Proc. Natl. Acad. Sci. USA **102:** 7766–7771.

Ballvora, A., Ercolano, M.R., Weiss, J., Meksem, K., Bormann, C.A., Oberhagemann, P., Salamini, F., and Gebhardt, C. (2002). The *R*1 gene for potato resistance to late blight (*Phytophthora infestans*) belongs to the leucine zipper/NBS/LRR class of plant resistance genes. Plant J. **30:** 361–371.

Bhattacharjee, S., Hiller, N.L., Liolios, K., Win, J., Kanneganti, T.D., Young, C., Kamoun, S., and Haldar, K. (2006). The malarial host-targeting signal is conserved in the Irish potato famine pathogen. PLoS Pathog. **2:** e50.

Bhattacharjee, S., van Ooij, C., Balu, B., Adams, J.H., and Haldar, K. (2008). Maurer's clefts of *Plasmodium falciparum* are secretory organelles that concentrate virulence protein reporters for delivery to the host erythrocyte. Blood **111:** 2418–2426.

Birch, P.R., Rehmany, A.P., Pritchard, L., Kamoun, S., and Beynon, J.L. (2006). Trafficking arms: Oomycete effectors enter host plant cells. Trends Microbiol. **14:** 8–11.

Bonello, J.-F., Sevilla-Lecoq, S., Berne, A., Risueno, M.-C., Dumas, C., and Rogowsky, P.M. (2002). Esr proteins are secreted by the cells of the embryo surrounding region. J. Exp. Bot. **53:** 1559–1568.

Bryan, G.T., Wu, K.-S., Farrall, L., Jia, Y., Hershey, H.P., McAdams, S.A., Faulk, K.N., Donaldson, G.K., Tarchini, R., and Valent, B. (2000). A single amino acid difference distinguishes resistant and susceptible alleles of the rice blast resistance gene Pi-ta. Plant Cell **12:** 2033–2046.

Buzzell, R.I., Anderson, T.R., and Rennie, B.D. (1987). Harosoy *Rps* isolines. Soyb. Genet. Newsl. **14:** 79–81.

Catanzariti, A.M., Dodds, P.N., Lawrence, G.J., Ayliffe, M.A., and Ellis, J.G. (2006). Haustorially expressed secreted proteins from flax rust are highly enriched for avirulence elicitors. Plant Cell **18:** 243–256.

Chang, M., Chou, J.C., Chen, C.P., Liu, B.R., and Lee, H.J. (2007). Noncovalent protein transduction in plant cells by macropinocytosis. New Phytol. **174:** 46–56.

Chang, M., Chou, J.C., and Lee, H.J. (2005). Cellular internalization of fluorescent proteins via arginine-rich intracellular delivery peptide in plant cells. Plant Cell Physiol. **46:** 482–488.

Cloutier, S., McCallum, B.D., Loutre, C., Banks, T.W., Wicker, T., Feuillet, C., Keller, B., and Jordan, M.C. (2007). Leaf rust resistance gene *Lr*1, isolated from bread wheat (*Triticum aestivum L.*) is a member of the large psr567 gene family. Plant Mol. Biol. **65:** 93–106.

Dangl, J.L., and Jones, J.D.G. (2001). Plant pathogens and integrated defence responses to infection. Nature **411:** 826–833.

Davis, E.L., and Mitchum, M.G. (2005). Nematodes. Sophisticated parasites of legumes. Plant Physiol. **137:** 1182–1188.

Dodds, P.N., Lawrence, G.J., Catanzariti, A.M., Ayliffe, M.A., and Ellis, J.G. (2004). The *Melampsora lini AvrL*567 avirulence genes are expressed in haustoria and their products are recognized inside plant cells. Plant Cell **16:** 755–768.

Dodds, P.N., Lawrence, G.J., and Ellis, J.G. (2001a). Six amino acid changes confined to the leucine-rich repeat beta-strand/beta-turn motif determine the difference between the P and P2 rust resistance specificities in flax. Plant Cell **13:** 163–178.

Dodds, P.N., Lawrence, G.J., and Ellis, J.G. (2001b). Contrasting modes of evolution acting on the complex *N* locus for rust resistance in flax. Plant J. **27:** 439–453.

Dou, D., et al. (2008). Conserved C-terminal motifs required for avirulence and suppression of cell death by *Phytophthora sojae* effector Avr1b. Plant Cell **20:** 1118–1133.

Eddy, S.R. (1998). Profile hidden Markov models. Bioinformatics **14:** 755–763.

Erwin, D.C., and Ribiero, O.K. (1996). *Phytophthora* Diseases Worldwide. (St. Paul, MN: APS Press).

Feuillet, C., Travella, S., Stein, N., Albar, L., Nublat, A., and Keller, B. (2003). Map-based isolation of the leaf rust disease resistance gene *Lr*10 from the hexaploid wheat (*Triticum aestivum* L.) genome. Proc. Natl. Acad. Sci. USA **100:** 15253–15258.

Förster, H., Coffey, M.D., Elwood, H., and Sogin, M.L. (1990). Sequence analysis of the small subunit ribosomal RNAs of 3 zoosporic fungi and implications for fungal evolution. Mycologia **82:** 306–312.

Forster, H., Tyler, B.M., and Coffey, M.D. (1994). *Phytophthora sojae* races have arisen by clonal evolution and by rare outcrosses. Mol. Plant Microbe Interact. **7:** 780–791.

Futaki, S. (2002). Arginine-rich peptides: Potential for intracellular delivery of macromolecules and the mystery of the translocation mechanisms. Int. J. Pharm. **245:** 1–7.

Gao, H., Narayanan, N.N., Ellison, L., and Bhattacharyya, M.K. (2005). Two classes of highly similar coiled coil-nucleotide binding-leucine rich repeat genes isolated from the *Rps*1-k locus encode *Phytophthora* resistance in soybean. Mol. Plant Microbe Interact. **18:** 1035–1045.

Gouget, A., Senchou, V., Govers, F., Sanson, A., Barre, A., Rouge, P., Pont-Lezica, R., and Canut, H. (2006). Lectin receptor kinases participate in protein-protein interactions to mediate plasma membrane-cell wall adhesions in *Arabidopsis.* Plant Physiol. **140:** 81–90.

Govers, F., and Gijzen, M. (2006). *Phytophthora* genomics: The plant destroyers' genome decoded. Mol. Plant Microbe Interact. **19:** 1295–1301.

Hahn, M., and Mendgen, K. (2001). Signal and nutrient exchange at biotrophic plant–fungus interfaces. Curr. Opin. Plant Biol. **4:** 322–327.

Halterman, D., Zhou, F., Wei, F., Wise, R.P., and Schulze-Lefert, P. (2001). The MLA6 coiled-coil, NBS-LRR protein confers AvrMla6-dependent resistance specificity to *Blumeria graminis* f. sp. *hordei* in barley and wheat. Plant J. **25:** 335–348.

Hardham, A.R. (2007). Cell biology of plant-oomycete interactions. Cell. Microbiol. **9:** 31–39.

Harper, J.T., Waanders, E., and Keeling, P.J. (2005). On the monophyly of chromalveolates using a six-protein phylogeny of eukaryotes. Int. J. Syst. Evol. Microbiol. **55:** 487–496.

Hiller, N.L., Bhattacharjee, S., van Ooij, C., Liolios, K., Harrison, T., Lopez-Estrano, C., and Haldar, K. (2004). A host-targeting signal in virulence proteins reveals a secretome in malarial infection. Science **306:** 1934–1937.

Huang, S., van der Vossen, E.A., Kuang, H., Vleeshouwers, V.G., Zhang, N., Borm, T.J., van Eck, H.J., Baker, B., Jacobsen, E., and Visser, R.G. (2005). Comparative genomics enabled the isolation of the *R*3a late blight resistance gene in potato. Plant J. **42:** 251–261.

Jiang, R.H.Y., Tripathy, S., Govers, F., and Tyler, B.M. (2008). RXLR effector reservoir in two *Phytophthora* species is dominated by a single rapidly evolving super-family with more than 700 members. Proc. Natl. Acad. Sci. USA **105:** 4874–4879.

Joliot, A. (2005). Transduction peptides within naturally occurring proteins. Sci. STKE **2005:** pe54.

Judelson, H., Tyler, B.M., and Michelmore, R.W. (1991). Transformation of the oomycete pathogen, *Phytophthora infestans.* Mol. Plant Microbe Interact. **4:** 602–607.

Kaplan, I.M., Wadia, J.S., and Dowdy, S.F. (2005). Cationic TAT peptide transduction domain enters cells by macropinocytosis. J. Control. Release **102:** 247–253.

Kemen, E., Kemen, A.C., Rafiqi, M., Hempel, U., Mendgen, K., Hahn, M., and Voegele, R.T. (2005). Identification of a protein from rust fungi transferred from haustoria into infected plant cells. Mol. Plant Microbe Interact. **18:** 1130–1139.

Langel, U. (2006). Handbook of Cell-Penetrating Peptides, 2d ed. (Boca Raton, FL: CRC/Taylor & Francis).

Lawrence, G.J., Finnegan, E.J., Ayliffe, M.A., and Ellis, J.G. (1995). The *L*6 gene for flax rust resistance is related to the *Arabidopsis* bacterial resistance gene *RPS*2 and the tobacco viral resistance gene *N.* Plant Cell **7:** 1195–1206.

Manning, V.A., and Ciuffetti, L.M. (2005). Localization of Ptr ToxA Produced by *Pyrenophora tritici-repentis* reveals protein import into wheat mesophyll cells. Plant Cell **17:** 3203–3212.

Marti, M., Good, R.T., Rug, M., Knuepfer, E., and Cowman, A.F. (2004). Targeting malaria virulence and remodeling proteins to the host erythrocyte. Science **306:** 1930–1933.

Martin, G.B., Brommonschenkel, S.H., Chunwongse, J., Frary, A., Ganal, M.W., Spivey, R., Wu, T., Earle, E.D., and Tanksley, S.D. (1993). Map-based cloning of a protein kinase gene conferring disease resistance in tomato. Science **262:** 1432–1436.

McLeod, A., Fry, B.A., Zuluaga-Duque, A.P., Meyers, K.L., and Fry, W.E. (2008). Toward improvements of oomycete transformation protocols. J. Eukaryot. Microbiol. **55:** 103–109.

Mindrinos, M., Katagiri, F., Yu, G.L., and Ausubel, F.M. (1994). The *A. thaliana* disease resistance gene *RPS*2 encodes a protein containing a nucleotide-binding site and leucine-rich repeats. Cell **78:** 1089–1099.

Orbach, M.J., Farrall, L., Sweigard, J.A., Chumley, F.G., and Valent, B. (2000). A telomeric avirulence gene determines efficacy for the rice blast resistance gene *Pi-ta.* Plant Cell **12:** 2019–2032.

Plano, G.V., Day, J.B., and Ferracci, F. (2001). Type III export: New uses for an old pathway. Mol. Microbiol. **40:** 284–293.

Qu, S., Liu, G., Zhou, B., Bellizzi, M., Zeng, L., Dai, L., Han, B., and Wang, G.L. (2006). The broad-spectrum blast resistance gene *Pi*9 encodes a nucleotide-binding site-leucine-rich repeat protein and is a member of a multigene family in rice. Genetics **172:** 1901–1914.

Qutob, D., Kamoun, S., and Gijzen, M. (2002). Expression of a *Phytophthora sojae* necrosis-inducing protein occurs during transition from biotrophy to necrotrophy. Plant J. **32:** 361–373.

Rehmany, A.P., Gordon, A., Rose, L.E., Allen, R.L., Armstrong, M.R., Whisson, S.C., Kamoun, S., Tyler, B.M., Birch, P.R., and Beynon, J.L. (2005). Differential recognition of highly divergent downy mildew avirulence gene alleles by *RPP*1 resistance genes from two Arabidopsis lines. Plant Cell **17:** 1839–1850.

Ridout, C.J., Skamnioti, P., Porritt, O., Sacristan, S., Jones, J.D., and Brown, J.K. (2006). Multiple avirulence paralogues in cereal powdery mildew fungi may contribute to parasite fitness and defeat of plant resistance. Plant Cell **18:** 2402–2414.

Romer, P., Hahn, S., Jordan, T., Strauss, T., Bonas, U., and Lahaye, T. (2007). Plant pathogen recognition mediated by promoter activation of the pepper *Bs*3 resistance gene. Science **318:** 645–648.

Sandhu, D., Gao, H., Cianzio, S., and Bhattacharyya, M.K. (2004). Deletion of a disease resistance nucleotide-binding-site leucine-rich-repeat-like sequence is associated with the loss of the *Phytophthora* resistance gene *Rps*4 in soybean. Genetics **168:** 2157–2167.

Senchou, V., Weide, R., Carrasco, A., Bouyssou, H., Pont-Lezica, R., Govers, F., and Canut, H. (2004). High affinity recognition of a *Phytophthora* protein by *Arabidopsis* via an RGD motif. Cell. Mol. Life Sci. **61:** 502–509.

Shan, W., Cao, M., Leung, D., and Tyler, B.M. (2004). The *Avr1b* locus of *Phytophthora sojae* encodes an elicitor and a regulator required for avirulence on soybean plants carrying resistance gene *Rps1b.* Mol. Plant Microbe Interact. **17:** 394–403.

Shen, K.A., Chin, D.B., Arroyo-Garcia, R., Ochoa, O.E., Lavelle, D.O., Wroblewski, T., Meyers, B.C., and Michelmore, R.W. (2002). *Dm*3 is one member of a large constitutively expressed family of nucleotide binding site-leucine-rich repeat encoding genes. Mol. Plant Microbe Interact. **15:** 251–261.

Slusarenko, A.J., and Schlaich, N.L. (2003). Pathogen profile. Downy mildew of *Arabidopsis thaliana* caused by *Hyaloperonospora parasitica* (formerly *Peronospora parasitica*). Mol. Plant Pathol. **4:** 159–170.

Snyder, E.L., and Dowdy, S.F. (2004). Cell penetrating peptides in drug delivery. Pharm. Res. **21:** 389–393.

Sogin, M.L., and Silberman, J.D. (1998). Evolution of the protists and protistan parasites from the perspective of molecular systematics. Int. J. Parasitol. **28:** 11–20.

Sokal, R.R., and Rohlf, F.J. (1995). Biometry. The Principles and Practice of Statistics in Biological Research. (New York: W.H. Freeman and Company).

Song, J., Bradeen, J.M., Naess, S.K., Raasch, J.A., Wielgus, S.M., Haberlach, G.T., Liu, J., Kuang, H., Austin-Phillips, S., Buell, C.R., Helgeson, J.P., and Jiang, J. (2003). Gene *Rb* cloned from *Solanum bulbocastanum* confers broad spectrum resistance to potato late blight. Proc. Natl. Acad. Sci. USA **100:** 9128–9133.

Srichumpa, P., Brunner, S., Keller, B., and Yahiaoui, N. (2005). Allelic series of four powdery mildew resistance genes at the *Pm*3 locus in hexaploid bread wheat. Plant Physiol. **139:** 885–895.

Staskawicz, B.J., Mudgett, M.B., Dangl, J.L., and Galan, J.E. (2001). Common and contrasting themes of plant and animal diseases. Science **292:** 2285–2289.

Tomasinsig, L., Skerlavaj, B., Papo, N., Giabbai, B., Shai, Y., and Zanetti, M. (2006). Mechanistic and functional studies of the interaction of a proline-rich antimicrobial peptide with mammalian cells. J. Biol. Chem. **281:** 383–391.

Torto, T.A., Li, S., Styer, A., Huitema, E., Testa, A., Gow, N.A., van West, P., and Kamoun, S. (2003). EST mining and functional expression assays identify extracellular effector proteins from the plant pathogen *Phytophthora.* Genome Res. **13:** 1675–1685.

Tyler, B., Forster, H., and Coffey, M.D. (1995). Inheritance of avirulence factors and restriction fragment length polymorphism markers in outcrosses of the oomycete *Phytophthora sojae.* Mol. Plant Microbe Interact. **8:** 515–523.

Tyler, B.M. (2002). Molecular basis of recognition between *Phytophthora* species and their hosts. Annu. Rev. Phytopathol. **40:** 137–167.

Tyler, B.M., et al. (2006). *Phytophthora* genome sequences uncover evolutionary origins and mechanisms of pathogenesis. Science **313:** 1261–1266.

van der Vossen, E., Sikkema, A., Hekkert, B.L., Gros, J., Stevens, P., Muskens, M., Wouters, D., Pereira, A., Stiekema, W., and Allefs, S. (2003). An ancient R gene from the wild potato species *Solanum bulbocastanum* confers broad-spectrum resistance to *Phytophthora infestans* in cultivated potato and tomato. Plant J. **36:** 867–882.

Wang, Z.-X., Yano, M., Yamanouchi, U., Iwamoto, M., Monna, L., Hayasaka, H., Katayose, Y., and Sasaki, T. (1999). The *Pib* gene for rice blast resistance belongs to the nucleotide binding and leucine-rich repeat class of plant disease resistance genes. Plant J. **19:** 55–64.

Whisson, S.C., et al. (2007). A translocation signal for delivery of oomycete effector proteins into host plant cells. Nature **450:** 115–119.

Wrather, J.A., and Koenning, S.R. (2006). Estimates of disease effects on soybean yields in the United States 2003 to 2005. J. Nematol. **38:** 173–180.

Wroblewski, T., Piskurewicz, U., Tomczak, A., Ochoa, O., and Michelmore, R.W. (2007). Silencing of the major family of NBS-LRR-encoding genes in lettuce results in the loss of multiple resistance specificities. Plant J. **51:** 803–818.

Yahiaoui, N., Srichumpa, P., Dudler, R., and Keller, B. (2004). Genome analysis at different ploidy levels allows cloning of the powdery mildew resistance gene *Pm*3b from hexaploid wheat. Plant J. **37:** 528–538.

Yamane, H., Lee, S.-J., Kim, B.-D., Tao, R., and Rose, J.K.C. (2005). A coupled yeast signal sequence trap and transient plant expression strategy to identify genes encoding secreted proteins from peach pistils. J. Exp. Bot. **56:** 2229–2238.

Yoon, H.S., Hackett, J.D., Pinto, G., and Bhattacharya, D. (2002). The single, ancient origin of chromist plastids. Proc. Natl. Acad. Sci. USA **99:** 15507–15512.

Supplemental Data. Dou et al. (2008) RXLR-mediated entry of *Phytophthora sojae* effector Avr1b into soybean cells does not require pathogen encoded machinery

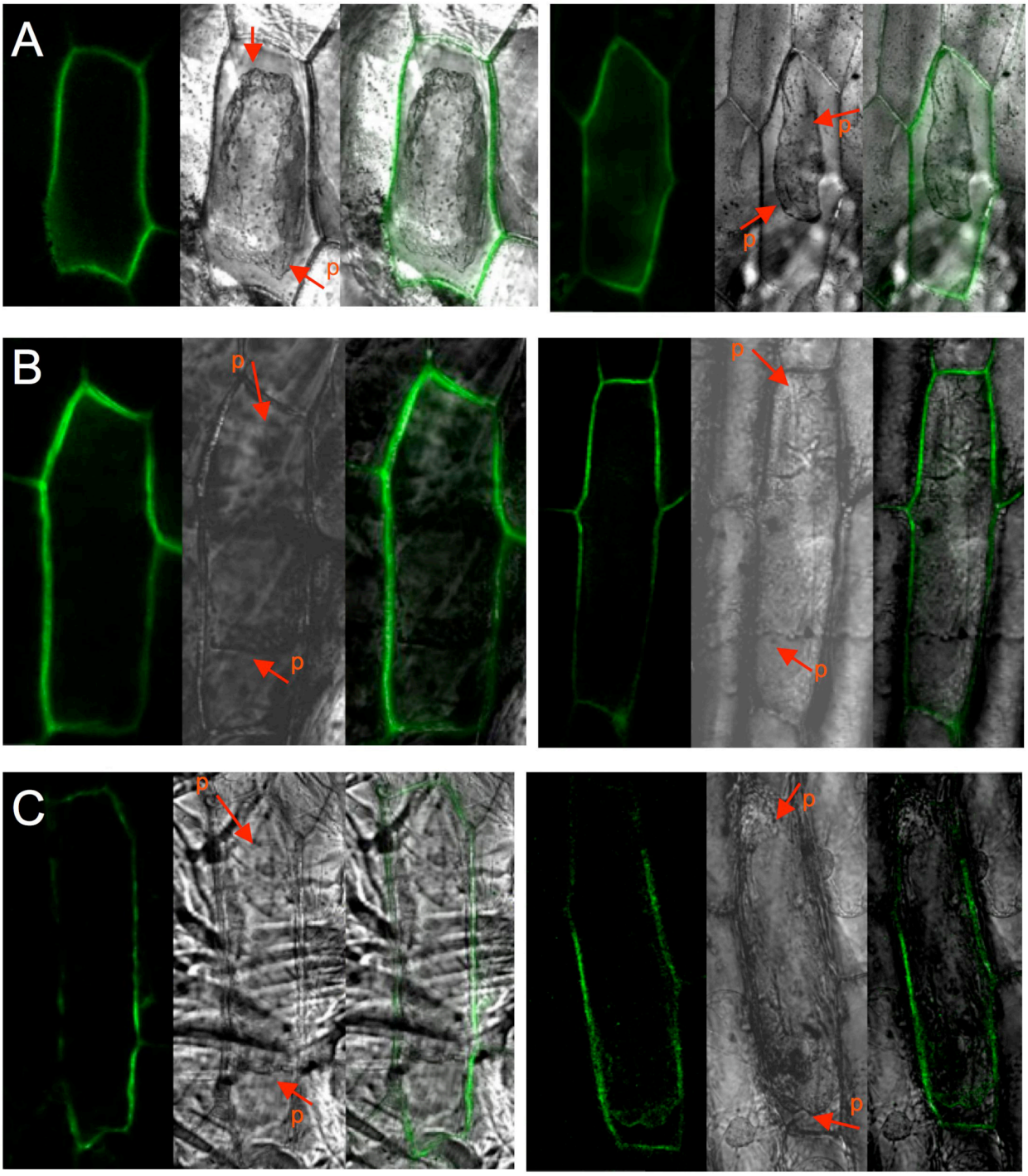

Supplemental Figure 1. Plasmolyzed onion bulb epidermal cells expressing secreted Avr1b-GFP fusion proteins.

DNA encoding various fusions of Avr1b with *Aequorea coerulescens* green fluorescent protein (GFP) was bombarded into onion epidermal cells. 24 hours later, plasmolysis was performed for 15 min in 0.8 M mannitol.

Each cell is shown three times in adjacent panels: fluorescent image (left), bright-field image (middle) and merged image (right). “p” indicates the plasma membrane in plasmolyzed cells.

(A) Fusion of GFP to the secretory leader of Avr1b alone (sGFP);
(B) GFP fused to Avr1b RXLR2^{AAAA} mutant including its secretory leader;
(C) GFP fused to Avr1b dEER^{A6} mutant including its secretory leader.

No	Name	Applications	Sequence (from 5' to 3')*
1	UF	*Hind* III and *Xma* I sites added to rpL41 promoter to drive G418 resistance gene	ataagcttgaatTCTGGCGTTCATCTCCGACG
2	UR		ttcccgggTGGATGCTCAGATGctagcGTC
3	HamF	*Bremia* Ham34 promoter internal primer	TTCTCCTTTTCACTCTCACG
4	HamR	*Bremia* Ham34 Terminator internal primer	AGACACAAAATCTGCAACTTC
5	Avr1bReF	*Avr1b*-1 internal primers for PCR	ACCTTCAGCGTGACTGACCT
6	Avr1bReR		GCGATTGCCAACCAGTTCT
7	ActinF	*P. sojae Actin* gene internal primers for the reference in RT-PCR	CGACATCCGTAAGGACCTGT
8	ActinR		TTCGAGATCCACATCTGCTG
9	PrimerC	*Kpn* I sites added flanking *Avr1b*-1 for insertion downstream of HAM34 promoter	ggggtaccgacaacaATGCGTCTATCTTTTGTGCT
10	PrimerD		ggggtaccTCAGCTCTGATACCGGTGAA
11	Avr1bF	*Xho* I site and initiation codon added to 5' end of mature *Avr1b*-1 for insertion downstream of CaMV 35S promoter	atcgcactcgagctttcgcagatcccgggggcaatgagatatgACTGAGTACTCCGACGAA
12	Avr1bR	*Xho* I site to 3' end of *Avr1b*-1 for insertion downstream of CaMV 35S promoter	atcgcactcgagcttgtcgatcgacagatccggtcggcatctactTCAGCTCTGATACCGGTG
13	Avr1bfull_F	Same as Avr1bF but for secretory *Avr1b*-1	atcgcactcgagctttcgcagatcccgggggcaatgagatATGCGTCTATCTTTTGTG
14	Motif1F	Introduction of RXLR1^{AAAA} mutation, creating a *Pst* I site	TCGTCCGTgctgcagctgctAACGGCGACATTGCCGGTGG
15	Motif1R		TCGCCGTTagcagctgcagcACGGACGAGATCTGGAGATT
16	Motif2F	Introduction of RXLR2^{AAAA} mutation, creating a *Pst* I site	CCGGTGGAgctgcagctgctGCTCATGAAGAGGACGATGC
17	Motif2R		TCATGAGCagcagctgcagcTCCACCGGCAATGTCGCCGT
18	Motif1+2F	Introduction of RXLR1^{AAAA} & RXLR2^{AAAA} mutations, creating 2 *Pst* I sites	gctgcagctgctAACGGCGACATTGCCGGTGGAgctgcagctgctGCTCATGAAGAGGACGATGC
19	Motif1+2R		agcagctgcagcTCCACCGGCAATGTCGCCGTTagcagctgcagcACGGACGAGATCTGGAGATT
20	Motif3F	Introduction of dEER^{A6} mutation, creating a *Pst* I site	gctgcagcagctGCGGGGgctgctACCTTCAGCGTGACTGACCT
21	Motif3R		agcagcCCCCGCagctgctgcagcATGAGCTCGAAGAAATCTTC
22	HpAvh341F	5' flanking *Xma* I site added to Hp Avh341 for insertion downstream of HAM34 promoter	attcccggggacaacaATGCGACTCCACTACGTG
23	HpAvh341R	For fusion with *Avr1b*-1	GTCAGTCACGCTGAAGGTlATCGAGAACGCCATGCCCAT
24	PsAvh171F	5' flanking *Xma* I site added to PsAvh171 for insertion downstream of HAM34 promoter	attcccggggacaacaATGGGCCTCCACAAGGGCT
26	PsAvh171R	For fusion with *Avr1b*-1	GTCAGTCACGCTGAAGGTlTAGGTGGTGTAGTCCGAC
26	1bRXLR(-)F	For deletion of N-terminus of *Avr1b*-1	aacccgggacaacaatgACCTTCAGCGTGACTGAC
27	Avr1b_EcoRI	Primers for making moving Avr1b expression cassette into pUC19 vector with *Xma* I and *Kpn* I sites flanking *Avr1b*-1 gene	GGAGgaaTTcGCTGGCTGGTGGCAGGAT
28	Avr1b_HindIII		GTATTGGCTAGAGaAGCTTGCCA
29	Avr1b_genegun_KpnI		AGAAACTCGAGCTTGTCGATCGACAGATCCGGTCGGCAggTACcTCAGCTCTGATAC
30	M2_F1	Replacement of RFLR with mutation encoding RFRL	GAAGATTTCgaCttGCTCATGAAG
31	M2_R1		CTTCATGAGCaaGtcGAAATCTTC
32	M2_F2	Replacement of RFLR with the mutation encoding FRLR	TGCCGGTGGAtttagaCTTCGAGCTC
33	M2_R2		GAGCTCGAAGtctaaaTCCACCGGCA
34	M2_F3	Replacement of RFLR with the	GAAGATTTgcaCGAGCTCAT

35	M2_R3	mutation encoding RFAR	ATGAGCTCGtgcAAATCTTC
36	M2_F4	Replacement of RFLR with the mutation encoding QFLQ	GGTGGAcagTTTCTTCaaGCTCATGAAG
37	M2_R4		AGCttGAAGAAActgTCCACCGGCAATG
38	GFPF	For fusion with *Avr1b*-1 to make *Avr1b*-1-*AcGFP*	CTTTCACCGGTATCAGAGCl<u>ggtaccg</u>cca<u>cc</u>l<u>atg</u>GTGAGCAAG GGCGCCGAG
39	GFPR	Addition of *Kpn* I after stop codon of GFP	AA<u>GgtaCC</u>tcaCTTGTACAGCTCATCCAT
40	Avr1bSac	Addition of NgoMIV site upstream of RFLR	TCAT<u>GAGCTC</u>GAAGAAATCTTCC<u>gCCGGC</u>AATG
41	AvrRFLQ	Replacement of RFLR with the mutation encoding RFLQ	CATT<u>GCCGGc</u>GGAAGATTTCTTCaAGC
42	AvrQFLR	Replacement of RFLR with the mutation encoding QFLR	CATT<u>GCCGGc</u>GGAcaATTTC
43	AvrRFVR	Replacement of RFLR with the mutation encoding RFVR	CATT<u>GCCGGc</u>GGAAGATTTgTTC
44	AvrKFLR	Replacement of RFLR with the mutation encoding KFLR	CATT<u>GCCGGc</u>GGA<u>Aag</u>TTTCTTC
45	Avr9R1	Replacement of RFLR with the sequence encoding the 9 arginine motif	cgtcgacgtcggcgacgcGCTCATGAAGAGGACGATG
46	Avr9R2		CATT<u>GCCGGc</u>GGAcgacggcgacgtcgacgtcggcgacg
47	AvrTAT1	Replacement of RFLR with the sequence encoding the TAT motif	taagaaacgccgtcagcgacgtcgaGCTCATGAAGAGGACGATG
48	AvfrTAT2		CATT<u>GCCGGc</u>GGAtatggacgtaagaaacgccgtcagc
49	GBPF1	Replacement of RFLR-dEER with the sequence from Pf GBP130	gaaggagaagactacactccggaaaagcaagcaaaag|ACCTTCAGCGTGA CTGACC
50	GBPF2		ctcgtatactggcagagggcgaagatacctgcgcaaggaaggagaagactacact
51	GBPF3		gtatgagaaagcggtagattacggctttcgagagtctcgtatactggcagag
52	GBPR		ctaccgctttctcatacttatc|TGCGTTGCAGGTCACGAC
53	HRPF1	Replacement of RFLR-dEER with the sequence from Pf HRPII	tgtcgacgatgcgcaccatgcacaccatgttgcagat|ACCTTCAGCGTGACT GACC
54	HRPF2		aacctcaacaagagactgttgcacgagacacaagcacatgtcgacgatgcgcacc
55	HRPF3		acaataacctgtgtagtaagaatgctaaaggcttgaacctcaacaagagactg
56	HRPR1		actacacaggttattgttaaa|TGCGTTGCAGGTCACGAC
57	1615F1	Replacement of RFLR-dEER with the sequence from Pf 1615c	cagtcaatgcattacaagaaatgttagatgatagtgtc|ACCTTCAGCGTGACT GACC
58	1615F2		ctcaagcagttggagttcatcacattggaagagaagacagtcaatgcattacaag
59	1615F3		aagatcaactcgtcatctacttatacacacagtagaatactcaagcagttggagttc
60	1615R1		agatgacgagttgatcttgttgtaact|TGCGTTGCAGGTCACGAC
61	AvrGFPF	Replacement of codons encoding nine arginine motif in pR9GFP with Avr1b residues 33 to 71 from wild type Avr1b or from Avr1b RXLR or dEER mutants	gatct<u>agatct</u>GTGGAATCTCCAGATCTC
62	AvrGFPR1		GTCATATGGATAGCCGGACAT|GTCAGTCACGCTGAAG GT
63	AvrGFPR2		GATC<u>CCATGG</u>AGCCAGCATAGTCTGGGACGTCATATGG ATAGCCGGA

Supplemental Table 1. Oligonucleotides used for PCR and plasmid construction.

Uppercase letters indicate bases that match the initial template. Lower case letters indicate mutations or 5' extensions that do not match the initial template. Restriction sites introduced into the amplicon are underlined. A pipe (|) indicates the boundary between *Avr1b*-1 sequences and fused sequences (Avh, GFP or *Plasmodium* RXLX motif) in the fusion oligonucleotides.

No	Plasmid Name	Sources	Construct	Construction strategy
1	pUN	pHAMT35N (*5*)	*Npt* II gene for G418 resistance fused to *P. sojae* rpL41 promoter in pUC19	Ham34 promoter of pHAMT35N replaced by *P. sojae* rpL41 promoter using primers UF and UR
2	pHamAvr1b	pHAMT35N	*Avr1b*-1 gene fused to Ham34 promoter and terminator for *P. sojae* transformation in pUC19	NptII gene of pHAMT35N replaced with *P. sojae Avr1b*-1 using PrimerC and PrimerD
3	M1	pHAMT35N	*Avr1b*-1(RXLR1^{AAAA}) mutant fused to Ham34 promoter and terminator	Same as pHamAvr1b with mutation introduced by primers motif1F and motif1R
4	M2	pHAMT35N	*Avr1b*-1(RXLR2^{AAAA}) mutant fused to Ham34 promoter and terminator	Same as pHamAvr1b with mutation introduced by primers motif2F and motif2R
5	M1+2	pHAMT35N	*Avr1b*-1(RXLR1^{AAA}A,2^{AAAA}) mutant fused to Ham34 promoter and terminator	Same as pHamAvr1b with mutation introduced by primers motif1+2F and motif1+2R
6	M3	pHAMT35N	*Avr1b*-1(dEER^{A6}) mutant fused to Ham34 promoter and terminator	Same as pHamAvr1b with mutation introduced by primers motif3F and motif3R
7	pHamAvh341	pHAMT35N	*HpAvh341* fused with C-terminal domain of *Avr1b*-1, driven by Ham34 promoter and terminator	NptII gene replaced with HpAvh341-Avr1b fusion using primers HpAvh341F, HpAvh341R and PrimerD
8	pHamAvh171	pHAMT35N	Ps *Avh171* (=*Avr*4/6) fused with C-terminal of *Avr1b*-1 driven by Ham34 promoter and terminator	NptII gene replaced with Ps Avh171-Avr1b fusion using primers PsAvh171F, PsAvh171R and PrimerD
9	pHamAvr1bCt	pHAMT35N	C-terminus of *Avr1b*-1 gene fused to Ham34 promoter and terminator for *P. sojae* transformation in pUC19	NptII gene of pHAMT35N replaced with *P. sojae Avr1b*-1 C terminus using primers 1bRXLR(-)F and PrimerD
10	UNM1	pUN and M1	Ham34::Avr1b (RXLR1^{AAAA}) inserted together with rpL41::NptII for *P. sojae* transformation	Selection and Gus expression cassettes in pCambia1305.2 replaced by inserts from pUN and M1, respectively
11	UNM2	pUN and M2	Ham34::Avr1b (RXLR2^{AAAA}) inserted together with rpL41::NptII for *P. sojae* transformation	Selection and Gus expression cassettes in pCambia1305.2 replaced by inserts from pUN and M2, respectively
12	UNM1+2	pUN and M1+2	Ham34::Avr1b (RXLR1^{AAAA}A,2^{AAAA}) inserted together with rpL41::NptII for *P. sojae* transformation	Selection and Gus expression cassettes in pCambia1305.2 replaced by inserts from pUN and M1+2, respectively
13	UNM3	pUN and M3	Ham34::Avr1b(dEER^{A6}) inserted together with rpL41::NptII for *P. sojae* transformation	Selection and Gus expression cassettes in pCambia1305.2 replaced by inserts from pUN and M3, respectively
14	pCambiaAvr1b	pCambia1305.2	CaMV 35S promoter fused to full length *Avr1b*-1 in GUS-containing vector	HMT gene in pCambia1305.2 replaced by *Avr1b*-1 using primers Avr1bfull_F and Avr1bR
15	pCambiaM2	pCambia1305.2	CaMV 35S promoter fused to *Avr1b*-1 (RXLR2^{AAAA}) in GUS-containing vector	HMT gene in pCambia1305.2 replaced by Avr1b(RXLR2) using primers Avr1bfull_F and Avr1bR
16	pCambia-mAvr1b	pCambia1305.2	CaMV 35S promoter fused to leaderless *Avr1b*-1 in GUS-containing vector	HMT gene in pCambia1305.2 replaced by mature *Avr1b*-1 using primers Avr1bF and Avr1bR
17	pCambia-mM2	pCambia1305.2	CaMV 35S promoter fused to leaderless *Avr1b*-1(RXLR2^{AAAA}) in GUS-containing vector	HMT gene in pCambia1305.2 replaced by mAvr1b(RXLR2) using primers Avr1bF and Avr1bR
18	pCa-GUS(-)	pCambia1305.2	Empty vector as the control	GUS expression cassette was removed by *Sph* I restriction and re-ligation for co-transformation experiments
19	pCaAvr1b	pCambiaAvr1b	CaMV 35S promoter fused to *Avr1b*-1 in GUS-free vector	
20	pCaM2	pCambiaM2	CaMV 35S promoter fused to *Avr1b*-1 (RXLR2^{AAAA}) in GUS-free vector	
21	pCa-mAvr1b	pCambia-mAvr1b	CaMV 35S promoter fused to leaderless *Avr1b*-1 in GUS-free vector	
22	pCa-mM2	pCambia-mM2	CaMV 35S promoter fused to leaderless *Avr1b*-1(RXLR2^{AAAA}) in GUS-free vector	
23	pUCAvr1b	pCambiaAvr1b	CaMV 35S promoter fused to *Avr1b*-1 with *Xma* I site	Avr1b expression cassette was inserted into pUC19 by PCR with primers Avr1b_EcoRI and Avr1b_HindIII

24	pUCAvr1bXK	pUCAvr1b	*Kpn* I site added to 3' end pUCAvr1b to facilitate later constructions	Amplification with primers Avr1b_EcoRI, Avr1b_HindIII and Avr1b_genegun_KpnI
25	pUCmAvr1b(dEER)	pUCAvr1bXK and M3	CaMV 35S promoter fused to mature *Avr1b*-1(dEER^{A6}) using *Xma* I and *Kpn* I sites	Ligation of *Xma* I-*Kpn* I fragment from M3 into pUCAvr1bXK
26	pUCmAvr1bGFP	pAcGFP1-N	Fusion of leaderless *Avr1b*-1 with *AcGFP* from pAcGFP1-N (Clontech, # 632485) placed under control of CaMV 35S promoter	AcGFP fused to relevant Avr1b sequence by PCR with primers Avr1bF or Avr1bfull_F plus GFPF and GFPR. PCR product inserted into pUCAvr1bXK using *Xma* I and *Kpn* I
27	pUCsAvr1bGFP	pUCAvr1bXK	Fusion of normal *Avr1b*-1 with *AcGFP* placed under control of CaMV 35S promoter	
28	pUCGFP	pUCsAvr1bGFP	CaMV 35S promoter fused to *AcGFP*	Deletion of Avr1b sequences by self-ligation of *Xma* I/*Age* I restricted pUCsAvr1bGFP
29	pUCsGFP		CaMV 35S promoter fusion of Avr1b secretory leader to *AcGFP* placed under control of CaMV 35S promoter	Deletion of Avr1b sequences encoding mature protein by self-ligation of *Nco* I restricted pUCsAvr1bGFP
30	pUCM2GFP	pUCAvr1bXK	*Avr1b*-1(RXLR2^{AAAA})-*AcGFP* fusion placed under control of CaMV 35S promoter	AcGFP fused to relevant Avr1b sequence by PCR with primers Avr1bfull_F, GFPF and GFPR. PCR product inserted into pUCAvr1bXK using *Xma* I and *Kpn* I
31	pUCM3GFP		*Avr1b*-1(dEER^{A6})*::AcGFP* fusion placed under control of CaMV 35S promoter	
32	pUCAvr1b(R9)GFP		*Avr1b*-1(RXLR2^{Arg9})::*AcGFP* fusion placed under control of CaMV 35S promoter	
33	pUCAvr1b(TAT)GFP		*Avr1b*-1(RXLR2^{TAT})::*AcGFP* fusion placed under control of CaMV 35S promoter	
34	pUCNgo	pUCAvr1bXK	Addition of NgoMIV site upstream of RFLR in N-terminus of Avr1b (T150C) in pUCAvr1bXK to facilitate later manipulations	GCCGGT in was mutated to GCCGGc using primer Avr1bSac
35	pUCRFRL	pUCAvr1bXK	CaMV 35S promoter fused to *Avr1b*-1 genes carrying indicated mutations	Wild type Avr1b in pUCAv1bXK was replaced with the corresponding mutants using *Xma* I and *Kpn* I
36	pUCFRLR			
37	pUCRFAR			
38	pUCQFLQ			
39	pUCQFLR	pUCNgo		Avr1b in pUCNgo was replaced with the corresponding mutants by *NgoMIV*I and *Kpn* I
40	pUCKFLR			
41	pUCRFLQ			
42	pUCRFVR			
43	pUCAvr9R			
44	pUCAvrTAT			
45	pUCAvrPfGBP	pUCAvr1bXK		Wild type Avr1b in pUCAvr1bXK was replaced with the corresponding mutants using *Xma* I and *Kpn* I
46	pUCAvrPfHRP			
47	pUCAvrPf1615			
48	pAvr1bGFP	pR9GFP	Replacement of codons encoding nine arginine motif in pR9GFP with Avr1b residues 33 to 71 from wild type Avr1b or from Avr1b RXLR or dEER mutants	Amplification with primers AvrGFPF, AvrGFPR1 and AvrGFPR2
49	pAvr1b(M1+2)GFP			
50	pAvr1b(M3)GFP			

Supplemental Table 2. Description of Plasmids Used

Transgene	Transformation Strategy[a]	Numbers of Positive Clones				Clones used in this study[f]
		G418 Growth[b]	PCR[c]	RT-PCR[d]	Efficiency[e]	
GUS	Single plasmid	22	NT	4[g]	18.2%	1
sAvr1b(WT)	Co-transformation	44	6	2	4.5%	2
sAvr1b(RXLR1^{AAAA})	Single plasmid	9	7	3	33.3%	3
sAvr1b(RXLR2^{AAAA})	Single plasmid	20	13	5	25.0%	2
sAvr1b(RXLR1^{AAAA}, 2^{AAAA})	Single plasmid	9	6	4	44.4%	2
sAvr1b(dEER^{A6})	Single plasmid	3	1	1	33.3%	1
sAvr1b(dEER^{A6})	Co-transformation	12	2	1	8.3%	1
Ps *Avh171-Avr1bCt*	Co-transformation	28	6	2	7.1%	2
Hp *Avh341-Avr1bCt*	Co-transformation	22	5	2	9.1%	2

Supplemental Table 3. Efficiency of PEG-mediated *P. sojae* protoplast transformation.

a For each transformation, 0.5~2x10^7 protoplasts were used and 1-3 transformation experiments were carried out. In some cases the transgene was inserted into the same plasmid as the selectable marker and in some cases the transgene was introduced by co-transformation.

b Number of G418 resistant colonies surviving after three rounds of selection on 50 ug/ml G418.

‡ Number of colonies in which the transgene could be detected by PCR from genomic DNA. NT = not tested.

d Number of colonies in which Avr1b mRNA could be detected by RT-PCR. In colonies with no detectable Avr1b transgene mRNA, the endogenous Avr1b gene was often silenced.

e percentage of G418 resistant colonies confirmed to express the transgene by RT-PCR.

f All the RT-PCR positive clones had similar expression levels for a give transgene.

g The 22 putative GUS gene transformants were assessed for transgene expression by staining for beta-glucuronidase activity with 5-bromo-4-chloro-3-indolyl- beta-D-glucuronic acid (X-gluc), rather than RT-PCR.

Cell

External Lipid PI3P Mediates Entry of Eukaryotic Pathogen Effectors into Plant and Animal Host Cells

Shiv D. Kale,[1] Biao Gu,[1,2] Daniel G.S. Capelluto,[3] Daolong Dou,[1,5] Emily Feldman,[1] Amanda Rumore,[1,3] Felipe D. Arredondo,[1] Regina Hanlon,[1] Isabelle Fudal,[4] Thierry Rouxel,[4] Christopher B. Lawrence,[1,3] Weixing Shan,[2,*] and Brett M. Tyler[1,*]

[1]Virginia Bioinformatics Institute, Virginia Polytechnic Institute and State University, Blacksburg, VA 24061, USA
[2]College of Plant Protection and Shaanxi Key Laboratory of Molecular Biology for Agriculture, Northwest A & F University, Yangling, Shaanxi 712100, China
[3]Department of Biological Sciences, Virginia Polytechnic Institute and State University, Blacksburg, VA 24061, USA
[4]INRA-Bioger, Campus AgroParisTech, 78850 Thiverval-Grignon, France
[5]Present address: Department of Plant Pathology, Nanjing Agricultural University, Nanjing 210095, China
*Correspondence: wxshan@nwsuaf.edu.cn (W.S.), bmtyler@vt.edu (B.M.T.)
DOI 10.1016/j.cell.2010.06.008

SUMMARY

Pathogens of plants and animals produce effector proteins that are transferred into the cytoplasm of host cells to suppress host defenses. One type of plant pathogens, oomycetes, produces effector proteins with N-terminal RXLR and dEER motifs that enable entry into host cells. We show here that effectors of another pathogen type, fungi, contain functional variants of the RXLR motif, and that the oomycete and fungal RXLR motifs enable binding to the phospholipid, phosphatidylinositol-3-phosphate (PI3P). We find that PI3P is abundant on the outer surface of plant cell plasma membranes and, furthermore, on some animal cells. All effectors could also enter human cells, suggesting that PI3P-mediated effector entry may be very widespread in plant, animal and human pathogenesis. Entry into both plant and animal cells involves lipid raft-mediated endocytosis. Blocking PI3P binding inhibited effector entry, suggesting new therapeutic avenues.

INTRODUCTION

Pathogens of both plants and animals produce effectors and/or toxins that act within the cytoplasm of host cells to suppress host defenses and cause disease (Bhavsar et al., 2007; Chisholm et al., 2006; Lafont et al., 2004; Tyler, 2009). Many bacterial pathogens use specialized secretion machineries to directly inject effectors into host cells (Tseng et al., 2009). In addition, many bacterial toxins can enter host cells by receptor-mediated endocytosis after binding glycolipid receptors (Lafont et al., 2004). Apicomplexan parasites such as *Plasmodium* that are enclosed within a parasitiphorous vacuole employ a host targeting signal (HTS), that includes the Pexel motif, to target secreted effectors for translocation across the parasitiphorous vacuolar membrane (Hiller et al., 2004; Marti et al., 2004; Bhattacharjee et al., 2006). Effectors from oomycete plant pathogens carry an HTS, containing RXLR and dEER motifs (Rehmany et al., 2005; Tyler et al., 2006; Jiang et al., 2008), that can translocate them into host cells in the absence of the pathogen (Dou et al., 2008; Whisson et al., 2007), but the mechanism of translocation was not identified. Oomycetes are fungus-like relatives of marine algae that cause many destructive plant diseases, such as potato late blight that caused the Irish potato famine in the nineteenth century (Tyler, 2007).

Effectors of fungal plant pathogens have also been predicted to translocate into host cells because many plants possess intracellular receptors, encoded by major resistance (R) genes, that mediate a rapid defense response when fungal effectors are present (Ellis et al., 2006; Tyler, 2002). For example, the R genes *L5*, *L6* or *L7* of flax (*Linum usitatissimum*) mediate a rapid defense response against lines of the flax rust fungus *Melampsora lini* that produce the effector AvrL567 (Ellis et al., 2007). Like many plant R genes, *L5*, *L6* and *L7* encode intracellular proteins with nucleotide binding sites and leucine-rich-repeats (NBS-LRR proteins) (Ellis et al., 2007). The L6 protein can bind directly to AvrL567 and binding is necessary to trigger a defense response (Ellis et al., 2007). Thus, AvrL567 is inferred to possess a mechanism to cross the flax plasma membrane. Fungal effectors with intracellular targets can also be found in wilt pathogens such as *Fusarium oxysporum* f.sp. *lycopersici* (*Fol*); the Avr2 effector of this tomato pathogen is found in the xylem but interacts with an NBS-LRR *R* gene product, I-2, in the host cytoplasm (Houterman et al., 2009). Furthermore, effectors of the rice blast fungus, *Magnaporthe oryzae* could be observed to enter rice cells from the pathogen (Khang et al., 2010). In the case of oomycetes, there are many plant NBS-LRR-class *R* genes that confer resistance against these pathogens, and in several cases an RXLR-dEER effector targeted by one of these *R* genes has been identified (Tyler, 2009). Examples include *Phytophthora sojae* effector Avr1b targeted by soybean *Rps*1b (Shan et al., 2004) and *P. infestans* effector Avr3a targeted by potato *R*3a

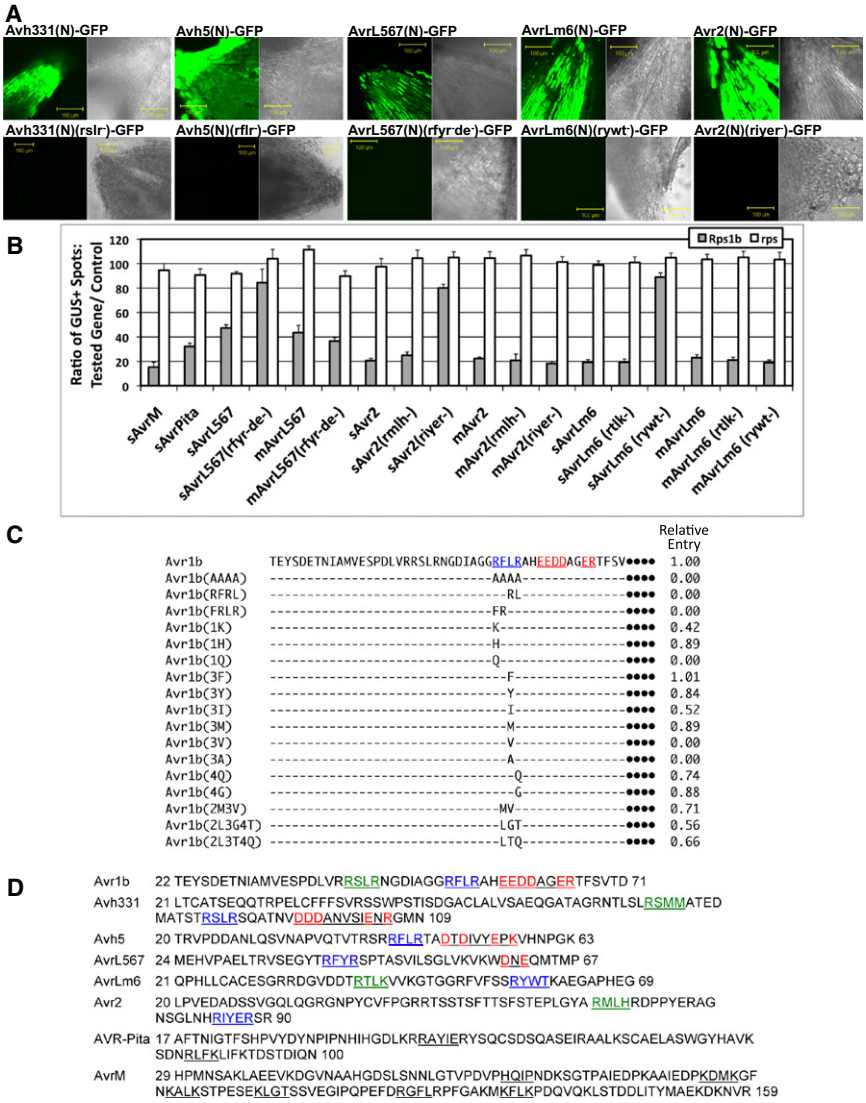

Figure 1. Identification of Motifs Mediating Cell Entry by Fungal Effectors

(A) Entry of wild-type and mutant effector-GFP fusion proteins into soybean root cells. Root tips were incubated with protein (1 mg/mL) for 12 hr, then washed for 2 hr. See also Figure S1 and Table S2.

(B) Double-barrel particle bombardment cell re-entry assays of fungal effectors fused to Avr1b. N-terminal sequences of each effector were fused to the C-terminal domain of Avr1b with (s) or without (m) the Avr1b secretory leader. Effector re-entry into soybean leaf cells resulting in cell killing was measured in the presence or absence of resistance gene *Rps*1b. Averages and standard errors shown. See also Table S1.

(C) Mutations of the Avr1b RXLR motif assayed using the double barrel particle bombardment assay. Cell entry activity measured as cell death in the presence of Rps1b relative to wild-type Avr1b. Dashes indicate identical residues; ●●●● indicates Avr1b sequences. Data for AAAA, RFRL, FRLR, 1K, 1Q, and 4Q mutants from Dou et al., (2008).

(D) Sequence of the cell entry domains of the effectors analyzed in (A) and (B). Active and inactive RXLR-like motifs are underlined in blue and green respectively, predicted RXLR-like motifs of unknown function are underlined in black; dEER motifs are underlined with the predicted active residues in red. Two predicted motifs in Avr-Pita overlap (RLFK and KLIF).

(Armstrong et al., 2005). Genes that encode effectors targeted by *R* gene products have historically been called avirulence genes because expression of the effector prevents infection when the plant host contains the cognate *R* gene (Jones and Dangl., 2006).

We show here that in order to carry effectors into host cells, oomycete RXLR-dEER host-targeting signals, and similar signals in fungal effectors, bind to host cell surface phosphatidylinositol-3-phosphate (PI3P).

RESULTS

Identification of Fungal Effector Translocation Motifs

The RXLR-dEER domain of *P. sojae* Avr1b enables translocation of green fluorescent protein (GFP) into plant cells without any pathogen-encoded machinery (Dou et al., 2008). The same is true for full-length Avr1b protein and for two additional bioinformatically predicted effectors, Avh5 and Avh331, based on uptake of effector-GFP fusion proteins into soybean root cells (Figure 1A and Figures S1A–S1J available online) and on re-entry of Avh331 protein after expression and secretion from soybean leaf cells following particle bombardment (Dou et al., 2008; Kale and Tyler, 2009) (Table S1). As in the case of Avr1b, both the RXLR and the dEER motifs of Avh5 and Avh331 (Figure 1D) were required for cell entry in the GFP root uptake assay (Figure 1A and Figures S1I and S1J) and the leaf bombardment assay (Table S1). To test whether fungal effectors contain N-terminal cell entry domains, we fused N-terminal segments from the fungal effectors AvrL567 from *M. lini* (Ellis et al., 2007), Avr2 from *Fol* (Houterman et al., 2009) and AvrLm6 from *Leptosphaeria maculans* (Fudal et al., 2007) to GFP. When the fusion proteins were incubated with soybean roots, strong accumulation of the proteins was observed in the root cells (Figure 1A), including the nuclei (Figures S1Q–S1S). The leaf bombardment assay confirmed that the N-terminal segments of all three fungal effectors could deliver Avr1b back into soybean leaf cells following secretion (Figure 1B), as could the N-terminal domains of AvrM from *M. lini* (Ellis et al., 2007) and of AVR-Pita from *M. oryzae* (Jia et al., 2000) (Figure 1B).

Since the fungal effectors contained no obvious RXLR or dEER motifs, we used the leaf bombardment assay to define the range of residues within the RXLR motif of Avr1b that could permit cell entry. The results (Figure 1C) revealed that lysine or histidine but not glutamine could replace the arginine at position 1 in the motif,

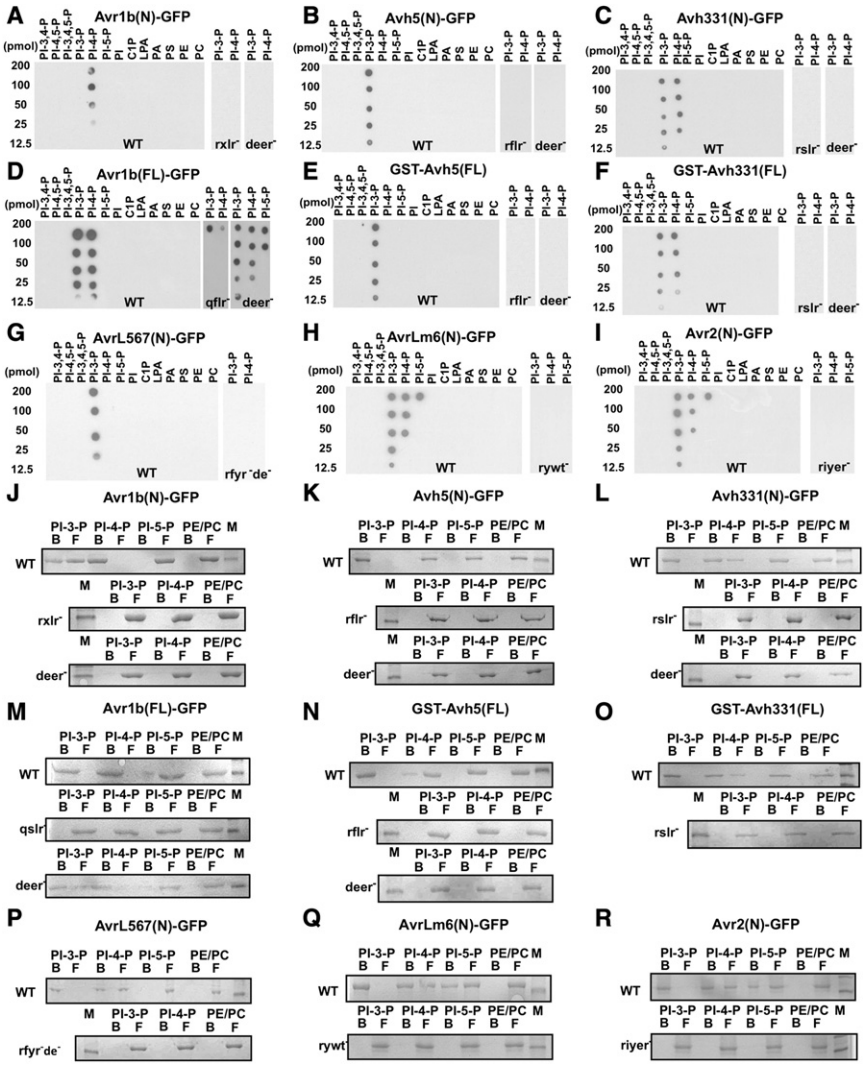

Figure 2. Binding of Oomycete and Fungal Effector Proteins to Phosphoinositides

(A–I) Filter-binding assays.

(J–R) Liposome-binding assays.

(N)-GFP and (FL)-GFP indicate a fusion of the N-terminal domain of an effector or the full-length protein, respectively, to the N terminus of GFP. GST-XXX(FL) indicates a fusion of a full-length effector protein (without signal peptide) to the C terminus of GST. PI-3,4-P = phosphatidylinositol-3,4-bisphosphate; PI-4,5-P = phosphatidylinositol-4,5-bisphosphate; PI-3,4,5-P = phosphatidylinositol-3,4,5-triphosphate; PI-3-P = phosphatidylinositol-3-phosphate; PI-4-P = phosphatidylinositol-4-phosphate; PI-5-P = phosphatidylinositol-5-phosphate; PI = phosphatidylinositol; C1p = ceramide-1-phosphate; LPA = lysophosphatidic acid; PA = phosphatidic acid; PS = phosphatidylserine; PE = phosphatidylethanolamine; PC = phosphatidylcholine. Except where shown, no mutant proteins bound to PI-3,4-P, PI-4,5-P, PI-3,4,5-P, PI-5-P, PI, C1P, LPA, PA, PS, PE, or PC (Figure S2). In the liposome binding assays (right panels), "B" and "F" indicate liposome-bound and -free proteins, respectively; "M" = size markers.

See also Figure S2.

that any large hydrophobic residue (isoleucine, methionine, phenylalanine, or tyrosine) could replace the leucine at position 3, but valine and alanine could not. At position 4, all residues tested allowed function. Furthermore, the presence of either an leucine or methionine residue at position 2 could substitute for leucine at position 3.

Using this information, we identified potential cell entry motifs in the N-terminal regions of the five fungal effectors (Figure 1D). A single motif in AvrL567, RFYR, was a close match to the oomycete RXLR motif. Alanine substitutions in the RFYR motif (Figure 1D) abolished the activity of the AvrL567 N-terminal domain in the leaf bombardment assay; when fused to Avr1b, cell killing in the presence of *Rps*1b was dependent on an intact RFYR motif, but only when the secretory leader was present (Figure 1B). When the alanine substitutions were introduced into the AvrL567(N)-GFP fusion protein, the protein did not accumulate in root cells (Figure 1A).

Substitution mutations were also introduced separately into two candidate cell entry motifs in each of AvrLm6 (RTLK and RYWT) and Avr2 (RMLH and RIYER). The mutations in the RYWT motif of AvrLm6 and in the RIYER motif of Avr2 abolished effector-GFP accumulation in root cells (Figures 1A and S1) and re-entry in the bombardment assay (Figure 1B). However the mutations in the RTLK motif of AvrLm6 and the RMLH motif of Avr2 had no measurable effect in either assay (Figure 1B and S1K,L). Mutations in the individual candidate motifs of AvrM and AVR-Pita had no effect on cell entry as measured by the bombardment assay (data not shown), indicating either that none of the candidates were involved in cell entry, or that each effector contained more than one functional motif.

Oomycete RXLR-dEER Domains Bind Phosphoinositides

In principle, a cell entry domain could bind either a (glyco)protein or (glyco)lipid receptor. After noting that beta-type phosphatidylinositol-4-phosphate (PI4P) kinases from rice and *Arabidopsis* contained PI4P binding domains that consisted of tandem repeats containing RXLR-dEER-like motifs (Lou et al., 2006), we tested whether oomycete RXLR-dEER domains could bind phosphoinositides. Thirteen lipids were spotted onto a membrane, which was probed with GFP fused to the N-terminal RXLR-dEER domains of Avr1b, Avh331 or Avh5, or to full-length Avr1b [Avr1b(FL)]. The Avr1b(FL)- and Avh331(N)-GFP fusions bound to both PI3P and PI4P (Figures 2C and 2D) while Avh5 (N)-GFP fusions bound mostly to PI3P (Figure 2B). The Avr1b N-terminus bound mostly to PI4P (Figure 2A); presumably this small difference in specificity arises from changes in the structure

of the N-terminus in the absence of the rest of the protein. No other phospholipids were bound, including PI5P, phosphatidylinositol-polyphosphates, or other anionic phospholipids. Substitution mutations in the RXLR or dEER motifs that abolished entry into soybean root and leaf cells (Dou et al., 2008; Figure 1 and Figure S1) also abolished binding, including interchanges of amino acids of the RXLR motif of Avr1b that preserved the positive charge (RFLR- > FRLR or RFLR- > RFRL) (Figure S2A). One exception was the dEER mutant of Avr1b which abolished binding only in the context of the N-terminal domain, suggesting a second redundant dEER-like motif further downstream. Fusions of full-length Avh5 or Avh331 proteins to the C terminus of glutathione S-transferase (GST) could also bind the same phosphoinositides as the N-terminal GFP fusions (Figures 2E and 2F). GST and GFP proteins alone did not bind any lipids (Figure S2A). Alanine substitutions in the RXLR or dEER motifs of full-length Avh5 proteins did not alter their far-UV circular dichroism spectra compared to wild-type Avh5, indicating that the substitutions did not significantly disturb the global fold of the effector protein (Figure S1T and Table S2).

To independently confirm binding of the RXLR-dEER domains to phosphoinositides, we tested the binding of the fusion proteins to liposomes composed of phosphatidylcholine (PC) and phosphatidylethanolamine (PE). None of the effector-GFP or GST-effector fusion proteins bound to liposomes (Figures 2J–2O and Figure S2B). However, when either PI3P or PI4P was included, all the fusion proteins bound to the liposomes. In every case, when any of the RXLR or the dEER motifs were mutated, the mutant fusion proteins lost their ability to bind to liposomes (Figures 2J–2O and Figure S2B) except for the dEER mutant of Avr1b(FL) which retained weak binding to several PI-Ps.

Fungal Effectors Also Bind Phosphoinositides

Both filter binding and liposome binding were used to test whether the N-terminal domains of AvrL567, AvrLm6, and AvrLm2 bound phosphoinositides. Figures 2G–2I show that all three fusions could bind PI3P, and more weakly to PI4P and/or PI5P (Figures 2G–2I and 2P–2R). Mutations in the functional RXLR-like motifs of each effector resulted in a loss of binding (2G–2I and 2P–2R) while mutations in the nonfunctional RXLR-like motifs of AvrLm6 and Avr2 did not affect binding (Figure S2). The host-targeting signals (HTS) of three *Plasmodium falciparum* effectors, PfGBP, PfHRPII, and Pf1615c, could carry Avr1b into plant cells (Dou et al., 2008; Figure S1M). The HTS regions of PfHRPII (Figure S2B) and the other two effectors (not shown) also could bind PI3P and/or PI4P, and the binding required intact pexel motifs.

PI3P Is Present on the Outer Surface of Plant and Human Cell Plasma Membranes

In order to test which, if any, phosphoinositide was present on the outer surface of plant cells, we created highly specific biosensors for PI3P and PI4P by fusing the PH domains of the human proteins PEPP1 and FAPP1 (Dowler et al., 2000; Vermeer et al., 2009) to GFP and to mCherry (Figure S3A). We also fused GFP to the PX domain of VAM7p, which binds preferentially to PI3P (Lee et al., 2006). Finally, we employed GFP and mCherry biosensors containing two tandem repeats of the PI3P-specific FYVE domain of the rat Hrs protein (Hrs-2xFYVE) (Vermeer et al., 2006). Each protein was incubated with soybean root suspension culture cells (Figure 3A) or with soybean roots (Figure 3B) and then the cells were subjected to plasmolysis to separate the plasma membranes from the cell walls. All three of the PI3P-GFP biosensors bound strongly and quite uniformly to the plasma membrane of the suspension and root cells, whereas no binding was observed to the PI4P biosensor FAPP1-PH-GFP. Figures 3E and 3F show that all four of the biosensor proteins showed the expected binding specificity.

Phosphatidylinositol phosphates are universally found in eukaryotic cells. Since a number of human and animal diseases are caused by fungi and oomycetes, we tested the possibility that cell surface PI3P or PI4P might be available to mediate effector protein entry into animal cells, using the human lung epithelial cell line A549 as a model. At 2°C, which inhibits endocytosis, all three of the PI3P-GFP biosensors bound strongly to the plasma membrane of the A549 cells, but no binding was observed to the PI4P biosensor (Figures 3C and 3D). In contrast to the root cells, binding to the surface of A549 cells was highly punctate. Since there are numerous reports that erythrocytes do not have cell surface phosphoinositides (reviewed in Quinn, 2002; Boon and Smith, 2002), we tested the binding of the four biosensors to human erythrocytes. No binding was observed to the erythrocytes by any of the biosensors nor by any effector GFP fusions (Figure 3D), which is in agreement with the literature, but which suggests that there may be differences among animal cell types with regard to the presence of outer surface phosphoinositides.

Inhibition of Effector Entry by PI3P Binding Proteins and Exogenous Inositol Phosphates

To test the hypothesis that the fungal and oomycete effectors bound external PI3P in order to enter plant cells, we incubated the effector-GFP fusions with the roots in the presence of a molar excess of each of the PI3P- and PI4P-binding biosensor proteins. All three PI3P-binding proteins completely abolished entry by the four effector-GFP fusions (Avr1b, AvrL567, AvrLm6 and Avr2) into soybean root cells (Figures 4A–4D, rows 2–4). In contrast, FAPP1-PH-mCherry did not inhibit uptake of any of the effector-GFP fusions (Figures 4A–4D, row 5), consistent with the hypothesis that PI3P, but not PI4P, is required for effector entry.

A synthetic cell entry motif composed of nine-arginine residues (Arg_9) was previously shown to deliver Avr1b and GFP into plant cells (Dou et al., 2008; Chang et al., 2005). The Arg_9-GFP fusion protein binds PI3P, PI4P, PI-polyphosphates and PS, albeit weakly in each case (Figure S4C). Figure 4E shows that none of the four biosensor proteins could inhibit the uptake of Arg_9-GFP, confirming that the PI3P biosensors did not cause a generalized inhibition of protein uptake.

To further confirm the role of PI3P binding in effector cell entry, we utilized inositol-1,3-diphosphate (1,3IP2) and inositol-1,4-diphosphate (1,4IP2); these compounds represent the hydrophilic head-groups of PI3P and PI4P, respectively, and thus were potential competitive inhibitors of effector binding. Preincubation with 100 μM 1,3IP2 inhibited binding of all the

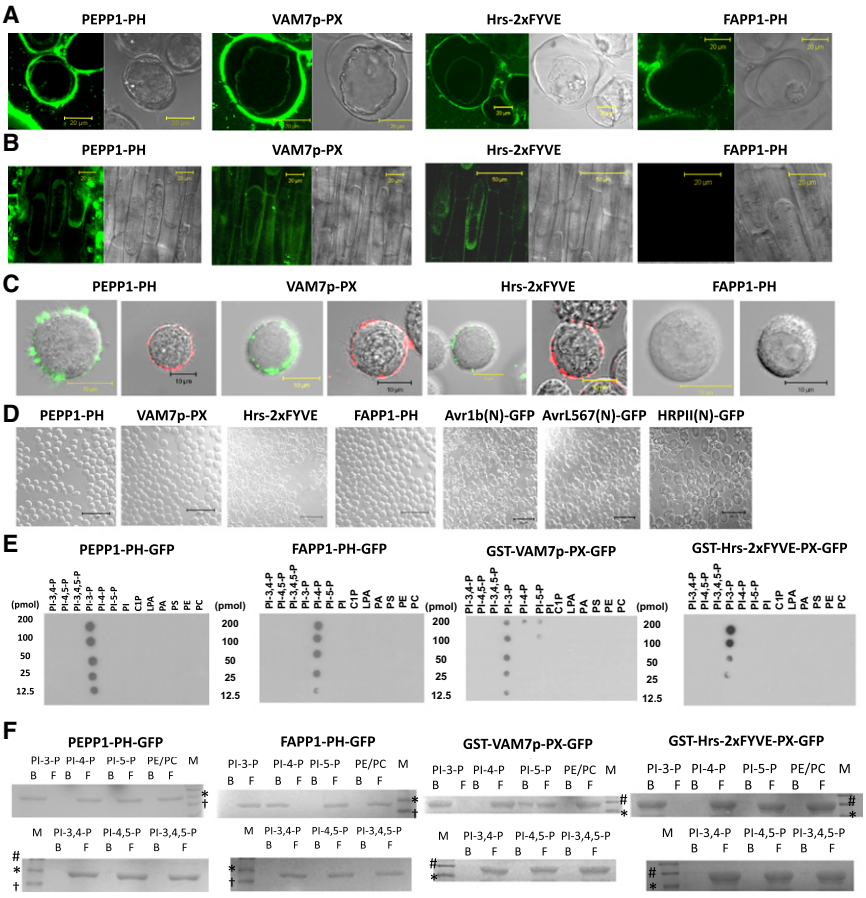

Figure 3. PI3P Occurs on the Outer Surface of Soybean Root Cells and Human Epithelial Cells

(A and B) Soybean root suspension culture cells (A) or root tips (B) incubated with GFP biosensors for 6 hr (A) or 12 hr (B) at 2°C, washed for 2 hr, then plasmolyzed with 0.8M Mannitol (A) or 4M NaCl (B) for 30 min. Left panels, fluorescence images; right panels, light micrographs. The scale bars represent 20 μm or 50 μm, respectively.

(C) A549 epithelial cells incubated with GFP biosensors (left panels) or mCherry biosensors (right panels) for 6 hr at 2°C, then washed twice briefly. Light micrographs are overlaid with fluorescence images. The scale bar represents 10 μm.

(D) Human erythrocytes incubated with GFP biosensors (panels 1-4) or effector-GFP fusions (panels 5–7) for 6 hr at 2°C, then washed twice briefly. Light micrographs are overlaid with fluorescence images. The scale bar represents 20 μm.

(E and F) Lipid blots (E) and liposome binding assays (F) validating the specificity of the biosensor proteins. Details as described in Figure 2. See also Figure S3.

effector-GFP fusions to PI3P-containing liposomes (Figure S4B). 1,4IP2 (100 μM) also inhibited binding to PI3P in every case, indicating that the specificity of binding was relaxed in the case of the soluble head group compounds. In concert with this observation, both 1,3IP2 and 1,4IP2 (500 μM) could completely inhibit root cell entry when preincubated with each of the effector fusions for 30 min prior to exposure to soybean roots (Figure 4A–4D, rows 6 and 7). Neither 1,3IP2 nor 1,4IP2 could inhibit the binding of Arg_9-GFP to liposomes (Figure S4B) and accordingly, uptake of Arg_9-GFP was unaffected by preincubation with either 1,3IP2 or 1,4IP2 (Figure 4E), confirming that neither compound caused a generalized inhibition of protein uptake.

As a further test of the ability of PI3P-binding proteins and IP2 to block effector entry into plant cells, full-length Avr1b protein and full-length Avh331 protein were infiltrated into soybean leaves containing the *Rps*1b or *Rps*1k resistance genes, respectively. As previously shown (Shan et al., 2004), Avr1b protein triggers programmed cell death (PCD) when infiltrated into *Rps*1b leaves (Figure 4F). As expected, no PCD was triggered when RXLR or dEER motif mutations were present (Figure S4A) or *Rps*1b was absent (Figure 4F). Avh331 is a candidate product of the *Avr1k* gene, and triggers programmed cell death (PCD) in *Rps*1k leaves when expressed in the leaf cells following particle bombardment, but not in leaves lacking *Rps*1k (Table S1). As predicted therefore, full-length Avh331 protein triggered PCD when infiltrated into *Rps*1k leaves but not when infiltrated into leaves lacking *Rps*1k (Figure 4G). Furthermore, infiltration of Avh331 protein containing an RXLR mutation did not trigger PCD (Figure S4A).

As shown in Figures 4F and 4G, 1,3IP2, 1,4IP2, and all three of the PI3P-binding proteins, but not the PI4P binding protein, strongly inhibited Rps1b- and Rps1k-mediated PCD when coinfiltrated with Avr1b or Avh331 protein, respectively.

Effector Entry into Human Cells

Given the presence of PI3P on the outside of the A549 human lung epithelial cells, we tested if RXLR-dEER motifs could mediate entry of effector proteins into these cells. GFP fusions with Avr1b and AvrL567 could enter A549 cells (Figures 5A and 5B) as could PfHRPII (from *Plasmodium*) (Figure S5V), and entry required intact RXLR or Pexel motifs (Figures 5A and 5B and Figure S5V). Localization of the GFP fusions inside the cells was confirmed by the accumulation of GFP within vesicle-like structures, and by the fact that the cells were treated with protease (trypsin) prior to photographing. Protein accumulation was strongly inhibited in each case by competing PI3P-binding proteins (which entered the cells instead) or by 1,3IP2 or 1,4IP2, but not by the PI4P mCherry biosensor (Figures 5A and 5B). No effector entry into erythrocytes was observed (Figure 3E), consistent with the absence of PI3P or PI4P from the outer surface of erythrocytes.

Arg9-GFP could also enter the A549 cells, but GFP itself could not (Figure 5C). Entry of Arg9-GFP was not inhibited by1,3IP2, 1,4IP2 or by PI3P- or PI4P-binding proteins, confirming that none of those inhibitors interfered generally with protein uptake by the A549 cells.

To determine if the effector-GFP fusions bound to the same sites on the cells as the PI3P-binding proteins, equimolar

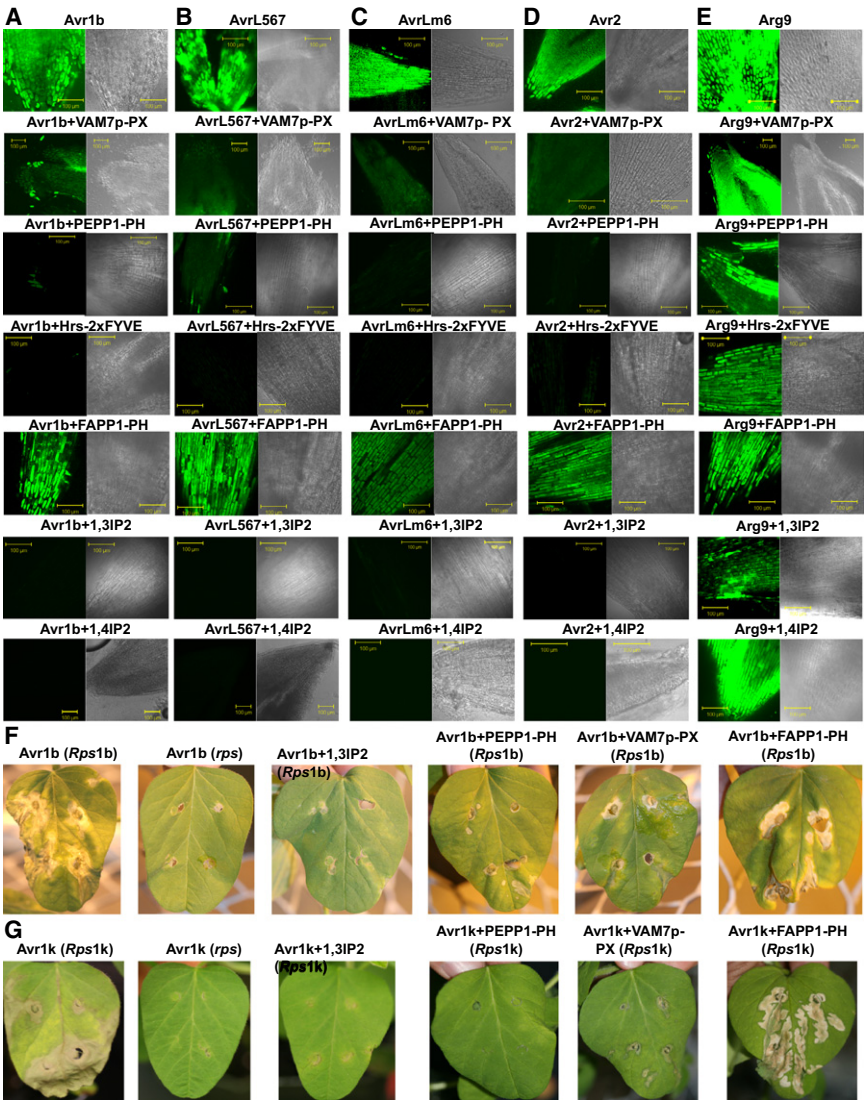

Figure 4. Inhibition of Effector Entry into Plant Cells by PI3P-Binding Proteins and Inositol Diphosphates

(A–E) Inhibition of effector-GFP entry into root cells. In each case, 1 mg/mL effector-GFP protein was incubated with soybean root tips for 12 hr then washed for 2 hr. For biosensor inhibition assays (rows 2–5), root tips were preincubated for 3 hr at room temperature in 5 mg/ml biosensor protein prior to addition of effector-GFP fusion proteins (final concentrations 2.5 mg/mL biosensor, 1.0 mg/mL effector). VAM7p-PX = PX domain alone, with no fluorescent protein fusion; PEPP1-PH, FAPP1-PH, and Hrs-2xFYVE biosensors were all mCherry fusions. For IP2 inhibition assays (rows 6 and 7) 500 μM 1,3IP2 or 1,4IP2 were preincubated with the effector-GFP proteins for 30 min prior to exposure to the roots. The scale bar represents 100 μm. See also Figures S4B and S4C.

(F and G) Inhibition of programmed cell death triggered by entry of Avr1b(FL) (F) and Avh331(FL) (G) into cells of soybean leaves containing cognate resistance genes. 0.25 mg/mL of each protein, lacking N-terminal or C-terminal fusions, were infiltrated into the primary unifoliate leaves from cultivars with no Rps gene (*rps*), *Rps*1b or *Rps*1k. Where indicated, the protein was coinfiltrated with 500 μM 1,3IP2 or with 1.0 mg/ml of the indicated biosensor protein (same biosensors as A-E, except that VAM7p-PX-mCherry was used instead of VAMp7-PX alone). The plant leaves were photographed 5 days after infiltration. See also Figure S4A.

concentrations of the biosensors and effectors were incubated with A549 cells at 2°C. The effector fusions colocalized with each biosensor in a punctate pattern on the surface of the cells (Figures 5D, 5F, and 5H and Figure S5). At 37°C, the three biosensors and the effector fusions were colocalized inside the cells within endosome-like structures (Figures 5E, 5G, and 5I). To support that the proteins were accumulating within endosome-like structures, the A549 cells were stained with FM4-64, a dye that binds to plasma membranes and then, following endocytosis, stains endosomes. The cells were washed and photographed after only 2.5 min, in order to observe the earliest events during entry. Figures 5J–5L shows that the Avr1b-GFP and AvrL567-GFP fusions accumulated within small endosome-like bodies and these bodies were stained with FM4-64.

To further characterize the binding of Avr1b and AvrL567 to the A549 cells, we measured the dissociation constants (K_d) for binding of Avr1b and AvrL567 to the surface of the cells; these were 190 ± 30 nM (standard error) and 330 ± 40 nM respectively (Figure 6A). The K_d's for binding of each effector to PI3P-containing liposomes were very similar, 210 ± 20 nM and 740 ± 120 nM respectively (Figure 6B). Measurements of binding by Avr1b and AvrL567 agreed that the number of PI3P molecules on the surface of each cell averaged 1.4 ± 0.1 × 10^8 (Figure 6A), which equates roughly to 1% of the plasma membrane outer leaflet lipid. The inhibition constants (K_i) for 1,3IP2 inhibition of binding to cells were 16 ± 1.6 μM for Avr1b and 13 ± 0.6 μM for AvrL567 (Figure 6C). The inhibition constants for 1,3IP2 inhibition of binding to PI3P-containing liposomes were of the same order, 1.9 ± 0.1 μM for Avr1b and 7.9 ± 0.7 μM for AvrL567 (Figure 6D).

Effector Cell Entry Is Inhibited by PI3P Depletion and by Inhibitors of Lipid Raft-Mediated Endocytosis

Quantitating the dynamics of effector-GFP accumulation revealed that the fusion proteins accumulated very rapidly, within 2.5 min of exposure to the A549 cells. Over the next hour however, the accumulated fluorescence declined steeply, before slowly recovering over the next 3 hr (Figure 6E). This pattern was also observed for GFP-biosensors and mCherry-biosensors and for Arg_9-GFP. A possible interpretation of this pattern is that the initial massive entry of binding proteins

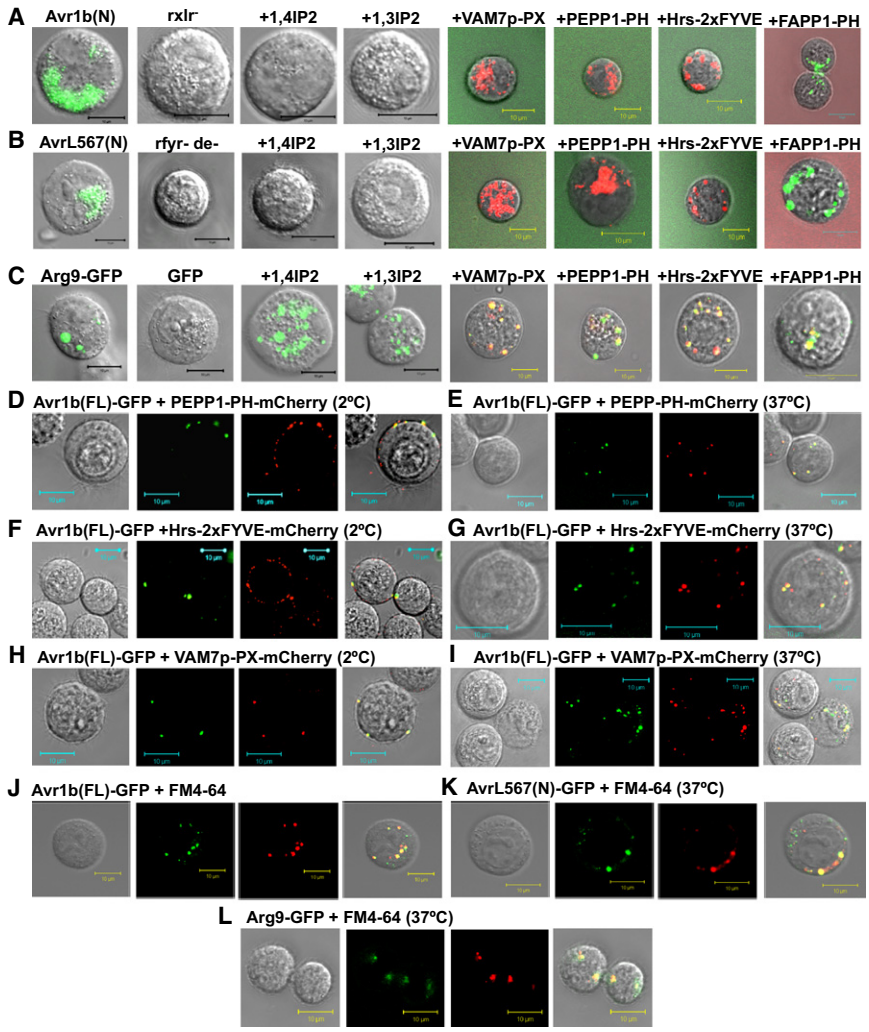

Figure 5. Effector Entry into Human Cells and Inhibition by Inositol Diphosphates and PI3P-Binding Proteins

(A–C) Human A549 cells were incubated with the indicated effector-GFP fusion proteins (25 μg/mL) for 8 hr, in the presence or absence of 500 μM inositol 1,3 diphosphate (1,3IP2), 520 μM inositol 1,4 diphosphate (1,4IP2), or 100 μg/ml of the indicated biosensor protein (mCherry fusion in each case), then washed either twice (panels 1–4) or once (panels 5–8) and photographed. Light micrographs are overlaid with fluorescence images (both red and green channels in panels 5–8). In panels 5–8, traces of the nonentering proteins can be observed in the background. The scale bars represent 10 μm. See also Figure S5.

(D–I) Colocalization of Avr1b(FL)-GFP with mCherry biosensor proteins on the surface (D, F, and H) or inside (E, G, and I) of A549 cells. 0.1 mg/ml Avr1b(FL)-GFP was incubated with 0.1 mg/ml biosensor at 2°C for 2 hr (D, F, and H) or 37°C for 8 hr (E, G, and I) then washed twice. Light micrograph (panel 1); GFP image (panel 2); mCherry image (panel 3); overlay (panel 4). The scale bars represent 10 μm.

(J–L) Colocalization of indicated GFP fusions with FM4-64. A549 cells were incubated with GFP fusion protein (0.1 mg/mL) for 2.5 min at 37°C, in the presence of 5 μM FM4-64, then washed. Light micrograph (panel 1); GFP image (panel 2); FM4-64 image (panel 3); overlay (panel 4). The scale bar represents 5 μm. See also Figure S5U, which shows FM4-64 entry alone.

depletes the surface of binding sites (based on the binding curves, nearly 90% of the binding sites are occupied at the protein concentrations used), bringing uptake to a temporary halt and resulting in a loss of fluorescence as the internalized GFP was degraded; accumulation presumably resumed only after PI3P was restored to the cell surface. This pattern resembles the endocytosis-mediated loss of cell surface receptors triggered by many ligands.

To test the role of endocytosis in effector-GFP accumulation, we measured the effect of compounds which inhibit several forms of endocytosis. Accumulation of Avr1b- and AvrL567-GFP fusions was inhibited by the phosphatidylinositol-3-kinase (PI3K) inhibitor wortmannin, that inhibits both clathrin-mediated endocytosis and PI3P biosynthesis, and by two inhibitors of lipid raft-mediated endocytosis, nystatin and filipin (Figure 6F and Figure S6A). Tyrphostin A23, N-ethylmaleimide, and LY294002, that inhibit clathrin-mediated endocytosis, and cytochalasin D, that inhibits macropinocytosis, did not inhibit accumulation (Figure 6F and Figure S6A). Although a high background fluorescence was observed in the presence of nystatin and filipin, no localized binding or entry of protein could be observed microscopically (Figure 6K and Figure S6D), suggesting that disruption of lipid rafts had disrupted the distribution of PI3P on the cell surface. To examine if wortmannin was acting by inhibiting endocytosis per se, or by depleting the cell surface of PI3P, A549 cells were preincubated for different periods of time with wortmannin. The longer that the cells were preincubated with wortmannin, the less effector-GFP protein entered, even at 2.5 min (Figure 6H and Figure S6B), suggesting that cell surface PI3P was becoming depleted during the preincubation. This was confirmed by measuring binding of the effectors and a PI3P biosensor at 2°C after 6 hr preincubation (Figure 6J). When the cells were only partially depleted of PI3P (by 30 or 60 min preincubation) entry of the effectors resumed after one hour as normal (Figure 6F), suggesting that endocytosis itself was unaffected. Binding and entry by the synthetic cell entry fusion Arg9-GFP was unaffected by wortmannin, nystatin or filipin, indicating that the action of these inhibitors was specific. Entry of Arg_9-GFP was instead inhibited by the macropinocytosis inhibitor cytochalasin D (Figures 6G and 6I), as reported previously for plant cells (Chang et al., 2007). Entry of Avr1b(FL)-GFP and AvrL567(N)-GFP into soybean root suspension culture cells was inhibited completely by filipin and partially by nystatin (Figure 6L and Figure S6E), indicating that lipid rafts are also required for PI3P-mediated entry into plant cells.

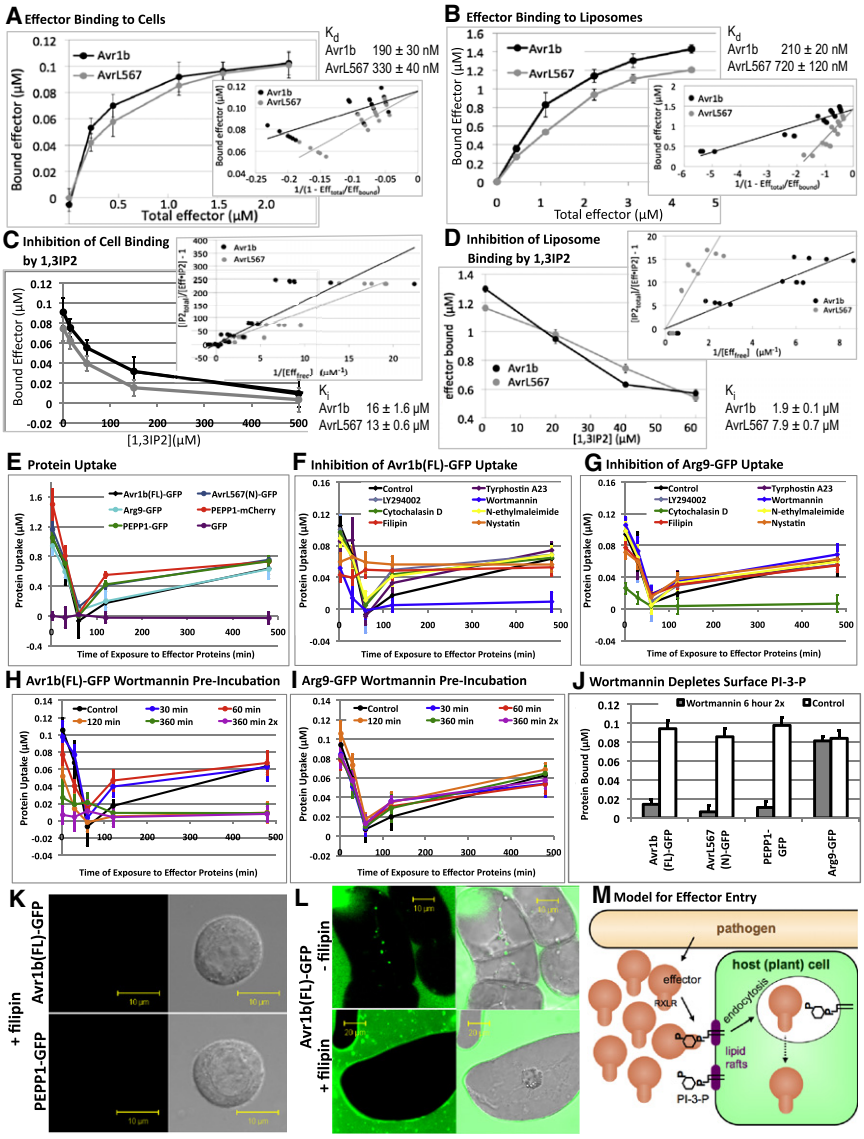

Figure 6. Mechanism of Binding and Entry of Effectors into Host Cells

Error bars in all panels indicate standard errors from four to six replicates.

(A and B) Quantitation of binding of Avr1b and AvrL567 to A549 cells (A) and PI3P-containing liposomes (B). Error bars indicate standard errors. Insets show plots of individual replicate data points used to estimate dissociation constants (K_d's).

(C and D) Quantitation of inhibition by 1,3IP2 of binding of Avr1b and AvrL567 to A549 cells (C) and PI3P-containing liposomes (D). Insets show plots of individual replicate data points used to estimate inhibition constants (K_i's).

(E) Kinetics of accumulation of effector fusions and biosensors in A549 cells.

(F and G) Inhibition of Avr1b(FL)-GFP (F) and Arg9-GFP accumulation at 37°C by endocytosis inhibitors. Inhibitors were added 2 hr before the proteins. See also Figure S6.

(H and I) Inhibition of Avr1b(FL)-GFP (F) and Arg9-GFP accumulation at 37°C by preincubation with wortmannin for different times. "360 min 2×" indicates two Wortmannin additions (at 0 and 180 min). Figure S6B shows data for AvrL567.

(J) Depletion of surface PI3P by incubation for 6 hr at 37°C with Wortmannin additions at 0 min and 180 min.). Binding was assayed at 2°C.

(K) Elimination of effector and biosensor binding sites on A549 cells by incubation with filipin for 2 hr. Binding was assayed at 2°C. Fluorescent images (left panels); overlays (right panels). Figure S6D shows additional photographs for PEPP1, Avr1b and AvrL567, and for nystatin.

(L) Entry of Avr1b(FL)-GFP into soybean root suspension cultures and inhibition by filipin. Cells were exposed to the protein (1.0 mg/mL) for 8 hr at 25°C, then photographed without washing. Note labeling of vesicles in the absence of filipin. Fluorescent images (left panels); overlays (right panels). See also Figure S6E.

(M) Proposed model for effector entry. Binding of effectors via their RXLR domains to PI3P, possibly located in lipid rafts, leads to entry by endocytosis. The mechanism of escape from endosomes is currently unknown. The moderate affinity of the effectors for PI3P facilitates binding on the outer surface but dissociation from PI3P inside the cell.

DISCUSSION

Domains containing RXLR and dEER motifs are responsible for entry of oomycete effector proteins into host plant cells (Dou et al., 2008; Grouffaud et al., 2008; Whisson et al., 2007). Entry of effector proteins into plant cells does not require the presence of the pathogen (Dou et al., 2008). We extend these findings here with similar experiments with full-length Avr1b protein and with two additional oomycete effectors, Avh331 and Avh5. Furthermore, our results with effectors from three fungal pathogens, AvrL567, AvrLm6 and Avr2, suggest that these effectors also can enter plant cells independently of the pathogen, mediated by RXLR-like motifs, though future, in planta experiments with fungal transformants would need to confirm the role of the RXLR-like motifs.

Our results show that all effectors (oomycete and fungal) could bind with high affinity only to PI3P and/or PI4P, via RXLR motifs, but not to other PI-polyphosphates or any anionic phospholipids tested. Thus, binding is very specific and not simply an electrostatic interaction with positive charges of the arginine residues (Langel, 2006). The affinity of binding of Avr1b and AvrL567 to PI3P in liposomes was comparable to those of characterized PI3P-binding proteins, yet the primary structures of the RXLR-dEER effector domains do not resemble any known phosphoinositide binding domains (Lemmon, 2008).

We identified PI3P on the surface of both soybean roots cells and human A549 cells using three structurally different PI3P-specific biosensors, but it was absent from the surface of erythrocytes. It remains to be determined whether the majority of animal cell types have PI3P on their surface, or whether this

Protein	Sequence	Lipid binding PI-3-P	Lipid binding PI-4-P	Leaf Cell Entry	Root Cell Entry	Human Cell Entry	Inhibition
Avr1b(FL)	|TEYSDETNIAMVESPDLVRRSLRNGDIAGGRFLRAHEEDDAGERTFSVTD...	+	+	1.00	Y	Y	Y
Avr1b(FL)rxlr^{rflr-}	|TEYSDETNIAMVESPDLVRRSLRNGDIAGGQFLRAHEEDDAGERTFSVTD...	–	–	0.00	N	N	nt
Avr1b(FL)deer^{-}	|TEYSDETNIAMVESPDLVRRSLRNGDIAGGRFLRAHAAAAAGAATFSVTD...	+	+	0.00	N	Y	nt
Avr1b(N)	|TEYSDETNIAMVESPDLVRRSLRNGDIAGGRFLRAHEEDDAGERTFSVTD|	–	+	1.00	Y	Y	Y
Avr1b(N) rxlr^{-}	|TEYSDETNIAMVESPDLVRAAAANGDIAGGAAAAAHEEDDAGERTFSVTD|	–	–	0.00	N	N	nt
Avr1b(N) deer^{-}	|TEYSDETNIAMVESPDLVRRSLRNGDIAGGRFLRAHAAAAAGAATFSVTD|	–	–	0.00	N	N	nt
Avr1b(N) rflr^{rflr}	|TEYSDETNIAMVESPDLVRRSLRNGDIAGGFRLRAHEEDDAGERTFSVTD|	–	–	0.00	N	N	nt
Avr1b(N) rflr^{rfrl}	|TEYSDETNIAMVESPDLVRRSLRNGDIAGGRFRLAHEEDDAGERTFSVTD|	–	–	0.00	N	N	nt
Avr1b(N) rflr^{qflr}	|TEYSDETNIAMVESPDLVRRSLRNGDIAGGQFLRAHEEDDAGERTFSVTD|	–	–	0.00	N	N	nt
Avr1b(N) rflr^{fyr}	|TEYSDETNIAMVESPDLVRRSLRNGDIAGGRFYRAHEEDDAGERTFSVTD|	–	+	0.84	Y	Y	nt
Avh331(N,FL)	|LTCATSEQQTRPELCFFFSVRSSWPSTISDGACLALVSAEQGATAGRNT LSLRSMMATEDMATSTRSLRSQATNVDDDANVSIENRGM|	+	+	1.07	Y	nt	Y
Avh331(N,FL)rslr^{-}	|LTCATSEQQTRPELCFFFSVRSSWPSTISDGACLALVSAEQGATAGRNT LSLRSMMATEDMATSTAAAASQATNVDDDANVSIENRGM|	–	–	0.00	N	nt	nt
Avh331(N) deer^{-}	|LTCATSEQQTRPELCFFFSVRSSWPSTISDGACLALVSAEQGATAGRNT LSLRSMMATEDMATSTRSLRSQATNVAAAANVSIANAGM|	–	–	0.00	N	nt	nt
Avh5(N,FL)	|TRVPDDANLQSVNAPVQTVTRSRRFLRTADTDIVYEPKVHNPGK|	+	–	nt	Y	nt	nt
Avh5(N,FL) rslr^{-}	|TRVPDDANLQSVNAPVQTVTRSRAAAATADTDIVYEPKVHNPGK|	–	–	nt	N	nt	nt
Avh5(N,Fl) deer^{-}	|TRVPDDANLQSVNAPVQTVTRSRRFLRTAATAIVYAPAVHNPGK|	–	–	nt	N	nt	nt
AvrL567(N)	|MEHVPAELTRVSEGYTRFYRSPTASVILSGLVKVKWDNEQMTMP|	+	±	0.70	Y	Y	Y
AvrL567(N) rfyr^{-}de^{-}	|MEHVPAELTRVSEGYTAAAASPTASVILSGLVKVKWANAQMTMP|	–	–	0.00	N	N	nt
AvrLm6(N)	|ESGRRDGVDDTRTLKVVKGTGGRFVFSSRYWTKAEGAPHEG|	+	+	0.95	Y	Y	Y
AvrLm6(N) RTLK^{qavq}	|ESGRRDGVDDTQAVQVVKGTGGRFVFSSRYWTKAEGAPHEG|	+	+	0.95	Y	Y	nt
AvrLm6(N) rywt^{tvvq}	|ESGRRDGVDDTRTLKVVKGTGGRFVFSSQVVQKAEGAPHEG|	-	-	0.00	N	N	nt
Avr2(N)	|LPVEDADSSVGQLQGRGNPYCVFPGRRTSSTSFTTSFSTEP LGYARMLHRDPPYERAGNSGLNHRIYERSR|	+	+	0.93	Y	Y	Y
Avr2(N) RMLHRD^{qvvnqn}	|LPVEDADSSVGQLQGRGNPYCVFPGRRTSSTSFTTSFSTEPLGYA QVVNQNPPYERAGNSGLNHRIYERSR|	+	+	0.89	Y	Y	nt
Avr2(N) riyer^{qvvqq}	|LPVEDADSSVGQLQGRGNPYCVFPGRRTSSTSFTTSFSTEPLGYA RMLHRDPPYERAGNSGLNHQVVQQSR|	-	-	0.00	N	N	nt
PfHRPII(N)	|FNNNLCSKNAKGLNLNKRLLHETQAHVDDAHHAHHVAD|	+	+	1.15	Y	Y	nt
PfHRPII(N) pexel^{-}	|FNNNLCSKNAKGLNLNKAAAAATQAHVDDAHHAHHVAD|	+	–	nt	N	N	nt
Arg9	|RRRRRRRRR|	±	±	1.13	Y	Y	N

Figure 7. Summary of Amino Acid Sequences and Cell Entry Activities of Effector Fusions and Mutants

Active and inactive RXLR-like motifs are blue and green respectively; dEER motifs, active residues are in red. (N) indicates N-terminal region only; (FL) indicates full-length protein; (N,FL) indicates identical results for N-terminal regions and full-length proteins. Leaf cell entry measured by particle bombardment. Lipid binding and root cell and human cell uptake are described qualitatively. Inhibition indicates whether protein entry into roots and A549 cells was blocked by the three PI3P-binding biosensors, 1,3IP2 and 1,4IP2 (in no case did the results differ among the two cell types and five inhibitors). Lipid binding measured by filter and liposome assays; +, strong; ±, weak; –, none; Y, yes; N, no; nt, not tested. See also Figure S7.

is restricted to certain cell types, such as epithelial cells. The presence of RXLR-dEER motif effectors in oomycete pathogens of a broad diversity of plants (Rehmany et al., 2005; Tyler et al., 2006; Jiang et al., 2008) suggests that cell surface PI3P should be widely present in plants, but this remains to be directly tested.

In aggregate, our data strongly support the hypothesis that RXLR-mediated binding to PI3P mediates entry of oomycete and fungal pathogen effectors into plant cells. The functional connection between PI3P binding and plant cell entry is underlined by the observation that all RXLR mutations that abolish PI3P binding also abolish cell entry (12 mutations in 9 effectors) and all RXLR mutations that fail to abolish PI3P binding also fail to abolish cell entry (3 mutations in 3 effectors) (Figure 7). Similar findings with the human A549 cells suggest the possibility that oomycetes and fungi that infect humans and other animals could utilize effectors that enter host cells via PI3P binding.

Our data on localization of the effector-GFP fusions shortly after their exposure to human cells and to soybean suspension culture cells, together with the effects of specific endocytosis inhibitors, support the hypothesis that the effectors enter both plant and animal cells via lipid raft-mediated endocytosis (Figure 6M). The K_d's of Avr1b and AvrL567 for PI3P are well above the threshold required for attachment to PI3P-containing intracellular membranes (must be less than 5–7 nM; Blatner et al., 2004), suggesting that oomycete and fungal effectors should readily release from PI3P-containing membranes once inside the host cell (Figure 6M), leaving them free to target a wide variety of host cellular compartments. A variety of bacterial toxins also enter host cells via lipid raft-mediated endocytosis following binding to a lipid receptor, most commonly a glycolipid (Lafont et al., 2004; Lord et al., 1999). The protein toxin PtrToxA from *Pyrenophora tritici-repentis*, enters via an RGD vitronectin-like adhesion motif, probably via receptor-mediated endocytosis (Sarma et al., 2005). The mechanism by which the RXLR effectors escape from endosomes is unknown. Bacterial toxins escape via several mechanisms including retrograde translocation from the ER and transit of partially unfolded proteins directly across membranes (Lafont et al., 2004; Lord et al., 1999). Although we observed that *Plasmodium* effectors also bound PI3P, and did so via their Pexel motif, the role of PI3P in the entry of *Plasmodium* effectors into erythrocytes across the parasitiphorous vacuolar membrane must be different than its role in oomycete and fungal effector translocation, since the Pexel motifs are cleaved within the parasite endoplasmic reticulum (Chang et al., 2008) and transported into the erythrocyte via a pathogen-derived translocon (de Koning-Ward et al., 2009; Maier et al., 2008). Perhaps PI3P binding is required for correct cleavage and targeting. Phosphoinositide levels are strongly elevated in *Plasmodium*-infected erythrocytes due to export of parasite phosphatidylinositol-3-kinase into the erythrocyte cytoplasm (Vaid et al., 2010). We do not know if oomycete or fungal RXLR motifs are ever cleaved, for example as part of the mechanism for escaping endosomes.

Our data demonstrate that effectors from diverse fungal plant pathogens, as well as oomycetes, utilize RXLR-mediated PI3P-binding to enter plant cells. The fungal pathogens include an obligately biotrophic basidiomycete that forms haustoria (*M. lini*; AvrL567), a xylem-dwelling ascomycete vascular wilt

pathogen (*F. oxysporum* f.sp. *lycopersici*; Avr2) and a hemibiotrophic ascomycete leaf and stem pathogens that remains confined to the apoplast (*L. maculans*; AvrLm6). Thus PI3P-mediated effector entry may have evolved independently in several lineages of fungi as well as in the oomycetes.

Our mutagenesis survey of the Avr1b RXLR motif and the diverse functional motifs found in the fungal effectors together suggest that a wide diversity of RXLR-related sequences may support cell entry via PI3P-binding. Bioinformatic screens with the highly redundant motif suggested by our data ([RHK]X[LMIFYW]) identify huge numbers of matches, most of which are likely spurious as judged by searches of permuted protein sequences (R. Jiang and B.M.T., unpublished data), and by the presence of inactive motifs in Avr1b, Avh331, AvrLm6, and Avr2 (Figure 7). Thus, it is very likely that there are additional requirements for cell entry, as noted by Bhattacharjee et al., (2006) and Dou et al. (2008). Biochemical screening for phosphoinositide binding will however provide a powerful tool for screening or directly isolating new candidate effector proteins from all classes of microbes. It may also enable detection of phosphoinositide-binding plant or animal proteins that can traffic through intercellular spaces and enter into target cells to transduce signals. Presumably cell surface PI3P plays a role in the normal physiology of plants and animals.

Understanding the role of phosphoinositides in pathogen effector entry also opens the possibility of targeting cell entry domains or external phosphoinositides for preventative or therapeutic intervention in both agriculture and medicine. The finding that PI3P-binding proteins and IP2 can block effector entry into both plant and human cells provides a proof-of-concept for this approach.

EXPERIMENTAL PROCEDURES

Plasmid Construction

Cloning strategies for all plasmids and the primers are reported in the Extended Experimental Procedures and in Table S3, Table S4, Table S5, and Table S6.

Protein Expression in *E. coli*

E. coli cells containing plasmids encoding each fusion protein were grown at 37°C to an OD_{600} of 0.6. Protein expression was induced with 1–5 mM IPTG and cell growth was continued at 16°C to 37°C for 1.5–16 hr depending on the protein (see Extended Experimental Procedures).

Purification of His-tagged GFP Fusion Proteins

Cells were lysed by sonication then the fusion proteins were collected from the supernatant using a Ni-NTA column (QIAGEN). Pooled fractions were concentrated and equilibrated to the appropriate assay buffer using a Amicon concentrator, and the purity was assessed by gel electrophoresis (Figure S7). See Extended Experimental Procedures for additional details.

Purification of GST-Fusion Proteins

GST fusion proteins were collected from the supernatant using glutathione-sepharose 4B beads (GE Healthcare). Where necessary, the GST tag was removed by digestion with thrombin. See Extended Experimental Procedures for additional details.

Lipid Filter-Binding Assays

Lipids were dissolved in chloroform: methanol: water (65:30:8) then spotted at appropriate concentrations onto membranes. Membranes were incubated in blocking buffer for 1 hr, then the probe protein (20 μg) was added and incubation continued overnight at 4°C. After washing, bound proteins were detected with rabbit anti-GFP or goat anti-GST antibody followed by an HRP-secondary antibody conjugate. Detection was carried out using ECL reagent. See Extended Experimental Procedures for additional details.

Liposome-Binding Assays

Liposomes were prepared from a suspension of PC, PE, and where appropriate a PI-x-P, in chloroform/methanol/water (65:30:8). Lipid mixtures were dried then rehydrated by three cycles of freeze/thawing. Large unilamellar vesicles were formed by extruding the lipid suspension through a 0.1 μM filter. After precentrifugation, protein was added to liposomes and incubated for 1 hr at room temperature. If needed 1,3IP2 or 1,4IP2 were incubated with the proteins for 30 min at room temperature before addition to the liposomes. Protein-liposome mixtures were centrifuged at 100,000 g for 15 min at 25°C. Pellets containing liposome-bound proteins and supernatants containing free proteins were then analyzed by SDS-PAGE. See Extended Experimental Procedures for additional details.

Soybean Root and Suspension Culture Protein Uptake Assays

1.5 cm root tips were cut from vermiculite-grown seedlings and placed into the effector or biosensor protein solution (1 mg/mL protein) and incubated for 12–15 hr at 28°C. For inositol diphosphate inhibition assays, the protein was preincubated with 500 μM 1,3IP2 or 1,4IP2 for 30 min at room temperature before the addition of root tips. For inhibition tests with biosensor proteins, the root tips were preincubated for 3 hr at room temperature in biosensor protein (5 mg/ml) before addition of the effector. After uptake, the root tips were washed in 75 ml of water for 2 hr. For assays with soybean root cell suspension cultures, effector-GFP fusion proteins (100 μg/ml) were incubated with 3 day old cultures for 6 hr at 25°C or at 2°C for 12 hr then photographed without washing. Filipin (50 μg/mL) and nystatin (50 μg/mL) were added 2 hr prior to protein addition. See Extended Experimental Procedures for additional details, including the confocal microscopy.

Human Cell Uptake Assays

Human A549 cells in a 96-well plate were cultured in 90 μl DMEM, 0.1% FBS (DMEM/FBS) at 37°C. Fusion protein was added to each well and incubated at 37°C for 2.5 min to 9 hr, as indicated, or at 2°C for 2 hr. Cells were washed twice and then suspended in 0.25% trypsin and photographed. Where used, the following were dissolved in DMSO and added to cells to final concentrations of: FM4-64, 5 μM; wortmannin, 1 μM; LY249002, 1 μM; tyrphostin A23, 350 μM; N-ethylmaleimide, 1 mM; cytochalasin D, 10 μM, filipin 50 μg/mL, nystatin 50 μg/mL. FM4-64 was added with the protein; the inhibitors were added 2 hr beforehand except where stated otherwise.

To assay inhibition by inositol diphosphate, effector fusion protein was preincubated with 1,3IP2 or I,4IP2 (1 mM) for 30 min at room temperature then added to an equal volume of cells. For inhibition assays, biosensor proteins (0.1 mg/mL) were incubated with the cells for 3 hr at 37°C before addition of effector protein. For dual staining, equal concentrations of the two proteins were added simultaneously to the cells. In all cases, the cells were incubated at 37°C a further 8–9 hr after effector addition (as indicated), then washed and photographed as described in the Extended Experimental Procedures.

To quantitate binding and uptake, GFP fluorescence was measured in the 96-well plates using a microplate spectrofluorometer. Four to six replicates were used, and 20 scans were averaged per replicate. A standard curve in the linear range of detection (0–100 μg/mL) was used to convert emission into protein concentration. See Extended Experimental Procedures for additional details.

Estimation of Binding and Inhibitor Constants

Binding constants and their standard errors were estimated by using the LINEST function of Microsoft Excel to fit a straight line to a plot of: E_b versus $P_t + K_d/(1\text{-}E_t/E_b)$ where E_b = [bound effector], E_t = [total effector], P_t = [available PI3P target] (the intercept), and K_d = the dissociation constant (the gradient). The number of PI3P molecules per cell was estimated from P_t. To estimate the inhibition constants and their standard errors for 1,3IP2, a straight line through the origin was fitted to a plot of I_t/EI - 1 versus K_i/E_f where E_f = [free effector] = $K_d/(P_t/E_b - 1)$, I_t = [total inhibitor], EI = [effector-inhibitor complex] = $E_t - E_b - E_f$ and K_i = the inhibition constant (the gradient). See Extended Experimental Procedures for additional details.

SUPPLEMENTAL INFORMATION

Supplemental Information includes Extended Experimental Procedures, Supplemental References, seven figures, and six tables and can be found with this article online at doi:10.1016/j.cell.2010.06.008.

ACKNOWLEDGMENTS

The project was conceived by B.M.T, W.S., and D.D., and the experiments were planned by all authors. S.D.K. and B.G. conducted most of the experiments with contributions from D.G.S.C., D.D., E.F., A.C., R.H., and F.A. S.D.K and B.M.T wrote the paper with input from all authors. We thank Furong Sun and Vincenzo Antignani for technical assistance; Rays Jiang (Broad Institute) for bioinformatics assistance; John McDowell, Ryan Anderson (Virginia Tech), and Frank Takken (University of Amsterdam) for useful discussions; Joop Vermeer and Teun Munnik (University of Amsterdam) for the Hrs-2xFYVE biosensor gene; Michael Klemba (Virginia Tech) for human erythrocytes, Saghai Maroof (Virginia Tech) for soybean seed and Maureen Lawrence, Lisa Gunderman and Emily Alberts for manuscript preparation. This work was supported by the National Research Initiative of the USDA National Institute of Food and Agriculture, grant number #2007-35319-18100 (to B.M.T), by the U.S. National Science Foundation, grant number IOS-0924861 (to B.M.T), in part by the 973 program of the Ministry of Science and Technology of China, grant #2006CB101901 and by grant 15 from the Earmarked Fund for Modern Agro-industry Technology Research System of China (to W.S.). S.D.K. was supported in part by a U.S. National Science Foundation predoctoral fellowship and B.G. was supported by a China Scholarship Council fellowship, #2007U27066, via NW A & F University.

Received: August 20, 2009
Revised: March 30, 2010
Accepted: May 10, 2010
Published: July 22, 2010

REFERENCES

Armstrong, M.R., Whisson, S.C., Pritchard, L., Bos, J.I., Venter, E., Avrova, A.O., Rehmany, A.P., Bohme, U., Brooks, K., Cherevach, I., et al. (2005). An ancestral oomycete locus contains late blight avirulence gene Avr3a, encoding a protein that is recognized in the host cytoplasm. Proc. Natl. Acad. Sci. USA *102*, 7766–7771.

Bhattacharjee, S., Hiller, N.L., Liolios, K., Win, J., Kanneganti, T.D., Young, C., Kamoun, S., and Haldar, K. (2006). The malarial host-targeting signal is conserved in the Irish potato famine pathogen. PLoS Pathog *2*, e50.

Bhavsar, A.P., Guttman, J.A., and Finlay, B.B. (2007). Manipulation of host-cell pathways by bacterial pathogens. Nature *449*, 827–834.

Blatner, N.R., Stahelin, R.V., Diraviyam, K., Hawkins, P.T., Hong, W., Murray, D., and Cho, W. (2004). The molecular basis of the differential subcellular localization of FYVE domains. J. Biol. Chem. *279*, 53818–53827.

Boon, J.M., and Smith, B.D. (2002). Chemical control of phospholipid distribution across bilayer membranes. Med. Res. Rev. *22*, 251–281.

Chang, H.H., Falick, A.M., Carlton, P.M., Sedat, J.W., Derisi, J.L., and Marletta, M.A. (2008). N-terminal processing of proteins exported by malaria parasites. Mol. Biochem. Parasitol. *160*, 107–115.

Chang, M., Chou, J.C., and Lee, H.J. (2005). Cellular internalization of fluorescent proteins via arginine-rich intracellular delivery peptide in plant cells. Plant Cell Physiol. *46*, 482–488.

Chang, M., Chou, J.C., Chen, C.P., Liu, B.R., and Lee, H.J. (2007). Noncovalent protein transduction in plant cells by macropinocytosis. New Phytol. *174*, 46–56.

Chisholm, S.T., Coaker, G., Day, B., and Staskawicz, B.J. (2006). Host-microbe interactions: shaping the evolution of the plant immune response. Cell *124*, 803–814.

de Koning-Ward, T.F., Gilson, P.R., Boddey, J.A., Rug, M., Smith, B.J., Papenfuss, A.T., Sanders, P.R., Lundie, R.J., Maier, A.G., Cowman, A.F., and Crabb, B.S. (2009). A newly discovered protein export machine in malaria parasites. Nature *459*, 945–949.

Dou, D., Kale, S.D., Wang, X., Jiang, R.H.Y., Bruce, N.A., Arredondo, F.D., Zhang, X., and Tyler, B.M. (2008). RXLR-mediated entry of Phytophthora sojae effector Avr1b into soybean cells does not require pathogen-encoded machinery. Plant Cell *20*, 1930–1947.

Dowler, S., Currie, R.A., Campbell, D.G., Deak, M., Kular, G., Downes, C.P., and Alessi, D.R. (2000). Identification of pleckstrin-homology-domain-containing proteins with novel phosphoinositide-binding specificities. Biochem. J. *351*, 19–31.

Ellis, J., Catanzariti, A.M., and Dodds, P. (2006). The problem of how fungal and oomycete avirulence proteins enter plant cells. Trends Plant Sci. *11*, 61–63.

Ellis, J.G., Dodds, P.N., and Lawrence, G.J. (2007). Flax rust resistance gene specificity is based on direct resistance-avirulence protein interactions. Annu. Rev. Phytopathol. *45*, 289–306.

Fudal, I., Ross, S., Gout, L., Blaise, F., Kuhn, M.L., Eckert, M.R., Cattolico, L., Bernard-Samain, S., Balesdent, M.H., and Rouxel, T. (2007). Heterochromatin-like regions as ecological niches for avirulence genes in the Leptosphaeria maculans genome: map-based cloning of AvrLm6. Mol. Plant Microbe Interact. *20*, 459–470.

Grouffaud, S., van West, P., Avrova, A.O., Birch, P.R., and Whisson, S.C. (2008). Plasmodium falciparum and Hyaloperonospora parasitica effector translocation motifs are functional in Phytophthora infestans. Microbiology *154*, 3743–3751.

Hiller, N.L., Bhattacharjee, S., van Ooij, C., Liolios, K., Harrison, T., Lopez-Estrano, C., and Haldar, K. (2004). A host-targeting signal in virulence proteins reveals a secretome in malarial infection. Science *306*, 1934–1937.

Houterman, P.M., Ma, L., van Ooijen, G., de Vroomen, M.J., Cornelissen, B.J., Takken, F.L., and Rep, M. (2009). The effector protein Avr2 of the xylem-colonizing fungus Fusarium oxysporum activates the tomato resistance protein I-2 intracellularly. Plant J. *58*, 970–978.

Jia, Y., McAdams, S.A., Bryan, G.T., Hershey, H.P., and Valent, B. (2000). Direct interaction of resistance gene and avirulence gene products confers rice blast resistance. EMBO J. *19*, 4004–4014.

Jiang, R.H.Y., Tripathy, S., Govers, F., and Tyler, B.M. (2008). RXLR effector reservoir in two Phytophthora species is dominated by a single rapidly evolving super-family with more than 700 members. Proc. Natl. Acad. Sci. USA *105*, 4874–4879.

Jones, J.D., and Dangl, J.L. (2006). The plant immune system. Nature *444*, 323–329.

Kale, S.D., and Tyler, B.M. (2009). Assaying effector function in planta using double-barreled particle bombardment. In Methods in Molecular Biology The Plant Immune Response, J.M. McDowell, ed. (Totowa, NJ: Humana).

Khang, C.H., Berruyer, R., Giraldo, M.C., Kankanala, P., Park, S.-Y., Czymmek, K., Kang, S., and Valent, B. (2010). Translocation of *Magnaporthe oryzae* effectors into rice cells and their subsequent cell-to-cell movement. Plant Cell *22* 10.1105/tpc.1109.069666.

Lafont, F., Abrami, L., and van der Goot, F.G. (2004). Bacterial subversion of lipid rafts. Curr. Opin. Microbiol. *7*, 4–10.

Langel, U. (2006). Handbook of cell-penetrating peptides, Second Edition (Boca Raton, FL: CRC / Taylor & Francis).

Lee, S.A., Kovacs, J., Stahelin, R.V., Cheever, M.L., Overduin, M., Setty, T.G., Burd, C.G., Cho, W., and Kutateladze, T.G. (2006). Molecular mechanism of membrane docking by the Vam7p PX domain. J. Biol. Chem. *281*, 37091–37101.

Lemmon, M.A. (2008). Membrane recognition by phospholipid-binding domains. Nat. Rev. Mol. Cell Biol. *9*, 99–111.

Lord, J.M., Smith, D.C., and Roberts, L.M. (1999). Toxin entry: how bacterial proteins get into mammalian cells. Cell. Microbiol. *1*, 85–91.

Lou, Y., Ma, H., Lin, W.H., Chu, Z.Q., Mueller-Roeber, B., Xu, Z.H., and Xue, H.W. (2006). The highly charged region of plant beta-type phosphatidylinositol

4-kinase is involved in membrane targeting and phospholipid binding. Plant Mol. Biol. *60*, 729–746.

Maier, A.G., Rug, M., O'Neill, M.T., Brown, M., Chakravorty, S., Szestak, T., Chesson, J., Wu, Y., Hughes, K., Coppel, R.L., et al. (2008). Exported proteins required for virulence and rigidity of *Plasmodium falciparum*-infected human erythrocytes. Cell *134*, 48–61.

Marti, M., Good, R.T., Rug, M., Knuepfer, E., and Cowman, A.F. (2004). Targeting malaria virulence and remodeling proteins to the host erythrocyte. Science *306*, 1930–1933.

Quinn, P.J. (2002). Plasma membrane phospholipid asymmetry. In Subcellular Biochemistry, P.J. Quinn and V.E. Kagan, eds. (London: Kluwer Academic/Plenum Publishers), pp. 39–60.

Rehmany, A.P., Gordon, A., Rose, L.E., Allen, R.L., Armstrong, M.R., Whisson, S.C., Kamoun, S., Tyler, B.M., Birch, P.R., and Beynon, J.L. (2005). Differential recognition of highly divergent downy mildew avirulence gene alleles by RPP1 resistance genes from two Arabidopsis lines. Plant Cell *17*, 1839–1850.

Sarma, G.N., Manning, V.A., Ciuffetti, L.M., and Karplus, P.A. (2005). Structure of Ptr ToxA: an RGD-containing host-selective toxin from Pyrenophora tritici-repentis. Plant Cell *17*, 3190–3202.

Shan, W., Cao, M., Leung, D., and Tyler, B.M. (2004). The *Avr1b* Locus of Phytophthora sojae Encodes an Elicitor and A Regulator Required for Avirulence on Soybean Plants Carrying Resistance Gene *Rps1b*. Mol. Plant Microbe Interact. *17*, 394–403.

Tseng, T.-T., Tyler, B.M., and Setubal, J.C. (2009). Protein Secretion Systems in Bacterial-Host Associations, and their Description in the Gene Ontology. BMC Microbiol. *9*(suppl 1), S2.

Tyler, B.M. (2002). Molecular Basis of Recognition Between *Phytophthora* species and their hosts. Annu. Rev. Phytopathol. *40*, 137–167.

Tyler, B.M. (2007). Phytophthora sojae: root rot pathogen of soybean and model oomycete. Mol. Plant Pathol. *8*, 1–8.

Tyler, B.M. (2009). Entering and breaking: virulence effector proteins of oomycete plant pathogens. Cell. Microbiol. *11*, 13–20.

Tyler, B.M., Tripathy, S., Zhang, X., Dehal, P., Jiang, R.H., Aerts, A., Arredondo, F.D., Baxter, L., Bensasson, D., Beynon, J.L., et al. (2006). Phytophthora genome sequences uncover evolutionary origins and mechanisms of pathogenesis. Science *313*, 1261–1266.

Vaid, A., Ranjan, R., Smythe, W.A., Hoppe, H.C., and Sharma, P. (2010). PfPI3K, a phosphatidylinositol-3 kinase from Plasmodium falciparum, is exported to the host erythrocyte and is involved in hemoglobin trafficking. Blood *115*, 2500–2507.

Vermeer, J.E., van Leeuwen, W., Tobena-Santamaria, R., Laxalt, A.M., Jones, D.R., Divecha, N., Gadella, T.W., Jr., and Munnik, T. (2006). Visualization of PtdIns3P dynamics in living plant cells. Plant J. *47*, 687–700.

Vermeer, J.E., Thole, J.M., Goedhart, J., Nielsen, E., Munnik, T., and Gadella, T.W., Jr. (2009). Imaging phosphatidylinositol 4-phosphate dynamics in living plant cells. Plant J. *57*, 356–372.

Whisson, S.C., Boevink, P.C., Moleleki, L., Avrova, A.O., Morales, J.G., Gilroy, E.M., Armstrong, M.R., Grouffaud, S., van West, P., Chapman, S., et al. (2007). A translocation signal for delivery of oomycete effector proteins into host plant cells. Nature *450*, 115–119.

Note Added in Proof

After this paper was accepted for publication, Rafiqi et al (Plant Cell 10.1105/tpc.109.072983) showed that fungal effectors AvrL567 and AvrM could enter plant cells in a pathogen-independent manner, mediated by RXLR-like sequences, and Murata-Kamiya et al (Cell Host & Microbe DOI 10.1016/j.chom.2010.04.005) showed that a Helicobacter pylori effector CagA enters human cells by binding cell surface phosphatidylserine.

EXTENDED EXPERIMENTAL PROCEDURES

Protein Expression in E. coli

Expression Vectors

The primers used for clone construction are listed in Table S3.

The polypeptides encoded by the protein expression vectors used in this study are listed in Table S5. pAvr1bXK was used for expression in planta using particle bombardment. All others were used for expression in *E. coli.* Further details of vector construction and utilization are given in Table S4.

Synthetic DNA Sequences

Several effector and biosensor proteins were produced using synthetic DNA sequences with codon usage optimized primarily for *E.coli* expression and/or for *Nicotiana* expression rather than the natural sequences of their genes. Those DNA sequences are listed in Table S6.

Growth and Induction of Protein Expression Cultures

BL21(DE3) *Escherichia coli* cells containing plasmids encoding each fusion protein were grown in 200 ml of Luria-Bertani media containing 100 μg/mL ampicillin in a 1 l baffled flask shaken at 240 rpm at 37°C to an OD_{600} of 0.6. Then for the following fusion proteins expression was induced with 2.5 mM IPTG and cell growth was continued under the same conditions for 4 hr at 37°C: control GFP, Avr1b(N)-GFP, Avh5(N)-GFP, PfGBP(N)-GFP, PfHRPII-GFP, their respective mutants, and Pf1615c(N)(pexel$^-$)-GFP. Expression of the following fusion proteins was induced with 1 mM IPTG and then cell growth was continued at 240 rpm at 17°C for 1.5 hr: AvrL567(N)-GFP, Avh331(N)-GFP, their respective mutants, and Pf1615c(N)-GFP. Expression of fusion proteins Avh5-GST, Avh331-GST, and their respective mutants was induced with 1 mM IPTG and then cell growth was continued at 240 rpm at 25°C for 2 hr. Expression of the following fusion proteins was induced with 5 mM IPTG and then cell growth was continued at 240 rpm at 16°C for 16 hr: PEPP1-PH-GFP, FAPP1-PH-GFP and all pSDK1 and pSDK2 clones. Cells were harvested by centrifugation at 7,000 g for 10 min and stored at −80°C.

Purification of His-Tagged GFP Fusion Proteins

Cells were lysed by sonication in chilled lysis buffer (50 mM NaH_2PO_4 (pH 7.2), 300 mM NaCl, 10 mM imidazole, 1 mg/mL lysozyme; 4 mL/g wet cell weight). Lysed cells were centrifuged at 10,000 g for 30 min at 4°C and then fusion proteins were collected from the supernatant using a column containing Ni-NTA superflow (QIAGEN). The column was then washed with 5 volumes of washing buffer (50 mM NaH_2PO_4, 300 mM NaCl, 20 mM imidazole, pH 7.2) and eluted in 1 ml fractions with elution buffer (50 mM NaH_2PO_4 (pH 7.2), 300 mM NaCl, 250 mM imidazole). Fractions were pooled then concentrated to 50-100 μl and equilibrated to 25 mM NaH_2PO_4 pH 7.2 (for the human cell uptake assay, the lipid filter-binding assay, and the liposome-binding assay) or 25 mM MES (2-(N-morpholino) ethanesulfonic acid) pH 5.8 (for the soybean root uptake assay) using a concentrator device (Amicon Centriplus MWCO-3 kDa or Amicon Ultra-4 Centrifugal Filter Unit with Ultracel-10 membrane). The protein concentration was measured by absorbance at 280 nm using a nanodrop spectrophotometer (ND-1000). The purity was assessed by gel electrophoresis (Figure S7). All proteins expressed using vectors pSDK1 and pSDK2 were purified by Nickel-NTA chromatography followed by size exclusion chromatography using Bio-Rad Bio-Gel P-100.

Purification of GST-Fusion Proteins

Cell lysis and centrifugation were performed as described above, except that the following lysis buffers were used: 50mM Tris-HCl (pH 6.8), 300mM NaCl (Avh5-GST) or 50mM Tris-HCl (pH 6.8), 500mM NaCl (Avh331-GST). The fusion proteins were collected from the supernatant using glutathione-sepharose 4B beads (GE Healthcare) at room temperature. The beads were washed in a column with 5 volumes of washing buffer (50mM Tris-HCl, 300 mM/500 mM NaCl, pH 6.8), then eluted in 1 ml fractions with GST elution buffer (50 mM Tris-HCl, 300 mM/500 mM NaCl, 10 mM reduced glutathione, pH 6.8). Fractions were pooled, concentrated to 50-100 μl and equilibrated to 50 mM Tris-HCl, 300 mM/500 mM NaCl, pH 6.8 using a 3 kDa concentrator device. Protein concentration was measured by absorbance at 280nm using a nanodrop spectrophotometer (ND-1000). The purity was assessed by gel electrophoresis (Figure S1). To obtain untagged Avh331 protein, purified GST-Avh331 (2 mg) was digested with 2 units of thrombin (Novagen, restriction grade) at 20°C for approximately 24 hr in a 1 ml reaction then fractionated on a glutathione sepharose 4B column. Nonbinding fractions containing untagged Avh331 protein were pooled and concentrated to 0.25 mg/mL in 10 mM MES buffer (pH5.8). Protein samples were immediately infiltrated onto leaves as Avh331 protein precipitated upon prolonged storage.

GST Cleavage and Purification

2 units of Novagen restriction grade thrombin was added to 1mg of purified protein from the following: GST-Avr1b-GFP, GST-Hrs-2xFYVE-GFP, GST-VAM7p-PX-GFP, GST-PEPP1-PH-mCherry, GST-FAPP1-PH-mCherry, GST-Hrs-FYVE-mCherry, GST-VAM7p-PX-mCherry, and the respective Avr1b mutant forms. Cleaved protein was purified by Nickel-NTA chromatography followed by size exclusion chromatography (Bio-Rad Bio-Gel P-100). Fractions were pooled, concentrated (as described above), and analyzed for purity by gel electrophoresis (Figure S7 and S3). Upon cleavage GST-Avr1b-GFP does precipitate between 20%–30%. Avr1b should never be concentrated above 1 mg/mL as it will increase precipitation overnight at 4°C. Avr1b-GFP protein samples were immediately infiltrated onto leaves as Avr1b-GFP protein precipitates slightly upon prolonged storage at 4°C.

Biosensors

The specificity of the biosensor proteins was validated by lipid filter-binding assays and by liposome binding assays (Figures 3E and 3F). The specificity of binding of the biosensors (and effectors) was further supported by the lack of binding to erythrocytes (Figure 3D), which carry a wide array of phospholipids, sphingolipids and glycolipids on their surface. PI3P was not previously reported on the outer surface of plant or animal cells (e.g., Quinn, 2002; Boon and Smith, 2002). An explanation for this oversight may be that nearly all studies of the membrane polarity of plasma membrane phosphoinositides were conducted on erythrocytes, and that most studies did not search specifically for PI3P (Quinn, 2002; Boon and Smith, 2002).

Lipid Filter-Binding Assay

Lipids (from Cayman Chemical, Ann Arbor, Michigan or Avanti Polar Lipids) were dissolved in DMSO. Lipid filters were prepared by spotting 1 μl of each lipid at appropriate concentrations onto Hybond-C-extra membranes (GE Healthcare). Membranes were incubated in 20 ml of blocking buffer (10mM Tris-HCl, pH 7.2, 150mM NaCl, 0.1% Tween-20, 3% fatty-acid free bovine serum albumin, Sigma # A-7030) for 1 hr at room temperature. The probe protein (20 μg) was added to the blocking buffer and incubated overnight at 4°C. After washing, bound proteins were detected with rabbit anti-GFP antibody (Immunology Consultants Laboratory) or with goat anti-GST (GE Healthcare) followed, after washing, with an HRP conjugate (anti-rabbit antibody or donkey-anti-goat IgG-HRP; Santa Cruz Biotechnology). Detection was carried out using ECL reagent (SuperSignal West Pico Chemiluminescent Substrate, Thermo Scientific).

Liposome-Binding Assay

Liposomes were prepared from a suspension of 0.733 μg/ml PC, 0.267 μg/ml PE (PC/PE) or 0.66 μg/ml PC, 0.24 μg/ml PE, 0.1 μg/ml phosphatidylinositol-phosphate (PC/PE/PI-x-P) in chloroform/methanol/water (65:30:8). Lipid mixtures were dried under vacuum overnight, then the resultant lipid films were rehydrated at 1 mg/mL (total lipid) in 20 mM Tris-HCl (pH 6.8) 100 mM NaCl, 2 mM dithiothreitol by three cycles of freeze/thawing. Large unilamellar vesicles were formed by extruding the lipid suspension through a 0.1-μM filter (nucleopore track-etch membrane, Whatman) 20 times and used immediately. Effector fusion proteins were centrifuged at 100,000 g for 20 min at 25°C prior to assay to remove protein aggregates. 10 μg of protein were added to 50 μg of liposomes and incubated for 1 hr at room temperature. If needed 1,3IP2 or 1,4IP2 (600 μM) were incubated with the proteins for 30 min at room temperature before addition to the liposomes. Protein-liposome mixtures were centrifuged at 100,000 g for 15 min at 25°C. Pellets containing liposome-bound proteins and supernatants containing free proteins were then analyzed by SDS-PAGE.

Soybean Root and Suspension Culture Protein Uptake Assay

Soybean seeds were germinated in vermiculite for 3-5 days. Roots were washed with water thoroughly to remove any debris. Approximately 1.5 cm root tips were cut and placed into the effector or biosensor protein solution (50 μl of 25 mM MES pH 5.8, 1 mg/mL protein) and incubated for 12-15 hr at 28°C. For inositol diphosphate inhibition assays, the protein was preincubated with 500 μM 1,3IP2 or 1,4IP2 for 30 min at room temperature before the addition of root tips. For inhibition tests with biosensor proteins, the root tips were preincubated for 3 hr at room temperature in 25 μl per root tip of biosensor protein (5 mg/ml in 25 mM MES pH 5.8). Then 25 μl of effector protein (2 mg/ml in 25 mM MES pH 5.8) was added and the roots were incubated for 12 hr at 28°C. After uptake, the root tips were rinsed with water and washed in 75 ml of water for 2 hr on an orbital shaker at 90 rpm.

In these experiments, accumulation of the GFP fusion proteins inside the root cells was confirmed by substantial accumulation of GFP in the nuclei of the cells (a property of *Aequorea coerulescens* GFP; Dou et al., 2008), and by plasmolysis experiments (Figure S1O; Dou et al., 2008). Fusion proteins with RXLR and dEER motif mutations accumulated within the root apoplast as readily as the non mutant proteins, and were not degraded, but were readily removed by the washing step (Figure S1P,U).

For assays with soybean root cell suspension cultures, effector-GFP fusion proteins (100 μg/ml final concentration) were incubated with 3 day old cultures for 6 hr at 25°C (for uptake experiments) or at 2°C for 12 hr (for binding experiments; cells were precooled for 2 hr before addition of protein) then washed for 2 hr and photographed. Plasmolysis was induced with 500 μl of 0.8M Mannitol (filter sterilized). Filipin (50 μg/mL) and nystatin (50 μg/mL) were added 2 hr prior to protein addition.

Soybean root suspension cultures were initiated from Glycine max cv. Williams. Hypocotyl sections were incubated on Gamborg Long Basal Medium (Phytotechnology Laboratories) with 2% sucrose (Sigma 5390), 0.2% Casein Hydrolysate (ICN Biomedicals), 1.0 mg/L 2,4-Dichlorophenoxyacetic acid (2,4-D), pH 5.7, and 0.4% Gelzan (Sigma) for 4-6 weeks at 22°C in the dark to generate callus. Clumps of callus were allowed to proliferate on plates. Rapidly growing sections were transferred to the same media without Gelzan and maintained in the dark at 27°C with shaking at 120 rpm. Cells were subcultured (8 mLs into 27 mLs of fresh medium) every 7 days and culture was maintained for 6 months before experiments were initiated.

Human Cell Uptake Assays

Human lung adenocarcinoma cells A549 (ATCC CCL-185) were harvested by trypsinization and centrifugation at 700 g for 5 min. Cells were seeded at a concentration of 2.5×10^4- 5.0×10^4 per well in a 96-well tissue culture plate. Cells were washed with Dulbecco's Phosphate Buffer Saline (Ca^{2+}/Mg^{2+} free) (DPBS; GIBCO) and cultured in 90 μl DMEM, 0.1% FBS (DMEM/FBS). Fusion protein (10 μg in DPBS) was added to each well (final concentration 25 μg/mL or 100 μg/mL, as indicated) and incubated in the same conditions at 37°C for 2.5 min to 9 hr, as indicated, or at 2°C for 2 hr. Cells were washed twice with 100 μl of DMEM/FBS

and then suspended in 50 μl DMEM/FBS plus 0.25% trypsin and photographed. Where used, the following were dissolved in DMSO at 100-fold final concentration and added to cells to final concentrations of: FM4-64, 5 μM; wortmannin, 1 μM; LY249002, 1 μM; tyrphostin A23, 350 μM; N-ethylmaleimide, 1 mM; cytochalasin D, 10 μM, filipin 50 μg/mL, nystatin 50 μg/mL. FM4-64 was added with the protein; the inhibitors were added 2 hr beforehand except where stated otherwise.

To assay inhibition by inositol diphosphate, effector fusion protein (0.2 mg/mL) was preincubated with 1,3IP2 or I,4IP2 (1 mM) in DPBS for 30 min at room temperature then added to an equal volume of cells in RPMI (final concentrations 500 μM IP2, 0.1 mg/mL effector proteins). For inhibition by biosensor proteins, biosensor protein (0.1 mg/mL in DPBS) was incubated with the cells for 3 hr at 37°C before addition of effector protein (final concentrations 100 μg/mL biosensor protein, 25 μg/mL effector proteins). For dual staining, the two proteins (100 μg/mL each final concentration in DPBS) were added simultaneously to the cells. In all cases, the cells were incubated at 37°C a further 8-9 hr after effector addition (as indicated), then washed and photographed.

To quantitate binding and uptake, GFP fluorescence was measured in 96 well plates (BD Falcon 353072 96-well Microplate, clear, tissue-culture treated, flat-bottom with lid) using a SpectraMax Gemini XS Microplate Spectrofluorometer and analyzed using the softmax Pro 4.3.1 software suite. GFP was excited at 488 nM and emission was captured at 509 nM using a cutoff of 495 nM. mCherry was excited at 587 nM and emission was captured at 610 nM using a cutoff of 590 nM. 20 scans were averaged per reading. A standard curve in the linear range of detection (0 to 100 μg/mL) was used to convert emission into protein concentration.

Estimation of Binding and Inhibitor Constants

To estimate binding constants for cell binding, cells were incubated with protein (100 μg/mL) for 3 hr at 2°C, then washed briefly and the binding quantitated as described above. To estimate binding constants for liposome binding, liposome-protein complexes were collected by centrifugation as described above, resuspended in 100 μl of 20 mM Tris-HCl (pH 6.8) 100 mM NaCl then added to a 96 well plate and measured as described above. Binding constants and their standard errors were estimated by using the LINEST function of Microsoft Excel to fit a straight line to a plot of: E_b versus $P_t + K_d/(1-E_t/E_b)$ where E_b = [bound effector], E_t = [total effector], P_t = [available PI3P target] (the intercept), and K_d = the dissociation constant (the gradient). The number of PI3P molecules per cell was estimated from P_t. To estimate the inhibition constants and their standard errors for 1,3IP2, a straight line through the origin was fitted to a plot of I_t/EI - 1 versus K_i/E_f where E_f = [free effector] = $K_d/(P_t/E_b - 1)$, I_t = [total inhibitor], EI = [effector-inhibitor complex] = $E_t - E_b - E_f$ and K_i = the inhibition constant (the gradient). For the liposome experiments, the estimated value of P_t (i.e., the available concentration) was used rather than the input concentration of PI3P. Six replicates were used for cell binding measurements and four replicates for liposome binding experiments. Transformed data from individual replicates (rather than their average) were entered into LINEST to estimate the constants and their standard errors.

Confocal Laser Scanning Microscopy

Microscopy analysis was performed using a Zeiss LSM 510 laser-scanning microscope. For the root uptake assay, excitation of GFP was done at 488 nm with the argon laser tube current set to 5.9 Amp. Emission was captured using a 505-530 nm broad pass filter. Imaging of mCherry was done using a HeNe Laser with an excitation of 543 nm and captured through a 580-615 broad pass filter. The detector gain was between 540-640(GFP) or 430-550(mCherry) with an amplifier offset of 0. Calibrations of gain settings were performed with multiple control roots with a range of background fluorescence to avoid capturing background fluorescence. Images of airway epithelial cells were taken with identical settings. The detector gain was between 600-800 (GFP) or 430-550(mCherry) with an amplifier offset between −0.2 and 0. Calibrations of detector gain and amplifier offset settings were performed with multiple controls to distinguish the range of background fluorescence to avoid capturing background fluorescence. For microscopy involving FM4-64 dye, the FM4-64 was excited at 514 nm and GFP was excited at 488 nm using the multi-track feature. Emissions passed through a dichroic beamsplitter NFT 545 that reflected wavelengths below 545 nm into a 505-530 nm broad pass filter (the GFP signal) and passed all wavelengths above 545 nm into a > 650 nm filter (the FM4-64 signal; 740 nm emission). For microscopy involving mCherry fusion proteins, the mCherry was excited at 543nm and GFP was excited at 488 nm using the multi-track feature. Emissions passed through a dichroic beamsplitter NFT 545 that reflected wavelengths below 545 nm into a 505-530 nm broad pass filter (the GFP signal) and passed all wavelengths above 545 nm into a 580-615 nm broad pass filter (the mCherry signal; 610 nm emission). Both signals were simultaneously processed using the multi-track feature. All images are representative of at least 8 scans.

SUPPLEMENTAL REFERENCES

Boon, J.M., and Smith, B.D. (2002). Chemical control of phospholipid distribution across bilayer membranes. Med. Res. Rev. *22*, 251–281.

Chang, M., Chou, J.C., and Lee, H.J. (2005). Cellular internalization of fluorescent proteins via arginine-rich intracellular delivery peptide in plant cells. Plant Cell Physiol. *46*, 482–488.

Dou, D., Kale, S.D., Wang, X., Jiang, R.H.Y., Bruce, N.A., Arredondo, F.D., Zhang, X., and Tyler, B.M. (2008). RXLR-mediated entry of *Phytophthora sojae* effector Avr1b into soybean cells does not require pathogen-encoded machinery. Plant Cell *20*, 1930–1947.

Quinn, P.J. (2002). Plasma membrane phospholipid asymmetry. In Subcellular Biochemistry, P.J. Quinn and V.E. Kagan, eds. (London: Kluwer Academic/ Plenum Publishers), pp. 39–60.

Sreerama, N., and Woody, R.W. (2004). Computation and analysis of protein circular dichroism spectra. Methods Enzymol. *383*, 318–351.

Whitmore, L., and Wallace, B.A. (2004). DICHROWEB, an online server for protein secondary structure analyses from circular dichroism spectroscopic data. Nucleic Acids Res. *32*, 668–673.

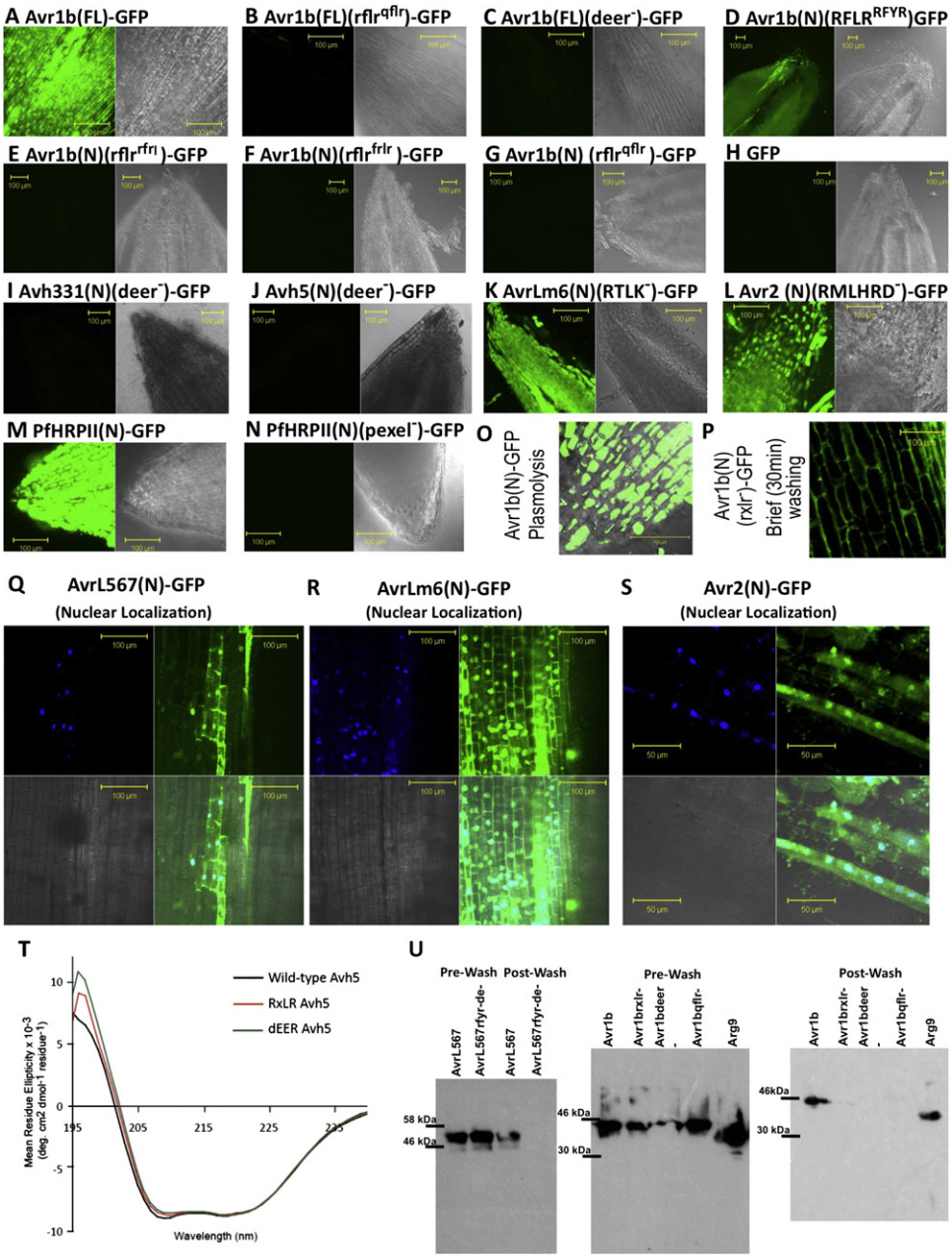

Figure S1. Plant Cell Entry by Oomycete, Fungal, and *Plasmodium* Effector Protein Fusions and Their Mutants, Related to Figure 1

(A–S) Root cell entry by fusion proteins. Fusion protein sequences are shown in Figure 7. Protein (1 mg/mL) was incubated with roots for 12 hr, then the roots were washed for 2 hr, except where indicated. Paired light micrographs and fluorescence optical sections are from the same root tips in each case. Fluorescent micrographs were taken with the same photographic exposure in every case. In (Q)–(S), roots were also stained with DAPI to unambiguously locate the nuclei; DAPI images (upper left panel), GFP images (upper right), light micrographs (lower left) were overlaid together in the bottom right panel.

(A) Avr1b(FL)-GFP.

(B) Avr1b(FL)-GFP qflr⁻ nonfunctional mutant.

(C) Avr1b(FL)-GFP deer⁻ partially functional mutant.

(D) Avr1b(N)-GFP functional RFLR mutant (RFYR).

(E) Avr1b(N)-GFP nonfunctional rflr⁻ mutant (rfrl).

(F) Avr1b(N)-GFP nonfunctional rflr⁻ mutant (frlr).

(G) Avr1b(N)-GFP nonfunctional rflr⁻ mutant (qflr).

(H) GFP alone with no fusion sequences.

(I) Avh331(N)-GFP nonfunctional deer- mutant.

(J) Avh5(N)-GFP nonfunctional deer- mutant.

(K) AvrLm6(N)-GFP RTLK$^-$ functional mutant.
(L) Avr2(N)-GFP RMLHRD$^-$ functional mutant.
(M) Plasmodium effector PfHRPII(N)-GFP.
(N) Plasmodium effector PfHRPII(N)-GFP pexel$^-$ nonfunctional mutant.
(O) Avr1b(N)-GFP; photographs taken 30 min after plasmolysis of the roots with 4 M NaCl for 30 min following washing.
(P) Avr1b(N)-GFP nonfunctional rxlr- mutant; photographed after brief (30 min) washing.
(Q) AvrL567(N)-GFP, DAPI costaining.
(R) AvrLm6(N)-GFP, DAPI costaining.
(S) Avr2(N)-GFP, DAPI costaining.
(T) Circular dichroism spectroscopy shows structure of Avh5 protein is unaffected by RXLR and dEER mutations. Spectra were collected using a Jasco J-720 spectropolarimeter. Far-UV circular dichroism spectra were measured for Avh5 proteins (20 μM in 10mM Tris-HCl, pH 5.8, 100 mM NaCl, 100 μM DTT) using a 1mm-slit-width cuvette. Five accumulated scans were recorded for each sample from 240 to 195 nm at 20°C using a bandwidth of 1-nm and a response time of 1 s at a scan speed of 20 nm/min. The background of the buffer alone was subtracted from each spectrum. Raw data were converted to mean residue ellipticity and analyzed for secondary structure composition using DICHROWEB (Whitmore and Wallace, 2004) and deconvoluted using CDSSTR (Sreerama and Woody, 2004). Detailed deconvolution data are shown in Table S2.
(U) Stability of RXLR mutant fusion proteins in soybean roots. Root tips were incubated with effector-GFP protein for approximately 12 hr. "Prewash" samples were quickly rinsed, ground, and resuspended in loading buffer and boiled for 5 min. "Post-wash" samples were washed in a manner identical to roots used for microscopy and then prepared as described above. Proteins were electrophoresed, transferred to nitrocellulose and then probed with anti-GFP antibodies. Left panel: prewash and post-wash samples of AvrL567(N)-GFP and mutant; center panel: prewash samples of Avr1b(N)-GFP and mutant proteins and Arg9-GFP; right panel: post-wash samples of Avr1b(N)-GFP and mutant proteins and Arg9-GFP.

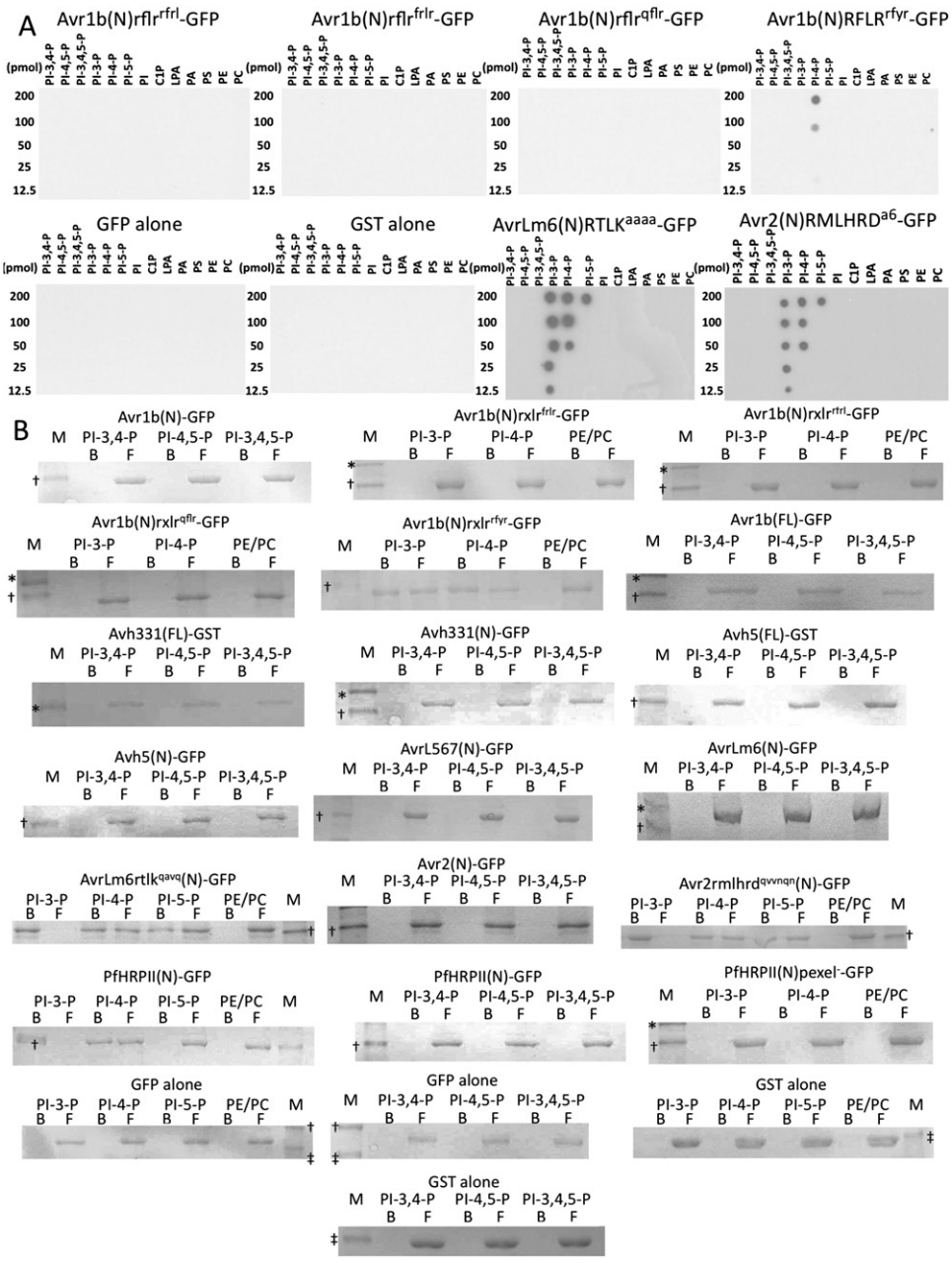

Figure S2. Binding of Oomycete, Fungal, and *Plasmodium* Effector Proteins to Phosphoinositides, Related to Figure 2

Filter-binding assays (A) and liposome-binding assays (B) of the binding of wild-type and mutant effector cell entry domains and control proteins to phospholipids. All mutations are summarized in Figure 7. (N)-GFP and (FL)-GFP indicate a fusion of the N-terminal domain of an effector or the full-length protein, respectively, to the N-terminus of GFP. GST-XXX(FL) indicates a fusion of a full-length effector protein (without signal peptide) to the C terminus of GST. PI-3,4-P = phosphatidylinositol-3,4-bisphosphate; PI-4,5-P = phosphatidylinositol-4,5-bisphosphate; PI-3,4,5-P = phosphatidylinositol-3,4,5-triphosphate; PI-3-P = phosphatidylinositol-3-phosphate; PI4P = phosphatidylinositol-4-phosphate; PI5P = phosphatidylinositol-5-phosphate; PI = phosphatidylinositol; C1P = ceramide-1-phosphate; LPA = lysophosphatidic acid; PA = phosphatidic acid; PS = phosphatidylserine; PE = phosphatidylethanolamine; PC = phosphatidylcholine. In the liposome binding assays (B), all liposomes contained PC and PE; lanes marked PE/PC lacked any other phospholipids; "B" and "F" indicate liposome-bound and -free proteins, respectively; "M" = size markers.

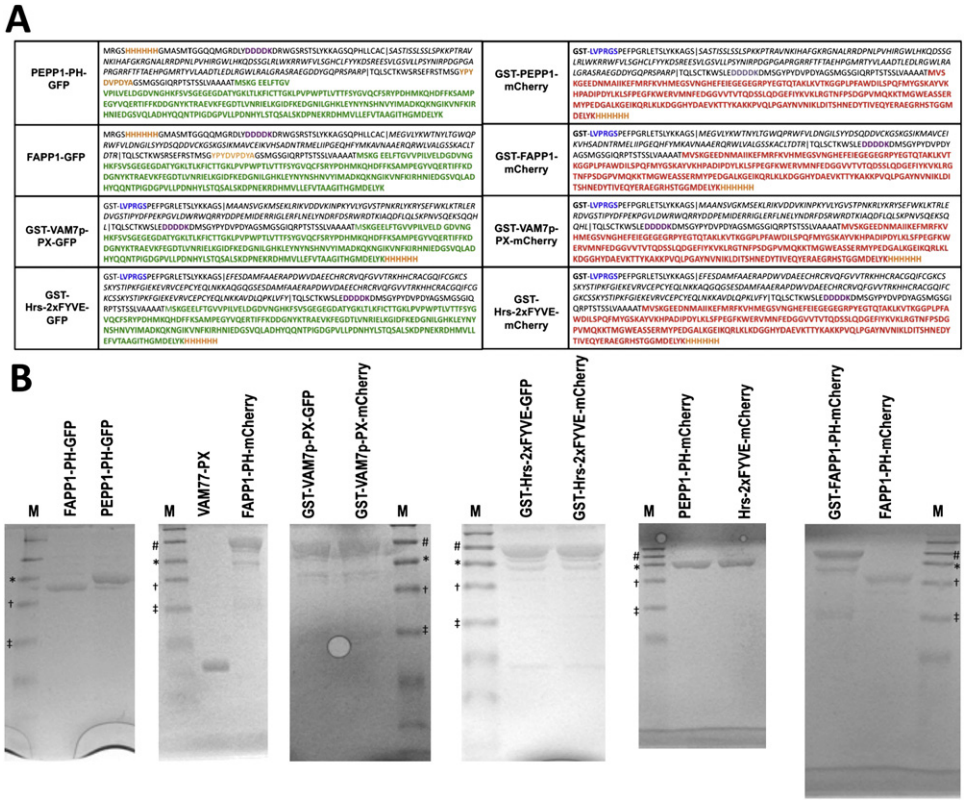

Figure S3. Sequence and Purity of Biosensor Proteins, Related to Figure 3

(A) Sequences of biosensor proteins. PI-P binding protein sequences are in italics, bounded by pipes ("|"). His tags are in orange; enterokinase cleavage sites are in purple; thrombin cleavage sites are in blue; haemaglutinin tags are in light brown; GFP is in green; mCherry is in red; all other unhighlighted sequences are linker sequences that span attB recombination sites. GST indicates N-terminal glutathione S-transferase fusion. Further details of vector construction and utilization are given in Table S4.

(B) Purity of biosensor protein preparations. The indicated fusion proteins were recovered from Ni-NTA columns, electrophoresed on SDS-polyacrylamide gels, then stained with Coomassie Brilliant Blue. M = size markers: # 80 kDa; *58 kDa marker; †46 kDa marker; ‡ 30kDa marker.

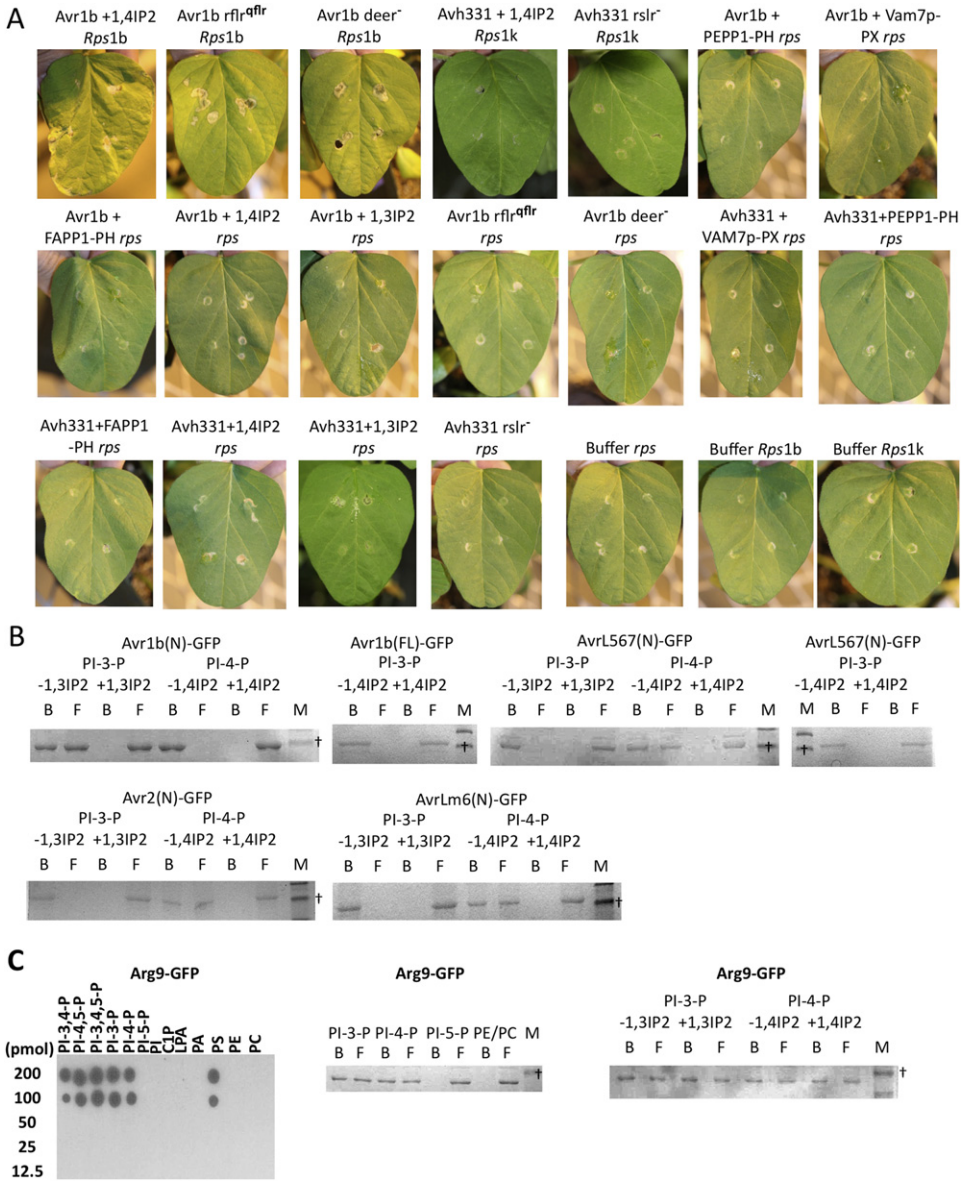

Figure S4. Inhibition of Effector Entry into Soybean Leaf Cells by RXLR and dEER Mutations, by PI-3-P-Binding Proteins and by Inositol Diphosphates, Related to Figure 4

(A) Entry of effectors into soybean leaf cells assayed by programmed cell death triggered by Avr1b and Avh331 in the presence of cognate resistance genes. Buffer or 0.25 mg/mL of each effector protein, lacking N-terminal or C-terminal fusions, were infiltrated into the primary unifoliate leaves of approximately 13 day old seedlings of cultivars with no Rps gene (*rps*; cultivar Williams), with *Rps*1b (cultivar L77-1863) or with *Rps*1k (Williams 82). Where indicated, the effector protein was coinfiltrated with 500 μM 1,3IP2 or 1,4IP2, or with 1.0 mg/ml of the indicated biosensor protein. VAM7p-PX, PEPP1-PH, FAPP1-PH and Hrs-2xFYVE biosensors were all added as mCherry fusions. Mutant effectors were as described in Figure 7. The plant leaves were photographed 5 days after infiltration.

(B) Inhibition of effector phosphoinositide-binding by inositol diphosphates, measured by liposome binding.

Binding of indicated effector-GFP fusion to liposomes containing PI-3-P or PI-4-P was measured in the presence or absence of 300 μM inositol 1,3 diphosphate (1,3IP2) or 1,4 diphosphate (1,4IP2) as described in Figure 2 and the Experimental Procedures. "B" and "F" indicate liposome-bound and -free proteins, respectively; "M" = size markers.

(C) Phospholipid-binding enabled by the synthetic cell entry motif, Arg9. Filter-binding assay (left panel) and liposome-binding assay (right panel) of the phospholipid binding specificity of the synthetic cell entry peptide, Arg9, fused to the N-terminus of GFP (sequence shown in Figure 6). Results for GFP and GST alone (no fusions) are shown in bottom of Figure S2B. PI-3,4-P = phosphatidylinositol-3,4-bisphosphate; PI-4,5-P = phosphatidylinositol-4,5-bisphosphate; PI-3,4,5-P = phosphatidylinositol-3,4,5-triphosphate; PI-3-P = phosphatidylinositol-3-phosphate; PI4P = phosphatidylinositol-4-phosphate; PI5P = phosphatidylinositol-5-phosphate; PI = phosphatidylinositol; C1P = ceramide-1-phosphate; LPA = lysophosphatidic acid; PA = phosphatidic acid; PS = phosphatidylserine; PE = phosphatidylethanolamine; PC = phosphatidylcholine. In the liposome binding assay (right panel), "B" and "F" indicate liposome-bound and -free proteins, respectively; "M" = size markers.

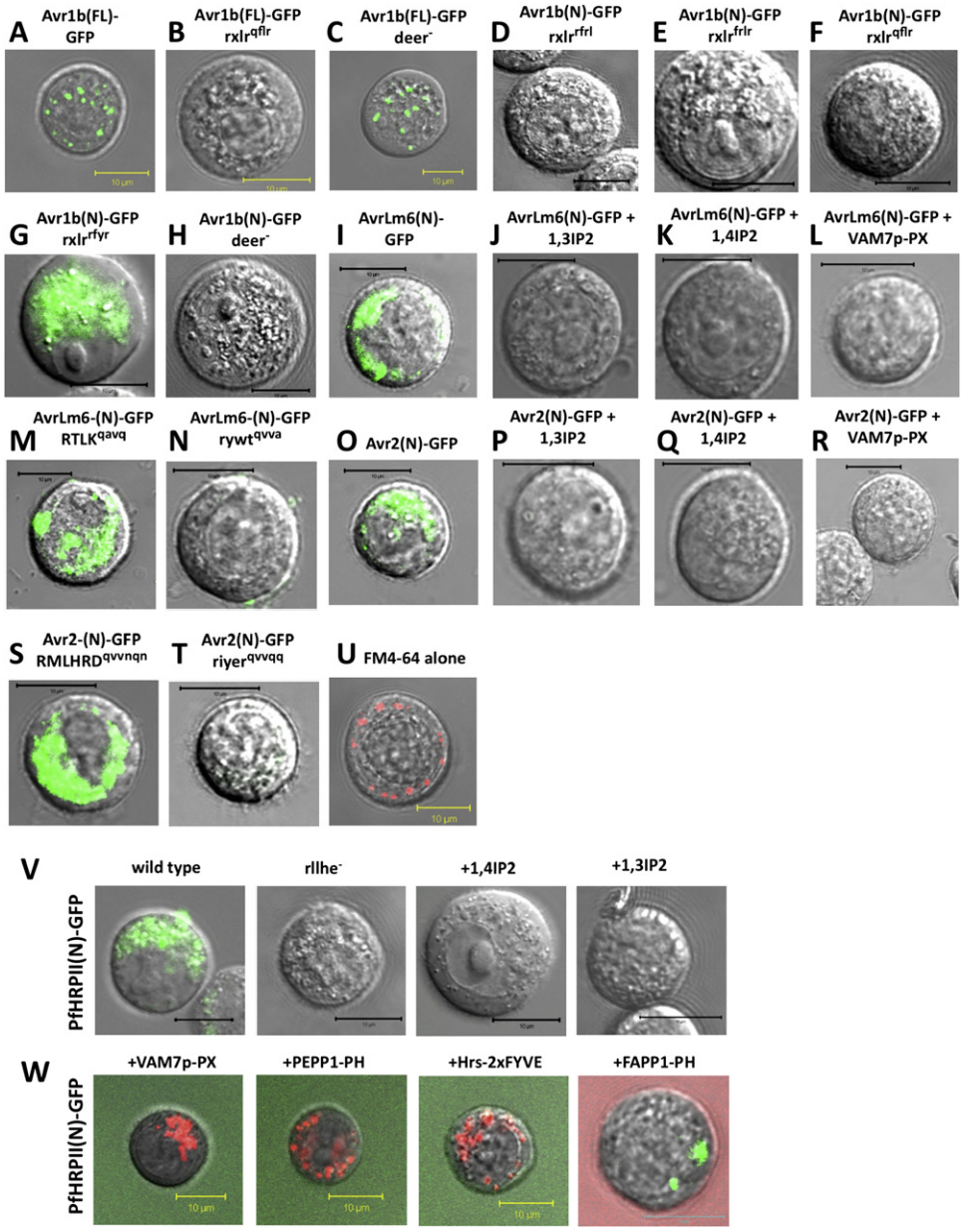

Figure S5. Entry of Effector-GFP Fusions and Their Mutants into A549 Cells, and Inhibition of Entry by PI3P-Binding Proteins and Inositol Diphosphates, Related to Figure 5

Human A549 cells were incubated with the indicated biosensors, effector-GFP fusion proteins or their mutants (described in Figure 7), in the presence or absence of 500 μM inositol 1,3 diphosphate (+1,3IP2), 520 μM inositol 1,4 diphosphate (+1,4IP2), as indicated below. Cells were then washed either twice (A-V) or once (W) and photographed. (N) = N-terminal domain; (FL) = full-length domain. Light micrographs are shown overlaid with fluorescence optical sections (both red and green channels in (W). Lighting and photographic exposure were identical for all photographs. Scale bars in every case represent 10 μm. In (W), traces of the nonentering proteins can be observed in the background.

(A–K, M–Q, S, T, and V) 100 μg/ml effector. 8 hr 37°C.

(U) 100 μg/ml effector. 5 μM FM4-64. 2.5 min 37°C.

(L, R, and W) 25 μg/ml effector, 100 μg/ml biosensor (L, R: VAM7p-PX alone; (W): mCherry fusion in each case). 8 hr 37°C.

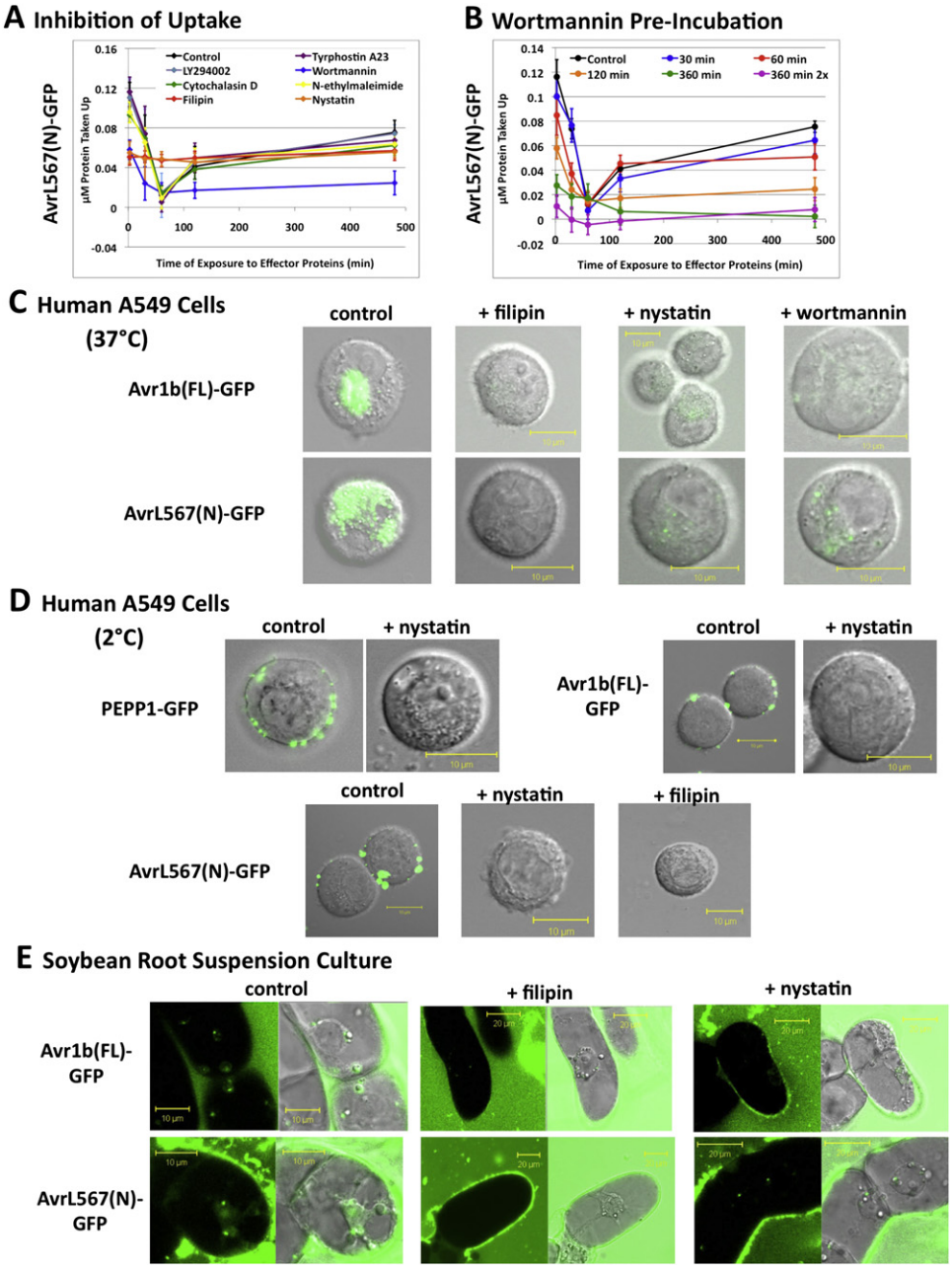

Figure S6. Mechanism of Binding and Entry of Effector Proteins into Host Cells, Related to Figure 6

(A) Inhibition of AvrL567(N)-GFP accumulation at 37°C by endocytosis inhibitors. Inhibitors were added 2 hr before the proteins. Concentrations are given in the Experimental Procedures. Error bars in (A) and (B) indicate standard errors from six replicates.

(B) Inhibition of AvrL567(N)-GFP accumulation at 37°C by preincubation with wortmannin for different times. 360 min 2× indicates two Wortmannin additions (at 0 min and 180 min).

(C) Inhibition of entry of Avr1b(FL)-GFP and AvrL567(N)-GFP into A549 cells at 37°C by filipin (50 μg/mL), nystatin (50 μg/mL) and wortmannin (1 μM). Cells were treated with each inhibitor for 2 hr, then protein (0.1 mg/mL final concentration) was added for 2.5 min before the cells were washed twice and photographed. Light micrographs are overlaid with fluorescent images. Scale bars represent 10 μM in each case.

(D) Elimination of effector and biosensor binding sites on A549 cells by incubation with filipin or nystatin (50 μg/mL each) for 2 hr at 37°C. Then binding was carried out at 2°C for 2 hr before the cells were washed briefly and photographed. Light micrographs are overlaid with fluorescent images. Scale bars represent 10 μM in each case.

(E) Entry of Avr1b(FL)-GFP and AvrL567(N)-GFP into soybean root suspension cultures and inhibition by filipin and nystatin (50 μg/mL each). Cells were exposed to the protein (1.0 mg/mL) for 8 hr at 25°C, then photographed without washing. Note labeling of vesicles in the absence of filipin. Nystatin only partially inhibited entry. Fluorescent images are shown alone (left panel) or laid over light micrograph (right panel). Scale bars represent 20 μM in each case.

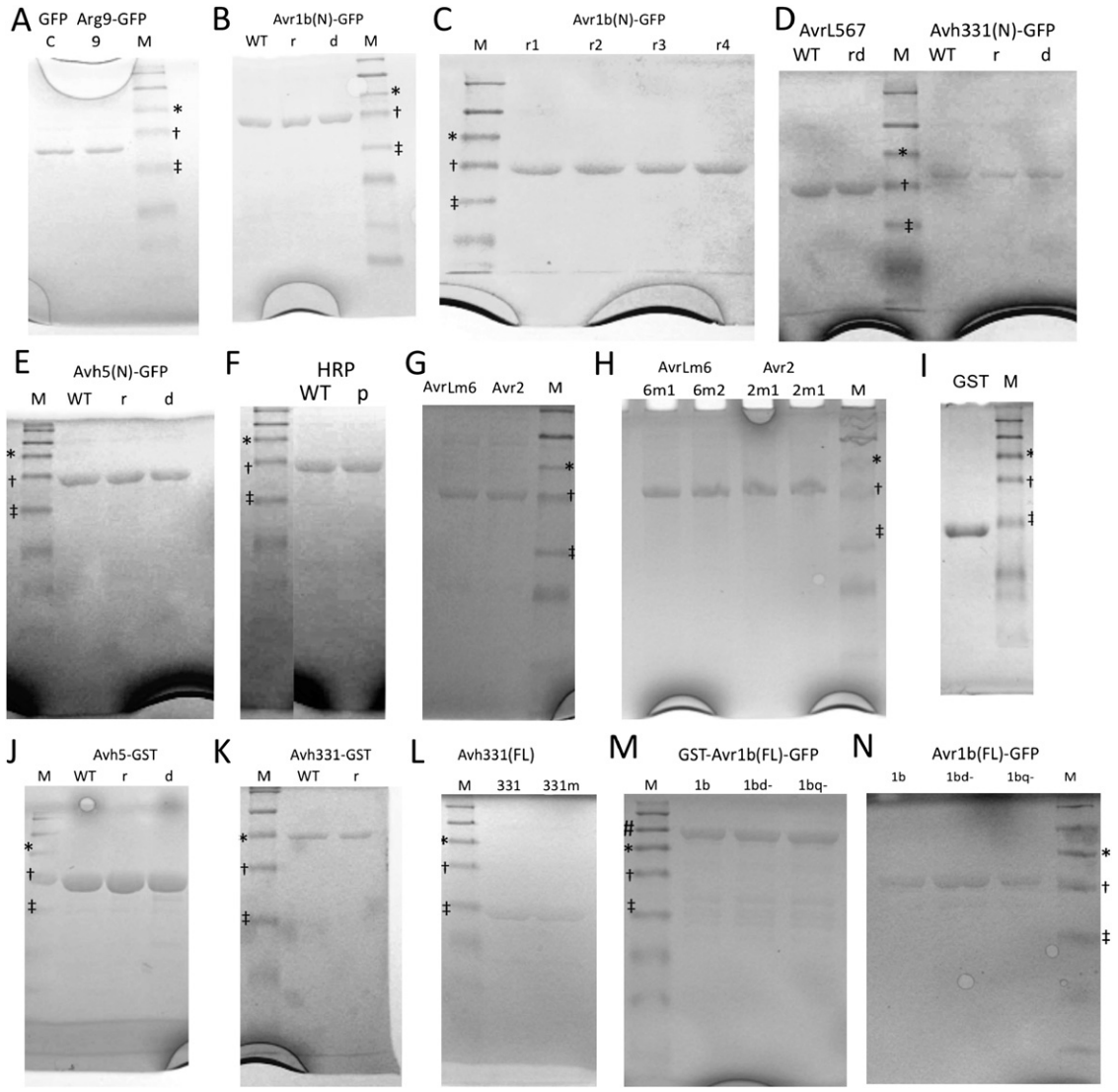

Figure S7. Purity of Effector Fusion Proteins Assessed by Gel Electrophoresis, Related to Figure 7

M- Marker, *58 kDa marker. †46 kDa marker. ‡ 30kDa marker.

(A) C = control GFP alone (no fusion), 9 = Arg9-GFP fusion protein.

(B) Avr1b(N)-GFP = N-terminal region of Avr1b fused to the N-terminus of GFP.

(C) Avr1b(N)-GFP proteins with mutations in the RXLR2 motif, RFLR: r1 = frlr; r2 = rfrl; r3 = qflr; r4 = RFYR.

(D) AvrL567(N)-GFP, Avh331(N)-GFP = N-terminal regions of AvrL567 or Avh331, respectively, fused to the N-terminus of GFP.

(E) Avh5(N)-GFP = N-terminal region of Avh5 fused to the N-terminus of GFP.

(F) GBP, HRP, 1615c = N-terminal regions of PfGBP, PfHRPII or Pf1615c, respectively, fused to the N-terminus of GFP.

(G) Lm6(N)-GFP, Avr2(N)-GFP = N-terminal regions of AvrLm6 or Avr2, respectively, fused to the N-terminus of GFP.

(H) AvrLm6(N)-GFP and Avr2(N)-GFP proteins with mutations in RXLR-like motifs: 6m1 = AvrLm6 RTLK to qavq; 6m2 = AvrLm6 rywt to qvva; 2m1 = Avr2 RMLHRD to qvvnqn; 2m2 = Avr2 riyer to qvvqq.

(I) GST = glutathione S-transferase with no fusion.

(J) Avh5-GST = Full-length mature Avh5 fused to the C terminus of GST.

(K) Avh331-GST Full-length mature Avh331 fused to the C terminus of GST.

(L) Full-length Avh331 with GST fusion removed from N-terminus: 331 = wild-type; 331 m = mutation of rslr to aaaa.

(M) GST-Avr1b(FL)-GFP - double fusion of full-length Avr1b with GST at the N-terminus and GFP at the C terminus: 1b = wild-type; 1bd- = replacement of dEER motif with alanine substitutions; 1bq- = mutation of rflr to qflr.

(N) Avr1b(FL)-GFP. Same proteins as (M) after removal of GST.

Encoded protein*	*Rps*1k†		*rps*†		p value¶	Rps1k interaction
	Survival‡	s.e.§	Survival‡	s.e.§		
sAvh331	0.16	0.013	0.96	0.03	< 0.001	yes
sAvh331 rxlr-	1.07	0.0006	0.97	0.035	> 0.1	no
sAvh331 deer-	1.00	0.05	0.94	0.04	> 0.1	no
mAvh331	0.44	0.09	1.21	0.21	< 0.001	yes
mAvh331 rxlr-	0.15	0.015	0.97	0.05	< 0.001	yes
mAvh331 deer-	0.14	0.02	1.06	0.03	< 0.001	yes

Table S1. Re-entry of Avh331 into soybean leaf cells requires the RXLR and dEER motifs.

This Table is associated with Figures 1 and 4.

* DNA encoding the indicated protein (see Figure 6) was mixed with DNA encoding beta-glucuronidase (GUS) prior to bombardment

† Soybean primary unifoliate leaves containing resistance gene *Rps*1k (cultivar HARO15) or not (*rps*; cultivar HARO(1-7)1 were bombarded.

‡ Using the double-barrel gene gun, each bombardment was accompanied by a control bombardment containing empty vector DNA and DNA encoding GUS. For each pair of bombardments, the ratio of the number of blue GUS-positive tissue patches produce by Avh331 compared to the control was calculated. Numbers shown are the geometric average of 13 to 15 bombardments.

§ Standard error of the survival, calculated from the log-ratios.

¶ Survival following bombardment was compared between the *Rps*1k soybean line and the near-isogenic non-Rps1k line, using the Wilcoxon rank sum test. A significant difference ($p < 0.001$) indicates an interaction between the Avh331 protein and the Rps1k gene product. The results show that the RXLR and dEER motifs of Avh331 are required for an interaction with the Rps1k gene product only when the protein contains a secretory leader.

Avh5	αR	αD	βR	βD	Turns	Unordered	# Valid solutions	NRMSD
WT	7	17	15	9	26	26	83	0.033
RXLR mutant	6	14	16	9	25	30	83	0.045
dEER mutant	7	14	17	10	24	29	102	0.040

Table S2. Prediction of secondary structure composition of Avh5 and its mutants (associated with Figure 1).

All secondary structural elements content are in %. R and D represent predicted regular and distorted secondary structure elements, respectively. NRMSD is the normalized root mean square difference of the experimental and calculated spectra. Predictions were generated using DICHROWEB and deconvoluted using CDSSTR. Spectra were collected using a Jasco J-720 spectropolarimeter. Far-UV circular dichroism spectra were measured for Avh5 constructs (20μM in 10mM Tris-HCl, pH 5.8, 100 mM NaCl, 100 μM DTT) using a 1 mm-slit-width cuvette. Five accumulated scans were recorded for each sample from 240 to 195 nm at 20°C using a bandwidth of 1-nm and a response time of 1 s at a scan speed of 20 nm/min. The background of the buffer alone was subtracted from each spectrum. Raw data were converted to mean residue ellipticity and analyzed for secondary structure composition using DICHROWEB (Whitmore and Wallace, 2004) and deconvoluted using CDSSTR (Sreerama and Woody, 2004).

Table S3. Primers used for clone construction, related to extended experimental procedures

Restriction sites are shown in bold. Mutations created by the primers are in lower case. Primers used by Dou et al. (2008) are marked with an asterisk (*).

Primer Name	Function	Sequence (5' to 3')
LinkerR2	Recreates the linker region between GFP and Arg9 for RXLR regions for all GFP expression constructs. NcoI	GCATC**CCATGG**AGCCAGCATAGTCTGGGACGT CATATGGATAGCCGGACATGG
Avr1bGFPF	Forward primer for Avr1b RXLR Region. BglII site for cloning into GFP expression vector	GATCT**AGATCT**GTGGAATCTCCAGATCTC
Avr1bGFPR1	Reverse primer for Avr1b RXLR region. Adds nucleotides to facilitate space between GFP and RXLR	GTCATATGGATAGCCGGACATGTCAGTCACGC TGAAGGT
Avr1bGFPR2	Reverse primer for Avr1b RXLR region. Adds remaining nucleotides to facilitate space between GFP and RXLR and NcoI cloning site.	GATC**CCATGG**AGCCAGCATAGTCTGGGACGTC ATATGGATAGCCGGA
cGFPF	Forward primer to add BglII site between the Arg9 sequence and the linker	ATGC**AGATCT**GAATTCAGATCCACCATGTCGG C
cGFPR	Reverse primer for control GFP	GCAT**CTCGAG**ACTGCAGGCTCTAGAGGCTCAC TTG
Avh331-GFPExp-BglII	Forward primer for Avh331 RXLR Region. BglII site for cloning into GFP expression vector	ATGC**AGATCT**CTCACTTGCGCCACCTCCGAGC
Avh331R2	Reverse primer for Avh331 RXLR region. Adds nucleotides to facilitate space between GFP and RXLR	CATATGGATAGCCGGACATGGTGGATCTGTCG ACTCTGTTTTCAATCG
Avh331dEERR2	Reverse primer for Avh331 RXLR region dEER mutant. Adds nucleotides to facilitate space between GFP and RXLR	CATATGGATAGCCGGACATGGTGGATCTGTCG ACTGCGTTTGCAAT
Avh5-GFPExp-BglII	Forward primer for Avh5 RXLR Region. BglII site for cloning into GFP expression vector	AGTC**AGATCT**ACAAGAGTCCCCGACGA
Avh5R2	Reverse primer for Avh5 RXLR region. Adds nucleotides to facilitate space between GFP and RXLR	CATATGGATAGCCGGACATGGTGGATCTGTCG ACTTGCCAGGATTATG
AvrL-GFPExp-BglII	Forward primer for AvrL567 RXLR Region. BglII site for cloning into GFP expression vector	ATCG**AGATCT**ATGGGAATGGAACATG
AvrLRevMod1	Reverse primer for AvrL567 RXLR region. Adds nucleotides to facilitate space between GFP and RXLR	GATAGCCGGACATGGTGGATCTGTCGACCCAC AGGTCAGTCACGC
AvrLRevMod2	Adds remaining nucelotides for linker sequence between GFP Expression vector and RXLR region	TC**CCATGG**AGCCAGCATAGTCTGGGACGTCAT ATGGATAGCCGGACATGGTGGATCT
PfHRPIIR2	Reverse primer for PfHRPII RXLR region. Adds nucleotides to facilitate space between GFP and RXLR	CATATGGATAGCCGGACATGGTGGATCTGTCG ACATCTGCAACATGG
PfHRPIIm-GFPExp-F1	Forward primer 1 for PfGBP RXLR Region. RLLHE to AAAAA	GGCTTGAACCTCAACAAGgcagcagcagcagcaACA CAAGCACATG
PfHRPIIm-GFPExp-F2	Forward primer 2 for PfGBP RXLR Region. RLLHE to AAAAA	GTAGTAAGAATGCTAAAGGCTTGAACCTCAAC AAG
PfHRPIIm-GFPExp-F3	Forward primer 3 for PfGBP RXLR Region. RLLHE to AAAAA	ATGC**AGATCT**TTTAACAATAACCTGTGTAGTAA GAATGCTAAAGGC
Avh331F-GST-BamHI	Forward primer for mature Avh331. BamHI site for cloning into PGEX4T1 vector	GCGT**GGATCC**CTCACTTGCGCCACCTCCG
Avh331R-GST-SalI	Reverse primer for mature Avh331. SalI site for cloning into PGEX4T1 vector	TCGA**GTCGAC**TCAGATAATCATGATGCTGT
Avh5F-GST-BamHI	Forward primer for mature Avh5. BamHI site for cloning into PGEX4T1 vector	GCGT**GGATCC**ACAAGAGTCCCCGACGA
Avh5R-GST-SalI	Reverse primer for mature Avh5. SalI site for cloning into PGEX4T1 vector	TCGA**GTCGAC**TCACTTGGCCTCTTGCGAT
Avh331F2-RXLR	Forward primer for producing RXLR mutation in Avh331. RSLR to AAAA	CAgcggcggcggcgTCTCAAGCTACGAACG
Avh331R2-RXLR	Reverse primer for producing RXLR mutation in Avh331. RSLR to AAAA	GTTCGTAGCTTGAGAcgccgccgccgcTGTCGAG
Avh331F2-dEER	Forward primer for producing dEER mutation in Avh331. DDDANVSIENR to AAAANVSIANA	GGCTAACGTTTCGATTgcgAACgcgGGATGAACC CTTCAG
Avh331R2-dEER	Reverse primer for producing dEER mutation in Avh331. DDDANVSIENR to AAAANVSIANA	GTTCGTAGCTTGAGAcgccgccgccgcTGTCGAG

Avh331F-NcoI	Forward primer for mature Avh331. NcoI site for cloning into transient assay vector with Avr1b signal peptide	GCGT**CCATGG**GAGCTCACTTGCGCCACCTCCG
Avh331F-XmaI	Forward primer for mature Avh331. XmaI site for cloning into transient assay vector without Avr1b signal peptide	agat**cccggg**gggcaatgagatatgCTCACTTGCGCCACCTCC
Avh331R-KpnI	Reverse primer for mature Avh331. KpnI site for cloning into transient assay vector	TCGA**GGTACC**TCAGATAATCATGATGCTGT
mAvrL567F	Forward primer for AvrL567 RXLR region. XmaI site for cloning into transient assay vector without Avr1b signal	agat**cccggg**gggcaatgagatATGATGGAACATGTACCAGCAG
AvrL567-F4	Forward primer for AvrL567 RXLR region	ACCAGAGTCAGCGAAGGGTATACACGATTTTACCGGTCCCCAACGGCTAGTGTAATAC
AvrL567-F3	Forward primer for AvrL567 RXLR region	CAACGGCTAGTGTAATACTGTCAGGATTGGTAAAGGTTAAATGGGATAATGAACAAATG
AvrL567-F2	Forward primer for AvrL567 RXLR region.	ACCAGAGTCAGCGAAGGGTATACACGATTTTACCGGTCCCCAACGGCTAGTGTAATAC
AvrL567-F1	Forward primer for AvrL567 RXLR region. NcoI site for cloning into transient assay vector with Avr1b signal peptide	atcg**ccatgg**gaATGGAACATGTACCAGCAGAGTTGACCAGAGTCAGCGAAGGG
AvrL567MR	Reverse primer for AvrL567 mutation. RFYR-DxE to AAAA-AxA	TCCTGACAGTATTACACTAGCCGTTGGGGAcgcagcggctgcTGTATACCCTTCGCTG
AvrL567MF	Forward primer for AvrL567 mutation. RFYR-DxE to AAAA-AxA	GTGTAATACTGTCAGGATTGGTAAAGGTTAAATGGgctAATgcaCAAATGACGATGCCG
Avr1b-KpnI †	Reverse Primer for Avr1b in the transient assay vector	AGAAA**CTCGAG**CTTGTCGATCGACAGATCCGGTCGGCAggTACcTCAGCTCTGATAC
Avr1bFull-F †	Forward primer for Avr1b with signal peptide. XmaI site	atcgcactcgagctttcgcagat**cccggg**gggcaatgagatATGCGTCTATCTTTTGTG
AvrPitaF	Forward primer for fusing N-terminus of AvrPita wild type on to Avr1b	ATCG**CCATGG**GACACCCAGTTTACGATTACAATC
AvrPitaF2mid	Forward primer for fusing N-terminus of AvrPita wild type on to Avr1b	CACGCCGTTAAAAATGACAATCGGTTATTTAGATTAATCTTTAAAACTGACAGCACAG
AvrPitaF1mid	Forward primer for fusing N-terminus of AvrPita wild type on to Avr1b	CTTTAAAACTGACAGCACAGATATTCAAAACACCTTCAGCGTGACTGACCTG
AvrPitaR1	Reverse primer for fusing N-terminus of AvrPita wild type on to Avr1b	CCACGAGGCGAGCTCGGCACAACTTTTTAGCGCGGCACGAATTTC
AvrPitaR2	Reverse primer for fusing N-terminus of AvrPita wild type on to Avr1b	CCGATTGTCATTTTTAACGGCGTGATAGCCCCACGAGGCGAGCTCGGCAC
AvrM-F3	Forward primer for fusing N-terminus of AvrM wild type on to Avr1b	ATCG**CCATGG**GAAACAACCTTGGAACAGTACCGGATGTGCCACATC
AvrM-F2	Forward primer for fusing N-terminus of AvrM wild type on to Avr1b	CAGTACCGGATGTGCCACATCAAATTCCAAATGACAAAAGTGGTACTCCTGCCATTG
AvrM-F1	Forward primer for fusing N-terminus of AvrM wild type on to Avr1b	CAAAAGTGGTACTCCTGCCATTGAAGACCCAAAAGATATGAAAGGATTCAATAAGGCTC
AvrM-R	Reverse Prmer for fusing N-terminus of AvrM wild type on to Avr1b	CCACAGGTCAGTCACGCTGAAGGTTCGTACATTTTTATCTTTTTCTGCCATGTATG
AvrM-Fmid	Forward primer for fusing N-terminus of AvrM wild type on to Avr1b	GAACCTTCAGCGTGACTGACCTGTGG
Lm6bmF	Forward primer for fusing N-terminus of AvrLm6 wild type and mutants on to Avr1b no signal peptide	agat**cccggg**gggcaataagatatgCAGCCACATCTGCTGTGTGCTTGT
Lm6bsF	Forward primer for fusing N-terminus of AvrLm6 wild type and mutants on to Avr1b signal peptide	atcg**ccatgg**gaCAGCCACATCTGCTGTGTGCTTGT
Lm6midF	Forward primer for fusing N-terminus of AvrLm6 wild type and mutants on to Avr1b	GCTGAAGGTGCTCCACATGAAGGGACCTTCAGCGTGACTGACCTGTGG
Lm6midR	Reverse primer for fusing N-terminus of AvrLm6 wild type and mutants on to Avr1b	CCACAGGTCAGTCACGCTGAAGGTCCCTTCATGTGGAGCACCTTCAGC
Avr2bmF	Forward primer for fusing N-terminus of Avr2 wild type and m1, m2 mutants on to Avr1b no signal peptide	agat**cccggg**gggcaataagatatgCTGCCAGTTGAAGATGCTGATTCT
Avr2bsF	Forward primer for fusing N-terminus of Avr2 wild type and m1, m2 mutants on to Avr1b signal peptide	atcg**ccatgg**gaCTGCCAGTTGAAGATGCTGATTCT
Avr2midF	Forward primer for fusing N-terminus of Avr2 wild type and m1 mutant on to Avr1b	CATCGTATTTATGAACGTTCTCGTACCTTCAGCGTGACTGACCTGTGG
Avr2midR	Reverse primer for fusing N-terminus of Avr2 wild type and m1 mutant on to Avr1b	CCACAGGTCAGTCACGCTGAAGGTACGAGAACGTTCATAAATACGATG
Avr2mmF	Forward primer for fusing N-terminus of Avr2 m2 mutant on to Avr1b	CAGGTGGTGCAGCAGTCTCGTACCTTCAGCGTGACTGACCTGTGG
Avr2mmR	Reverse primer for fusing N-terminus of Avr2 m2mutant on to Avr1b	CCACAGGTCAGTCACGCTGAAGGTACGAGACTGCTGCACCACCTG

Avr1b(KFLR)F †	Forward primer for replacing RFLR motif of Avr1b with KFLR. NgoMIV	CATT**GCCGGc**GGAAagTTTCTTC
Avr1b(HFLR)F	Forward primer for replacing RFLR motif of Avr1b with HFLR. NgoMIV	CGACATT**GCCGGC**GGAcacTTTCTTCGAGCTCA TGAAGAGGACGATG
Avr1b(QFLR)F †	Forward primer for replacing RFLR motif of Avr1b with QFLR. NgoMIV	CATT**GCCGGc**GGAcaATTTC
Avr1b(RFFR)F	Forward primer for replacing RFLR motif of Avr1b with RFFR. NgoMIV	CGACATT**GCCGGC**GGAAGATTTtTTCGAGCTCA TGAAGAGGACGATG
Avr1b(RFYR)F	Forward primer for replacing RFLR motif of Avr1b with RFYR. NgoMIV	CGACATT**GCCGGC**GGAAGATTTtaTCGAGCTCA TGAAGAGGACGATG
Avr1b(RFIR)F	Forward primer for replacing RFLR motif of Avr1b with RFIR. NgoMIV	CGACATT**GCCGGC**GGAAGATTTaTTCGAGCTC ATGAAGAGGACGATG
Avr1b(RFMR)F	Forward primer for replacing RFLR motif of Avr1b with RFMR. NgoMIV	CGACATT**GCCGGC**GGAAGATTTaTgCGAGCTC ATGAAGAGGACGATG
Avr1b(RFVR)F †	Forward primer for replacing RFLR motif of Avr1b with RFVR. NgoMIV	CATT**GCCGGc**GGAAGATTTgTTC
Avr1b(RFAR)F †	Forward primer for replacing RFLR motif of Avr1b with RFAR. NgoMIV	CATT**GCCGGc**GGAAGATTTgcTCG
Avr1b(RFLQ)F †	Forward primer for replacing RFLR motif of Avr1b with RFLQ. NgoMIV	CATT**GCCGGc**GGAAGATTTCTTCaAGC
Avr1b(RFLG)F	Forward primer for replacing RFLR motif of Avr1b with RFLG. NgoMIV	CGACATT**GCCGGC**GGAAGATTTCTTgGAGCTC ATGAAGAGGACGATG
Avr1b(RMVR)F	Forward primer for replacing RFLR motif of Avr1b with RMVR. NgoMIV	CGACATT**GCCGGC**GGAAGAaTggTTCGAGCTC ATGAAGAGGACGATG
Avr1b(RLGT)F	Forward primer for replacing RFLR motif of Avr1b with RLGT. NgoMIV	CGACATT**GCCGGC**GGAAGAcTTggaacAGCTCA TGAAGAGGACGATG
Avr1b(RLTQ)F	Forward primer for replacing RFLR motif of Avr1b with RLTQ. NgoMIV	CGACATT**GCCGGC**GGAAGAcTTacTCaAGCTCA TGAAGAGGACGATG
GWGFPF	Forward primer for Cloning Gateway cassette in GFP expression vector	GTCA**AGATCT**ACAAGTTTGTACAAAAAAGCTGA AC
GWGFPR	Reverse primer for Cloning Gateway cassette in GFP expression vector	GCAT**AGATCT**GGACCACTTTGTACAAGAAAGC TGAAC
GWGFPFBglII	Removes internal BglII site	GGGGCGTAAACGCGTGGATCCGGCTTACT
GWGFPRBglII	Removes internal BglII site	AGTAAGCCGGATCCACGCGTTTACGCCCC
attB1F	For cloning genes containing attB1 site	ATGCACAAGTTTGTACAAAAAAGCAGGCTC
attB2R	For cloning genes containing attB2 site	ATGCACCACTTTGTACAAGAAAGCTGGGT
AvrLm6m1R	Reverse primer mutating RTLK to qavq in AvrLm6	AGTACCTTTAACAACctgcaccgcctgGGTATCATC AACACC
AvrLm6m1F	Forward primer mutating RTLK to qavq in AvrLm6	GGTGTTGATGATACCcaggcggtgcagGTTGTTAAA GGTACT
AvrLm6m2R	Reverse primer mutating RYWT to qvvq in AvrLm6	TGGAGCACCTTCAGCTTTcgccaccacctgAGAAGA GAAAACAAAACG
AvrLm6m2F	Forward primer mutating RYWT to qvvq in AvrLm6	CGTTTTGTTTTCTCTTCTcaggtggtggcgAAAGCTG AAGGTGCTCCA
Avr2m1R	Reverse primer mutating RMLHRD to qvvnqn in Avr2	AGCACGTTCATATGGTGGGTTctggttcaccacctgA GCATAACCCAGTGGTTC
Avr2m1F	Forward primer mutating RMLHRD to qvvnqn in Avr2	GAACCACTGGGTTATGCTcaggtggtgaaccagAAC CCACCATATGAACGTGCT
Avr2m2R	Reverse primer mutating RIYER to qvvqq in Avr2	TGTACAAGAAAGCTGGGTACGAGActgctgcaccac ctgATGATTCAGACCAGAATTAC
Vam7pXGWF	Forward primer adding attB1 site infront of VAM7p-PX domain	atgcACAAGTTTGTACAAAAAAGCAGGCTccATG GCAGCTAATTCTGTAGGGAAAATGAGTG
Vam7pXGWR	Reverse primer adding attB2 site at the end of VAM7p-PX domain	GCATACCACTTTGTACAAGAAAGCTGGGTTAG ATGCTGCTGTGACTTTTCTTG
2xFYVEGWF	Forward primer adding attB1 site infront of Hrs-2xFYVE	atgcACAAGTTTGTACAAAAAAGCAGGCTccGaatt cgaaagtgatgccatgttcgctg
2xFYVEGWR	Reverse primer adding attB2 site at the end of Hrs-2xFYVE	GCATACCACTTTGTACAAGAAAGCTGggtatagaat acaagcttgggctgcaggtcg
Avr1bGWF	Forward primer adding attB1 site infront of Avr1b	gatcACAAGTTTGTACAAAAAAGCAGGCTccACT GAGTACTCCGACGAAACC

Avr1bGWR	Reverse primer adding attB2 site at the end of Avr1b	GATCACCACTTTGTACAAGAAAGCTGGGTTCAGCTCTGATACCGGTGAAAGGTG
GFPF	Forward primer for PCR hybridization removing the NotI site from the linker sequence preceeding GFP from pArg9	GTCGCGGCGGCGGCCACCatgagcaagggcgaggaactgttc
GFPHISR	Reverse primer adding a poly His tag and a NotI site to the end of GFP	gcatGCGGCCGCTCAATGATGATGATGATGATGcttgtacagctcgtccatgccatg
mCHerryF	Forward primer adding part fof the linker sequence preceeding GFP lacking the NotI site to the front of mCherry	GTCGCGGCGGCGGCCACCATGGTTTCTAAAGGTGAAGAAG
mCherryHISR	Reverse primer adding a poly His tag and a NotI site to the end of mCherry	gcatGCGGCCGCTCAATGATGATGATGATGATGTTTATACAGTTCATCCATACC
LinkerF	Forward primer of the linker sequence adding a enterokinase site and a xmaI site	atgcCTCGAGGACGATGACGATAAGGATATGTCCGGCTATCCATAT
LinkerR	Reverse primer removing the NotI site of the linker sequence	GGTGGCCGCCGCCGCGACTAGTGAGCTCGTCGA
GWFXmaI	Forward primer adding a XmaI site to the front of the Gateway Cassette	gatc**ctcgag**ACAAGTTTGTACAAAAAAGCTGAAC
GWRXmaI	Reverse primer adding a XmaI site to the front of the Gateway Cassette	gcat**ctcgag**ggACCACTTTGTACAAGAAAGCTGAAC

Table S4. Description of plasmids used in this study (associated with supplemental experimental procedures).

- * Amino acid sequences of the proteins encoded by the plasmids are shown in Figures 7 and S3.
- † Sequences of primers used for the cloning strategy are shown in the Supplemental Experimental Procedures

Plasmid	Recipient	Expression	Description*	Cloning Strategy†
Arg9-GFP		*E. coli*	9Arg fused to the N-terminus of GFP.	Received from Han-Jung Lee[25]
Avr1b(N)-GFP	Arg9-GFP	*E. coli*	Amino acids 33-71 of Avr1b fused to the N-terminus of GFP.	Described by Dou et al[8]
Avr1b(N)(rxlr$^-$)-GFP	Arg9-GFP	*E. coli*	Amino acids 33-71 of Avr1b fused to the N-terminus of GFP. RSLR and RFLR both mutated to AAAA.	Described by Dou et al[8]
Avr1b(N)(deer$^-$)-GFP	Arg9-GFP	*E. coli*	Amino acids 33-71 of Avr1b fused to the N-terminus of GFP. EEDDAGER mutated to AAAAAGAA.	Described by Dou et al[8]
Avh5(N)-GFP	Arg9-GFP	*E. coli*	Amino acids 19-63 of Avh5 fused to the N-terminus of GFP.	2-Step PCR of Avh5 using Avh5-ExpGFP-BglII and Avh5R2 then Avh5-ExpGFP-BglII and LinkerR2. BglII and NcoI.
Avh5(N)(rflr$^-$)-GFP	Arg9-GFP	*E. coli*	Amino acids 19-63 of Avh5 fused to the N-terminus of GFP. RFLR mutated to AAAA.	2-Step PCR of Avh5RXLR mutant from pGEX4T1 using Avh5-ExpGFP-BGlII and Avh5R2 then Avh5-ExpGFP-BglII and LinkerR2. BglII and NcoI.
Avh5(N)(deer$^-$)-GFP	Arg9-GFP	*E. coli*	Amino acids 19-63 of Avh5 fused to the N-terminus of GFP. DTDIVYEPK mutated to ATAIVYAPA	2-Step PCR of Avh5dEER mutant from pGEX4T1 using Avh5-ExpGFP-BGlII and Avh5R2 then Avh5-ExpGFP-BglII and LinkerR2. BglII and NcoI.
Avh331(N)-GFP	Arg9-GFP	*E. coli*	Amino acids 21-108 of Avh331 fused to the N-terminus of GFP.	2-Step PCR of Avh331 using Avh331-ExpGFP-BglII and Avh331R2 then Avh331-ExpGFP-BglII and LinkerR2. BglII and NcoI cloning.
Avh331(N)(rslr-)-GFP	Arg9-GFP	*E. coli*	Amino acids 21-108 of Avh331 fused to the N-terminus of GFP. RSLR mutated to AAAA	2-Step PCR of Avh331RXLR mutant from pGEX4T1 using Avh331-ExpGFP-BglII and Avh331R2 then Avh331-ExpGFP-BglII and LinkerR2. BglII and NcoI.
Avh331(N)(deer-)-GFP	Arg9-GFP	*E. coli*	Amino acids 21-108 of Avh331 fused to the N-terminus of GFP. DDDANVSIENR mutated to AAAANVSIANA	2-Step PCR of Avh331dEER mutant from pGEX4T1 using Avh331-ExpGFP-BglII and Avh331dEERR2 then Avh331-ExpGFP-BglII and LinkerR2. BglII and NcoI.
AvrL567(N)-GFP	Arg9-GFP	*E. coli*	Amino acids 24-67 of AvrL fused to the N-terminus of GFP	2-Step PCR of AvrL567 from pUCmAvrL567 using AvrL-ExpGFP-BglII and AvrLRevMod1 then AvrL-ExpGFP-BglII and AvrLRevMod2. BglII and NcoI.
AvrL567(N)(rfyr$^-$de$^-$)-GFP	Arg9-GFP	*E. coli*	Amino acids 24-67 of AvrL fused to the N-terminus of GFP. RFYRSPTASVILSGLVKVKWDNE mutated to AAAASPTASVILSGLVKVKWANA	2-Step PCR of AvrL567m from pUCmAvrL567(rfyr$^-$de$^-$) using AvrL-ExpGFP-BglII and AvrLRevMod1 then AvrL-ExpGFP-BglII and AvrLRevMod2. BglII and NcoI.
PfGBP(N)-GFP	Arg9-GFP	*E. coli*	Amino acids 70-107 of PfGBP fused to the N-terminus of GFP	2-Step PCR of PfGBP using PfGBP-ExpGFP-BglII and PfGBPR2 then PfGBP-ExpGFP-BglII and LinkerR2. BglII and NcoI.
PfGBP(N)(pexel$^-$)-GFP	Arg9-GFP	*E. coli*	Amino acids 70-107 of PfGBP fused to the N-terminus of GFP. RILAE mutated to AAAAA	3-Step PCR of PFGBP mutating RILAE to AAAAA using PfGBPF1 & PfGBPR2, then PfGBPF2 and PfGBPR2, then PfGBPExp-BglII and LinkerR2. BglII and NcoI.
PfHRPII(N)-GFP	Arg9-GFP	*E. coli*	Amino acids 27-63 of PfHRPII fused to the N-terminus of GFP	2-Step PCR of PfHRPII using PfHRPII-ExpGFP-BglII and PfHRPIIR2 then PfHRPII-ExpGFP-BglII and LinkerR2. BglII and NcoI.
PfHRPII(N)(pexel$^-$)-GFP	Arg9-GFP	*E. coli*	Amino acids 27-63 of PfHRPII fused to the N-terminus of GFP. RLLHE mutated to AAAAA	4-Step PCR of PfHRPII mutating RLLHE to AAAAA using PfHRPIIF1 and PfHRPIIR2, then PfHRPIIF2 and PfHRPIIR2, then PfHRPIIF3 and PfHRPIIR2, then PfHRPII-

				ExpGFP-BglII and LinkerR2. BglII and NcoI.
Pf1615c(N)-GFP	Arg9-GFP	*E. coli*	Amino acids 25-65 Pf1615c fused to the N-terminus of GFP	2-Step PCR of Pf1615c using Pf1615c-ExpGFP-BglII and Pf1615cR2 then Pf1615c-ExpGFP-BglII and LinkerR2. BglII and NcoI cloning.
Pf1615c(N)(pexel$^-$)-GFP	Arg9-GFP	*E. coli*	Amino acids 25-65 Pf1615c fused to the N-terminus of GFP. RILKQ mutated to AAAAA	3-Step PCR of Pf1615c mutating RILKQ to AAAAA using Pf1615cF1 and Pf1615cR2, then Pf1615cF2 and Pf1615cR2, then Pf1615c-ExpGFP and LinkerR2. BglII and NcoI.
GST-Avh331	pGEX4T1	*E. coli*	mature Avh331 fused to the C-terminus of GST	PCR of Avh331 using Avh331F-GST-BamHI and Avh331R-GST-SalI. BamHI and SalI.
GST-Avh331(rslr-)	pGEX4T1	*E. coli*	mature Avh331 fused to the C-terminus of GST. RSLR mutated to AAAA	2-Step PCR of Avh331RXLR using Avh331F-GST-BamHI and Avh331R2-RXLR, and Avh331F2-RXLR and Avh331R-GST-SalI. Products were fused using Avh331F-GST-BamHI and Avh331R-GST-SalI. BamHI and SalI.
GST-Avh5	pGEX4T1	*E. coli*	mature Avh5 fused to the C-terminus of GST	PCR of Avh5 using Avh5F-GST-BamHI and Avh5R-GST-SalI. BamHI and SalI
GST-Avh5(rflr$^-$)	pGEX4T1	*E. coli*	mature Avh5 fused to the C-terminus of GST.RFLR mutated to AAAA	2-Step PCR of Avh5 using Avh5F-GST-BamHI and Avh5-RXLRF, and Avh5-RXLRR and Avh5R-GST-SalI. Products were fused using Avh5F-GST-BamHI and Avrh5R-GST-SalI. BamHI and SalI.
GST-Avh5(deer$^-$)	pGEX4T1	*E. coli*	mature Avh5 fused to the C-terminus of GST. DTDIVYEPK mutated to ATAIVYAPA	2-Step PCR of Avh5 using Avh5F-GST-BamHI and Avh5-dEERF, and Avh5-dEER and Avh5R-GST-SalI. Products were fused using Avh5F-GST-BamHI and Avrh5R-GST-SalI. BamHI and SalI.
pUCsAvh331	pUCAvr1bXK	Transient soybean expression	mature Avh331 fused to the secreted leader of Avr1b in the transient assay vector	PCR of Avh331 using Avh331F-NcoI and Avh331R-KpnI. NcoI and KpnI.
pUCsAvh331(rslr-)	pUCAvr1bXK	Transient soybean expression	mature Avh331 fused to the secreted leader of Avr1b in the transient assay vector. RSLR mutated to AAAA	PCR of Avh331(rflr-) using Avh331F-NcoI and Avh331R-KpnI. NcoI and KpnI.
pUCsAvh331(deer-)	pUCAvr1bXK	Transient soybean expression	mature Avh331 fused to the secreted leader of Avr1b in the transient assay vector. AAAANVSIANA	PCR of Avh331(deer-) using Avh331F-NcoI and Avh331R-KpnI. NcoI and KpnI.
pUCmAvh331	pUCAvr1bXK	Transient soybean expression	mature Avh331 cloned into transient bombardment vector with Avr1b signal peptide	PCR of Avh331 using Avh331F-XmaI and Avh331R-Kpn.I XmaI and KpnI.
pUCmAvh331(rslr-)	pUCAvr1bXK	Transient soybean expression	mature Avh331 cloned transient bombardment vector with Avr1b signal peptide. RSLR mutated to AAAA	PCR of Avh331(rflr-) using Avh331F-XmaI and Avh331R-KpnI. XmaI and KpnI.
pUCmAvh331(deer-)	pUCAvr1bXK	Transient soybean expression	mature Avh331 cloned into transient bombardment vector with Avr1b signal peptide.	PCR of Avh331(deer-) using Avh331F-XmaI and Avh331R-KpnI. XmaI and KpnI.
pUCsAvrL567-Avr1b	pUCNgo	Transient soybean expression	Amino acids 24-67 of AvrL replaced the RXLR region of sAvr1b in the transient assay vector	4-Step PCR Avr1b. AvrLF4 and Avr1b-KpnI, then AvrLF3 Avr1b-KpnI, then AvrLF2 and Avr1b-KpnI, then AvrLF1 and Avr1b-KpnI. NcoI and KpnI.
pUCsAvrL567(rfyr$^-$de$^-$)-Avr1b	pUCNgo	Transient soybean expression	Amino acids 24-67 of AvrL replaced the RXLR region of sAvr1b in the transient assay vector. RFYR-DE of AvrL muated to AAAA-AA	2-Step PCR AvrL567-Avr1b. AvrLF1 and AvrLmR. AvrLmF and Avr1b-KpnI. Fuse the two pieces using AvrLF1 and Avr1b-KpnI. NcoI and KpnI.
pUCmAvrL567-Avr1b	pUCAvr1bXK	Transient soybean expression	Amino acids 24-67 of AvrL replaced the RXLR region of mAvr1b in the transient assay vector	PCR pUCsAvrL567. mAvrL567F and Avr1b-KpnI of. XmaI and KpnI.
pUCmAvrL567(rfyr$^-$de$^-$)-Avr1b	pUCAvr1bXK	Transient soybean expression	Amino acids 24-67 of AvrL replaced the RXLR region of mAvr1b in the transient assay vector. RFYR-DE of AvrL muated	PCR pUCsAvrL567(rfyr-de-). mAvrL567F and Avr1b-KpnI. XmaI and KpnI.

			to AAAA-AA	
pUCsAvrM-Avr1b	pUCAvr1bXK	Transient soybean expression	N-terminus of AvrM replaced the RXLR region of sAvr1b in the transient assay vector.	5 Step PCR. AvrM mini gene amplified with AvrM-F1 and AvrM-R, then AvrM-F2 and AvrM-R, AvrM-F3 and AvrM-R. Avr1b C-terminus was amplified with AvrM-Fmid and Avr1b-KpnI. The products were fused together using AvrM-F3 and Avr1b-KpnI.
pUCsAvrPita-Avr1b	pUCAvr1bXK	Transient soybean expression	N-terminus AvrPita replaced the RXLR region of sAvr1b in the transient assay vector.	5 step PCR. Pita mini gene was amplified with AvrPitaF and AvrPitaR1 then AvrPitaR2. Avr1b C-terminus was amplified with AvrPitaF1mid and Avr1b-KpnI then AvrPitaF2mid and Avr1b-KpnI. The products were fused together using AvrPitaF and Avr1b-KpnI.
pUCsAvrLm6-Avr1b	pUCAvr1bXK	Transient soybean expression	N-terminus AvrLm6 replaced the RXLR region of sAvr1b in the transient assay vector.	2-Step PCR using AvrLm6, Lm6bsF and Lm6midR and Avr1b, Lm6midF and Avr1b-KpnI. Products were fused using Lm6bsF and Avr1b-KpnI. NcoI and KpnI.
pUCsAvrLm6-Avr1b(rtlk^{qavq})	pUCAvr1bXK	Transient soybean expression	N-terminus AvrLm6 rxlr mutant 1 replaced the RXLR region of sAvr1b in the transient assay vector.	2-Step PCR using AvrLm6(rtlk^{qavq}), Lm6bsF and Lm6midR and Avr1b, Lm6midF and Avr1b-KpnI. Products were fused using Lm6bsF and Avr1b-KpnI. NcoI and KpnI.
pUCsAvrLm6-Avr1b(rywt^{qvva})	pUCAvr1bXK	Transient soybean expression	N-terminus AvrLm6 rxlr mutant 2 replaced the RXLR region of sAvr1b in the transient assay vector.	2-Step PCR using AvrLm6(rywt^{qvva}), Lm6bsF and Lm6midR and Avr1b, Lm6midF and Avr1b-KpnI. Products were fused using Lm6bsF and Avr1b-KpnI. NcoI and KpnI.
pUCmAvrLm6-Avr1b	pUCAvr1bXK	Transient soybean expression	N-terminus AvrLm6 replaced the RXLR region of mAvr1b in the transient assay vector.	2-Step PCR using AvrLm6, Lm6bmF and Lm6midR and Avr1b, Lm6midF and Avr1b-KpnI. Products were fused using Lm6bmF and Avr1b-KpnI. XmaI and KpnI.
pUCmAvrLm6-Avr1b(rtlk^{qavq})	pUCAvr1bXK	Transient soybean expression	N-terminus AvrLm6 rxlr mutant 1 replaced the RXLR region of mAvr1b in the transient assay vector.	2-Step PCR using AvrLm6(rtlk^{qavq}), Lm6bmF and Lm6midR and Avr1b, Lm6midF and Avr1b-KpnI. Products were fused using Lm6bmF and Avr1b-KpnI. XmaI and KpnI.
pUCmAvrLm6-Avr1b(rywt^{qvva})	pUCAvr1bXK	Transient soybean expression	N-terminus AvrLm6 rxlr mutant 2 replaced the RXLR region of mAvr1b in the transient assay vector.	2-Step PCR using AvrLm6(rywt^{qvva}), Lm6bmF and Lm6midR and Avr1b, Lm6midF and Avr1b-KpnI. Then Lm6bmF and Avr1b-KpnI. XmaI and KpnI.
pUCsAvr2-Avr1b	pUCAvr1bXK	Transient soybean expression	N-terminus Avr2 replaced the RXLR region of sAvr1b in the transient assay vector.	2-Step PCR using Avr2, Avr2bsF and Avr2midR, and Avr1b, Avr2midF and Avr1b-KpnI. Products were fused using Avr2bsF and Avr1b-KpnI. NcoI and KpnI.
pUCsAvr2-Avr1b(RMLHRD^{qvvnqn})	pUCAvr1bXK	Transient soybean expression	N-terminus Avr2 rxlr mutant 1 replaced the RXLR region of sAvr1b in the transient assay vector.	2-Step PCR using Avr2(RMLHRD^{qvvnqn}), Avr2bsF and Avr2midR, and Avr1b, Avr2midF and Avr1b-KpnI. Products were fused using Avr2bsF and Avr1b-KpnI. NcoI and KpnI.
pUCsAvr2-Avr1b(RIYER^{qvvqq})	pUCAvr1bXK	Transient soybean expression	N-terminus Avr2 rxlr mutant 2 replaced the RXLR region of sAvr1b in the transient assay vector.	2-Step PCR using Avr2(RIYER^{qvvqq}), Avr2bsF and Avr2mmidR, and Avr1b, Avr2mmidF and Avr1b-KpnI. Products were fused using Avr2bsF and Avr1b-KpnI. NcoI and KpnI.
pUCmAvr2-Avr1b	pUCAvr1bXK	Transient soybean expression	N-terminus Avr2 replaced the RXLR region of mAvr1b in the transient assay vector.	2-Step PCR using Avr2, Avr2bmF and Avr2midR, and Avr1b, Avr2midF and Avr1b-KpnI. Products were fused using Avr2bmF and Avr1b-KpnI. XmaI and KpnI.
pUCmAvr2-Avr1b(RMLHRD^{qvvnqn})	pUCAvr1bXK	Transient soybean expression	N-terminus Avr2 rxlr mutant 1 replaced the RXLR region of mAvr1b in the transient assay vector.	2-Step PCR using Avr2(RMLHRD^{qvvnqn}), Avr2bmF and Avr2midR, and Avr1b, Avr2midF and Avr1b-KpnI. Products were fused using Avr2bmF and Avr1b-KpnI XmaI and KpnI.
pUCmAvr2-Avr1b(RIYER^{qvvqq})	pUCAvr1bXK	Transient soybean expression	N-terminus Avr2 rxlr mutant 2 replaced the RXLR region of mAvr1b in the transient assay vector.	2-Step PCR using Avr2(RIYER^{qvvqq}), Avr2bmF and Avr2mmidR, and Avr1b, Avr2mmidF and Avr1b-KpnI. Products were fused using Avr2bmF and Avr1b-KpnI. XmaI and KpnI.
pUCsAvr1b(KFLR)	pUCAvr1bNgo	Transient soybean	RFLR motif of Avr1b was replaced with KFLR by PCR and fused to	Described by Dou et al[8]

		expression	pUCAvr1bXK. NgoMIV/KpnI	
pUCsAvr1b(HFLR)	pUCAvr1bNgo	Transient soybean expression	RFLR motif of Avr1b was replaced with HFLR by PCR and fused to pUCAvr1bXK. NgoMIV/KpnI	PCR of Avr1b using Avr1b(HFLR)F and Avr1b-KpnI. NgoMIV and KpnI.
pUCsAvr1b(QFLR)	pUCAvr1bNgo	Transient soybean expression	RFLR motif of Avr1b was replaced with QFLR by PCR and fused to pUCAvr1bXK. NgoMIV/KpnI	Dou et al[8]
pUCsAvr1b(RFFR)	pUCAvr1bNgo	Transient soybean expression	RFLR motif of Avr1b was replaced with RFFR by PCR and fused to pUCAvr1bXK. NgoMIV/KpnI	PCR of Avr1b using Avr1b(RFFR)F and Avr1b-KpnI. NgoMIV and KpnI.
pUCsAvr1b(RFYR)	pUCAvr1bNgo	Transient soybean expression	RFLR motif of Avr1b was replaced with RFYR by PCR and fused to pUCAvr1bXK. NgoMIV/KpnI	PCR of Avr1b using Avr1b(RFYR)F and Avr1b-KpnI. NgoMIV and KpnI.
pUCsAvr1b(RFIR)	pUCAvr1bNgo	Transient soybean expression	RFLR motif of Avr1b was replaced with RFIR by PCR and fused to pUCAvr1bXK. NgoMIV/KpnI	PCR of Avr1b using Avr1b(RFIR)F and Avr1b-KpnI. NgoMIV and KpnI.
pUCsAvr1b(RFMR)	pUCAvr1bNgo	Transient soybean expression	RFLR motif of Avr1b was replaced with RFMR by PCR and fused to pUCAvr1bXK. NgoMIV/KpnI	PCR of Avr1b using Avr1b(RFMR)F and Avr1b-KpnI. NgoMIV and KpnI.
pUCsAvr1b(RFVR)	pUCAvr1bNgo	Transient soybean expression	RFLR motif of Avr1b was replaced with RFVR by PCR and fused to pUCAvr1bXK. NgoMIV/KpnI	Described by Dou et al[8]
pUCsAvr1b(RFAR)	pUCAvr1bNgo	Transient soybean expression	RFLR motif of Avr1b was replaced with RFAR by PCR and fused to pUCAvr1bXK. NgoMIV/KpnI	Described by Dou et al[8]
pUCsAvr1b(RFLG)	pUCAvr1bNgo	Transient soybean expression	RFLR motif of Avr1b was replaced with RFLG by PCR and fused to pUCAvr1bXK. NgoMIV/KpnI	PCR of Avr1b using Avr1b(RFLG)F and Avr1b-KpnI. NgoMIV and KpnI.
pUCsAvr1b(RMVR)	pUCAvr1bNgo	Transient soybean expression	RFLR motif of Avr1b was replaced with RMVR by PCR and fused to pUCAvr1bXK NgoMIV/KpnI	PCR of Avr1b using Avr1b(RMVR)F and Avr1b-KpnI. NgoMIV and KpnI.
pUCsAvr1b(RLGT)	pUCAvr1bNgo	Transient soybean expression	RFLR motif of Avr1b was replaced with RLGT by PCR and fused to pUCAvr1bXK NgoMIV/KpnI	PCR of Avr1b using Avr1b(RLGT)F and Avr1b-KpnI. NgoMIV and KpnI.
pUCsAvr1b(RLTQ)	pUCAvr1bNgo	Transient soybean expression	RFLR motif of Avr1b was replaced with RLTQ by PCR and fused to pUCAvr1bXK NgoMIV/KpnI	PCR of Avr1b using Avr1b(RLTQ)F and Avr1b-KpnI. NgoMIV and KpnI.
pUCAvr1b(Arg9)	pUCAvr1bNgo	Transient soybean expression	RFLR motif of Avr1b was replaced with 9 Arg residues by PCR and fused to pUCAvr1bXK NgoMIV/KpnI	Described by Dou et al[8]
Control GFP	Arg9-GFP	*E. coli*	Removal of nucleotides encoding the 9 Arg	PCR of GFP plus linker sequence using cGFPF and cGFPR. Cloned into BglII and XhoI site of Arg9-GFP. BglII and XhoI.
Avr1b(N)(rxlr^{rfrl})-GFP	Arg9-GFP	*E. coli*	Amino acids 33-71 of Avr1b fused to the N-terminus of GFP. RFLR both mutated to rfrl.	2-step PCR of Avr1b(N)rxlr^{rfrl} from pUCsAvr1b(RFLR) using Avr1bGFPF, Avr1bGFPR1, and Avr1bGFP2. BglII and NcoI.
Avr1b(N)(rxlr^{frlr})-GFP	Arg9-GFP	*E. coli*	Amino acids 33-71 of Avr1b fused to the N-terminus of GFP. RFLR both mutated to frlr.	2-step PCR of Avr1b(N)rxlr^{frlr}from pUCsAvr1b(RFLR) using Avr1bGFPF, Avr1bGFPR1, and Avr1bGFP2. BglII and NcoI.
Avr1b(N)(rxlr^{qflr})-GFP	Arg9-GFP	*E. coli*	Amino acids 33-71 of Avr1b fused to the N-terminus of GFP. RFLR both mutated to qflr.	2-step PCR of Avr1b(N)rxlr^{qflr} from pUCsAvr1b(RFLR) using Avr1bGFPF, Avr1bGFPR1, and Avr1bGFP2. BglII and NcoI.
Avr1b(N)(rxlr^{rfyr})-GFP	Arg9-GFP	*E. coli*	Amino acids 33-71 of Avr1b fused to the N-terminus of GFP. RFLR both mutated to rfyr.	2-step PCR of Avr1b(N)rxlr^{rfyr} from pUCsAvr1b(RFLR) using Avr1bGFPF, Avr1bGFPR1 and Avr1bGFP2. BglII and NcoI.
GWGFP	Control GFP	*E.coli*	Gateway compatible construct of the GFP expression vector	2-step PCR of gateway cassette from pEG100 removing internal BglII site using GWGFPF and GWGFPRBglII, and GWGFPFBglII and GWGFPR. Products were fused using GWGFPF and GWGFPR. BglII.
AvrLm6(N)-GFP	GWGFP	*E.coli*	Amino acids 21-69 of AvrLm6 fused to the N-terminus of GFP.	Synthesized by Genescript with AttB cloning sites. Gateway BP reaction into pDONR and

				then Gateway LR reaction GWGFP.
AvrLm6(N)(rtlk^{qavq})-GFP	GWGFP	*E.coli*	Amino acids 21-69 of AvrLm6 fused to the N-terminus of GFP. RTLK mutated to qavq	2 Step PCR using attB1 and AvrLm6m1R, and AvrLm6m1F and AttB2. Products were fused using with attB1 and attB2. Gateway cloning.
AvrLm6(N)(rywt^{qvva})-GFP	GWGFP	*E.coli*	Amino acids 21-69 of AvrLm6 fused to the N-terminus of GFP. RYWT mutated to qvva	2 Step PCR using attB1 and AvrLm6m2R, and AvrLm6m2F and AttB2. Followed by PCR with AttB1 and AttB2. Gateway cloning
Avr2(N)-GFP	GWGFP	*E.coli*	Amino acids 20-90 of Avr2 fused to the N-terminus of GFP.	Synthesized by Genescript with AttB cloning sites. Gateway reaction into pDONR and then into GWGFP
Avr2(N)(RMLHRD^{qvvnqn})-GFP	GWGFP	*E.coli*	Amino acids 20-90 of Avr2 fused to the N-terminus of GFP. RMLHRD mutated to qvvnqn.	2 Step PCR using attB1 and Avr2m1R, and Av2m1F and attB2. Products were fused using attB1 and attB2. Gateway cloning.
Avr2(N)(RIYER^{qvvqq})-GFP	GWGFP	*E.coli*	Amino acids 20-90 of Avr2 fused to the N-terminus of GFP. RIYER mutated to qvvqq.	2 Step PCR using attB1 and Avr2m2R and attB2. Products were fused using attB1 and attB2. Gateway cloning.
PEPP1-PH-GFP	GWGFP	*E.coli*	PEPP1-PH domain fused to the N-terminus of GFP	Synthesized by Genescript with AttB cloning sites. Gateway reaction into pDONR and then into GWGFP
FAPP1-PH-GFP	GWGFP	*E.coli*	FAPP1-PH domain fused to the N-terminus of GFP	Synthesized by Genescript with AttB cloning sites. Gateway reaction into pDONR and then into GWGFP
pSDK1	pGEX4T1	*E.coli*	Protein expression vector designed with N-terminus GST tag, thrombin cleavage site, gateway cloning site, enterokinase site, GFP followed by poly-histidine tag	2 Step PCR hybridization of the product of LinkerF and LinkerR and the product of GFPF and GFPHisR all from pArg9 using LinkerF and GFPHisR. XmaI and NotI into pGEX4T-1. Resultant vector was the cut with XmaI and the PCR of the Gateway cassette using GWFXmaI and GWRXmaI cut with XmaI was ligated in and screened for correct orientation.
pSDK2	pGEX4T1	*E.coli*	Protein expression vector designed with N-terminus GST tag, thrombin cleavage site, gateway cloning site, enterokinase site, mCherry followed by poly-histidine tag	2 Step PCR hybridization of the product of LinkerF and LinkerR and the product of GFPF and mCherryHisR using LinkerF and mCherryHisR. XmaI and NotI into pGEX4T-1. Resultant vector was the cut with XmaI and the PCR of the Gateway cassette using GWFXmaI and GWRXmaI cut with XmaI was ligated in and screened for correct orientation.
pSDK1-VAM7pPX	pSDK1	*E.coli*	Vam7p-PX domain inserted into pSDK1expression cassette	PCR with AttB sites using Vam7pXGWF and Vam7pXGWR and gateway reactiond into pDONR and then into pSDK1
pSDK1-Hrs-2xFYVE	pSDK1	*E.coli*	Hrs-2xFYVE domain inserted into pSDK1 expression cassette	PCR with AttB sites using 2xFYVEGWF and 2xFYVEGWR and gateway reactiond into pDONR and then into pSDK1
pSDK1-Avr1b(FL)	pSDK1	*E.coli*	Avr1b(FL) inserted into pSDK1 expression cassette	PCR with AttBs sites using Avr1bGWF and Avr1bGWR and gateway reaction into pDONR and then into pSDK1
pSDK1-Avr1b(FL)rxlr^{qflr}	pSDK1	*E.coli*	Avr1b(FL)rxlr^{qflr} inserted into pSDK1 expression cassette	PCR with AttBs sites using Avr1bGWF and Avr1bGWR and gateway reaction into pDONR and then into pSDK1
pSDK1-Avr1b(FL)deer^{-}	pSDK1	*E.coli*	Avr1b(FL)deer^{-} inserted into pSDK1 expression cassette	PCR with AttBs sites using Avr1bGWF and Avr1bGWR and gateway reaction into pDONR and then into pSDK1
pSDK2-VAM7pPX	pSDK2	*E.coli*	Vam7p-PX domain inserted into pSDK2 expression cassette	PCR with AttB sites using Vam7pXGWF and Vam7pXGWR and gateway reaction into pDONR and then into pSDK2
pSDK2-Hrs-2xFYVE	pSDK2	*E.coli*	Hrs-2xFYVE domain inserted into pSDK2 expression cassette	PCR with AttB sites using 2xFYVEGWF and 2xFYVEGWR and gateway reactiond into pDONR and then into pSDK2
pSDK2-PEPP1-PH	pSDK2	*E.coli*	PEPP1-PH domain inserted into pSDK2 expression cassette	Synthesized by Genescript with AttB cloning sites. Gateway reaction into pDONR and then into pSDK2
pSDK2-FAPP1-PH	pSDK2	*E.coli*	FAPP1-PH domain inserted into pSDK2 expression cassette	Synthesized by Genescript with AttB cloning sites. Gateway reaction into pDONR and then into pSDK2

Table S5. Polypeptides encoded by the protein expression vectors, related to extended experimental procedures

pAvr1bXK was used for expression in planta using particle bombardment. All others were used for expression in *E. coli.* . Underlined sequences represent expressed sequences that were replaced as needed with other effector or biosensor sequences. Pipes ("|") indicate sites of replacement. Avr1b secretion signal peptide is in italics; his tags (HHHHHH), enterokinase cleavage sites (DDDDK); thrombin cleavage sites (LVPRGS) and haemaglutinin tags (YPYDVPDYA) are highlighted in bold; all other unhighlighted sequences are linker sequences that in the last three vectors span attB recombination sites. GST indicates N-terminal glutathione-S-transferase fusion.

Vector	**Expressed polypeptide**
pAvr1bXK	*MRLSFVLSLVVAIGYVVTCNA*|TEYSDETNIAMVESPDLVRRSLRNGDIAGGRFLRAHEEDDAGER|-Avr1b(66-138)
Arg9-GFP	MRGS**HHHHHH**GMASMTGGQQMGRNLY**DDDDK**DRWGSRS|RRRRRRRRR|EFRSTMSG**YPYDVPDYA**GSMGSGIQRPTSTSSLVAAAAT-GFP(full length)
pGEX4T-1-Avh331	GST-**LVPRGS**|LTCATSEQQTRPELCFFFSVRSSWPSTISDGACLALVSAEQGATAGRNTLSLRSMMATEDMATSTRSLRSQATNVDDDANVSIENRGMNPSVLTKLGEFASTLTAGNTANKLWLMADVDPKSAFKLLGLDMPGVRFIDNPKMLQWLKFTKAYLDMKKSGFGETSAHALLYEKIGGPDLSLLLSLKDAPDANSLVQKLTNSQFGMWHDARIEPEQLAQTVFKIQDVRKLPKNDPKLQVIDDYAKYHRKHRKFLNSIMII|
pGWGFP-Lm6	MRGS**HHHHHH**GMASMTGGQQMGRDLY**DDDDK**DRWGSRSTSLYKKAGSQPHLLCAC|ESGRRDGVDDTRTLKVVKGTGGRFVFSSRYWTKAEGAPHEG|TQLSCTKWSRSEFRSTMSG**YPYDVPDYA**GSMGSGIQRPTSTSSLVAAAAT-GFP(full length)
pSDK1-Avr1b	GST-**LVPRGS**PEFPGRLETSLYKKAGS|MTEYSDETNIAMVESPDLVRRSLRNGDIAGGRFLRAHEEDDAGERTFSVTDLWNKVAAKKLAKAMLADPSKEQKAYEKWAKKGYSLDKIKNWLAIADPKQKGKYDRIYNGYTFHRYQS|TQLSCTKWSLE**DDDDK**DMSGYPYDVPDYAGSMGSGIQRPTSTSSLVAAAAT-GFP(full length)-**HHHHHH**
pSDK2-PEPP1	**GST**-**LVPRGS**PEFPGRLETSLYKKAGS|SASTISSLSSLSPKKPTRAVNKIHAFGKRGNALRRDPNLPVHIRGWLHKQDSSGLRLWKRRWFVLSGHCLFYYKDSREESVLGSVLLPSYNIRPDGPGAPRGRRFTFTAEHPGMRTYVLAADTLEDLRGWLRALGRASRAEGDDYGQPRSPARP|TQLSCTKWSLE**DDDDK**DMSGYPYDVPDYAGSMGSGIQRPTSTSSLVAAAAT-mCherry(full length)-**HHHHHH**

Table S6. Synthetic DNA sequences, related to extended experimental procedures

Sequences designed and synthesized by GenScript Corporation are marked with an asterisk.

AvrL567(N) (*E.coli* optimized) ATGGGAATGGAACATGTACCAGCAGAGTTGACCAGAGTCAGCGAAGGGTATACACGATTTTACCGGTCCCCAAC GGCTAGTGTAATACTGTCAGGATTGGTAAAGGTTAAATGGGATAATGAACAAATGACGATGCCG
AvrM(N) (*E.coli* optimized) ATGGGAAACAACCTTGGAACAGTACCGGATGTGCCACATCAAATTCCAAATGACAAAAGTGGTACTCCTGCCATT GAAGACCCAAAAGATATGAAAGGATTCAATAAGGCTCTCAAATCTACTCCAGAATCCGAAAAACTTGGAACTTCG TCAGTTGAAGGGATCCCTCAACCAGAATTTGACAGAGGATTCCTTAGACCTTTTGGAGCAAAAATGAAATTCCTC AAGCCGGACCAAGTTCAGAAACTTTCTACAGATGATCTCATCACATACATGGCAGAAAAAGATAAAAATGTACGA
Avr-Pita(N) (*E.coli* optimized) CACCCAGTTTACGATTACAATCCAATTCCAAACCATATCCACGGAGATTTAAAAAGGCGGGCTTATATTGAACGC TATTCCCAATGTTCAGATTCGCAGGCCTCCGAAATTCGTGCCGCGCTAAAAAGTTGTGCCGAGCTCGCCTCGTG GGGCTATCACGCCGTTAAAAATGACAATCGGTTATTTAGATTAATCTTTAAAACTGACAGCACAGATATTCAAAAC
AvrLm6(N) (*E.coli*, *Nicotiana* optimized)* CATCTGCTGTGTGCTTGTGAATCTGGTCGTCGTGATGGTGTTGATGATACCCGTACCCTGAAAGTTGTTAAAGGT ACTGGTGGTCGTTTTGTTTTCTCTTCTCGTTATTGGACCAAAGCTGAAGGTGCTCCACATGAAGGG
Avr2(N) (*E.coli*, *Nicotiana* optimized)* GTTGAAGATGCTGATTCTTCTGTTGGTCAGCTGCAGGGTCGTGGTAATCCATATTGTGTTTTTCCAGGTCGTCGT ACCTCTTCTACCTCTTTTACCACCTCTTTTTCTACCGAACCACTGGGTTATGCTCGTATGCTGCATCGTGATCCAC CATATGAACGTGCTGGTAATTCTGGTCTGAATCATCGTATTTATGAACGTTCTCGT
hPEPP1-PH (*E.coli*, *Nicotiana* optimized)* GTACTATTTCTTCACTGAGCAGTCTGTCTCCTAAAAAACCTACACGTGCTGTTAACAAGATCCATGCATTCGGTAA ACGCGGCAATGCTCTGCGTCGCGATCCGAACCTGCCAGTGCATATTCGTGGTTGGCTGCATAAACAGGATTCTT CAGGCCTGCGCCTGTGGAAACGTCGCTGGTTTGTTCTGTCAGGTCATTGTCTGTTCTATTACAAAGATTCTCGTG AAGAATCAGTTCTGGGCAGCGTGCTGCTGCCTAGCTATAACATTCGTCCTGATGGTCCGGGCGCACCACGCGGT CGTCGCTTTACCTTCACTGCGGAACATCCAGGCATGCGCACATACGTGCTGGCTGCAGATACCCTGGAGGATCT GCGTGGTTGGCTGCGTGCTCTGGGTCGTGCAAGTCGCGCGGAAGGTGATGATTATGGCCAACCTCGTTCTCCG GCACGCCCA
hFAPP1-PH (*E.coli*, *Nicotiana* optimized)* TGGAAGGTGTTCTGTATAAATGGACAAATTACCTGACCGGCTGGCAGCCACGTTGGTTTGTTCTGGATAACGGTA TTCTGTCTTATTACGATTCACAAGATGATGTGTGTAAAGGTAGCAAAGGCAGTATCAAGATGGCTGTTTGCGAAA TCAAGGTGCATTCTGCAGATAATACCCGTATGGAACTGATTATTCCTGGCGAACAGCATTTCTATATGAAAGCTG TTAACGCTGCAGAACGTCAACGCTGGCTGGTTGCTCTGGGTTCTTCAAAAGCGTGTCTGACCGATACTCGC
mCherry (*E.coli*, *Nicotiana* optimized)* TGGTTTCTAAAGGTGAAGAAGATAACATGGCTATCATCAAAGAATTTATGCGTTTCAAGGTTCATATGGAAGGTTC TGTTAACGGTCATGAATTTGAAATTGAAGGTGAAGGTGAAGGTCGTCCATATGAAGGTACTCAGACCGCTAAACT GAAAGTTACCAAAGGTGGTCCACTGCCATTTGCTTGGGATATTCTGTCTCCACAGTTTATGTATGGTTCTAAGGC TTACGTTAAACATCCAGCTGATATTCCAGATTATCTGAAACTGTCTTTTCCAGAAGGTTTTAAATGGGAACGTGTT ATGAATTTTGAAGATGGTGGTGTTGTTACCGTTACCCAGGATTCTTCTCTGCAGGATGGTGAATTTATTTATAAAG TTAAACTGCGTGGTACTAATTTTCCATCTGATGGTCCAGTTATGCAGAAAAAGACTATGGGTTGGGAAGCATCTT CTGAACGTATGTATCCAGAAGATGGTGCTCTGAAAGGTGAAATTAAACAGCGTCTGAAACTGAAAGATGGTGGTC ATTATGATGCTGAAGTTAAAACCACCTATAAAGCTAAAAAACCAGTTCAGCTGCCAGGTGCTTACAACGTTAACAT CAAACTGGATATCACCTCTCATAACGAAGATTACACCATCGTTGAACAGTATGAACGTGCTGAAGGTCGTCATTC TACCGGTGGTATGGATGAACTGTATAAA

Chapter 6: Conclusions and Personal Outlook

Introduction

The previous chapters focus on two important aspects of pathogen host interactions: effector translocation and function in virulence. Chapter 2 describes a novel technology utilized to test the ability of effectors to induce cell death or suppress different triggers of cell death. Chapter 3 provides evidence that effectors have the ability to suppress different inducers of cell death via conserved C-terminal domains. In the case of Avr1b these C-terminal domains are also required for the interaction with Rps1b. Chapter 4 shows the role of the RXLR-dEER motif in protein translocation. The highlight of this chapter focuses on the finding of RXLR effector translocation without the need of any pathogen encoded machinery. Chapter 5 greatly expands on the findings in Chapter 4 and identifies several fungal effectors capable of translocation independent of the pathogen via an RXLR-like motif. These effectors are able to enter cells by binding phosphatidylinositol-3-phosphate (PtdIns-3-P) found in lipid rafts on the outer leaflet of animal and plant cells. A proof-of-concept is shown by blocking effector entry through the use of biosensors that are able to sequester PtdIns-3-P or by competitive inhibition.

Suppression of Cell Death

Chapter 3 highlights the role of effectors in the suppression of different types of host induced cell death. Cell death as a strategy for defense is well understood. The host sacrifices a region of cells to develop a physical barrier. The purpose of this physical barrier is to prevent the movement of the pathogen, but it is equally as

important to cut off nutrient acquisition. Biotrophic and hemi-biotrophic organisms must keep the host cell alive to facilitate the acquirement of nutrients, and allow pathogenesis to progress to a point of critical mass. Visualizing the differences that occur during a compatible and incompatible interaction at early time points can be challenging. Only at points well after initial penetration do differences arise between two interactions. Even in an incompatible interaction the oomycete is able to reach the endodermis indicating that the resistance mechanism is not instantaneous and may occur due to starvation **(1)**. The hypersensitive response either triggered by PTI or ETI is key to the prevention of pathogenesis **(2)**, but one can speculate there is more involved than simply the creation of physical barrier that prevents nutrient acquisition. Regardless of the unknown complexities association with pathogenesis, prevention of cell death in host cells does facilitate pathogenesis for biotrophs and hemi-biotrophs.

P. sojae *Avr1b* is expressed during the early stages of infection and contributes to the virulence of the pathogen **(3,4)**. The expression profile of *Avr1b* indicates that the gene aids the biotrophic phase of infection by suppressing host cell death mechanism **(3,4)**. Chapter 3 shows that *Avr1b* and several other oomycete effectors have the ability to suppress programmed cell death induced by the mouse BAX protein and hydrogen peroxide **(4)**. These findings illuminate the role of early expressed effectors in keeping the host cells alive to maximize nutrient acquisition. Avr1b contains highly conserved K, W, and Y-domains in the C-terminus of the protein **(4)**. These domains are found in a large number of putative effectors in the genomes of *P. sojae* and *P. ramorum* **(5)**. The presence of these domains in tandem implies that many effectors share similar secondary structure and that a core structure may exist for effectors. These core

structures would allow effectors to interact with a specific type of protein such as those containing conserved domains associated with cell death pathways. *P. infestans* Avr3a, which also contains K, W, and Y domains, is able to stabilize the U-box protein CMPG1, which is required for efficient activation of defense responses associated with ETI **(6)**. U-box proteins are involved in the ubiquitination pathway and these U-box proteins make up a family of E3 enzymes **(7)**. Thus by interacting with these U-box proteins, effectors are able to modulate host cell ubiquitination. Due to the diversity in amino acid sequence associated with the C-terminal domains, many effectors may also interact with different plant domains associated with defense pathways.

Protein Translocation

Protein translocation from pathogen to host occurs through a variety of mechanisms. RXLR or RXLR-like motif mediates translocation of effectors into host cells for oomycete and fungal effectors **(8,9,10,11)**. The mechanism of translocation is mediated by the binding of phosphatidylinositol-3-phosphate (PtdIns-3-P) found on the surface of plant and animal cells in lipid raft structures **(10)**. Several pathogen-secreted proteins are able to enter host cells mediated by phospholipid-binding endocytosis **(10)**. Tetanus, cholera and botulinum toxins enter cells via binding surface glycolipids **(12)**. The CagA effector of *Helicobacter pylori,* enters host epithelial cells by binding Ptd-Ser on the outer leaflet **(13)**. Certain fungal ribotoxins bind surface phospholipids to enter cells via a number of mechanisms of endocytosis **(14)**. Recently evidence also implicates certain allergens entry via RXLR-like motifs (Rumore, Kale, Tyler, Lawrence, unpublished). Pathogen-secreted proteins may enter through other mechanisms.

Pseudomonas exotoxin A enters via binding to alpha2-macroglobulin/LDL receptor **(15)**. Thus many pathogen-secreted proteins are able to utilize a variety of host macromolecules to enter cells without the requirement of any pathogen encoded machinery.

The identification of the oomycete RXLR and fungal RXLR-like effector entry mechanism has stimulated discussion in several scientific foci. The presence of PtdIns-3-P has previously not been identified on the external leaflet of cells. Is phosphatidylinositol phosphorylated on the outer leaflet or is PtdIns-3-P localized to the raft by a flippase or unknown mechanism? How do these effector proteins escape endosomes? In soybean suspension culture and human airway epithelial cells, Avr1b-GFP and AvrL567-GFP can be seen entering the cell in small punctate structures that move towards what is believed to be the endoplasmic reticulum or golgi apparatus. Is there a fusion that transpires in the golgi apparatus that mediates release or do these effectors escape during translocation of the vesicle? The answers to these questions will allow us to gain further insight into the mechanism of entry and the role of phospholipids in translocation and pathogenesis.

Development of Biotechnology

One of the discoveries highlighted in Chapter 5 is the proof of concept that effector entry can be blocked by either sequestering PtdIns-3-P on the cell surface through the use of a biosensor or by competitive inhibition of the RXLR binding pocket through the use of 1,3IP2 **(10)**. By preventing effector entry into host cells, the pathogen is unable to effectively utilize its arsenal of effectors to modulate host cell defense

responses. The loss of a significant number, if not all, effector entry would prevent mechanisms such as ETI; however the loss of suppression of PTI and other primary defense responses by effectors could conceivably be enough to allow the basal defense response to mediate immunity.

A potential caveat of blocking effector entry is that this function might disrupt normal cellular processes. Effectors hijack an innate host cell entry mechanism that has remained available regardless of selection pressure associated with its removal. The presence of these receptors indicates they have an innate function in cellular communications. Blocking such communication avenues may produce adverse effects *in-planta*, though there is no experimental evidence indicating such findings. Currently one effector has been identified that utilizes the RXLR-phospholipid mediated cell entry mechanism creating a beneficial interaction between fungus and plant (Plett, Kale, Tyler, Martin, unpublished). These findings add clout to the hypothesis that effectors hijack a mechanism of entry that is beneficial to the plant. Identification of host RXLR proteins will enable an understanding why the host cells retaining this entry mechanism when there is much selection pressure against it.

Identification of RXLR-like motifs

The functional flexibility of the RXLR motif sits in contrast with its genomic conservation. Simple string searches for RXLR-like motifs in fungal genomes produce results enriched in false positives. Currently, identification of RXLR-like motifs can only be done effectively with known intracellular effectors. Further work is required both experimentally and bioinformatically to remove false positives in search of RXLR-like

sequences. A reason for strong RXLR sequence preservation in oomycetes may lie in the full-length protein. A large subset of oomycete effectors possess conserved C-terminal domains that are predicted amphipathic helices **(4,5)**. These domains may present a core structure. Efficient binding of PtdIns-3-P and structural stability of the entire effector may purify for an RXLR motif of a specific structure. Likewise fungal effectors share little similarity therefore selection pressure would not generate identical RXLR translocation motifs. A hypothesis may be these RXLR-like effectors originated independently in taxa. Defining an RXLR sequence based on specific taxa may elucidate the full effector repertoire during bioinformatic searches. However, an RXLR-like effector reservoir was identified in the genome of *Leptosphaeria maculans* **(16)**, though no statistical test has been developed to separate true positives from false positives. Interestingly, known translocated effectors AvrLm6 and AvrLm4/7 were found in this reservoir indicating that there is an inherit information in the primary structure to identify translocation motifs. The next challenge, computationally, is to develop a reliable method to identify RXLR-like motifs.

Rationale for effector reservoirs

Evolution occurs in a variety of environments and settings. The assumed randomness of phenomena we cannot currently comprehend leads to the occurrence of novel features that are advantageous for fitness of a given organism. Under these circumstances the excessively large reservoirs of effectors makes sense. Effectors arise through duplication events and mutate randomly. This can be documented through the fact that these effectors are found in highly repetitive regions of the genome filled with

transposable elements, and a large subset of effectors share sequence homology **(5,16,17)**. Only a subset of effectors are active during pathogenesis (Tyler, unpublished), while the remaining effectors are believed to lay dormant waiting for "random" activation that may benefit pathogenesis. Intense selection pressure towards beneficial, newly activated effectors allows for strong purifying effects in the population, especially in the face of a novel resistance gene. Thus the fitness costs of maintaining such a large reservoir is balanced by the ability to "randomly" activate a new component of the effector-ome relatively quickly. Another hypothesis for the large reservoir of putative effectors is the diverse host range of many oomycetes. Effectors may be activated depending on the site of infection or others might be host specific. This hypothesis makes sense for broad host range oomycetes such as *P. cinnamomi*, but does not mesh well with other oomycetes such as *P. sojae* and *P. infestans*, who are believed to have a limited host range. However this limited host range may be a product of common agriculture practices where disease is only visualized and noted on crops that have importance. There is a possibility that many narrow range oomycetes simply cannot successfully infect other plant species due to a lack of coevolution mediated by an initial resistance protein that could not be overcome and/or relatively low fitness on that host. These questions can be easily answered by looking at microscopy of infection assays with non-traditional pathogen host combinations. In many cases the pathogen may not be able to adhere or penetrate the host. However, there are bound to be cases of successful penetration that is limited by a host specific defense response to an effector(s). The mechanism of activation of effectors is of great interest due to the

implications in understanding co-evolution between pathogen and host, and potential evolution in a given organism.

References:

1. Tyler BM (2007) *Phytophthora sojae*: root rot pathogen of soybean and model oomycete. *Molec Plant Path*: 8, 1-8.
2. Jones JDG, Dangl JL (2006) The plant immune system. *Nature:* 444, 323-329.
3. Shan W, et al (2004) The Avr1b locus of Phytophthora sojae encodes an elicitor and a regulator required for avirulence on soybean plants carrying resistance gene Rps1b. *Mol Plant Micro Interact:* 17, 394-403.
4. Dou D, et al (2008) Conserved C-terminal motifs required for avirulence and suppression of cell death by *Phytophthora sojae* effector Avr1b. *The Plant Cell*: 20,1118-1133.
5. Tyler BM, et al (2006) Phytophthora genome sequences uncover evolutionary origins and mechanisms of pathogenesis. *Science*: 313, 1261–1266.
6. Bos JIB, et al (2010) *Phytophthora infestans* effector AVR3a is essential for virulence and manipulates plant immunity by stabilizing host E3 ligase CMPG1. *Proc Nat Acad Sci USA*: 107, 9909-9914.
7. Hatakeyama S, et al (2001) U-box proteins as a new family of ubiquitin-protein ligases. J boil chem: 276, 33111-33120.
8. Whisson SC, et al (2007) A translocation signal for delivery of oomycete effector proteins into host plant cells. *Nature:* 450, 115-118.
9. Dou D, et al (2008) RXLR-Mediated Entry of *Phytophthora sojae* Effector *Avr1b* into Soybean Cells Does Not Require Pathogen-Encoded Machinery. *The Plant Cell* 20:1930-1947.
10. Kale SD, et al (2010) External lipid PI3P mediates entry of eukaryotic pathogen efectors into plant and animal host cells. *Cell:* 142, 284-295.
11. Rafiqi M, et al (2010) Internalization of flax rust avirulence proteins into flax and tobacco cels can occur in the absence of the pathogen. *The Plant Cell*: 22, 2017-2032.
12. Lalli G, et al (1999) Functional characterization of tetanus and botulinum neurotoxins binding domains. *J Cell Sci*: 122, 2715-2724.
13. Murata-Kamiya N, et al (2010) *Helicobacter pylori* Exploits Host Membrane Phosphatidylserine for Delivery, Localization, and Pathophysiological Action of the CagA Oncoprotein. *Cell Host Microbe:* 7, 338-339.
14. Lacadena J, et al (2007) Fungal ribotoxins: molecular dissection of a family of natural killers. *FEMS Microbiol Rev*: 31, 212-237.
15. Kounnas MZ, et al (1992) The alpha 2-macroglobulin receptor/low density lipoprotein receptor-related protein binds and internalizes *Pseudomonas* exotoxin A. *J Biol Chem:* 267, 12420-12423.

16. Rouxel T, et al (2011) Effector diversification within compartments of the *Leptosphaeria maculans* genome affected by Repeat-Induced Point mutations. *Nat Comm*: doi:10.1038/ncomms1189.
17. Jiang RHY, et al (2008) RXLR effector reservoir in two *Phytophthora* species is dominated by a single rapidly evolving super-family with more than 700 members. *Proc Natl Acad Sci USA*: 105, 4874–4879.